THE IMPLICATIONS OF ADOPTING EUROCODES FOR DESIGNING DISASTER RESILIENT BUILDINGS IN SRI LANKA

H.A. Pathirana

218113B

Master of Science

Department of Civil Engineering
Faculty of Engineering

University of Moratuwa
Sri Lanka

June 2025

THE IMPLICATIONS OF ADOPTING EUROCODES FOR DESIGNING DISASTER RESILIENT BUILDINGS IN SRI LANKA

H.A. Pathirana

218113B

Thesis submitted in partial fulfillment of the requirements for the degree

Master of Science

Department of Civil Engineering

Faculty of Engineering

University of Moratuwa

Sri Lanka

June 2025

DECLARATION OF THE CANDIDATE

I declare that this is my own work and this thesis does not incorporate without acknowledgement any material previously submitted for a degree or diploma in any other University or Institute of higher learning and to the best of my knowledge and belief it does not contain any material previously published or written by another person except where the acknowledgement is made in the text. I retain the right to use this content in whole or part in future works (such as articles or books).

Signature: Date: 17.06.2025

Hashini Ayeshika Pathirana

Department of Civil Engineering,

University of Moratuwa.

DECLARATION OF THE SUPERVISOR

The above candidate has carried out research for the Masters thesis under our supervision. We confirm that the declaration made above by the student is true and correct.

Signature of the Supervisor: Date: 22.06.2025

Prof. M.T.R. Jayasinghe,

Senior Professor,

Department of Civil Engineering,

University of Moratuwa.

Signature of the Supervisor: Date: 21.06.2025

Prof. C.S. Lewangamage,

Professor,

Department of Civil Engineering,

University of Moratuwa.

Signature of the Supervisor: Date: 18.06.2025

Dr. A.U. Weerasuriya,

Senior Lecturer,

Department of Construction and Quality Management,

The Hong Kong Metropolitan University,

Hong Kong

Signature of the Supervisor: Date: 17.06.2025

Dr. P.L.N. Fernando,

Senior Lecturer,

Department of Civil Engineering,

University of Moratuwa.

DEDICATION

I would like to dedicate this thesis to the professional engineers in Sri Lanka, who endeavor to make sure safety, and disaster resilience in both new and existing built environments, benefiting the general public of Sri Lanka.

ACKNOWLEDGEMENT

I express my deepest gratitude to my supervisor, Prof. M.T.R. Jayasinghe, Senior Professor, Department of Civil Engineering, University of Moratuwa, Sri Lanka, for granting me an incredible opportunity to conduct a research study in collaboration with the National Building Research Organization, Sri Lanka. He provided directions to initiate this research study and advice throughout the research study with constructive feedback during each milestone of the research study. His invaluable research vision made my research experience very effective in forming a strong foundation for my future professional career.

I sincerely thank my supervisor, Prof. C.S. Lewangamage, Professor, Department of Civil Engineering, University of Moratuwa, for providing directions during the critical stages of this research study as well as for providing valuable feedback during the milestones of the research study.

I gratefully acknowledge my supervisor, Dr. A.U. Weerasuriya, Senior Lecturer, Department of Construction and Quality Management, The Hong Kong Metropolitan University, Hong Kong, for his precious contribution to this research study through his invaluable guidance, encouragement, methodological advice, and critical feedback. His kind assistance has been incredibly helpful in shaping this research study with continuous progress throughout this research study, successfully attending to each milestone of this research study, effectively communicating research findings, and completing this research study on time. His research expertise and knowledge shared through a series of scholarly interactions and critical technical discussions greatly contributed to enhancing the research quality as well as my analytical thinking, research interests, communication skills, and professional growth. I am also thankful for his assistance in accessing important literature and permitting me to utilize remote computer facilities. I am genuinely appreciative of the valuable time he dedicated to supervising my research study, correcting and proofreading my research papers, presentations, and thesis for communicating the research findings in the best manner. His constant support and patience were instrumental in guiding this research in the right direction from its beginning to the end.

I express my sincere gratitude to my supervisor, Dr. P.L.N. Fernando, Senior Lecturer, Department of Civil Engineering, University of Moratuwa, for sharing research ideas, directions and providing feedback during the milestones of this research study.

I also extend my gratitude to the Department of Civil Engineering, University of Moratuwa, for offering this valuable opportunity to pursue a Master of Science degree with a major component of research.

I sincerely appreciate, Dr. Gobirahavan Rajeswaran, Senior Lecturer, Department of Civil and Environmental Engineering, University of Ruhuna, Sri Lanka, for supporting me in conducting nonlinear analyses in this study, accessing key literature, and providing positive feedback on the research progress. I am also grateful to Prof. Priyan Dias, Emeritus Professor, Department of Civil Engineering, University of Moratuwa, for helping me to access research data and refine the research methods. My thanks also go to Dr. Isuru Nanayakkara, Department of Civil and Structural Engineering, University of Sheffield, United Kingdom, for his directions in shaping the research methodology.

I acknowledge with gratitude, Eng. (Dr.) Asiri Karunawardena, Director General, National Building Research Organization, for granting me this tremendous research opportunity and providing the necessary facilities to conduct this research study in collaboration with the National Building Research Organization (NBRO). I am genuinely appreciative of positive feedback and suggestions for improvements given to me during the milestones of this research study. I sincerely appreciate his recognition of my abilities and his encouragement to be involved in several key projects related to my research study. These opportunities I received throughout this research journey made me confident in facing new challenges at work. I truly appreciate all these opportunities, which laid a good start and a strong foundation for my professional career and made me confident in communicating research findings to technical audiences.

I extend my sincere gratitude to Eng. (Ms.) K.M.D.N.K. Kahahengoda, Director, Structural Engineering Research and Project Management Division, NBRO, and its Engineering Staff; Eng. (Ms.) Ajantha Basnayake, Eng. (Ms.) Raneesha Gunathunga, Eng. Isuru Ramawickrama, Eng. Rakhitha Amarathunga, Eng. (Ms.) Nelum Perera, Eng. Dilantha Gunathunga, Eng. Tharuka Lakshan, Eng. (Ms.) Sathya Bandaranayake, and Eng. K. Raakulan for their constant support and motivation in completing this research study. I am thankful for the shared knowledge on civil engineering projects, and for creating a collegial and supportive workplace environment of learning and creativity, which provided an excellent opportunity to be involved in both research and official project works, broadening my research and learning experience. I am also grateful for the financial assistance provided by the NBRO, throughout my research studies.

I am also grateful to my friends who contributed ideas and perspectives that enriched this research study.

Last but not least, I am deeply thankful for my parents and my brother for their endless support, constant encouragement, patience, and understanding throughout this research journey.

ABSTRACT

Sri Lanka has prioritized designing disaster-resilient buildings and evaluating the degree of disaster-resilience of the existing buildings due to the challenges posed by natural and man-made hazards. This approach challenges the common practice of the Sri Lankan construction industry to use British Standards as its industrial standards. Since the British Standards had been replaced by Eurocodes, Sri Lanka has started using Eurocodes but without critically evaluating the effectiveness of Eurocodes and national annexes in designing buildings with disaster resilience features. Therefore, it is crucial to evaluate the structural vulnerability of buildings to gravity, wind, and seismic loads. To fulfill these timely needs, this study envisages to examine the effectiveness of Eurocodes and national annexes to design disaster-resilient buildings in Sri Lanka, assessing the degree of disaster resilience of the existing buildings, and examining cost implications. To this end, this study put forwards a novel framework to evaluate the structural resilience of code-compliant and non-code-compliant reinforced concrete buildings under extreme wind and seismic loads. The framework constitutes non-linear static pushover analysis for wind assessments, non-linear dynamic time-history analysis, incremental dynamic analysis, and fragility assessments for seismic evaluations. The framework was first applied to a typical office building before assessing a three-story school building, an eight-story university building, and a six-story hospital building, designed according to Eurocodes (EN1990. (2005), EN 1991-1-1. (2002), EN 1991-1-4. (2010), EN 1992-1-1. (2004), EN 1998-1. (2013)) and Sri Lankan national annexes, as well as a seven-story mixed-use defective building and its retrofitted version. The results showed that the Eurocode-based building designs have a significantly larger base shear capacity than the base shear force triggered by a wind with a 1700-year return period, the highest return period considered for the wind performance evaluation. Although these buildings have reasonable structural resilience against extreme seismic loading, they do not meet the more stringent performance requirements, such as Fully Operational and Operational, in the seismic performance objectives. Therefore, Eurocode-based designs can sometimes fail to meet the performance objectives for structural resilience, even though these objectives are assumed to be implicitly satisfied by the design codes and standards. The analysis of the defective building confirmed the building's inadequate capacity to carry gravity, wind, and seismic loads. The retrofitted building with structural jacketing had enhanced load carrying capacities, indicating the effectiveness of structural jacketing as a retrofitting measure for defective buildings in Sri Lanka. The comparison of material properties, partial safety factors, load combinations, and design methodologies of Eurocodes and British Standards for designing beams and columns revealed that British Standards generally require more reinforcement for a given section size, mainly due to more conservative partial safety factors in load combinations. However, the differences in section sizes and reinforcement requirements strongly depend on the building type and loading conditions, such as gravity loading alone or a combination of gravity and lateral loading.

Keywords: Eurocodes, Buildings, Disaster resilience, Wind loading, Seismic loading

TABLE OF CONTENTS

LIST OF FIGURES

Figure **Description** **Page**

LIST OF TABLES

Table **Description** **Page**

LIST OF ABBREVIATIONS

Abbreviation	Description
AEL	Annual Expected Loss
ASCE	American Society of Civil Engineers
ATC	Applied Technology Council
BSI	British Standards Institution
BSSC	Building Seismic Safety Council
CIDA	Construction Industry Development Authority
COV	Coefficient of Variation
CPT	Cone Penetration Test
CTBUH	Council on Tall Buildings and Urban Habitat
DDI	Deformation Damage Index
DM	Damage Measure
DOL	Duration of Load
DV	Decision Variable
EC	Eurocode
EDP	Engineering Demand Parameter
EN	Euro Norms
EU	European Union
FEMA	Federal Emergency Management Agency
FO	Fully Operational
FPHLM	Florida Public Hurricane Loss Model
GDP	Gross Domestic Product
IBC	International Building Code
IDA	Incremental Dynamic Analysis
IM	Intensity Measure
ISO	International Organization for Standardization
LRFD	Load and Resistance Factor Design
LS	Life Safe
MEP	Mechanical, Electrical, Plumbing

MRI	Mean Recurrence Interval
MWFRS	Main Wind Force Resisting System
NBRO	National Building Research Organization
NC	Near Collapse
NDTHA	Non-linear Dynamic Time-History Analysis
NEHRP	National Earthquake Hazards Reduction Program
NSPA	Non-linear Static Pushover Analysis
O	Operational
OMRF	Ordinary Moment Resisting Frame
PBD	Performance-Based Design
PBEE	Performance-Based Earthquake Engineering
PBWE	Performance-Based Wind Engineering
PEER	Pacific Earthquake Engineering Research
QST	Quenched and Self-Tempered
RB	Reinforcement Bar
RC	Reinforced Concrete
RMS	Root of Mean Squares
SDOF	Single Degree of Freedom
SEAOC	Structural Engineers Association of California
SL	Sri Lankan
SMRF	Special Moment Resisting Frame
SPT	Standard Penetration Test
UBC	Uniform Building Code
UDA	Urban Development Authority
UK	United Kingdom
UNDRR	United Nations Office for Disaster Risk Reduction
UNISDR	United Nations International Strategy for Disaster Reduction
US	United States Dollar

LIST OF APPENDICES

Appendix **Description** **Page**

CHAPTER 1 : INTRODUCTION

1.1. General

During their lifetime, buildings encounter various hazards, such as earthquakes, volcanoes, glaciers, tsunamis, floods, windstorms, and fire (Anwar & Ahmed, 2021). Sri Lanka experiences some of these natural hazards, most often floods, droughts, landslides, and storms (World Bank Climate Change Knowledge Portal). However, seismic activities are less common in Sri Lanka. Figure 1.1 shows the average annual incidence of natural hazards in Sri Lanka from 1980 to 2020.

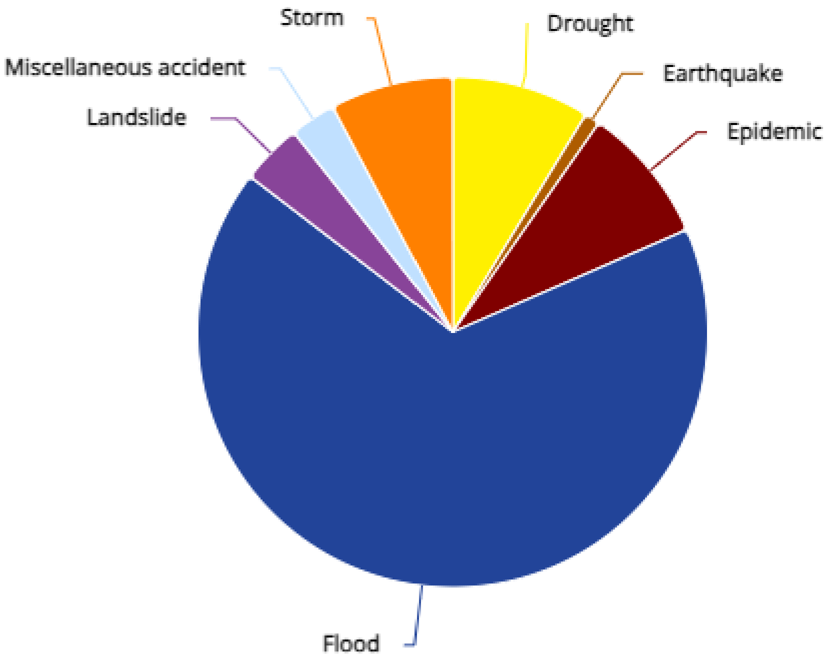

Figure 1.1: Average annual natural hazard occurrence between 1980 – 2020 (World Bank Climate Change Knowledge Portal)

As illustrated in Figure 1.1, Sri Lanka's hazard risk profile is featured by a mix of frequent, low-impact incidents and some occasional high-impact, large-loss incidents. Floods are more common, with a relatively low impact, than other catastrophic events. Cyclones and earthquakes. Although less frequent, cyclones and earthquakes typically result in severe consequences when they occur (World Bank Group, 2016).

Natural disasters impose financial burdens on nations, stemming from various consequences, such as casualties, infrastructure damage, recovery costs, downtime, and more. However, with strategic mitigation efforts, these burdens can be reduced. The World Bank conducted a preliminary analysis of the direct and indirect impacts on physical and property damage caused by previous disasters. These losses encompass expenses related to relief assistance and the reconstruction of housing and roads. Over an extended period, the average annual combined losses in these sectors due to natural disasters are estimated to be SL Rs 50 billion. This sector-specific Annual Expected Loss (AEL) constitutes 0.50% of Sri Lanka's Gross Domestic Product (GDP) and represents 3% of the government's total expenditure (World Bank Group, 2016). These natural disasters' frequency and intensity, driven by climate change, are expected to elevate these estimated values further, but with proactive measures, these impacts can be mitigated.

To guarantee a disaster-resilient built environment, it's crucial to understand the difference between disasters and hazards. The United Nations Office for Disaster Risk Reduction (UNDRR) defines a disaster as a significant disruption to the functioning of a community or society, arising from the interaction between hazardous events and factors like exposure, vulnerability, and capacity. This disruption results in various types of losses and consequences, including those affecting people, resources, economies, and the environment (Disaster | UNDRR, 2007). Hence, disaster is defined by three key components: hazard, exposure, and vulnerability, as shown in Eq. (1) below.

$$\text{Disaster} = \text{Hazard} \times \text{Exposure} \times \text{Vulnerability} \qquad [1]$$

A hazard is a natural or man-made event; exposure encompasses anything of value that is exposed to that hazard, and vulnerability accounts for the weak points in structures being hit by the event. Therefore, a disaster with a high risk, vulnerability, and exposure is deemed severe. Hazards are uncontrollable, but exposure can be controlled by proper land use planning (e.g., selecting low-hazard-prone areas). Crucially, the responsibility of maintaining the vulnerability of structures to hazards lies within the scope of the structural design engineers. Therefore, the structures will remain safe from disasters if the vulnerability is low (Anwar & Ahmed, 2021).

To minimize the risk of disasters, it is crucial to accurately evaluate potential hazards and implement measures to decrease exposure and vulnerability. The strategies for reducing exposure and vulnerability can be categorized into two types: structural, focusing on designing infrastructure to reduce the chances of failure, and non-structural, prioritizing public education and policy development. Since Sri Lanka is exposed to numerous hazards and has high exposure and vulnerability, it is imperative to prioritize the disaster resilience of structures in Sri Lanka. Of the natural hazards depicted in Figure 1, floods, storms, landslides, earthquakes, and tsunamis pose significant threats to the built environment.

In 2021, Tavares & Krausmann (2021) investigated methods for mitigating disaster risk in their work titled "Impacts of Natural Hazards and Climate Change on EU Security and Defense." The suggested structural measures for each disaster are detailed as follows. Structural measures for mitigating the flood/tsunami disaster include constructing flood defenses, enhancing drainage systems, and river engineering measures. Elevating buildings to at least one meter above the base flood level is critical, especially for mission-critical facilities. Establishing flood shelters for rapid access to higher floors or roofs enhances emergency response capabilities. Deploying debris barriers, flood-proofing existing structures with appropriate building materials, and scour protection strengthens buildings against flood forces. Moreover, improving corrosion resistance and incorporating protective coatings and inhibitors on building elements prolong the life of critical assets exposed to floodwaters (Tavares & Krausmann, 2021). Mitigating landslide risks requires a comprehensive approach to slope stability and terrain management. These structural approaches enhance community resilience to landslide hazards, safeguarding buildings and inhabitants in vulnerable regions (Tavares & Krausmann, 2021).

Implementing structural measures to enhance resilience against wind hazards necessitates a comprehensive approach to building design. Hurricane shelter design, construction, and maintenance play a vital role in providing safe havens for individuals during severe windstorms. Debris barriers help mitigate the risk of flying objects causing damage. Another critical strategy is constructing buildings with impact-resistant materials to withstand the forces exerted by high wind loads. Careful orientation of buildings minimizes exposure to likely wind directions, reducing vulnerability. Ensuring the secure attachment of building roofs to foundations is crucial for preventing potential lift-offs during intense wind events. (Tavares & Krausmann, 2021). Ensuring earthquake resilience, too, involves a comprehensive approach to building design. Seismic design and earthquake-resistant construction techniques are essential for structural protection (Tavares & Krausmann, 2021).

The measures above for reducing the risk of disasters suggest that taking actions such as planning land use properly before construction and building well-designed defenses/debris barriers can significantly reduce the exposure of constructed areas to natural hazards like floods/tsunamis and landslides with less emphasis on the buildings themselves. These steps can effectively minimize the impact of frequent but less severe events such as floods and landslides. Consequently, in many cases, disasters caused by these hazards, such as floods and landslides, don't necessarily need specific building design codes and standards for mitigation. Unlike floods and landslides, cyclones and earthquakes occur less frequently but pose a higher risk when they do occur. While effective land use planning is crucial to lessening the exposure to hazards, the design of buildings also plays a vital role in minimizing the effects of cyclones and earthquakes on buildings, thereby reducing vulnerability. Therefore, this research study concentrates on the design aspects linked with the built environment, explicitly addressing the disaster resilience in buildings against cyclonic and seismic hazards - two types of natural disasters that happen less often in Sri Lanka but carry significant severity when they occur.

Nissanka et al. (2020) reviewed the current status of building codes for improving the disaster resilience of Sri Lankan built environments. Accordingly, building codes that set forth the minimum construction standards are influential in guaranteeing the safety of buildings during natural hazards. Their research states that the probable damage to human lives and property could be minimized by incorporating probable risks from natural disasters and their consequences into building codes. Moreover, their research revealed that the studies on Sri Lankan building codes are still in the initial stage. However, several studies have been undertaken to showcase how disaster-resilient built environments are created. Their research is particularly significant as it sheds light on the existing need for understanding how these codes should be more widely adopted to enable disaster resilience; hence, it forms a critical foundation for the present study, which aims to build upon examining the degree of disaster resilience of code-based building designs and vulnerability of non-code-based buildings or the defective buildings concerning wind and seismic hazard. These code-based building designs are the building designs that strictly follow the provisions, procedures, and limitations outlined in national or international building design codes and standards, such as the Eurocodes or BS Standards. These buildings are assumed to follow established engineering principles, ensuring structural safety and compliance with regulatory frameworks. In contrast, non-code-based building designs refer to existing structures that exhibit defects primarily due to non-compliance with formal design and construction codes. These buildings may have been constructed without adherence to systematic engineering design, oversight, or enforcement mechanisms, often relying on informal practices. In the context of this study, such non-code-based buildings represent cases where code violations or the absence of proper design documentation have led to structural deficiencies or vulnerabilities.

Sri Lanka has prioritized designing disaster-resilient buildings because relentless climate change increases the frequency and intensity of cyclones, and the continuous tectonic plate movements impose a significant threat of disastrous earthquakes – two natural disasters likely to occur in Sri Lanka. Given the challenges posed by natural disasters and the susceptibility of the built environment to disasters, establishing a unified multidisciplinary national building code for Sri Lanka has been recognized as a priority to ensure a safer and disaster-resilient built environment in the country. Therefore, the National Building Research Organization (NBRO), the Construction Industry Development Authority (CIDA), and the Urban Development Authority (UDA) lead the building code establishment, with input from relevant stakeholders. Adopting a unified, multi-disciplinary building code will bring substantial changes for stakeholders. For example, there is significant international investment in construction, which requires flexibility in the compliance pathway. Hence, determining the compliance approach in the code is crucial for its successful adaptation throughout the country.

The first option for the compliance pathway is the prescriptive regulations stipulating how a building must be built, including what materials can be used, how they may be used, and what design solutions can be accepted. This is a book of rules that the user can follow to achieve compliance. The second option is to follow performance-based regulations, which define the outcomes required to be achieved by the completed building. They set performance requirements to be met rather than prescriptive requirements that the code user must follow. The performance statements are the mandatory legal requirements of the code, where the designer can choose how the performance criteria are met. The third option is to follow a hybrid compliance regulation where both performance-based and prescriptive requirements are provided, and the conditions under which deviation from the prescribed methods is permitted are included. The recommendation for the structural design section of the Sri Lankan building code should take a hybrid approach (mixed performance and prescriptive) with a clear set of functional statements or requirements for each discipline. This allows for performance-based design if the designer chooses. In addressing each functional requirement, it is essential to provide an acceptable solution with a prescriptive methodology suitable for the most common building typologies. Simultaneously, it is advisable to develop a manual or guideline to provide a pathway for compliance with the performance statements for small-scale housing appropriate for use by a less technical audience, including local builders, artisans, and self-builders. Significantly, this manual should be developed and published in parallel with the code.

The Sri Lankan construction industry mainly adopts British Standards as its industrial standards for designing buildings. Nevertheless, these building design codes and standards follow the prescriptive design approach. As this new building code is to adopt the most fitting from the previously utilized British Standards and the latest Eurocodes as its structural design code, it becomes crucial to examine whether these standards align with the recommendations outlined in the requirements for structural design section of the Sri Lankan building code development process; i.e., the capability of buildings designed using building codes and standards in meeting performance requirements stipulated for disaster resilience.

On the other hand, the British Standards Institution (BSI) ceased updating the British Standards in 2010 and subsequently replaced them with Eurocodes. Eurocodes are preferred over the British Standards because the former allows users to modify some country-specific parameters (e.g., design wind speed, design peak ground acceleration) and adjust minor design guidelines by national annexes. Eurocodes give flexibility to design engineers so they can use Eurocodes with adjustments in any country. Moreover, design engineers can easily communicate ideas with others who use Eurocodes. This flexibility of Eurocodes leverages its broad adoption, starting from Europe and the United Kingdom in 2000 and continuing to later non-European countries, such as Singapore and Malaysia.

Sri Lanka started using Eurocodes as early as 2010 but did not dedicate much effort to fine-tuning country-specific parameters or preparing national annexes. After identifying their importance, Sri Lanka has produced national annexes for many Eurocodes in recent years, largely thanks to the relentless efforts of universities and relevant government institutions. However, to date, neither the accuracy of Eurocodes nor the effectiveness of national annexes has been subjected to critical evaluation. As a result, designers, engineers, and researchers are sometimes reluctant to adopt these national annexes for unique designs such as disaster-resilient buildings. Therefore, there is a timely need to critically evaluate the accuracy and effectiveness of Eurocodes and Sri Lankan annexes for designing disaster-resilient buildings. Disaster-resilient buildings are an ultimate challenge for design codes and standards because these buildings need to stand against extreme external loadings while maintaining acceptable deformation, displacement, and member forces.

On the other hand, almost all the high-rise buildings in Sri Lanka are designed, constructed, and consulted by experts in relevant disciplines. Some of the low-rise and medium-rise buildings in Sri Lanka do not receive the same attention from industrial professionals. As a result, those buildings are poorly designed and constructed. For instance, Cels et al. (2023) conducted an engineering survey on Sri Lankan school buildings exposed to the 2004 Tsunami. Their study revealed plenty of important information regarding school buildings that might make them vulnerable to other disasters, such as cyclones, earthquakes, etc. As per their survey findings, school building designs in Sri Lanka are primarily based on the gravity load design, thus causing consistency in element sizes and detailing. Almost all the surveyed school buildings have been made up of three archetypes. This practice of type plans in the school building construction tends to utilize the same column type, beam type along the shorter direction, beam type along the longer direction, and one slab thickness regardless of the exposure conditions of each school building; thus, no significant difference in the structural arrangement of buildings across the surveyed districts. Moreover, the survey results indicated that most of the school buildings had been provided with gable pitched roofs, supported by truss systems made of steel, timber, or a combination of reinforced concrete and wood, with roof coverings consisting of clay tiles, metal sheets, or asbestos sheets. Hence, many school buildings in Sri Lanka have been noted as posing a potential threat despite their categorization under a higher importance class due to their pivotal role in shaping the country’s future.

Such practice hinders Sri Lanka's priority to design disaster-resilient buildings to withstand severe and frequent natural disasters triggered by future climate change. Moreover, as the World Bank estimated, Sri Lanka incurs $380 million in average losses yearly due to natural disasters (World Bank Group, 2016). Therefore, Sri Lanka faces a significant challenge in evaluating the susceptibility of the existing structures to natural disasters and providing strategies to reduce the vulnerability. The existing buildings have not been subjected to critical performance evaluations under gravity, wind, and seismic loadings to benchmark the structural vulnerability according to well-accepted criteria.

Therefore, this study's scope considers both code-compliant and non-code-compliant high-importance low-rise buildings made of reinforced concrete to evaluate their performance requirements to achieve disaster resilience and the cost implications of adhering to the previously used British Standards as well as the latest Eurocodes.

1.2. Research Problem

Sri Lanka currently lacks a comprehensive legal mandate to regulate the construction industry. As a result, a significant proportion of low- to medium-rise buildings, particularly in urban areas such as Colombo, exhibit notable design and construction deficiencies. In many instances, buildings are constructed without adherence to design codes and standards; structural designs are altered without proper approval, safety measures are compromised, and additional floors are added without adequate structural assessment. These practices significantly undermine the structural integrity of buildings, thereby placing occupants at serious risk. Notable incidents such as the Buwelikada and Wellawatta building collapses serve as dark reminders of the consequences of non-compliance with design codes and standards. In contrast, high-rise developments typically receive greater attention from qualified professionals. This disparity in construction quality renders a large portion of the built environment highly vulnerable to both natural and man-made hazards.

Exacerbating this issue is the increasing frequency and intensity of climate-induced hazards, such as cyclones, and the seismic activity associated with tectonic plate movements. In response to these risks, Sri Lanka has prioritized the design and construction of disaster-resilient buildings. However, achieving such resilience presents a significant challenge for the country's current building design codes and standards, which must ensure that buildings maintain structural performance during and after extreme events.

At present, Sri Lanka predominantly relies on outdated British Codes and Standards and occasionally on Eurocodes and Sri Lankan National Annexes. The latest generation of Eurocodes has not yet been critically evaluated for their applicability and effectiveness in ensuring disaster resilience within Sri Lanka's specific context. This lack of evaluation creates uncertainty regarding their relevance and adaptability to the country's unique hazard profile and construction practices.

In response to these challenges, Sri Lanka has recently initiated the development of a National Building Code, which will include two key chapters: Structures and Existing Structures. These sections are expected to play a vital role in promoting the resilience of both new constructions and the existing building stock. However, a significant limitation lies in the absence of a validated framework for assessing the disaster resilience of code-compliant and non-code-compliant buildings. Similarly, there is a critical need to identify and recommend effective retrofitting strategies that can be integrated into the Existing Structures chapter to enhance the safety and performance of vulnerable buildings.

Therefore, there is a demanding need for research that develops a robust framework for resilience assessment of code-compliant and non-code-compliant buildings, evaluates the implications of adopting Eurocodes for designing disaster-resilient buildings in Sri Lanka, evaluates the vulnerability of existing buildings in Sri Lanka, and proposes effective retrofitting strategies for existing structures.

1.3. Aims and Objectives

The proposed study aims to investigate the effectiveness of Eurocodes and the Sri Lankan annexes for designing disaster-resilient buildings in Sri Lanka.

The present study envisages providing the following deliverables:

1) Vivid explanations for the differences in the approaches, parameters, and provisions in the previous British Standards and the latest Eurocodes.
2) Demonstrate the accurate use of Eurocodes and the Sri Lankan national annexes for designing disaster-resilient buildings against wind and earthquake loading.
3) Guide further development of Sri Lankan annexes to comply with Eurocodes and national annexes of other countries with similar conditions.

To accomplish the goals outlined above, the present study sets the following objectives:

1) Identify the differences in wind and earthquake loads estimated using British Standards and Eurocodes by conducting an in-depth analysis of their approaches, provisions, and design parameters.
2) Perform a comprehensive literature survey to compare the values and use of similar design parameters in British Standards, Eurocodes, Sri Lankan national

annexes, and national annexes of countries with geographical and climate conditions similar to Sri Lanka.

3) Evaluate the ultimate and serviceability limit state performance of several disaster-resilient buildings designed according to the British Standards and Eurocodes using state-of-the-art finite element modeling.
4) Develop guidelines for accurately using Eurocodes and Sri Lankan national annexes for designing disaster-resilient buildings in Sri Lanka and further improving Sri Lankan national annexes.

1.4. Methodology

The present study outlines the following methodological approach to achieving each of the objectives above:

1) Conducting a comprehensive literature review to understand the latest findings of designing disaster-resilient buildings and how British Standards and Eurocodes include disaster-resilient features in their design approaches.
2) Creating state-of-the-art finite element models for several ordinary buildings with disaster-resilient features to evaluate their ultimate and serviceability limit state performance and testing for extreme wind and earthquake loads. These building designs include various architectural features (roof shapes, openings, structural components).
3) Analyzing design approaches, parameters, and provisions in British Standards and Eurocodes to estimate the influence on the effectiveness of their provisions for disaster resilience, ultimate and serviceability limit state performance, and the overall construction and operational cost of several typical buildings.
4) Preparing a set of guidelines based on the study's findings to leverage the accurate use of Eurocodes and Sri Lankan national annexes for designing disaster-resilient buildings in Sri Lanka and for further development of Sri Lankan national annexes for Eurocodes.

1.5. Significance of the Research

This research is significant as Sri Lanka moves toward developing a Unified Multidisciplinary National Building Code, with the principal goal of enhancing the resilience of its built environment. By examining the implications of adopting Eurocodes for designing disaster-resilient buildings within the Sri Lankan context, this study offers timely and relevant insights into how internationally recognized best practices can be effectively adapted for local application.

In terms of its specific contributions, the research supports national efforts in several meaningful ways. First, it introduces a systematic evaluation framework for assessing both the degree of disaster resilience in code-compliant buildings and the vulnerability of the existing building stock. This is especially valid as the forthcoming National Building Code is expected to include dedicated chapters on Structures and Existing Structures, requiring robust tools for assessment and decision-making.

Second, the study provides a focused evaluation of the level of disaster resilience inherent in Eurocode-compliant building designs and vulnerability in existing buildings. This is of particular relevance given Sri Lanka’s increased exposure to climate-induced hazards and underlying seismic risks. Gaining a deeper understanding of the performance of Eurocodes under such conditions will support informed decisions regarding their applicability and any necessary local adaptations. These insights are essential for bridging the gap between global design standards and Sri Lanka’s unique environmental and construction conditions.

In addition, the research addresses a critical gap in current practice by identifying effective retrofitting strategies for the country’s vulnerable existing buildings. This is particularly important for low- to medium-rise structures, which often receive limited attention from industry professionals yet represent a significant portion of the built environment at risk.

More broadly, the study contributes to capacity building within Sri Lanka’s engineering and regulatory sectors. It provides a valuable knowledge base for policymakers, practitioners, and academics, thereby supporting efforts to align the country's construction practices with international resilience objectives.

In essence, this research not only informs the development of national policy but also contributes meaningfully to the long-term resilience of Sri Lanka’s built environment. This outcome is increasingly critical in the face of growing natural and man-made hazards.

1.6. Arrangement of the report

Chapter 1 of the thesis provides an in-depth exploration of the study's background and introduction, encompassing Sri Lanka's disaster risk profile, common practices in building design and construction, and the identified deficiencies of disaster resilience in built environments. Furthermore, it outlines the research problem, presents the aims and objectives of the study, states the methodological approach adopted for the study, and highlights the significance of the research.

Chapter 2 provides an extensive literature review focusing on the historical occurrences of cyclones and earthquakes and the effectiveness of various design approaches, including code-based, performance-based, and resilience-based designs, in mitigating their impacts. Additionally, it offers detailed descriptions of various initiatives, frameworks, and methodologies previously employed to evaluate the level of disaster resilience exhibited by code-based building designs from a global perspective.

Chapter 3 provides a literature review-based analysis to provide guidelines for designing and constructing buildings' substructures to resist extreme lateral loading conditions.

Chapters 4, 5, 6, and 7 provide the methodological approach adopted in the proposed framework for evaluating the degree of disaster resilience of code-compliant buildings, along with the analysis conducted on a typical Eurocode-based building and four additional Eurocode-based case study buildings. These chapters tailor the proposed framework for evaluating the disaster resilience of code-based building designs to accommodate non-code-compliant buildings. Also, this chapter employs this modified framework to evaluate the degree of disaster resilience of a defective building and subsequently evaluate the performance enhancement achieved through retrofit measures applied to the considered defective building.

Chapter 8 provides the cost implications for designing buildings per the previously used British Standards and the latest Eurocodes.

Chapter 9 encompasses conclusions from the current study, recommendations, and future research endeavors.

CHAPTER 2 : LITERATURE REVIEW

2.1. General

Assessing the level of disaster resilience in buildings in Sri Lanka concerning wind and earthquake loading necessitates a comprehensive understanding of Sri Lanka's hazard risk profile regarding wind and earthquake aspects, historical occurrences of such hazards, implemented building design codes and standards within the country, and internationally recognized engineering practices for evaluating the disaster resilience of code-based building designs. Therefore, this chapter critically examines Sri Lanka's vulnerability to wind and earthquake hazards alongside the knowledge of disaster resilience locally and globally.

2.2. Wind and earthquake disaster profile in Sri Lanka

2.2.1. Documented wind disasters in Sri Lanka’s history

Sri Lanka, an island country in South Asia, is located in the Indian Ocean southwest of the Bay of Bengal. It delineates its boundary with the Indian subcontinent by the Gulf of Mannar and the Palk Strait. Despite the strategic advantage of its location in the Indian Ocean, the natural geography poses a disadvantage for Sri Lanka. For instance, the Bay of Bengal is considered a region with intense wind events on Earth. One of the cyclonic paths falls close to the island's northern and northeastern parts. Consequently, the country is susceptible to extremely destructive wind events during the North Indian cyclone and monsoon seasons each year.

Of the previous cyclones that affected Sri Lanka from 1900 to 2000, the one in 1978 was the strongest and most devastating of the century. A maximum northerly wind speed of 145 km/h (cyclone events 1900-2000) was recorded during this cyclone. According to the satellite estimates and as reported in the satellite disturbance summary of Washington, the maximum wind speeds were 222 km/h and 206 km/h, respectively (cyclone events from 1900 to 2000). The cyclone in 1978 is, therefore, documented as the most severe cyclone to affect Sri Lanka in the previous century, leading to significant losses and damages in the Northern and Eastern areas of the country. This massive cyclone led to the blowing off of nearly 50% of the roofs of buildings along its path and caused significant losses to paddy cultivation and coconut tree plantations.

Subsequently, the 2000 cyclone was recorded as the strongest tropical cyclone to strike Sri Lanka since 1978. It attained a peak wind speed of 120 km/h, impacting the country's eastern region at its maximum strength. It eventually dissipated over southern India by slightly weakening while crossing the island.

Strong winds and gales occur more frequently than cyclones in many parts of Sri Lanka yearly. While fatalities due to gales or strong winds are rare, property damage is more common.

Therefore, Sri Lankan history has documented many cyclones, strong winds, and gales, resulting in extensive damage across the country. This stresses the importance of addressing the impact of wind events in the context of disaster resilience.

2.2.2. Documented earthquake disasters in Sri Lanka's history

Sri Lanka is in the North Western region of the Indo-Australian tectonic plate, distant from its plate boundaries. Despite the natural geographical location of Sri Lanka minimizing its susceptibility to earthquakes, the country has recorded several significant earthquake events in its history, in addition to the minor tremors experienced over the country.

The first recorded account of an earthquake impacting Sri Lanka is revealed in a pamphlet published in Lisbon in 1616, describing an event that occurred near Colombo on 14th April 1615 (N. Seneviratne et al., 2020). This event resulted in 2000 casualties and 200 building collapses. It is written in Sri Lankan history as the most significant earthquake ever. Since then, there have not been similarly large-scale earthquakes. Although no casualties or significant damage were recorded, the 1938 and 1940 earthquakes affected many parts of the island.

The catalog of past earthquakes that have impacted Sri Lanka indicates that it cannot be regarded as a seismic-free area. Consequently, earthquake hazards should be considered in the design of structures and incorporated into assessing their degree of disaster resilience.

2.3. Sri Lankan practice of designing buildings to resist wind and earthquake hazards

2.3.1. Codes for designing buildings in Sri Lanka

The Sri Lankan construction industry adopts British Standards as its industrial standards for building design. British Standards are the structural design codes implemented by the British Standards Institution (BSI), and have been adopted by other countries.

However, the British Standards Institution (BSI) ceased updating the British Standards in 2010. It declared the implementation of a set of new British Standards (BSs) for structural design, derived from European Standards commonly referred to as Eurocodes, and the associated withdrawal of conflicting BS design standards.

Therefore, in the UK, the British Standards Institution (BSI) has adopted the Eurocode (EN) Standards as British Standards (BS ENs).

British Standards Institution (BSI) has also published the corresponding national annexes for use with the BS ENs. These national annexes furnish details about nationally determined parameters utilized in designing buildings and civil engineering projects within the country in question. These encompass specific national safety criteria, geographical and climatic conditions, and procedural guidelines.

The flexibility of structural Eurocodes enables their adoption not only in Europe but also on a global scale. Several countries outside Europe have recognized this feature, and many have already committed to adopting Eurocodes. As a result, Eurocodes are considered to be the leading structural codes.

Sri Lanka, too, started using Eurocodes as early as 2010 but did not dedicate much effort to fine-tuning country-specific parameters or preparing national annexes. After identifying their importance, Sri Lanka has produced national annexes for many Eurocodes in recent years, largely thanks to the relentless efforts of universities and relevant government institutions. However, Sri Lanka predominantly adheres to British Standards, with only occasional adoption of Eurocodes.

In addition to the codes for design structures in Sri Lanka, the construction industry is paying growing attention to wind and seismic engineering practices. This heightened focus is driven by the country's significant impact of wind and seismic forces, prompting ongoing development and progress in these domains.

2.3.2. Evolution of wind engineering practices in the Sri Lankan context

Special safety measures for resisting cyclones have not been considered in ancient building designs in Sri Lanka due to the infrequent occurrence of cyclones. The 1978 cyclone, the most robust and most devastating cyclone to strike Sri Lanka, resulted in significant failures in buildings along its cyclonic path. These damages highlighted the application of low-wind-resistant building technologies, low-quality building materials, and poor artistry as inadequacies in Sri Lankan building designs, thus informing the necessity of considering wind loading in the building design practice.

To fulfill the first step of the program initiated by the Government of Sri Lanka for developing an appropriate methodology for estimating wind loads, the Government of Australia directed a crew of specialists to work cooperatively with a team of consultants led by the United Nations Development Program and the officers from the Building Department, Sri Lanka. These efforts focused on two significant areas: proposing wind zones and wind speeds for Sri Lanka and an improved technology for designing and constructing buildings to suit high wind situations. Due to this initiative, Sri Lanka has been divided into three wind zones, and the wind speeds have been proposed separately for typical and post-disaster structures. A design manual, "Design of Buildings for High Winds – Sri Lanka," had also been formulated to address the construction of low-rise buildings and their structural integrity.

As reported in the history of wind engineering in Sri Lanka, the "Design Buildings for High Winds – Sri Lanka" manual had been the sole compulsory guide on wind engineering in the country. At the same time, CP3 was the most common exercise for estimating wind forces on buildings. Nevertheless, over time, there has been a trend towards adopting international wind codes like British Standards (BS 6399-:1997), Australian Standards (AS 1170-2: 1989), Australian / New Zealand Standards (AS/NZS 1170-2: 2002), etc. due to the restricted application of the design manual and CP3 for the low to high rise buildings rising in the urban zones in the country. Further, the Sri Lanka Standards Institution (SLSI) has decided to use Eurocodes (EN 1991-1-4:2005) along with the Sri Lankan national annex to evaluate wind loading on buildings as practical from the withdrawal of British Standards in 2010.

Hence, alongside the primary building design codes and standards (British Standards and Eurocodes), design engineers in Sri Lanka employ wind loading standards like the "Design of Buildings for High Winds – Sri Lanka" manual, along with a range of international standards such as British Standard, Eurocode with Sri Lankan national annex, Australian Standard, and Australian/New Zealand Standard, to address the design of buildings vulnerable to wind loading.

2.3.3. Evolution of earthquake engineering practices in the Sri Lankan context

Over the past years, some investigations have been conducted in Sri Lanka to explore the domain of earthquake engineering. Despite the limited data available in Sri Lanka, these research studies have provided valuable insights to improve the field.

Herath et al. (2017) study is mainly concerned with the geological setting of Sri Lanka. Their remarkable study highlights the Mannar rift zone and Comorin ridge, a failed rift basin formed due to the crustal thinning associated with continental rifting before or during the Gondwana breakup.

In 2020, H. N. Seneviratne et al. extensively investigated the seismic behavior around the country and its engineering considerations. The research utilized historical records, a suite of over 300 earthquakes near Sri Lanka, for the investigation. Their study uncovered that the 1615 earthquake was the most significant earthquake to strike Sri Lanka. H. N. Seneviratne, et al.'s research, is particularly noteworthy as it also reveals the Mannar rift zone and Comorin ridge as the crucial areas capable of producing a seismic event with a magnitude of 6.9, occurring at a depth of 10 – 15 km underneath the sea level and exhibiting a return period of 475 years. Therefore, this study serves as a crucial groundwork for the current research. It seeks to utilize its findings to decide on the earthquake ground motion parameters representative of the local context.

In 2020, N. Seneviratne et al. undertook a comprehensive study to identify the seismicity of Sri Lanka and present a macro seismic hazard zonation for Sri Lanka. Their study also uncovered that the main seismic threat to Sri Lanka is oceanic earthquakes at the failed Mannar rift zone and Comorin ridge. This research estimates that the magnitude of the 1615 earthquake amounts to 6.5, with the epicenter close to Colombo, considering the extent of the damage caused. Therefore, N. Seneviratne et al.'s work is a pivotal base for the current study to gain insight into the potential earthquake occurrences in Sri Lanka.

Kularathna et al. (2013) focused on preparing national guidelines for seismic analysis and designing buildings in the country. Since "Earthquake Resistant Detailing for Buildings in Sri Lanka" issued by the Society of Structural Engineers, Sri Lanka is the only available document in Sri Lanka for designing buildings to withstand earthquake loading, their research study envisaged to guide analyzing and designing buildings for seismic loading. There, national guidelines have been put forward to practice along with the Eurocode 8 (EN 1998-1: 2004) "Design of Structures for Earthquake Resistance" until Sri Lanka produces its national annex for Eurocode 8, which is currently in its early stages of preparation.

In addition to the manual "Earthquake Resistant Detailing for Buildings in Sri Lanka," design engineers in Sri Lanka also incorporate international earthquake codes such as Eurocode (EN 1998-1:2004) with national guidelines, Australian Standard (AS 1170.4-2007), Australian/New Zealand Standard (AS/NZS 1170.0: 2002), and others. These are used alongside the primary building design codes and standards (British Standards and Eurocodes) to address the design of buildings susceptible to earthquake loading.

2.4. The necessity of disaster resilience

Most older buildings can withstand natural disasters due to conventional construction techniques and conservatism in the design and construction. In contrast, contemporary structures might face risk from extreme events since they are being built in a construction age where the design optimizations are accommodated in the building designs while adhering to exceptional architectural requirements (Brett & Lu, 2013). For instance, taller and larger structures are being built despite the increasing construction pace and the developing conditions. Therefore, the disastrous collapses of buildings and infrastructure schemes occur due to natural and artificial extreme events triggered by climatic change and general societal changes, such as design optimization and sustainability (Stochino et al., 2019). This increases attention on the robustness concepts among structural engineering research and design communities (Brett & Lu, 2013).

The robustness of structures gained attention over time due to extreme events and the failure of structures. The Ronan Point gas explosion that occurred in London in 1968 is one such occurrence that added depth to understanding the importance of robustness (Stochino et al., 2019). An internal gas-related blast in this building caused the partial collapse of the structure, leading to four casualties and 17 injuries. During post-investigations, it was found that the faults in both design and construction had led this apartment to undergo partial collapse. Furthermore, the safety and integrity of the buildings could not be guaranteed by the current building codes. Subsequently, this phenomenon has caused building codes in many countries to adopt robustness provisions (Pearson & Delatte, 2005).

For instance, the Institution of Structural Engineers has established new guidance regarding design strategies to resist disproportionate collapse. This guidance is based on approaches employed in the UK over the past 40 years, mainly tracing the incident of the partial collapse of Ronan Point. Notably, this guidance coincides with the UK construction industry's transition period from British to European Standards. Robustness is also defined by Eurocode 1 as a structure's capacity to sustain impacts, fires, explosions, and human error without experiencing damage that is disproportionate to the original cause.

Also, robustness gained attention after the World Trade Center attacks in New York in 2001 (Stochino et al., 2019). It was the first time in history that a complete collapse of an extraordinary structure was witnessed. This failure has informed the requirement to enhance the design considerations of such high-rise skyscrapers and extraordinary building structures.

In 2008, Henderson & Ginger examined the role of building codes and construction standards in mitigating wind disasters by utilizing the lessons learned from a tropical cyclone, Larry, which crossed the North Queensland coast of Australia on 20th March 2006 and caused drastic losses to the country, including severe damage to buildings along its way. Their study compared wind loading on buildings and the structural provisions outlined in the Building Code of Australia (BCA) along with the eye-witnessed damage on site, stressed-out employment of unconservative design criteria, poor construction techniques, unsuitable use of materials for durability needs, and the use of unconfirmed items in the building construction as leading to devastative damage.

It is evident that even the contemporary structural design codes and standards tend to verify the individual members but do not sufficiently address the system behavior of buildings (Stochino et al., 2019). According to Marjanishvili et al., discrepancies between anticipated and actual structural performance arises from the assumption that designing at the individual member level will sufficiently impact the overall resistance, which forms the basis of structural robustness.

The attributes like stiffness, strength, ductility, and stability describe the fundamental characteristics of structures. The codified design procedures that set forth specific requirements address these properties well; therefore, the structures that follow the codified design procedures are equipped with these properties. During their lifespan, buildings might undergo unpredictable extreme events not covered in the design criteria. Considering the economic feasibility, it is not a solution to directly incorporate such uncontrollable and extreme events into the design (Brett & Lu, 2013).

Historically, the conventional method of mitigating risk faced by structures is by incorporating protective measures – specifically increasing the structural elements' resistance, thus enhancing the structure's robustness (Stochino et al., 2019). However, it is impossible to protect buildings against all types of hazards. Enhancing structural robustness may become economically infeasible once a particular acceptable risk threshold has been exceeded (Stochino et al., 2019). Therefore, the latest research initiatives have gained attention in the field of resilient design concepts (Almufti & Willford, 2013).

In addition to limiting damage from disastrous actions, it is crucial to plan for efficient and timely recovery after a disaster. The emphasis on an infrastructure's capacity to adapt to and recover from disruptions or damages at the time of a disaster is the concept of resilience, which is gaining growing attention with extreme events.

Disaster resilience is the ability to endure, adapt, and recover from various hazards (National Academies 2012). The prime goal of employing a resilient design approach is to enhance these capacities (Disaster Resilience, 2012). As stated by UNISDR, disaster resilience is defined as the capability of a system, community, or society exposed to hazards to withstand, absorb, adapt to, and recover from the impacts of a hazard efficiently and promptly, while maintaining or restoring its essential structures and functions. This generic and broad definition implies that resilience accounts for a specific time-related aspect, which must be incorporated when addressing resilience strategies. This temporal dimension can be demonstrated concerning the “resilience triangle” provided in Figure 2.1 (Bruneau et al., 2003).

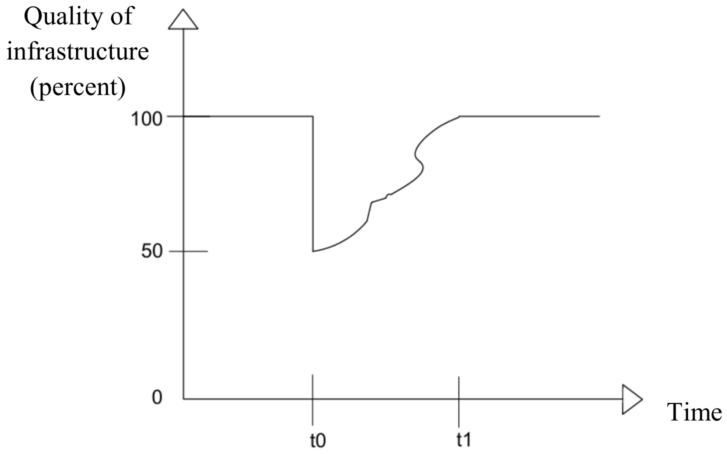

Figure 2.1: Measure of seismic resilience - conceptual definition (Reproduced from Bruneau et al., 2003)

The resilience triangle applies to technological systems like built infrastructure and visualizes the sudden decline in performance and the progressive restoration over time. Unlike robustness, which is viewing as an inherent and fixed characteristic feature of a system, resilience is considered a dynamic property dependent on the design choices. Suppose resilience is regarded as a structure's capability to resist, adapt to, and recover from extreme events. In that case, resistance can reflect the engineer's endeavors in making structures capable of withstanding a specified hazard. Even in the face of the design magnitude of an extreme event, structures might experience a particular extent of damage. Adaptation to extreme events encompasses the availability of pre-planned contingency plans for emergencies to restore the structure's functionality after an extreme event. At the same time, recovery signifies the time-dependent restoration process via remedial measures. Therefore, corrective measures may be required, and they will disrupt the structure's functionality for a specific period despite the limited damage and the non-failure of individual members (Stochino et al., 2019).

Bruneau et al. (2003) suggested a conceptual structure for defining the resilience of communities to seismic hazard, along with the measurable parameters of resilience. "Lower likelihood of failure," "Minimized impact of failure in terms of casualties, damage, and adverse economic and social outcomes," and "Faster recovery – returning to normal performance levels" are the complementary measures. At the same time, "Ends of robustness and rapidity" and "Means of resourcefulness and redundancy" are the quantitative measures incorporated into this framework. Therefore, robustness, redundancy, resourcefulness, and rapidity were defined as the four attributes of resilience (Bruneau et al., 2003). Robustness and resilience are two concepts that relate to different properties of structures. From this point of view, robustness is considered a component of resilience, and it relates to the decline in performance within the resilience triangle, as shown in Figure 2.1.

2.5. Role of building codes in disaster resilience

Depending on the requirements outlined in the building design codes and standards, designs can be categorized as code-based, performance-based, or resilience-based. Consequently, the effectiveness of these codes in addressing structures' disaster resilience varies between categories.

Structural design approaches have evolved from intuitive, code-based, performance-based, and resilience-based designs. In ancient times, master builders constructed structures based on their experience and intuition without utilizing formal design calculations. With the commencement of mass construction, builders started using codes and standards to design and construct structures, thereby incorporating code-based designs into the building. Over time, shortcomings in the code-based designs and the impacts of climate change informed the requirement for performance-based and resilience-based designs (Anwar & Ahmed, 2021).

2.5.1. Role of code-based building designs in disaster resilience

Ensuring the safety of building occupants from harm or fatalities is the foremost concern in structural design. Therefore, existing codes and standards aim to avoid failures of buildings that could result in casualties in the event of infrequent occurrences. Although this goal has primarily been accomplished for buildings in the United States exposed to wind or earthquake events, the financial losses and societal disturbance linked to many of these events have become intolerable. It has become evident that buildings designed to meet the life safety requirements outlined in codes may not fulfill other requirements expected by building owners and occupants (Ellingwood et al., 2004). Conventional design practices have primarily emphasized achieving the goal of protecting human life. There has been minimal consideration given to serviceability concerns, which, although not directly affecting life safety, could impose notable social and economic consequences (Ellingwood et al., 2004). Therefore, the aftermath of natural disasters and increased public expectations have drawn attention to real code shortcomings and their enforcement (Rosowsky & Ellingwood, 2002).

The provisions in code-based building designs are prescriptive. Building codes set the baseline or the minimum requirements to sufficiently safeguard the safety of building occupants by safe design and construction of residential, educational, occupational, and a variety of other structures. These codes account for the capacity of the buildings to withstand natural disasters and the consequences of climate change. However, the building codes lack the means of evaluating the performance of buildings against these extreme events. Instead, it is assumed that the anticipated performance is implicitly fulfilled by complying with the minimum requirements outlined in the code for designing and detailing the structural elements of a building. For instance, Eurocode 8 for designing structures for seismic resistance intends to satisfy "No Collapse Requirement" at an earthquake occurence having a 475-year return period and "Damage Limitation Requirement" at an earthquake occurrence having a 95-year return period provided that the building design followed the prescriptive standards and guidelines outlined in the code [Eurocode 8]. Nevertheless, the code does not verify these performances on its own.

Therefore, it is evident that current code-based designs do not explicitly aim for the performance objectives. While prioritizing life safety and preventing collapse is crucial, it may not fully account for the functionality of buildings after hazards, such as repairing damages that occur (Joyner & Sasani, 2018).

Although the code-based building designs do not provide flexibility to deviate from the prescribed rules outlined in the code, code-based designs are accepted over performance-based and resilience-based designs because the former grants simplicity and uniformity, making it convenient for the users to apply across varying projects. Also, the code-based designs are formulated conservatively to ensure the ease of application over a wide range of scenarios, resulting in either overestimating or underestimating.

2.5.2. Role of performance-based building designs in disaster resilience

Sometimes, the building developers and the public seek explicit confirmation of the safety of their buildings. However, it is impossible to explicitly comment on the safety of design outcomes even though the code-based procedures are intended to provide safe structures (Anwar & Ahmed, 2021).

Performance-based engineering necessitates a more comprehensive understanding of structural design objectives compared to code-based engineering (Ellingwood et al., 2004). The performance-based structural design approach is a practical, economical, and appropriate substitute for prescriptive design approaches. Performance-based design (PBD) is occasionally employed to supplement code-based design.

PBD aims to establish performance predictions while explicitly adhering to pre-defined performance objectives. Performance-based regulations define the outcomes that a building must achieve to carry out performance prediction analyses. These outcomes are performance requirements rather than prescriptive requirements that the code user must follow.

These analyses of performance predictions follow systematic procedures, incorporating advanced computer programs to simulate 3D mathematical models of structures using actual recorded hazards such as wind and earthquake time histories.

Sometimes, the building developers' target performance objectives exceed the code objectives. However, the PBD is utilized to validate that the code-intended performance objectives are met. By employing performance-based designs effectively, it can be confirmed later that the desired performance has been attained (Almufti & Willford, 2013).

Since the performance-based design approaches are equipped with explicit performance indicators and procedures, engineers can address inquiries concerning structural safety. Furthermore, it gives engineers the flexibility to employ innovative analysis and design techniques, thereby enhancing the efficiency of structural design (Anwar & Ahmed, 2021).

Nevertheless, the trustworthiness of computer-based models in capturing the actual behavior of buildings declines when the structure is pushed to its limits. Consequently, the computer models alone cannot accurately predict damage when the structure undergoes substantial harm. Additionally, performance-based building designs do not explicitly showcase the performance of the non-structural elements. Moreover, these designs do not account for the external factors that could obstruct the functionality of buildings (Almufti & Willford, 2013). Such deficiencies in performance-based design motivate the adoption of resilience-based designs.

2.5.3. Role of resilience-based building designs in disaster resilience

Resilience-based design is a comprehensive approach that identifies and lessens risks resulting from hazards, aiming to expedite rapid recovery in the aftermath. This approach surpasses the performance objectives outlined in the code-based designs and, therefore, the typical goals of the performance-based design. It incorporates integrated multidisciplinary design and contingency planning with performance-based assessments to align with the resilience objectives of the owner. In resilience-based design approaches, buildings are designed to endure minimal damage, decreasing the uncertainty in the building's behavior. This builds up confidence in its intended performance. In contrast to code-based and performance-based designs, resilience-based designs specifically address design and performance verification of both structural and non-structural elements. Moreover, resilience-based designs distinguish themselves from code- and performance-based designs by incorporating preparedness for post-hazard recovery. This distinctive feature of resilience-based designs ensures the continuity of operations and livable conditions immediately after the hazard, if desired (Almufti & Willford, 2013).

Assessing repair costs and the loss of functionality during repairs throughout the lifetime of a building also measures resilience. This assessment can help gauge the effectiveness of existing codes and, more importantly, highlight potential shortcomings (Joyner & Sasani, 2018).

Also, utilizing locally relevant, disaster-resilient building codes is the most efficient strategy for ensuring that the new and reconstructed structures meet resilience standards.

2.6. Structural resilience

Since it is impossible to address adaptation to and recovery of structures from extreme events using structural design, Marjanishvili et al. set forth a modified definition for resilience by excluding adaptation and recovery. Therefore, the newly introduced structural resilience concentrates on the resistance element of the general resilience concept. Further, the term structural resilience is subdivided into two primary characteristics: robustness and hazard. Structural resilience is connected with a particular hazard magnitude, which is expected to be mitigated by a design featuring a designated robustness. Therefore, the new definition of structural resilience forwarded by Marjanishvili et al. provides a sound basis for structural designers to quantify the structural resilience of structures via measures of robustness and hazard.

Therefore, evaluating the performance of buildings designed to comply with existing codes is the first step in determining the disaster resilience they provide (Joyner & Sasani, 2018). Instead of serving as an alternative to code-based prescriptions, performance-based design is essentially an approach that incorporates prescriptions while aiming directly at attaining and optimizing clearly defined performance objectives. It's worth noting that until recently, the code provisions implemented to fulfill performance objectives have primarily been established empirically (Paulotto et al., 2004).

2.6.1. Intensity measures and engineering demand parameters

When evaluating the performance of code-based building designs, it is imperative to recognize suitable intensity measures that represent the demand placed on the buildings, along with engineering demand parameters that characterize the buildings' response.

2.6.2. Performance objectives and limit states

Performance-based engineering aims to ensure that buildings or structures achieve specific performance targets when faced with different natural or human-caused dangers. Recent suggestions for this approach, presented by organizations like FEMA, NEHRP, and SEAOC, have similar characteristics. They all focus on protecting human lives during severe events first, then preventing buildings from collapsing during extreme situations (collapse prevention, or CP), and ensuring that buildings remain functional during moderate events (known as continued function or immediate occupancy, IO). The explanations of severity levels (severe, extreme, moderate) are still developing but are likely based on how likely it is to encounter the hazard over a specific period. For example, a building might be required to withstand events that have a 50% chance of happening in 50 years (called a 50%/50-year event) without losing functionality, ensure life safety during events that have a 10% chance of happening in 50 years, and avoid collapsing during events that have a 2% chance of happening in 50 years. These performance goals are displayed in a matrix that matches objectives with hazard intensities, and particular buildings are categorized based on their use. This categorization is usually outlined in standards like Table 1-1 of the ASCE Standard 7-02 (Ellingwood et al., 2004).

Ensuring that a building meets its performance requirements involves linking the qualitatively indicated objective, such as immediate occupancy post a 50%/50-year event, to a response level and limit state (determining force or deformation) that can be verified through structural analysis and mechanics principles.

This typically involves assessing the structural integrity of the entire building system. If the performance objective relates to localized damage, a limit state focusing on the strength or deformation of individual members/connections may suit. However, relying solely on the performance of individual parts might not reflect the overall system's capacity.

Although equating performance-based design with deformation-based design is an oversimplification, in situations where it is required to assess how a system responds using just a single structural response quantity (usually calculated with finite element structural analysis), it's often better to focus on deformation of the structure rather than member strength. This is especially true when the structural behavior exhibits non-linear characteristics. Recent efforts, like FEMA Report 356 and its predecessor (FEMA Report 273), have also linked structural deformations to performance levels.

It is widely acknowledged that performance-based design (PBD) is the most logical approach for evaluating and mitigating the risks posed by infrastructure due to natural and man-made events in designing structures and rehabilitating existing ones. The initial formal implementations of PBD were primarily focused on earthquake engineering and design, with subsequent extensions to other engineering disciplines, such as Blast Engineering and Fire Engineering. Wind Engineering, too, has emerged as an area with significant potential for further advancements in PBD.

2.7. Performance-based wind engineering (PBWE)

2.7.1. Current practice of wind engineering

In wind engineering, the usual practice involves selecting hazard intensities from established codes or standards to calculate loadings and then design the structural elements of buildings accordingly (Spence & Arunachalam, 2022). For instance, in Eurocode 1: Actions on Structures - Part 1-4: General actions - Wind actions (EN 1991-1-4:2005+A1), the hazard intensity is determined by the characteristic 10-minute mean wind velocity for a specified mean return period. The selection of this mean return period involves the degree of resilience that the stakeholder expects from the structure. Wind loads are then computed based on the prescribed wind speed at the desired mean return period, considering seasonal variations, wind directionality, exposure conditions, topography, structure geometry, and more. These loads are primarily utilized for strength-based design, i.e., the ultimate limit state determined to ensure life safety. Aspects related to serviceability design are usually left to the engineer and stakeholders' choice. After the loads are specified for a specific structure, a suitable material code, like "Eurocode 2: Design of concrete structures - Part 1-1: General rules and rules for buildings" (EN 1992-1-1:2004) for reinforced concrete buildings and "Eurocode 3: Design of steel structures - Part 1-1: General rules and rules for buildings" (EN 1993-1-1:2005) for structural steel buildings, is mostly employed in the design. The aforementioned codes outline detailed prescriptive requirements that engineers must follow to ensure life safety.

2.7.2. Limitations of the current practice of wind engineering

The procedures provided in existing codes for designing buildings to wind actions have several notable shortcomings:

1) The procedure is prescriptive, assuming the performance is implicitly achieved by following the prescriptions. Therefore, the system's performance remains unknown (Griffis et al., 2013).
2) It tends to be deterministic despite recognizing that modeling assumptions greatly influence outcomes (Griffis et al., 2013).
3) Damage to non-structural components from the large drift of the leading wind force resisting system isn't explicitly accounted for, though it can significantly affect overall building performance in terms of economic roles (Griffis, 1993).
4) Mitigation of debris impact risk on building envelopes relies solely on prescribed measures like glazing that is resistant to impact or storm shutters, without a thorough assessment of associated risks.

5) Losses from wind-driven rain, which causes water ingress and damage to interior non-structural components, are disregarded despite their potential to contribute significantly to total losses during severe wind events (G et al., 2000).

The challenges outlined in existing wind engineering practices can only be overcome by establishing a comprehensive performance-based design philosophy similar to earthquake-resistant design principles. However, directly applying these principles to wind engineering encounters obstacles due to the unique characteristics of wind loading and wind-excited structures, which differ from earthquake loading and earthquake-excited structures (Spence & Arunachalam, 2022).

Despite the differences between wind and earthquake situations, the framework presented by FEMA (Federal Emergency Management Agency) in 2012 offers a valuable and established foundation for applying Performance-based Design (PBD) principles to other natural hazards, together with severe wind events. It's vital to note that performance goals like fully operational and immediate occupancy stem from Performance-based Earthquake Engineering (PBEE) and outline preferred functions of buildings at specific load levels. Therefore, when defining target performance goals for buildings subjected to wind loading, the qualitative aims of the goals set for performance-based earthquake engineering can be maintained. Nevertheless, it's crucial to acknowledge the potential need for other performance goals, like evacuation before severe wind events, when developing frameworks for effectively implementing Performance-based Wind Engineering (PBWE) (Spence & Arunachalam, 2022).

2.7.3. Performance-based wind engineering (PBWE) frameworks

The first formal implementations of performance-based design were focused on earthquake engineering. Over time, performance-based design applications rapidly expanded to other domains, notably Wind Engineering.

Similarly, Performance-based design (PBD) has primarily evolved within the United States, particularly in seismic risk and design. The significant economic losses and widespread devastation triggered by four hurricanes, Hugo, Andrew, Iniki, and Opal, during the 1990s, alongside the growing recognition of performance-based earthquake engineering, served as catalysts for interest in applying performance-based engineering principles to the design of buildings exposed to wind loads (Ellingwood et al., 2004).

Early efforts in this direction involved proposing frameworks aimed at evaluating the performance of residential wood buildings (Rosowsky & Ellingwood, 2002). Significant advancements resulting from Rosowsky & Ellingwood's research encompass the development of a comprehensive set of performance objectives, ranging from serviceability to ultimate load levels, tailored for residential structures subjected to wind loads. Additionally, recognizing the necessity for system-level analysis, rather than traditional component-level assessments, emerged as a crucial aspect for enhancing confidence in performance predictions. Moreover, the importance of accounting for uncertainty in the analysis was underscored. The following sections provide a detailed discussion of these efforts.

Later on, there was a growing interest in simulating the performance of engineered structures exposed to wind loading, within a PBWE framework (Paulotto et al., 2004).

"Performance-based Wind Engineering," PBWE, was first introduced in an Italian research project by Paulotto et al. in 2004. This marked the initial extension of performance-based design, initially developed in the USA for seismic risk and design, to wind engineering. In many performance-based wind engineering initiatives, it's common to observe the adoption of the PEER framework (Porter, 2003), initially developed for performance-based earthquake engineering. This initial attempt was also built on the PEER equation [2] and was restricted to a specific type of building (i.e., tall buildings) for simplicity.

$$\mathbf{p(DV) = \iiint |p(DV|DM)|.|p(DM|EDP)|.|p(EDP|IM)|.dp(IM)} \qquad [2]$$

In Paulotto et al.'s initial endeavor to expand performance-based design to wind engineering, emphasis is only placed on a term in Eq. (2), which pertains to vulnerability analysis (e.g., dp(DM|EDP)).

Initial endeavors on performance-based wind engineering primarily aimed to establish the suitability of the PEER framework or comparable methods for assessing the performance of skyscrapers and spanning bridges subjected to wind loading.

After these early research endeavors, there has been a significant increase in interest in PBWE, with several frameworks introduced for residential buildings (Rosowsky and Ellingwood, 2002) and engineered systems (Griffis et al., 2013; Mohammadi et al., 2019).

Griffis et al. (2013) introduced a novel framework for performance-based wind engineering. They concentrated on establishing building performance objectives, related acceptance criteria, and, importantly, explicitly integrating methods to account for non-linear behavior. Accordingly, the proposed performance-based wind engineering framework, whether it pertains to strength or serviceability, at any designated load level, comprises four primary constituents, as depicted in Figure 2.2 below.

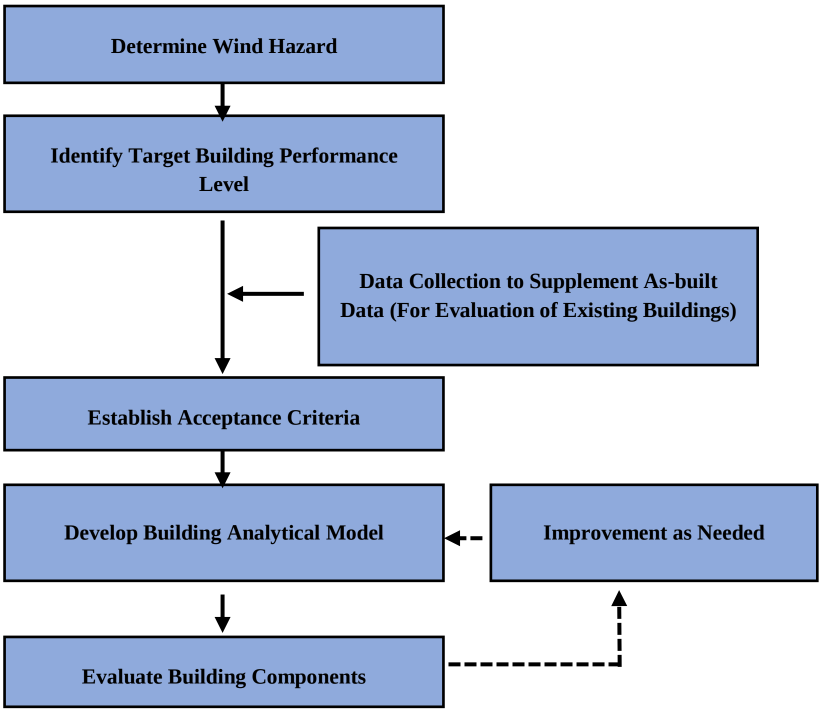

Figure 2.2: Performance-based wind engineering framework. Adapted from (Griffis et al., 2013)

As illustrated above, the approach is not prescriptive. The choice of the target building performance level enables input from end users. Establishing an analytical model that accurately accounts for the fitting non-linear behavior necessitates considerably larger work compared to the traditional design procedure. As this method focuses on evaluating a building via component assessment (except motion comfort performance objective), it is well-suited for assessing existing buildings. However, additional effort is needed for new building designs to update the analytical model to reflect required modifications to member sizes to meet acceptance criteria or strategically remove unnecessary material to achieve cost-effectiveness. Further research on various primary structural systems for buildings may update this method by introducing a Response Modification Factor (R_{wind}). This factor would allow the design engineer to lower the wind loads detailed by the code, establishing a base design that serves as a good initiation for the assessment (Griffis et al., 2013).

It is worth mentioning that there has been significant progress in developing PBWE frameworks for probabilistic evaluation and optimal design of engineered structures experiencing extreme wind events. Considerable advancements have originated in the simulation of structural and non-structural damage and losses caused by various winds by utilizing probabilistic system-level metrics related to repair expenses, downtime, life cycle costs, and occupant comfort (Griffis et al., 2013; Mohammadi et al., 2019).

As well, methodologies have been developed for design optimization while adhering to the abovementioned probabilistic system-level metrics. Although most of these frameworks were initially simulated by the fragility/consequence function-based damage/loss simulation methods presented by the PEER framework (and afterward developed in the P-58 methodologies), they have since grown to take in extra factors, such as life cycle costs, and wind-specific performance criteria like occupant comfort. Throughout this development, they have maintained mainly the core concept of the PEER framework for explicitly evaluating the probabilistic system-level metrics.

2.7.4. Performance levels, performance objectives, acceptance criteria, and assessment methodologies

Rosowsky & Ellingwood (2002) introduced various performance objectives for wind-excited residential buildings in four key levels: maintaining serviceability under ordinary occupancy conditions, ensuring immediate occupancy following moderate events, providing life safety during design-basis events, and preventing collapse during maximum considered events. These objectives address varying degrees of hazard to ensure safety and functionality throughout a building's lifecycle.

These early suggestions typically rely on broadly defined goals for buildings with various occupancy types (Rosowsky & Ellingwood, 2002). Rosowsky & Ellingwood (2002) suggested that these objectives, like "serviceability," "immediate occupancy," and "collapse prevention," must be defined using structural responses that can be assessed by the structural engineer utilizing existing analytical tools or supportive testing methods.

Paulotto et al.’s work, which builds upon the PEER framework, emphasizes that defining performance is the initial stage in applying performance-based design (PBD). Based on the performance criteria, suitable Damage Measures (DMs) and Engineering Demand Parameters (EDPs) need to be selected (Paulotto et al., 2004). Paulotto et al.’s proposal for defining performance didn't specifically concentrate on building structural performance differences. Instead, it addressed various aspects such as the buildings’ ultimate limit state, serviceability limit state, envelope, and surroundings.

Figure 2.3 below displays the performance objective matrix proposed by Griffis et al. (2013). It illustrates the possible performance objectives corresponding to different risk categories across various wind hazard levels.

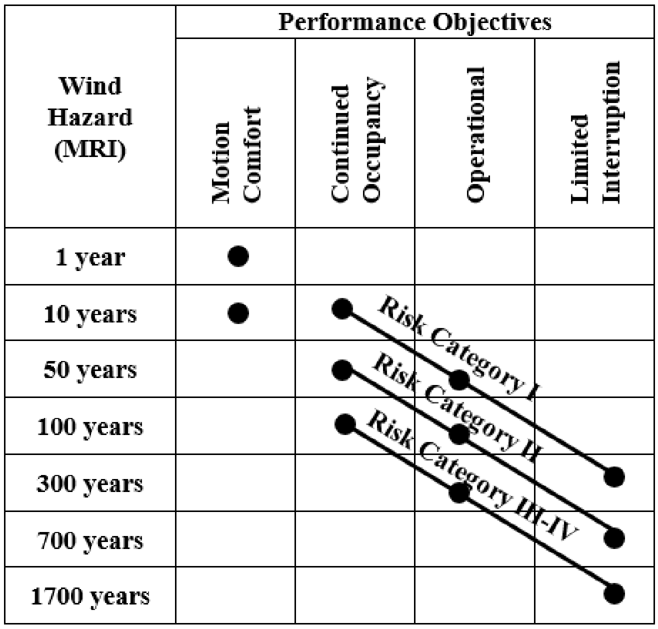

Figure 2.3: Performance objective matrix. Adapted from (Griffis et al., 2013)

2.7.5. Component-level performance evaluation of buildings subjected to extreme wind loads

Griffis et al. (2013) introduced a framework for evaluating the performance of wind-induced buildings at the component level, consisting of three performance levels: (1) continued occupancy, (2) operational, and (3) limited interruption. As appropriate, these performance levels will be assessed based on the force and deformation levels experienced by deformation-controlled and force-controlled elements.

Figures 2.4 and 2.5 provide a qualitative illustration of the deformation limits for "continued occupancy," "operational," and "limited interruption" performance objectives.

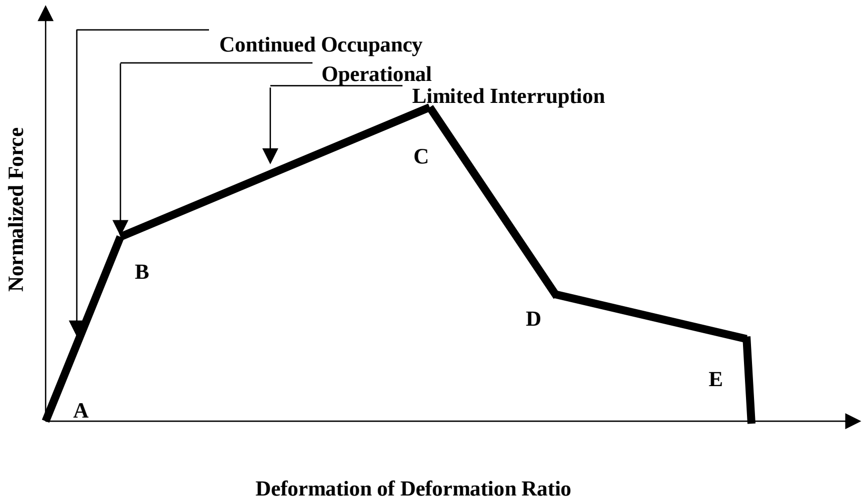

Figure 2.4: Component deformation acceptance criteria – deformation controlled actions. Adapted from (Griffis et al., 2013)

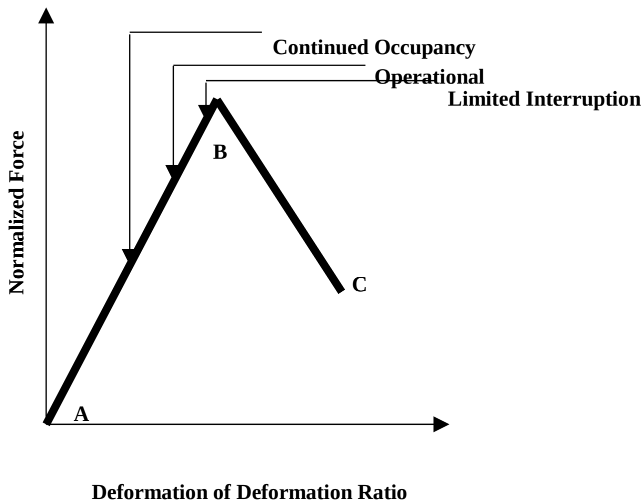

Figure 2.5: Component deformation acceptance criteria – force-controlled actions. Adapted from (Griffis et al., 2013)

For each designated hazard intensity, the deformations of individual structural elements can be determined from non-linear models representing the buildings in question. These deformations can then be compared to the force-deformation relationships of the elements to ascertain their performance levels.

Mohammadi et al. (2019) adjusted the performance levels suggested by Griffis et al. (2013) to better suit wind loading conditions than seismic loading conditions. The performance levels introduced by Mohammadi et al. (2019) offer a more elaborate version, incorporating an additional performance level, collapse prevention, to signify an unstable performance range. Figure 2.6 shows the performance limits developed for steel beams and columns of the building model.

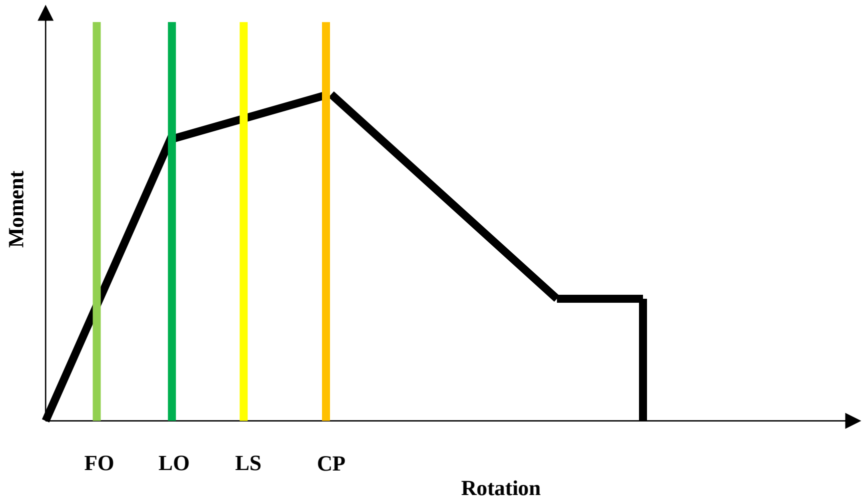

Figure 2.6: Component acceptance criteria – steel beam and column elements. Reproduced from (Mohammadi et al., 2019)

For the first two performance levels - continued occupancy and operational (entire operational and limited operations as per Mohammadi et al. (2019)) - the matrix outlined by Griffis et al. (2013) establishes stricter performance thresholds concerning the mean recurrence interval. Conversely, the opposite is observed for the third performance level, limited interruption (life safety as stated in Mohammadi et al. (2019)).

After establishing these performance thresholds, Mohammadi et al. (2019) proceeded to evaluate the performance of individual components, assessing the dynamic behavior of all structural elements in an existing 47-story steel frame building subjected to incremental dynamic analysis at various hazard intensity levels denoted by relevant basic wind speeds.

2.7.6. System-level performance evaluation of buildings subjected to extreme wind loads

If the objective is "collapse prevention" or "life safety," employing a system evaluation centered on the first failure, as exemplified by Folz and Foschi in 1989, might result in a pessimistic evaluation of the system's capacity. Alternatively, according to other research studies, such as those conducted by Rosowsky and Ellingwood in 1991, failures in assemblies of typical size often arise when two adjacent members fail, leaving the residual structure unable to connect over the damaged area. However, if the aim is to prevent local damage, first-failure analysis may be a suitable limit state for the structure (Rosowsky & Ellingwood, 2002).

According to Rosowsky & Ellingwood (2002), confirmation that a building meets a specific performance requirement, such as immediate occupancy during moderate wind events or life safety during design-basis earthquakes, involves linking the qualitative performance objective to a measurable response parameter, such as force or deformation, which can be calculated using structural analysis and mechanics principles. When design relies on the behavior of members, this linkage is typically straightforward. However, it's important to note that the performance of individual members within the system may not accurately reflect the overall system performance (Rosowsky & Ellingwood, 2002). Therefore, Rosowsky & Ellingwood (2002) identified the importance of system-level analysis over traditional component-level analysis in achieving confidence in predicting the performance of buildings.

In recent years, numerous studies have evaluated the system-level wind performance of both new and existing buildings using various analytical methods, including modal analysis, non-linear static pushover analyses, non-linear response history analysis, and non-linear incremental dynamic analysis (Mohammadi et al., 2019), fragility assessment, inter-storey shear strain deformation assessment, motion perception assessment, and more.

2.8. Performance-based earthquake engineering (PBEE)

2.8.1. Current practice of performance-oriented earthquake engineering

The conventional prescriptive requirements in seismic codes are performance-oriented, as these codes are developed to achieve specific performance goals, such as preventing collapse and ensuring the safety of lives. For instance, Eurocode 8 (EN 1998-1:2004) aims to fulfill two key objectives: firstly, it ensures that structures designed under its guidelines adhere to the "no collapse requirement." This mandates that structures must endure the designated earthquake forces without suffering either local or global failure, thereby preserving their structural integrity and retaining some capacity to bear loads following seismic activity. Secondly, Eurocode 8 (EN 1998-1:2004) seeks to meet the "damage limitation requirement," which requires that structures should be resilient enough to withstand seismic events with a higher likelihood of incidence than the design action without incurring destruction that would significantly obstruct their use or result in disproportionately high repair costs compared to the structure's original construction expenses.

At the preparation stage of these conventional codes, engineers have assumed that the buildings constructed following these prescriptive provisions will satisfy the specific performance objectives outlined in the code. Nonetheless, these codes do not evaluate a design’s ability to meet performance objectives (Whittaker et al., 2003).

The deficiencies in code-based designs in presenting an accurate assessment of performance have been proven by the earthquake damage to buildings caused by minor, moderate, and intense earthquakes recorded in the United States of America. This has led to substantial revisions in their prescriptive provisions. For instance, the expectations for the performance of mission-critical buildings started to change after the extensive damage that occurred in numerous emergency response amenities, particularly hospitals, during the 1971 San Fernando earthquake. Accordingly, engineers determined that mission-critical buildings, including hospitals, fire stations, communications centers, etc., are crucial for post-earthquake response and recovery. Hence, designing them to remain operational even after severe earthquakes is necessary. Further, engineers assumed that achieving this performance objective could be accomplished by increasing the strength of these buildings by 50% relative to non-essential buildings and implementing more stringent quality assurance strategies during construction (Whittaker et al., 2003). The primary method for adjustment is using arbitrary importance factors that change the required strength (Whittaker et al., 2003).

Substantial economic losses and the functional loss in mission-critical facilities after the 1989 Loma Prieta and 1994 Northridge earthquakes informed the establishment of the performance-based earthquake engineering field to create resilient built environments. During the early 1990s, designers and academic community fellows, mainly structural and geotechnical engineers, identified the requirement for new and fundamentally different design approaches. This requirement stemmed from the shortcomings of existing prescriptive force-based provisions. Prescriptive provisions were sometimes identified as complicated, often containing confusing and conflicting requirements. Furthermore, these prescriptive force-based procedures are frequently not appropriately targeted at performance objectives, not directly aligned with the intended performance goals, hence lack the reliability in achieving desired societal protection, and sometimes they are excessively costly to implement (Whittaker et al., 2003).

2.8.2. Performance-based earthquake engineering (PBEE) frameworks

Performance-based earthquake engineering (PBEE) involves evaluating, designing, and constructing buildings to achieve earthquake performance goals that matter to the stakeholders, whether about financial costs, human lives, or operational disruptions (Goulet et al., 2007).

In different versions, Performance-based earthquake engineering (PBEE) could potentially turn into the main method for assessing seismic performance in both new and existing structures, replacing load-and-resistance-factor design (LRFD). The main contrast between the two approaches is their focus: LRFD primarily evaluates the likelihood of failure in discrete components (with some attention to system-level factors like the strong-column-weak-beam requirement), while PBEE mainly deals with system-level performance, concentrating on the risk of collapse, casualties, repair expenses, and loss of functionality after an earthquake (Porter, 2003).

Early efforts to establish and standardize PBEE methodologies led to the publication of SEAOC's Vision 2000 report (1995) (Porter, 2003). In the early to mid-1990s, the Federal Emergency Management Agency (FEMA) funded the Applied Technology Council (ATC) and the Building Seismic Safety Council (BSSC) to develop NEHRP (National Earthquake Hazards Reduction Program) guidelines and commentary for seismic rehabilitation of buildings (FEMA 273). This initiative indicated a significant achievement in the progression of performance-based earthquake design methods and clarified some crucial perceptions vital to a performance-based earthquake methodology (Whittaker et al., 2003).

Other notable early PBEE initiatives consist of ATC-32 (1996a), ATC-40 (1996b), and FEMA 356 (2000) (Porter, 2003). Further to FEMA-273/274, additional initiatives such as ATC-40, Methodology for Evaluation and Upgrade of Concrete Buildings, and Vision-2000 Framework for Performance-based Seismic Design Project improved and expanded the technology introduced in FEMA-273/274. Later, the American Society of Civil Engineers further refined these technologies when converting the FEMA-273/274 reports into the Prestandard for Seismic Rehabilitation of Buildings, known as FEMA 356 (Whittaker et al., 2003).

Therefore, the FEMA-356, ATC-40, and Vision-2000 outline contemporary standards and practices in performance-based seismic engineering (Whittaker et al., 2003).

The literature highlights several deficiencies in the FEMA 273/356 performance-based approach (Whittaker et al., 2003). These include:

1. The PBEE methodology predicts structures' responses depending on the structure's overall behavior, yet it assesses performance by examining damage sustained by individual components. Consequently, the prediction of structural performance tends to be influenced by the performance of the weakest elements.
2. Many of the acceptance criteria outlined in the document, which engineers rely on to evaluate the performance of structures, are subjective and dependent on judgment rather than empirical data or direct evidence. This raises concerns about the procedures' reliability.
3. Engineers perceive the guidelines as overly cautious compared to designs based on prescriptive criteria. Nevertheless, there is no established evidence regarding their reliability and effectiveness in achieving the desired performance.

4. The performance levels defined by FEMA 273/356 do not specifically focus on specific critical concerns of stakeholders, like anticipated repair exenses and the downtime resulting from earthquake destruction.

After the unexpected identification of brittle fracture damage in welded moment-resisting steel frame buildings after the 1994 Northridge earthquake, FEMA initiated a significant project, commonly called the SAC Steel Project, to formulate earthquake evaluation and design criteria for this category of structures. Central outcomes of this initiative encompassed a set of endorsed design documents (FEMA-350, FEMA-351, and FEMA-352), which introduced performance-based design approaches to address shortcomings identified in the existing FEMA 273/356 guidelines. These FEMA technical reports provided an extensive research dataset on such buildings' structural performance, facilitating the establishment of less subjective acceptance criteria for design applications.

Moreover, they devised a methodology for evaluating a building's structural performance dependent on its overall behavior, rather than just focusing on the damage to individual components. While the SAC procedure has not gained extensive reception, the prescriptive processes outlined in FEMA-350 and FEMA-351, confirmed through performance-based approaches, have been broadly embraced and integrated into national design standards and building codes (Whittaker et al., 2003).

The Pacific Earthquake Engineering Research (PEER) Center, located at the University of California, Berkeley, is one of the three earthquake engineering research centers supported by federal funding. PEER Center proposed a performance-based earthquake engineering approach focusing on system-level aspects like hazard assessment, structural assessment, damage assessment, and loss assessment, which were not covered within the first-generation efforts (Porter, 2003).

Identifying the shortcomings of FEMA 273/356, FEMA has partnered with the Applied Technology Council (ATC) to implement a project referred to as ATC-58 for creating the next generation of performance-based seismic design guidelines for buildings. These guidelines are envisioned for new constructions and retrofitting projects covering structural and non-structural elements within buildings, primarily focusing on designing structures to withstand seismic forces (Whittaker et al., 2003).

2.8.3. Performance levels, performance objectives, acceptance criteria, and assessment methodologies

Performance-based design approaches employ various matrices to specify the damage limit state at which a particular building should function for a given return period, depending on its importance level. For instance, in SEAOC's Vision 2000 report

(1995) and FEMA 273 (1997), which originated from the ATC-33 project, performance-based earthquake engineering is defined as a method to guarantee specific groupings of anticipated system performance across varying levels of seismic activity (Porter, 2003).

Figure 2.7 illustrates the performance objectives outlined in Vision 2000. Accordingly, designers and owners can collaborate to select a combination of performance level and seismic activity level to establish the performance objective for the design.

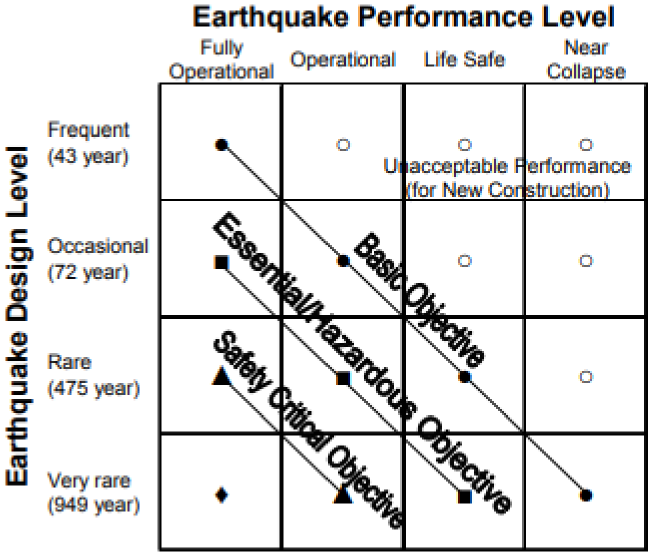

Figure 2.7: Vision 2000 recommended seismic performance objectives for buildings (after SEAOC, 1995)

FEMA 273 also outlines its performance objectives employing a comparable methodology, but with some differences in the descriptions of performance and seismic activity intensities (Porter, 2003).

A key concept in the performance-based procedures outlined in FEMA 273/274 performance-based framework is the performance objective, which includes specifying the design event (earthquake hazard) that the building should withstand and determining an acceptable damage level if that incident occurs. Another noteworthy aspect of the NEHRP (National Earthquake Hazards Reduction Program) Guidelines (FEMA 273/274) involves the specification of standard performance levels. Outlining of these standard performance levels involved quantification of the degrees of both structural and non-structural damage based on standard structural response parameters (Whittaker et al., 2003).

Figure 2.8 displays the qualitative performance levels of FEMA 273/274 overlaid onto a global force-displacement curve for a representative building. The associated levels of damage are also indicated in Figure 2.8 (Whittaker et al., 2003).

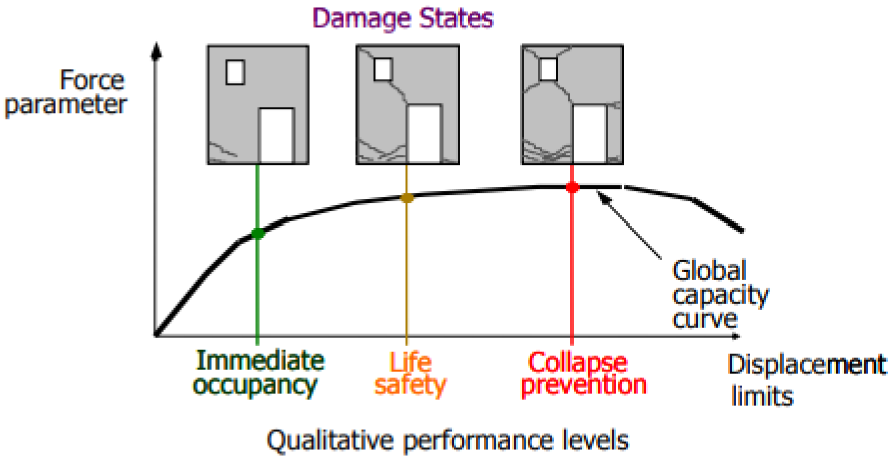

Figure 2.8: Qualitative performance levels of FEMA 273/274/356

NEHRP guidelines present four linear and non-linear procedures for predicting response parameters for a given shaking level. These procedures can be applied to assess the expected performance of buildings in relation to the target performance levels specified in the performance objectives (Whittaker et al., 2003).

Figure 2.9 demonstrates the non-linear static method of FEMA 273/274 used to evaluate the performance. One or more elastic acceleration response spectra initially characterize the seismic hazard. Subsequently, a non-linear computer model of the structure is developed and exposed to gradually incrementing forces/displacements to generate the capacity curve depicted in Figure 2.9. This curve typically presents base shear (on the y-axis/ordinate) versus roof displacement (on the x-axis/abscissa). Using an equivalent single-degree-of-freedom (SDOF) non-linear representation of the building frame, a maximum roof displacement is determined for each design spectrum. Following this, component deformations and force actions necessary for performance assessment are derived based on the outcomes of the non-linear static analysis. These deformations and force demands are compared to the respective component deformation and force capacities, as outlined in the materials chapters of FEMA 273 for the performance levels depicted in Figure 2.8. If the demands on components do not surpass their capacities, the building is considered to have achieved the desired performance objectives (Whittaker et al., 2003).

Likewise, each overall performance level is defined based on the performance of individual components. A structural design is deemed successful if analysis demonstrates that the forces or deformations experienced by each component remain within predetermined bounds. Performance is either pass or fail, based on whether the forces or deformations exceed the limit. If the acceptance criteria are met, the design is considered to have achieved its performance objective, though without specifying a quantified probability (Porter, 2003).

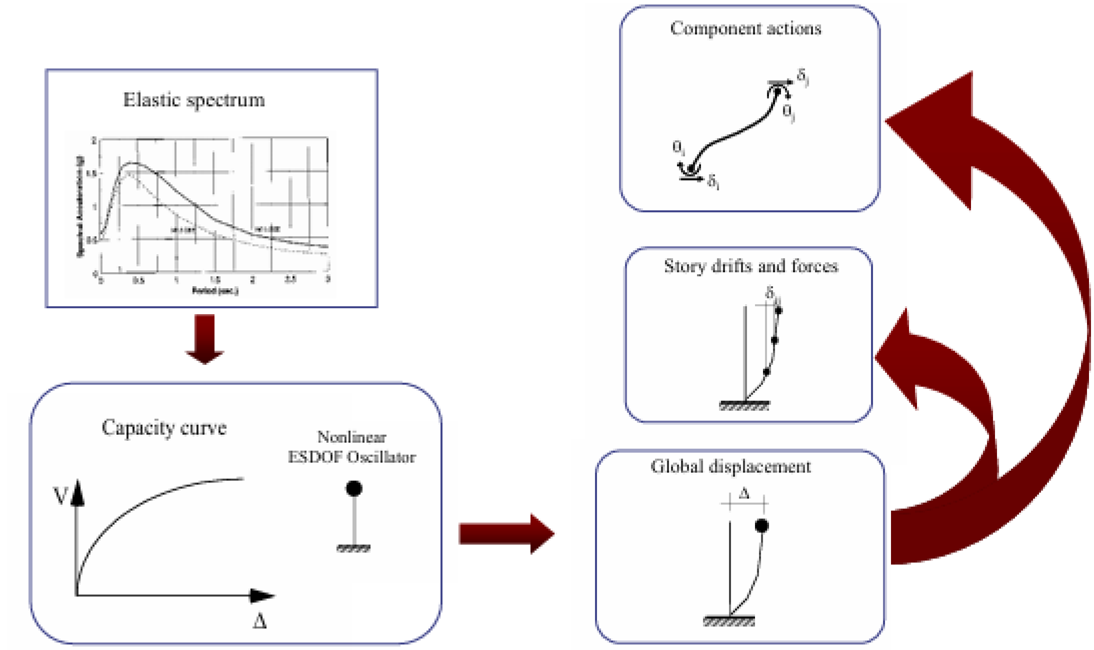

Figure 2.9: Performance assessment procedure of FEMA 273/274/356 (after Comartin)

These documents offer the same concept of performance levels but use different definitions, damage states, and acceptance criteria. In 2001, Ghobarah grouped the performance levels in Vision 2000, FEMA 273, and ATC 40 in equivalent categories, as illustrated in Table 2.1 below (Ghobarah, 2001).

Table 2.1: Common criteria for performance levels

Performance Level	Damage State	Drift
Fully operational, Immediate occupancy	No damage	<0.2%
Operational, Damage control, moderate	Repairable	<0.5%
Life safe – Damage state	Irreparable	<1.5%
Near collapse, Limited safety, Hazard reduced	Severe	<2.5%
Collapse	Collapse	>2.5%

A significant aspect of PEER's approach is its emphasis on delivering performance indicators at the system level. These indicators involve probabilistic evaluations of repair expenses, casualties, and the duration of functionality loss (Porter, 2003).

Figure 2.10 depicts the PBEE method created by the Pacific Earthquake Engineering Research (PEER) Center. It consists of four phases: hazard assessment, structural assessment, damage assessment, and loss assessment.

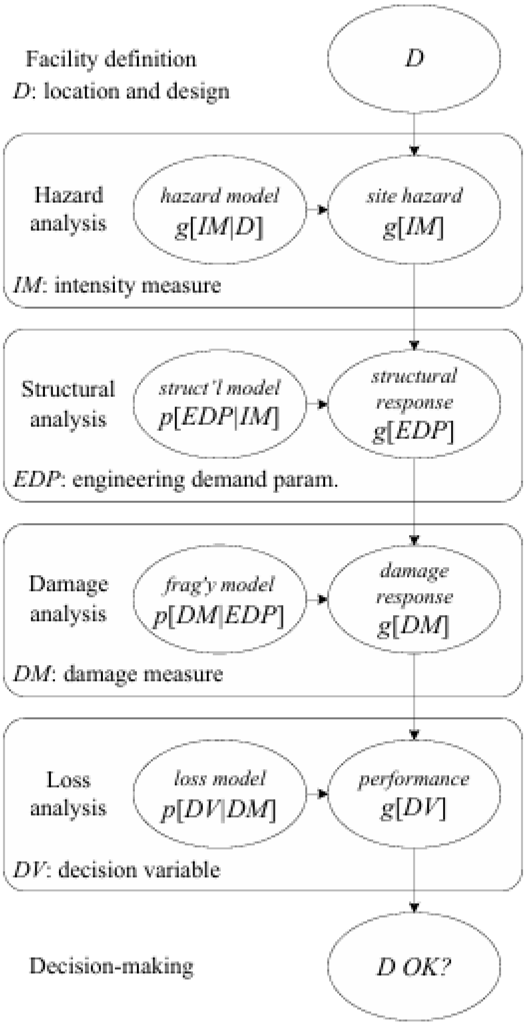

Figure 2.10: PEER analysis methodology (Porter, 2003)

The performance-based design methodology outlined in ATC 58 incorporates processes for assessing risk tailored to the design-basis. This risk assessment can be conducted either deterministically, based on specific scenarios or events, or probabilistically. Risk is quantified in terms of particular losses, such as the cost of restoring a damaged facility to functionality, loss of life, and periods of downtime, rather than relying solely on traditional metrics like ensuring the safety of human lives during the design event.

The process for predicting performance shares similarities with the methodology employed in the HAZUS national loss estimation software, even though the individual steps are executed distinctly. Figure 2.11 illustrates the flow chart outlining the ATC-58 performance prediction process. This methodology is primarily based on techniques developed by the Pacific Earthquake Engineering Research (PEER) Center, supported by funding from the U.S. National Science Foundation (Whittaker et al., 2003).

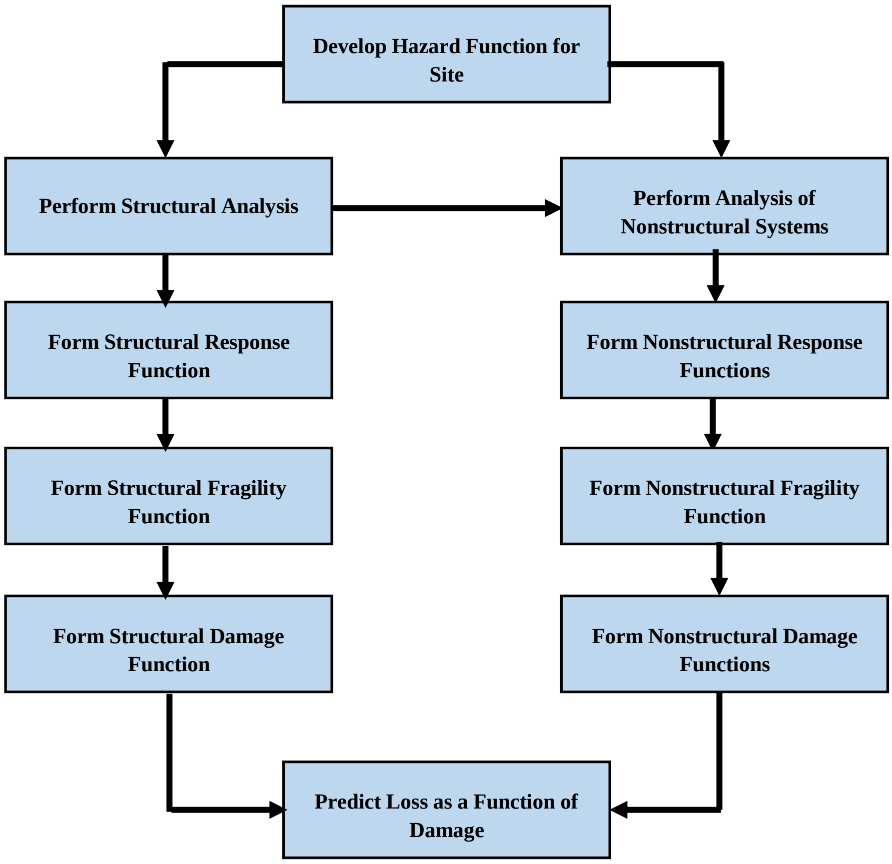

Figure 2.11: ATC-58 performance prediction flowchart

The ATC-58 project employs performance goals that are foreseeable and meaningful for both designers and decision-makers. Initial tasks within the project have shown that these decision-makers, or stakeholders, encompass a diverse range of individuals representing various interests and levels of expertise. Each category of decision-maker approaches performance considerations from a distinct angle and employs different decision-making processes when selecting performance goals (Whittaker et al., 2003).

2.8.4. Performance assessment of buildings under extreme earthquake loads

Various researchers have previously examined the seismic behavior of reinforced concrete (RC) buildings designed and constructed according to current codes, utilizing different frameworks proposed in performance-based earthquake engineering.

Goulet et al. (2007) showcased the implementation of the PBEE methodology by employing PEER Performance-based Earthquake Engineering (PBEE) methodology to predict how well eight variations of a four-story, reinforced concrete (RC), special moment-resisting frame (SMRF) building, built to comply with the 2003 IBC, would withstand seismic activity. Addressing the workflow in the PEER PBEE framework, this work utilized site-specific seismic hazard evaluations, non-linear dynamic structural response analysis up to the point of collapse, damage assessments, and loss estimation to assess the performance concerning structural and non-structural damage, repair expenses, collapse probabilities, and fatality-related losses. Accordingly, performance was measured in terms of economic losses and collapse safety metrics.

2.8.4.1. Non-linear static pushover analysis

Pushover analysis subjects buildings to increasing lateral loads until a predetermined target level is achieved. Pushover analysis can be conducted in two ways: force-controlled and displacement-controlled. In force-controlled analysis, lateral forces are exerted in small increments on the structure. Conversely, displacement-controlled analysis involves gradually increasing the top story displacement, causing the building to deform laterally under the required horizontal force. The magnitude of displacement is proportional to the fundamental horizontal translational mode of the building. In both approaches, adjustments to the building's stiffness matrix may be necessary with each increment, especially during the transition from elastic to inelastic states. The displacement-controlled pushover method is often favored over the force-controlled approach as it allows for analysis up to the desired displacement level without converging issues, allowing the full range of structural responses to be observed (Hyderkhan & Murnal, 2018).

Non-linear static pushover method is a widely acknowledged methodology for assessing the seismic behavior of existing buildings, as well as in the performance-based design of new buildings, which count on ductility or redundancies to withstand seismic loads (Taghinezhad et al., 2018 & Khan, 2013). Since the pushover approach usually is involved in evaluating the capacity of buildings subjected to seismic loads, it is featured in the latest retrofitting guidelines for seismic design (Khan, 2013).

Pushover analysis is a static approach that employs a simplified non-linear method to predict deformations of buildings. In this procedure, a static lateral force distribution is imposed on the building, typically in proportion to the design force profiles specified by building codes. This force profile undergoes gradual increments in small steps, with the building being evaluated at each stage (Hyderkhan & Murnal, 2018). When structures undergo earthquake forces, they redesign themselves (Khan, 2013). As the applied load increases, specific locations within the building experience yield (Hyderkhan & Murnal, 2018). When individual structural components are subject to yielding or failure, the remaining structural components bear an additional share of the dynamic forces previously catered by the failed element (Khan, 2013). With each yielding event, the structural properties are adjusted to estimate the effects of yielding (Hyderkhan & Murnal, 2018). The pushover method illustrates this incident by imposing loads on the building until the analysis identifies the initial structural component to fail. Subsequently, it revises the model to address the structural alterations induced by the weakened component. After completing the initial iteration, the second iteration begins redistributing the loads. Again, the structure is pushed until the analysis identifies the second component to fail (Khan, 2013). This process persists until the analysis identifies a yielding pattern for the overall structure on a global scale and of form, and the structure either collapses or reaches a predetermined level of lateral displacement (Khan, 2013).

This iterative process produces a load-deflection curve, illustrating the structural response from a resting stage to ultimate failure. The load represents the equivalent static load associated with the fundamental mode of the structure, often expressed as the base shear. The deflection is usually measured at the top story. This method's precise, appropriate lateral load distribution choice is crucial (Hyderkhan & Murnal, 2018).

Although pushover analysis cannot accurately assess the structure's performance against dynamic earthquake loading, literature provides some evidence from the studies that used non-linear static pushover analysis, as discussed below.

Goulet et al. (2007) employed the static pushover method to examine the overall load-deflection behavior of the benchmark building and assess the impact of different modeling assumptions on the results. These analyses adhered to a static lateral force distribution in line with seismic design requirements. Patil & Kori (2021) utilized non-linear static analysis to measure the performance of five-moment resisting frames with 4, 8, 12, 16, and 20 stories, which were analyzed and designed following the guidelines of the seismic codes. Pierre & Hidayat (2020) analyzed an eighteen-story office building comprising a reinforced concrete frame using the pushover method. As per their conclusions, the analyzed building falls within the Immediate Occupancy performance level. This implies that while the building has sustained some damage, its strength and stiffness remain nearly unchanged compared to its pre-earthquake condition, allowing the building to be reused.

Since pushover analysis is a static, non-linear method that does not fully capture the dynamic effects of earthquakes, extensive research studies have not been undertaken in this area. The literature highlights the inherent limitations of pushover analysis when used solely for seismic assessment of buildings. However, it presents the implications of applying pushover analysis to assess the behavior of buildings experiencing the combined effect of wind and earthquake forces. Hence, further research and development are required in this area.

2.8.4.2. Non-linear dynamic time-history analysis (NDTHA) and incremental dynamic analysis (IDA)

Non-linear dynamic time-history analysis (NDTHA) linked with incremental dynamic analysis (IDA) is a technique utilized to evaluate how structures perform under various earthquake intensities. It is essential to note that this method is time-consuming, similar to other time-history approaches, and heavily depends on the availability of records. However, relying solely on a single seismic record in IDA may not fully capture a structure's behavior for future earthquakes, as the accuracy of IDA heavily depends on the chosen records. Hence, conducting IDA studies using multiple records representing a range of seismic conditions for a given structural model is crucial. This approach produces a series of IDA curves illustrating how the structure responds to different seismic inputs, all standardized using the same intensity measures (IMs) and engineering demand parameters (EDPs). Carefully selecting intensity measures and engineering demand parameters is a crucial aspect of incremental dynamic analysis (Hyderkhan & Murnal, 2018).

Notably, this method has gained acceptance in the Federal Emergency Management Agency (FEMA) guidelines, endorsing its suitability for evaluating the potential collapse capacity of entire structures. Because earthquakes are dynamic and non-linear, IDA results are believed to closely estimate the structural behavior during seismic events relative to other kinds of analyses, making it a more realistic approach than alternative analyses (Hyderkhan & Murnal, 2018). Several research studies have highlighted the suitability of time-history methodology followed by incremental dynamic analysis over pushover analysis to assess the performance of structures under earthquake loading.

In 2018, Taghinezhad et al. evaluated the reliability of pushover analysis in predicting the story drifts of buildings subjected to various lateral load patterns. For this work, they analyzed a few reinforced concrete moment frames of different heights under pushover and time-history methodologies. They found that none of the horizontal load patterns considered in the pushover methodology can estimate a story drift distribution close enough to that of the non-linear time-history analysis. They underscored that it is essential to gauge the potential error that could impact the accuracy of the story drift because of the constraints and assumptions associated with the pushover methodology. Taghinezhad et al. (2018) emphasized that it is crucial to accurately predict the story drifts and their distribution along the building's height to assess the seismic behavior of buildings, since damages to non-structural components are directly associated with the story drifts of the building.

Hyderkhan and Murnal (2018) investigated the effectiveness of incremental dynamic analysis curves and pushover curves in evaluating the seismic behavior of reinforced concrete buildings. Their research focused on buildings employing extraordinary and ordinary moment-resisting systems, all sharing identical floor plans and consistent story heights. In their study, incremental dynamic analysis and pushover analysis were carried out on G+3, G+6, and G+12 structures using SMRF and OMRF frames to assess their seismic behavior concerning the recorded maximum displacement at the top floor. Their outcomes indicated that structures show a higher response in maximum top story displacement when subjected to incremental dynamic analysis than pushover analysis, even when the base shear value remains the same. Also, they concluded that the findings from the incremental dynamic analysis are more accurate and generally yield higher values than those obtained from non-linear static pushover analysis (Hyderkhan & Murnal, 2018).

Further to the magnitude change in response of a building subjected to incremental dynamic analysis and pushover analysis, Goulet et al. (2007) stated that different ground motions trigger various collapse mechanisms, and the collapse mechanism expected from the non-linear static pushover method is not the major collapse mechanism witnessed in the time-history response method.

As discussed below, most studies that used non-linear dynamic time-history analysis, incremental dynamic analysis, and fragility analysis have yielded significant results.

Goulet et al. (2007) utilized non-linear dynamic analyses to evaluate the seismic behavior of code-based reinforced concrete frames. They used ground motion suites corresponding to seven selected intensity levels for this evaluation. Their study found that it's crucial to consider the response spectral shape when choosing earthquake records for non-linear dynamic assessments aligned with a specific level of hazard indicated by a response spectral value at the fundamental period of the building, mainly when dealing with higher hazard levels. They have also stated that ignoring these factors when selecting records might result in a 5-10 times overprediction of the mean annual collapse rate.

Patil & Kori (2021) utilized non-linear dynamic analysis to measure the behavior of five-moment resisting frames with 4, 8, 12, 16, and 20 stories. These frames were analyzed and designed following the guidelines of the seismic codes. These assessments concerned member failures and structural performance regarding displacement and ductility.

Taking into account the uncertainties in structural modeling and the variability among earthquake records, Goulet et al. (2007) found that the likelihood of collapse of eight variations of a four-story, reinforced concrete (RC), special moment-resisting frame (SMRF) built to comply with the 2003 IBC falls between 2% and 7% for seismic ground motions, with a 2% likelihood of occurrence over 50 years.

The research detailed in the paper by Haselton et al. (2011) highlights how non-linear dynamic analysis can effectively assess collapse scenarios. It emphasizes the importance of such evaluations in forming and improving building code regulations to ensure consistent safety standards for buildings.

These investigations underscore the vulnerability of buildings constructed per code-based standards to seismic occurrences characterized by return periods surpassing those anticipated during the design process. Consequently, such buildings cannot be deemed resilient solely based on their compliance with design-level seismic requirements.

2.9. Summary

The literature highlights Sri Lanka's vulnerability to wind and earthquake hazards and emphasizes the importance of enhancing disaster resilience in its built environment. Ensuring disaster resilience involves extensive analyses, including hazard analysis, structural analysis, damage analysis, and loss analysis. Together, these analyses provide a concise picture of disaster resilience, encompassing the fatalities, repair costs, and downtime. The structural engineering aspect of disaster resilience pertains explicitly to “structural analysis” and aligns well with performance-based engineering. The literature underlines the importance of integrating performance-based design methodologies alongside code-based approaches to strengthen the structural resilience of buildings within the broader framework of "disaster resilience."

Building design codes and standards are vital in maintaining disaster resilience in the built environment. Adopting Eurocodes for designing disaster-resilient buildings in Sri Lanka holds significant promise for enhancing the structural integrity and safety of the built environment. They provide comprehensive guidelines and standards encompassing various natural disasters, including earthquakes and windstorms, pertinent to Sri Lanka's diverse climatic and geological conditions.

Sri Lanka started using Eurocodes as early as 2010 and has recently produced national annexes for many Eurocodes. However, up to date, neither the accuracy of Eurocodes nor the effectiveness of national annexes for designing disaster-resilient buildings.has been subjected to critical evaluation in the Sri Lankan context.

Non-linear static pushover analysis is an effective method for assessing the behavior of buildings under extreme wind conditions. It can also be utilized to determine the response of buildings subjected to the combined action of wind and seismic loadings. However, it is less suitable for buildings subjected solely to seismic loading. In contrast, non-linear dynamic time-history analysis, linked with incremental dynamic analysis and fragility assessment, has a proven track record in the literature for assessing the behavior of buildings subjected to extreme seismic action. These analyses help determine the level of structural resilience in both code-compliant and non-code-compliant buildings. Additionally, they can appraise proposals for retrofitting existing defective buildings for their structural resilience.

Building on the identified research gaps and best practices highlighted in the literature, the subsequent chapters of this thesis will conduct thorough analyses and interpret the results to provide conclusions, offer recommendations, and suggest future research directions regarding adopting Eurocodes for designing disaster-resilient buildings in Sri Lanka.

CHAPTER 3 : PLANNING, DESIGNING AND CONSTRUCTING SUBSTRUCTURES FOR BUILDING RESILIENCE

3.1. General

Geotechnical engineers face the complex task of designing new foundations for seismic loading and retrofitting existing foundations. Designing foundations for seismic loading necessitates expertise in soil mechanics, foundation engineering, soil-structure interaction, and structural dynamics (Pecker & Pender, 2000).

The foundations should be safe from the static and dynamic/seismic loads induced by earthquakes. The conventional static design of foundations focuses on the failure behavior concerning the bearing capacity. Moreover, the static design of foundations utilizes a suitable factor of safety (around 3) and considers the short-term settlements acceptable. Sound settlement predictions require knowledge of soil behavior (Pecker & Pender, 2000).

Following the failures of foundations witnessed in the earthquakes in Mexico City in 1985 and Kobe, Japan, in 1995, several studies attempted to estimate seismic bearing capacity. Since the soil-structure interactions govern the structural behavior of seismic-excited buildings, the seismic design of foundations should consider the non-linear behavior of soils and the cyclic deformations of foundations. With the advancement in knowledge, building codes started considering these aspects of designing foundations to withstand seismic forces. Eurocode 8: Design of structures for earthquake resistance - Part 5: Foundations, retaining structures, and geotechnical aspects (EN 1998-5:2004 (E)) is one such pioneering code (Pecker & Pender, 2000).

Although the present study, “The Implications of Adopting Eurocodes for Designing Disaster Resilient Buildings in Sri Lanka,” basically concentrates on the structural resilience of building superstructures, this chapter provides a literature review-based overview of the basic principles of designing foundations for earthquake resistance, foundation failure modes, damages incurred in past earthquake events, new knowledge, and the best practices of designing and constructing foundations. First, this chapter briefly discusses current knowledge to identify gaps that should be addressed in future research.

3.2. Philosophy of foundation design to seismic loading

As Pender (1995) explained, designing foundations to withstand seismic forces is an extensive process that requires understanding, innovation, technical expertise, and practical experience. According to Pecker & Pender (2000), it is an iterative process rather than a linear progression that involves the key stages: (i) the soil profile's geological setting and geotechnical properties, (ii) the characterization of the loads on the foundation soil by the structure, (iii) structure's performance requirements, (iv) examination of probable solutions, including load capacity evaluation, safety factor calculations, and deformation predictions, (v) accounting for construction techniques and practical limitations such as budget and schedule, (vi) applying judgment to evaluate possible risks.

3.2.1. Fundamentals of soil-structure interaction for the evaluation of seismic loads

When buildings experience seismic activity, the forces of inertia develop in the superstructures, and soil deformations induce earthquake loads on the foundation. These inertial forces, generated due to the acceleration felt by the structure, are proportional to the acceleration of the mass and act opposite to the ground motion. Soil deformations occur due to the passage of seismic waves through the ground. Literature defines these two phenomena as inertial and kinematic loading. The two phenomena together make the Soil-Structure Interaction (SSI) which depends on the characteristics of the foundation and the incoming wave field (Pecker & Pender, 2000).

Due to the inherent complexity in evaluating kinematic interaction effects compared to inertial interaction effects, most building codes exclude kinematic interaction effects except a few, such as Eurocodes. Often, geotechnical engineers ignore the kinematic component and consider the inertial component as the soil-structure interaction (Pecker & Pender, 2000).

Gazetas-Mylonakis (1998) presented a schematic diagram of these key features of soil-structure interaction for a building with an embedded foundation supported on piles (Figure 3.1). However, the conclusions drawn herein from this study apply to any foundation type.

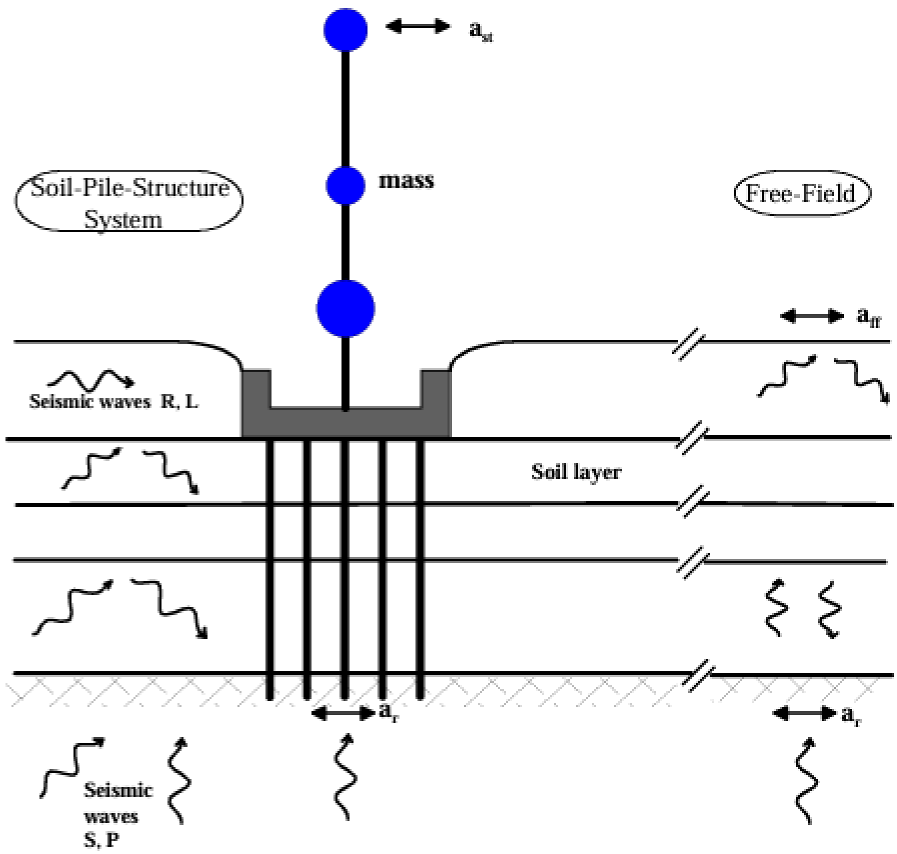

Figure 3.1: Sketch of the soil-structure interaction problem

As shown in Figure 3.1, the soil layers distant from the building are subject to seismic excitation comprising incident waves, namely primary/dilatational waves (P waves) and secondary/shear waves (S waves), which are the body waves, and love waves (L waves) and Rayleigh waves (R waves) which constitute the surface waves. Seismological conditions govern the characteristics of these incoming waves, and the geometry, stiffness, and damping features of soil deposits alter this motion. The resulting modified motion is referred to as the free field motion at the foundation's site.

As Lysmer (1978) explained, determining this modified/free-field motion is difficult since the design ground motion is generally stated at a single point on the ground surface. A back-calculation from incomplete information cannot derive the whole wave field. Since a satisfactory solution is not yet available, assumptions need to be formulated concerning the precise composition of the free-field motion.

When looking at the movement in the vicinity of the structure and its foundation, it is worth mentioning that the seismically deforming soil causes the piles and embedded foundation to move, which will then cause the supported structure to move as well. Even without the superstructure, the foundation's motion will differ from free field motion because of the soil's rigidity relative to the piles and foundations. The incoming waves are reflected and dispersed by the foundation and piles, causing stresses that lead to curvatures and bending moments. This phenomenon is referred to as kinematic interaction.

The movement created at the foundation level causes oscillations in the superstructure, leading to inertia forces and overturning moments at the structure's base. Therefore, additional dynamic forces and displacements occur in the foundation, the piles, and the surrounding soil. This is the inertial interaction phenomenon. The foundations should be evaluated for the joint effect of inertial and kinematic loads.

3.3. Foundation failure modes

The shaking of the ground during an earthquake may impact the shallow foundations in the ways listed below (Puri & Prakash, 2013).

(1) Bearing capacity failure caused by the gradual weakening of soil strength under cyclic loading.

(2) Sliding/overturning of the foundation due to large horizontal inertial forces.

(3) Large settlements and tilting of the foundation due to the liquefaction of soil beneath and around the foundation.

(4) Foundation instability due to ground softening or failure triggered by the pore water pressure redistribution during the post-earthquake stage.

3.4. Lessons from past earthquake events

Earthquake damages to buildings built with wood, masonry, or mixed-construction materials occur due to exceeding the structural elements' load-bearing capacity. With the growing interest in reinforced concrete structures equipped with seismic loading resistance, building damage during the following historical earthquakes has revealed that those building failures were triggered by the reduction in soil-bearing capacity while preserving the structures' integrity (Zięba et al., 2023). For instance, the toppling and leaning of high-rise buildings (Figure 3.2) occurred after an earthquake of magnitude 6.0 struck Hualien (Taiwan) because of the loss of soil-bearing capacity (Zięba et al., 2023).

Figure 3.2: Collapsed an apartment building after reaching the ultimate limit state of the sub-soil, Taiwan 2018.

Failures in the bearing capacity of soils underneath shallow foundations were also reported in Mexico City due to the 1985 Michoacan earthquake (Mendoza and Avunit (1988), Zeevart (1991)) and in Adapazari City during the 1999 Kocaeli earthquake (Karaca (2001), Bakir et al. (2002), and Yilmaz et al. (2004)). Figure 3.3 shows some instances of failures in the bearing capacity of soils underneath foundations after the Adapazari earthquake.

Figure 3.3: Typical examples of bearing capacity failure in the city of Adapazari during the 1999 Kocaeli earthquake. Adapted from (Yilmaz et al., 2004)

The surface soils encountered at these sites fit the CL/ML group. However, the soils in this group are usually considered non-liquefiable (Puri & Prakash, 2013). 0.5-0.7m and 0.5-1.0m settlements were recorded in loose sands in Hachinohe at the time of the 1968 Tokachioki earthquake (magnitude 7.9) and Port and Roko Island in Kobe during the Hygoken Nanbu earthquake (magnitude 6.9), respectively (Puri & Prakash,2013).

Therefore, it is evident that failures of the foundation may happen as a result of a decrease in bearing capacity, extreme settlement, and tiltation, in both liquefying and non-liquefying soils (Puri & Prakash, 2013).

3.5. New knowledge/findings from research

Recently, several researchers have investigated the causes of the massive destruction caused by earthquakes. For instance, Gazetas et al. (2004) carried out a study to understand the causes of the building tiltation after the 1999 Turkey earthquake. An in-depth investigation of the building failures in Adapazari city has indicated that the tilting and toppling were common for slender buildings with an aspect ratio (H/B) greater than two and no adjacent buildings on their lateral sides. In contrast, wider and adjoining buildings experienced a little or no rotation. A summary of their findings stated that overturning occurred in most buildings with H/B greater than 1.8, and only vertical settlements with no visible tilting appeared in buildings with H/B less than 0.8.

Furthermore, Gazetas et al. (2004)) examined soil profiles of a few case study buildings using the SPT and CPT tests. These tests confirmed that the soil profiles from the surface to about 15 m deep contained some alternating sandy-silt and silty-sand layers with point resistance values, $q_c \approx (0.4 - 5.0)$ MPa. The seismo-cone measurements indicated wave velocities (Vs) of less than 60 m/s up to a depth of 15 m. This, too, indicates the presence of extremely soft soil layers. According to their conclusion, even relatively small acceleration values between 0.20g and 0.30g liquefied at least the upper-most 1-2 m thick loose sandy silt layer and generated excess pore-water pressures in the deeper layers, causing heavy destruction (PURI & Prakash, 2007).

3.6. Good practice for the design and construction of foundations for seismic loads

The literature presents that the following good practices should be considered when designing and constructing buildings, especially the foundations, to resist seismic loading.

1. When liquefiable soils are present, the following should be avoided:
   (i) The foundation should not be directly on top of potentially liquefiable soil layers because even foundations with minimal loads can settle into the soil.

(ii) A sufficient depth of soil that does not liquefy should be present to avoid sand boils and surface fissuring from damaging the foundation.

If these requirements are not satisfied, deep foundations or ground improvement may be required (Puri & Prakash, 2013).

2. As per the conclusions drawn by Pecker & Pender (2000) from their study on "Earthquake resistant design of foundations: New construction,"
   (i) Foundations should be located away from major active faults or not span across them. Ground motions in the near field are impossible to predict; hence, designing structures to account for those movements in the near field is not practical.
   (ii) If liquefiable deposits and unstable slopes are present, those should be treated before construction. Pile foundations can resist cyclic deformations of a liquefied layer. However, the larger magnitude quasi-static displacements occurring due to the post-earthquake ground movement can result in distress of the foundation (e.g., Kobe earthquake).
   (iii) The foundation should be planned and constructed homogeneously. Otherwise, construction joints should be provided appropriately. In the case of individual footings, situations where some footings rest on manufactured fills while the other footings rest on natural soils should not be accepted. It is also advisable to plan the foundations to align with the building's symmetry. Upkeeping symmetry in the foundation aids in preserving structural balance and stability, which is vital for surviving seismic loads and other forces.
   (iv) The foundation type should be selected by considering the secondary effects, such as settlements in medium-dense or loose dry sands, consolidation settlements in clay layers following an earthquake, and the settlements triggered by the post-earthquake dissipation of non-liquefiable sand deposit's pore pressures. If the expected settlement exceeds the limits or significantly varies across the building, raft foundations or end-bearing piles must be used.
   (v) At the foundation level, individual footings should be connected with tie beams to avoid uneven footing settling.
   (vi) Piles should be reinforced throughout their lengths, although calculations do not suggest reinforcements throughout. Pile-raft connections and interfaces between soil layers with different stiffnesses should be carefully handled. For example, the pile-raft connection can be designed to form a plastic ductile hinge, as stated in Eurocode 8.
   (vii) It is not recommended to use inclined piles since soil densification after an earthquake can induce parasitic bending stresses. This leads to significant

forces transferring onto pile caps. If the pile arrangement is asymmetrical, permanent rotations may occur due to the dissimilar stiffness of the pile group in different loading directions.

3.7. Summary

Extensive research has been dedicated to examining the failure patterns and causes of foundation failures triggered by earthquakes. Moreover, research has been undertaken to outline the failure surfaces beneath shallow foundations exposed to static and earthquake loads and foundation settlements.

As evident from structural damage by earthquakes, a thorough understanding of the soil-structure interaction is of utmost importance in preventing earthquake-induced damage to structures, alongside maintaining the structural resilience of the buildings' superstructure to extreme seismic loading. Several researchers have described the methods used to design foundations for static and seismic loading and compared design methodologies with different codes and standards, such as Eurocodes. However, to the author's knowledge, building superstructures and their substructures/foundations have not been modeled, focusing on the soil-structure interaction to simulate how well the code-compliant/non-code-compliant foundations perform under extreme seismic loading.

Although Sri Lanka is less susceptible to earthquakes and hence earthquake-induced foundation failures, it is advisable to have an in-depth knowledge of how the soil-structure interaction can lead to foundation failure. Applying appropriate measures after analyzing the soil-structure interaction during the planning, designing, and construction stages of buildings can protect structures from seismic loading, which has a highly unpredictable occurrence. Despite being considered a low-risk seismic zone, Sri Lanka has experienced perceptible ground shaking from time to time (e.g., the 1938 earthquake) and minor tremors across the island. Therefore, this understanding is particularly crucial for designing disaster-resilient cities in Sri Lanka, especially in developments like Port City, which is built on reclaimed land in a coastal environment.

CHAPTER 4 : LINEAR ELASTIC MODELING, ANALYSIS, DESIGN, AND DESIGN REVIEW

1.1. General

The structural modeling, analysis, and design process is initiated by preparing general arrangement drawings for the structural system based on Architectural & MEP service drawings. Next, the preliminary sizes of structural elements are calculated by using ultimate and serviceability design loads, ensuring structural safety and integrity, architectural requirements and aesthetics, durability, sustainability, constructability, economic aspects, etc.

Accurate modeling and analysis of structures are essential for determining member forces, which are crucial for the design and construction of safe, stable, and functional buildings. Linear elastic modeling and analysis enable engineers to foresee how structures respond to various anticipated loads even before the construction stage. Assuming that materials exhibit linear elastic behavior, linear elastic analysis evaluates the linear relationships between applied forces and structural responses.

This chapter presents the application of linear elastic modeling and analysis in the design of the selected buildings for this study. Moreover, this chapter discusses the adoption of linear elastic modeling and analysis to review the design of an existing building in Sri Lanka. For these tasks, the present study utilizes SAP2000 software, which is well-recognized in the industry for its comprehensive suite of features for creating structural models, performing analyses, and visualizing results, thereby facilitating the building design process.

4.2. Case studies

This study focuses on six case study buildings: a typical building, a school building, a university building, a hospital building, an existing defective building, and its retrofitted version. These buildings were selected based on various criteria to effectively address the research needs.

The typical building was included as the first case study to illustrate the workflow of the proposed research methodology with a simple example. An office building was selected as the representative example solely to facilitate structural load calculations, given the need for a clearly defined occupancy type under Eurocode loading conditions, its suitability for representation with a low-rise, simple structural layout, and its exclusion from the occupancy categories examined in the main case studies of this research.

The other case study buildings, excluding the existing buildings, were chosen because each serves a crucial role during and after disasters. Therefore, they are expected to include disaster-resilient features. Along with the typical building, the case studies constitute a school building, which functions as a refuge shelter during various disasters; a university building, assumed to oversee the country's telecommunications systems, requiring uninterrupted operation during disasters; and a hospital building, which must operate at full capacity, especially during disasters that threaten public health.

The defective building is a mixed-use building as it serves various types of occupancies on its floors. The basement floor is used for general stores, while the ground floor houses shops. The first, second, and third floors are dedicated to offices. Moving up, the fourth and fifth floors are occupied by residential/duplex houses, with the fifth floor also featuring an open terrace. The sixth floor comprises the roof slab and another open terrace. On the seventh floor, there is a lift machine room and a 4000-liter water tank, and finally, the roof floor consists solely of the roof slab. Although these types of occupancies are not critical during and after disasters, extreme events can easily cause the collapse of buildings with design or construction faults. Therefore, this defective building was included as a case study in this research, as the behavior of such structures is crucial for ensuring the safety of their occupants, as well as the safety of nearby structures, their occupants, and people using nearby roads.

The case study buildings for this research were also selected to represent a variety of features commonly found in modern buildings. These include a three-story typical building and a three-story school building, both with rectangular plan views. The study also includes an eight-story university building with a free-form plan that incorporates several rectangular wings extending perpendicular to the plan's longitudinal axis, as well as a six-story hospital building with a free-form plan and an interior courtyard. In addition to these code-compliant buildings, a seven-story building suspected of having design flaws, along with its retrofitted version, was also included. This defective building has a nearly rectangular plan view with vertical setbacks along its height. All six case study buildings' structural systems are multi-story reinforced concrete frames with columns, beams, floor slabs, roof slabs, and brick or block masonry infill walls. The general arrangement drawings of the case study buildings are provided in Appendix A.

The typical building and school building with disaster-resilient features are assumed to be constructed in Colombo. The university and hospital buildings considered in this study are slightly modified versions of their existing structures, which are located in the Colombo and Nuwara Eliya districts, respectively. The defective building is located in the Colombo district.

4.3. Linear elastic modeling

The three-dimensional finite element models of the typical building, school building, university building, and hospital building, created using Finite Element Modeling software, along with their basic geometric features, are shown in Figures 4.1-4.4, respectively. The member sizes were assigned to these models based on the results of the initial design.

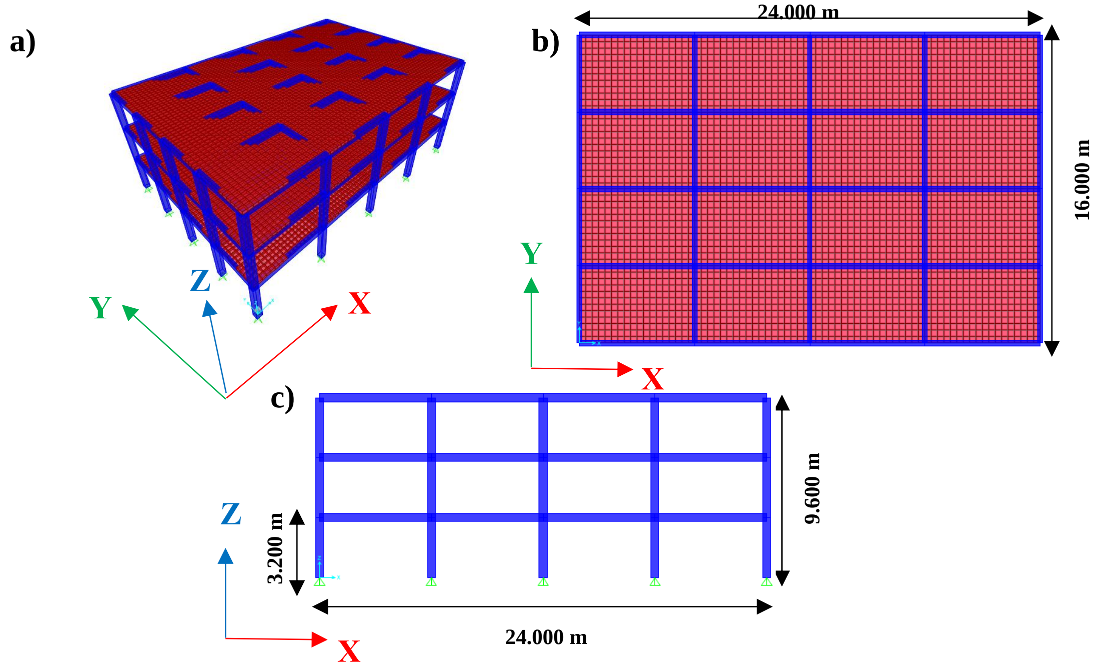

Figure 4.1: Finite element model of the typical office building in SAP2000 software (a) 3D view, (b) plan view, (c) a sectional view

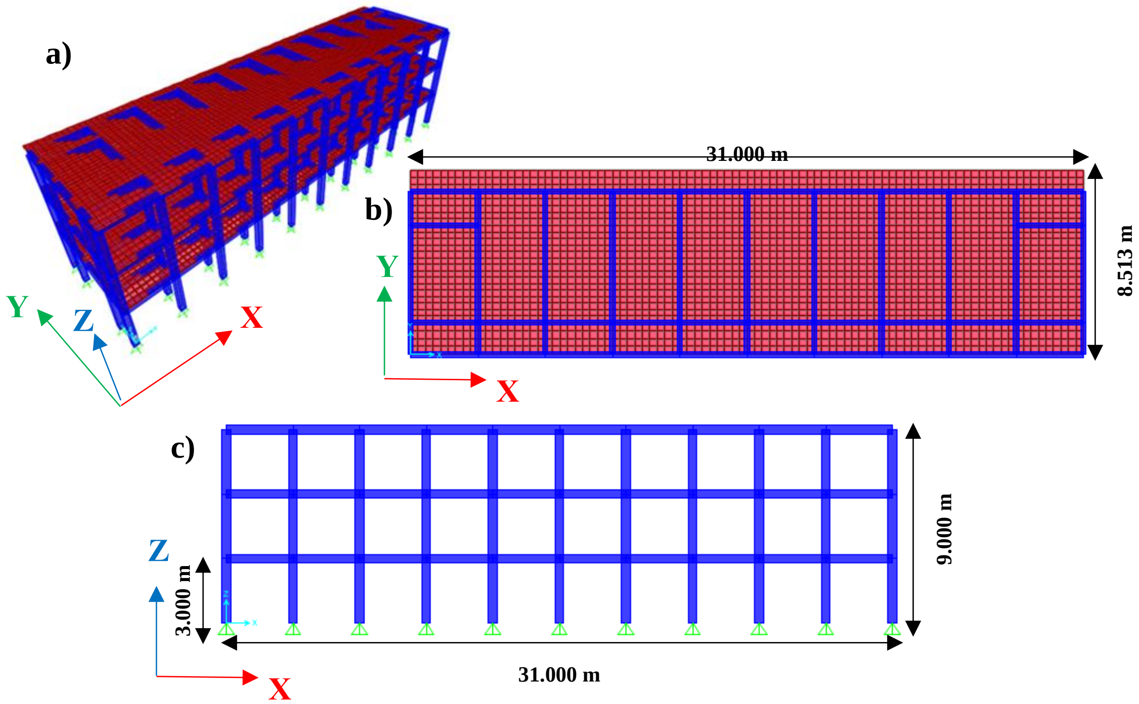

Figure 4.2: Finite element model of the school building in SAP2000 software (a) 3D view, (b) plan view, (c) a sectional view

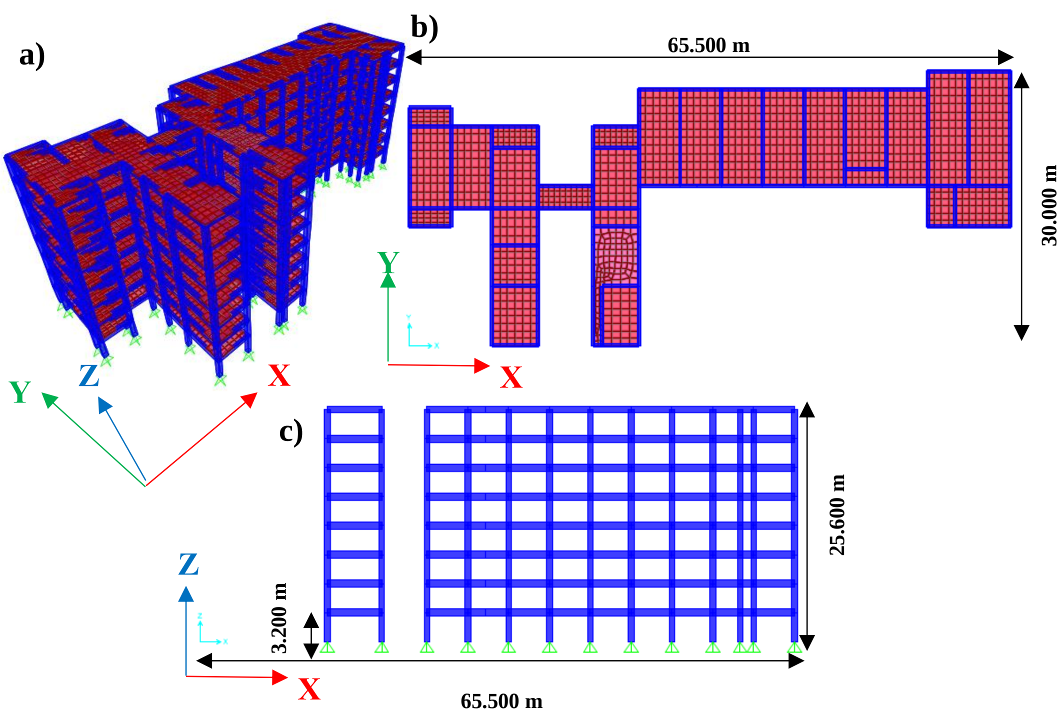

Figure 4.3: Finite element model of the university building in SAP2000 software (a) 3D view, (b) plan view, (c) a sectional view

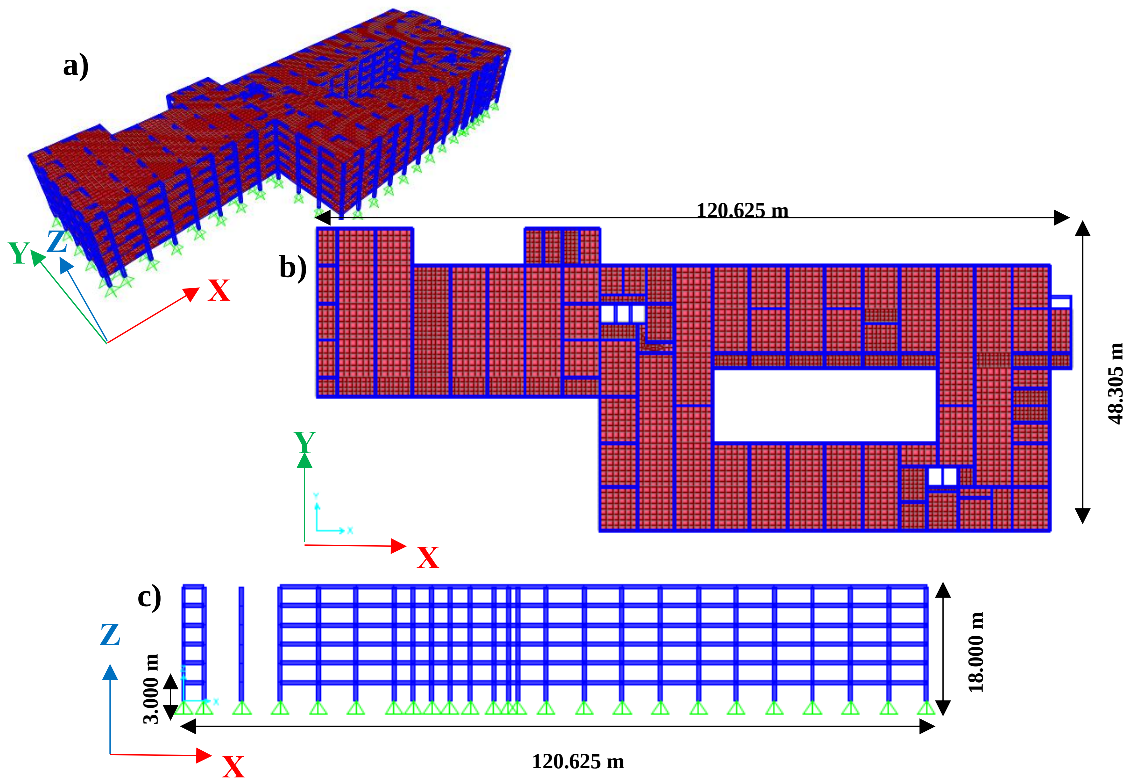

Figure 4.4: Finite element model of the hospital building in SAP2000 software (a) 3D view, (b) plan view, (c) a sectional view

The existing building considered in this study has received objections from nearby residents and local authorities against its faulty construction and has been classified as a threat to the neighbors' safety. At the request of the building owner, a site visit was conducted and the original structural design drawings were provided by the building owner for reference. During the visit, it was observed that only the structural frame and a few infill walls had been constructed; finishes, partitions, and ceiling installations were not yet completed, and the building had not been occupied. After gathering on-site visual observations, it was suspected that this building might have some deficiencies in both its construction and the design utilized for its construction.

Therefore, this building was subjected to thorough visual inspections to identify its architectural features, structural system arrangement, load path, and any visible defects. By the time of the site inspection, the main structural system had been completed, and further construction had been terminated. An internal staircase and a lift provide vertical circulation to the upper floors.

This building was tested for the material properties (i.e., material strengths), section sizes, and reinforcement arrangements to check whether it was constructed as per the original structural drawings. Core tests were conducted to determine the compressive strength of concrete in the slabs. Rebound hammer tests were used to estimate the compressive strength of concrete in beams and columns. Cover meter tests were carried out to determine the dimensions of structural members, the concrete cover to reinforcement, and the reinforcement layout, including bar diameters and spacing. The test locations and relevant tests were chosen based on engineering judgment and previous experience to ensure that those locations accurately represent the overall building, provide sufficient data to interpret building stability, minimize structural impact, and remain financially viable.

The existing building was found to deviate from the original structural drawings provided by the building owner, particularly in the sizing and detailing of load-bearing elements such as beams and columns, as well as in construction quality. These deviations were identified through on-site observations and by comparing the original design drawings with the actual site conditions, as revealed through material testing. Typical issues observed included variations in cross-sectional dimensions and reinforcement arrangements. However, the original design drawings provided by the building owner were found to be adequate for safely carrying the gravity and wind loads. Therefore, if the building had been constructed in accordance with these original design drawings, it would have qualified as a code-based building.

Since this building was not constructed according to the original structural design drawings, it was decided to simulate it using the actual site conditions to assess the impact of the design efficiencies and construction faults on achieving resilience targets, rather than relying on the original design drawings that resulted in a code-based building. The dimensions and the member sizes shown in the as-built drawings and the building material test report, along with the strength properties obtained from the building material test report, were utilized when creating a finite element model of the existing building. However, only the geometric properties were considered in the finite element model, even though the reinforcement details of the existing building were known. Due to modeling complexities, reinforcement details were not included in the finite element analysis; however, they were taken into account during the structural design checks. The omission of rebar modeling was due to simplification assumptions aimed at reducing computational complexity.

A retrofitting proposal was developed to address the structural design deficiencies identified in the existing building. This approach aimed to apply a practical retrofitting technique commonly used in Sri Lanka, known as concrete jacketing or section enlargement with reinforcements. The proposed method involved the structural concrete jacketing of all beams and columns, which was found to be structurally inadequate, wherein a new layer of concrete with embedded reinforcement was added to the original members. Specifically, this retrofitting strategy focused on enlarging the cross-sectional dimensions of the deficient beams and columns to meet the minimum code-based requirements, including structural adequacy and the required concrete cover to new reinforcement. The proposal was formulated by estimating the necessary increases in member dimensions, as well as the appropriate reinforcement bar diameters and quantities to be embedded within the jackets. Several iterations were carried out to refine the assumed section sizes and reinforcement layouts. The analysis presented in this study is based exclusively on Iteration I, and the enlarged member dimensions specified in Retrofitting Proposal I were incorporated into the finite element model of the retrofitted building.

For example, Figures 4.5 and 4.6 show the existing and retrofitted sections of a defective column and beam in the building.

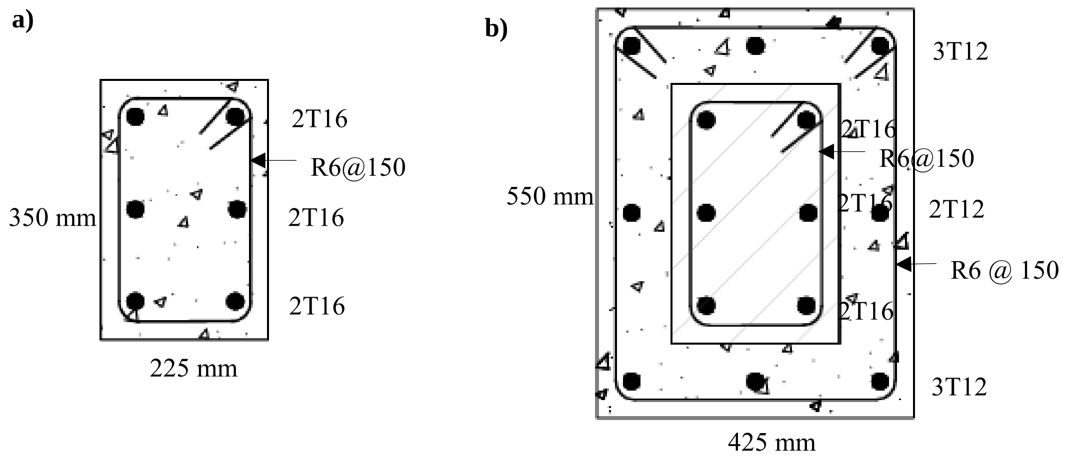

Figure 4.5: Section sizes and reinforcement details (a) defective column, (b) retrofitted column

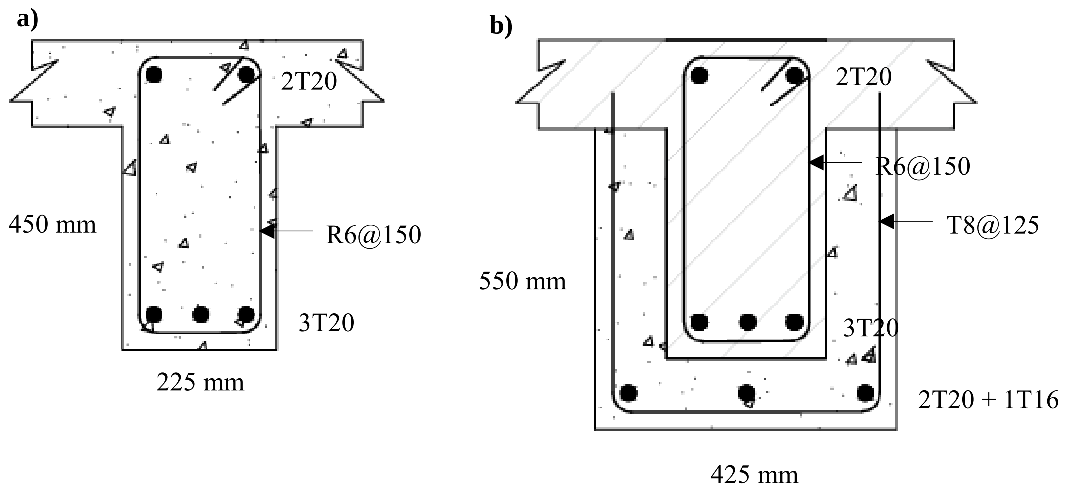

Figure 4.6: Section sizes and reinforcement details (a) defective beam, (b) retrofitted beam

The retrofitted building was modeled by replacing the beam and column dimensions in the existing building model with the corresponding enlarged dimensions specified in Retrofitting Proposal I. However, only the geometric properties were considered in the finite element model, despite the availability of reinforcement details for the existing building. Due to modeling complexities, reinforcement was not included in the finite element analysis, although it was considered during the structural design checks. The omission of rebar modeling was due to simplification assumptions aimed at reducing computational complexity. In addition, material interface effects such as the bond and potential slip between the existing and newly added concrete were not incorporated in the model due to modeling limitations.

Figures 4.7 and 4.8 illustrate the three-dimensional finite element models of the defective and retrofitted buildings, simulated in the finite element modeling software, along with their basic geometric features.

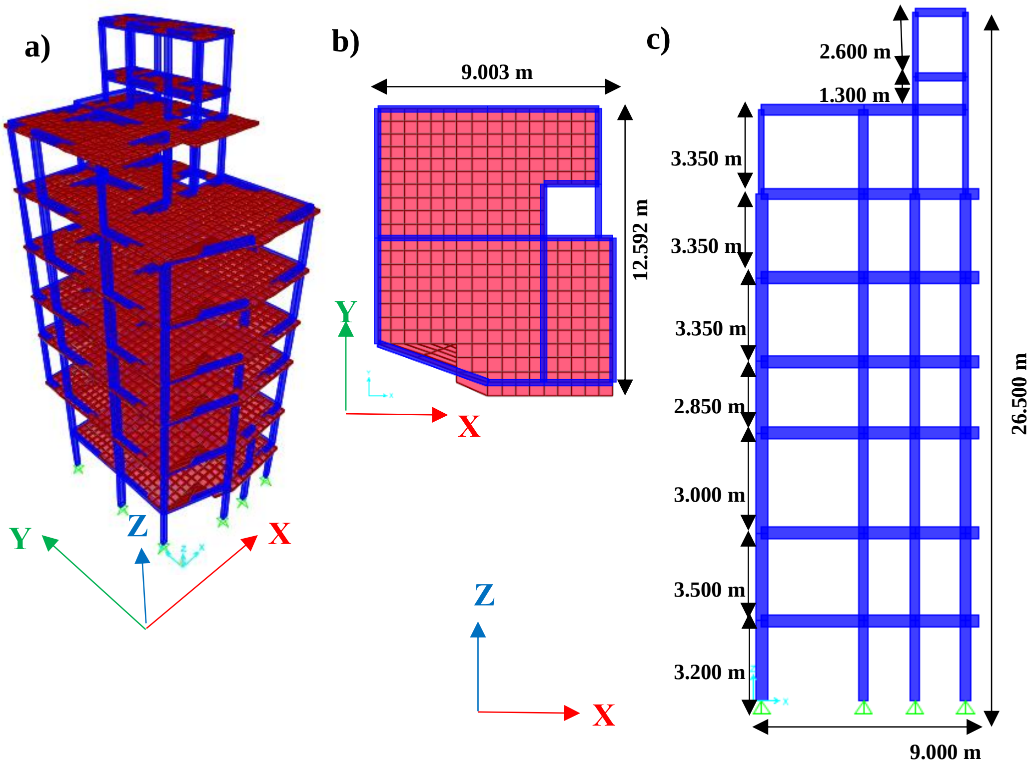

Figure 4.7: Finite element model of the defective building in SAP2000 software (a) 3D view, (b) plan view, (c) a sectional view

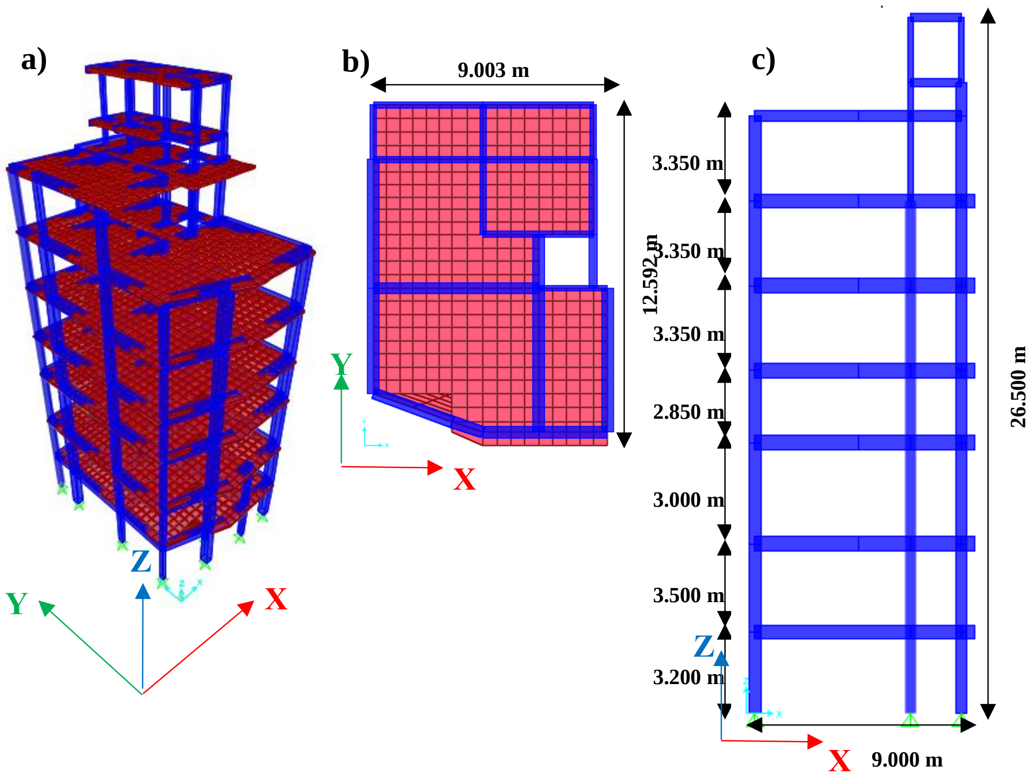

Figure 4.8: Finite element model of the retrofitted building in SAP2000 software (a) 3D view, (b) plan view, (c) a sectional view

4.3.1. Load schedule

Various loads acting on the case study buildings were identified during the conceptual design stage of this study. These loads include gravity loads and lateral loads. Gravity loads comprise permanent and imposed loads. Lateral loads comprise wind and seismic forces, relating to the focus of the current study.

Since only the dead loads, superimposed dead loads, imposed loads, and wind loads had been considered in the defective building's original structural design and the existing building was not constructed as per the original structural drawings, it was tested only for dead, superimposed dead, imposed, and wind loads. Seismic loads were not considered for the defective building, as it would be irrelevant to evaluate the seismic load-bearing capacity of a building that was not designed to accommodate such loads.

All the loads considered in this study are based on each building's occupancy type and are per the relevant Eurocodes and their Sri Lankan national annexes.

4.3.1.1. Permanent loads

Permanent loads can be classified into two main types based on their nature: dead loads and superimposed dead loads. Self-weights of building elements, including columns, beams, slabs, and walls, constitute dead loads, while loads due to partitions, finishes, ceilings, and services are considered superimposed dead loads.

Dead loads from the columns, beams, and slabs were assigned to the building models by the Finite Element Modeling software based on the member sizes and concrete unit weight. Wall loads were calculated based on the wall thickness, height, and the unit weight of walling materials. Then, the wall loads were applied as line loads on the beams. Accordingly, material densities/unit weights were the input to the Finite Element Modeling software and utilized to calculate the dead loads. The unit weights of reinforced concrete, steel reinforcement, brick masonry, and block masonry were considered 25.0 kN/m^3, 78.5 kN/m^3, 19.0 kN/m^3, and 21.0 kN/m^3, respectively.

Superimposed dead loads from partition loads, finishes, ceilings, and services were chosen based on the recommendations in the IStructE Manual for the design of concrete building structures to Eurocode 2. Accordingly, the superimposed dead loads should be sufficient and not be lower than the recommended levels during the initial design stage. These loads were subjected to variations depending on the usage of some floor areas (e.g., MEP rooms, toilets, roof slabs).

Accordingly, the superimposed dead loads listed in Table 4.1 were considered for the case study buildings.

4.3.1.2. Imposed loads

In this study, the imposed loads on the buildings were determined according to EN 1991-1-1: 2002: Eurocode 1: Actions on structures - Part 1-1: General actions – Densities, self-weight, imposed loads for buildings.

Accordingly, the superimposed dead loads and imposed loads outlined in Table 4.1 were considered for the case study buildings based on their usage type. These loads varied depending on the usage of some floor areas (e.g., MEP rooms, toilets, and roof slabs).

Table 4.1: Schedule of loads on the case study buildings

Building	Floor	Superimposed Dead Load (kN/m²)			Imposed Load (kN/m²)
		Partitions	Finishes	Ceiling and Services	
Typical building	Typical floors	1.0	1.8	0.5	2.0
	Roof floor	0.0	2.8	0.5	0.4
School building	Typical floors	-	1.8	0.5	3.0
	Roof floor	0.0	2.8	0.5	0.4
University building	Typical floors	1.0	1.8	0.5	4.0
	Roof floor	0.0	2.8	0.5	0.4
Hospital building	Typical floors	1.0	1.8	0.5	5.0
	Roof floor	0.0	2.8	0.5	0.4
Defective / retrofitted buildings	Basement floor - General stores	1.0	1.5	0.5	5.0
	Ground floor - Shops	1.0	1.5	0.5	4.0
	First floor - Offices	1.0	1.5	0.5	2.5
	Second floor - Offices	1.0	1.5	0.5	2.5
	Third floor - Offices	1.0	1.5	0.5	2.5
	Fourth floor - Residential/duplex houses	1.0	1.5	0.5	2.0
	Fifth floor - Residential/duplex houses and open terrace	1.0	1.5 (2.5 for open terrace)	0.5	2.0 (4.0 for open terrace)
	Sixth floor - Roof slab and open terrace	0	2.5	0.5	4.0
	Seventh floor - Lift machine room and 4000 L water tank	0	2.5	0.5	7.5
	Eighth floor - Roof slab	0	2.5	0.5	2.0
	A staircase on every floor - Foot traffic only	0	2.5	0.5	4.0

4.3.1.3. Wind loads

Wind loads on the first four case study buildings and the defective, retrofitted buildings were calculated according to Eurocode 1: Actions on structures - Part 1-4: General actions - Wind actions (EN 1991-1-4:2005) and the Sri Lankan national annex, considering the post-disaster functionality of disaster-resilient buildings and normal structures, respectively. The wind forces on each floor were calculated by multiplying the pressure distribution derived from the code with the tributary area. This calculation involved multiplying half the height of both the stories below and above by the building's width on that particular side, which varies depending on the wind loading direction.

Appendix B provides a summary of the calculated wind loads on the case study buildings.

4.3.1.4. Seismic loads

Seismic loads on the buildings were calculated following the EN 1998-1:2004+A1:2013: Eurocode 8: Design of structures for earthquake resistance - Part 1: General rules, seismic actions and rules for buildings. Since the preparation of the Sri Lankan national annex for Eurocode 8 is at an initial stage, national guidelines established by Kularathna et al. (2013) for the seismic assessment and design of (engineered) buildings in Sri Lanka were employed in this study.

The earthquake forces on each building floor were computed by multiplying the seismic mass of each floor by the corresponding spectral acceleration. This seismic mass calculation involved the total permanent load and 30% of the total imposed load, as specified by Eurocode 8.

Appendix C provides a summary of the calculated seismic loads on the case study buildings.

4.4. Linear elastic analysis

In this study, the structural analysis of the typical building, school building, university building, and hospital building was conducted by applying the expected loads on the Finite Element Models. The structural analysis of the defective building and the retrofitted building was performed by applying the existing loads (self-weight of the structural elements and walls) and the expected loads (superimposed dead loads, imposed loads, and wind loads) to the finite element model. The load combinations, derived from EN 1990:2002+A1:2005: Eurocode - Basis of structural design, and the envelope of these load combinations were considered for the analyses. The maximum member forces in the critical structural elements of each building were obtained from the finite element model to utilize in the structural design and structural design review.

Appendix D provides a summary of the maximum member forces in the basic structural elements of the newly designed buildings.

4.5. Linear elastic design

All structural elements of the first four case study buildings: Typical Building, School Building, University Building, and Hospital Building were designed based on the limit state design principle while meeting the serviceability limit state and ultimate limit state design criterion specified in the Eurocodes. The structural design was conducted per Eurocode 2: Design of concrete structures-Part 1-1: General rules and rules for buildings (EN 1992-1-1:2004), and the Sri Lankan national annex. These documents proposed section sizes and reinforcement arrangements for the maximum member forces. Appendix E provides a summary of the section sizes and the reinforcement details.

4.6. Structural design review

Based on the building material test report, it was confirmed that the existing building considered in this study was not constructed according to the section sizes and the reinforcement arrangement given in the original structural drawings. Therefore, this building was classified as non-compliant with the provided structural design drawings. However, the building remains without major structural defects, likely because only the dead loads and minimal superimposed loads are currently applied to the structure. Therefore, the key focus of this section of the study is to check the adequacy of this existing building to resist both the existing and anticipated loads.

The structural design review conducted per Eurocode 2: Design of concrete structures - Part 1-1: General rules and rules for buildings (EN 1992-1-1:2004) and its Sri Lankan national annex revealed that the member section sizes and reinforcement arrangements of several beams and columns in the existing building are insufficient to bear the member forces resulting from the existing dead loads and superimposed loads, despite the building currently supporting these loads without any visible signs of distress. This is likely due to the higher design loads considered in the analysis compared to the actual loads currently acting on the building, as well as the inclusion of material safety factors in the structural design checks. Furthermore, a significant portion of the beams and columns in the existing building are insufficient to bear the member forces under the full range of expected loads, including superimposed dead loads, imposed loads, and wind loads associated with the building’s intended future use. Therefore, the design calculations confirmed that while the building can safely transfer the existing loads in its present actual condition, it cannot handle the expected loads.

Unlike the first four code-based case studies, this existing building is classified as a non-code-based structure or a defective structure. Structural design checks revealed several design deficiencies, particularly in the sizing and detailing of load-bearing elements such as beams and columns. Common issues observed include undersized cross-sections and inadequate reinforcement.

Since the structural arrangement, section sizes, and reinforcement details are inadequate to cater to the expected loads, a retrofitting measure has been proposed to strengthen this building. The proposed retrofitting involves adding new columns, beams, and required slab panels to the structure and jacketing the existing foundation, columns, and beams that are vulnerable to failure. Therefore, the present study also focuses on evaluating the adequacy of this retrofitting proposal to bear future loads, intending to use these results to determine the effectiveness of retrofitting in improving the wind and seismic performance of buildings.

With retrofitting, the permanent loads from the self-weight of the structural elements were increased due to the addition of new columns, beams, slab panels, and reinforced concrete jackets introduced to some of the beams and columns. Additionally, the superimposed dead loads, imposed loads, and wind loads were slightly increased in the area where the extent of the ground floor was expanded by adding extra columns, beams, and slab panels.

A linear elastic analysis of the retrofitted building was conducted to find the additional member forces on the structural elements due to the added loads. The modified structure was analyzed with modified element stiffness with additional dead loads, superimposed dead loads, imposed loads, and wind loads. Responses of the two analyses conducted for the existing and the modified buildings were superimposed to get the final design responses.

The structural design checks conducted for the retrofitted building based on Retrofitting Proposal I found that the columns are capable of safely carrying all anticipated loads under the serviceability limit state (unfactored loads). However, some columns failed to meet the requirements under the ultimate limit state (factored loads), indicating the need for further revisions to Retrofitting Proposal I.

Regarding the beam design checks, it was confirmed that the beams can adequately resist the sagging bending moments and shear forces induced by the expected loads under the ultimate limit state (factored loads). However, some beams did not satisfy the requirements for resisting hogging bending moments at the supports under both serviceability (unfactored loads) and ultimate limit states (factored loads).

This is because reinforced concrete jacketing with additional reinforcement placed at the bottom primarily enhances a beam's sagging bending moment capacity while having minimal effect on its hogging moment capacity near the supports. However, alternative methods, such as attaching a steel plate to the top of the beam, can be employed to improve hogging moment capacity.

It was confirmed that the retrofitting proposal I is not adequate for enhancing the gravity and wind load-bearing capacity of the defective building. Also, the substructure of the building, which is a raft foundation, necessitates further modifications, such as an overlay on the existing raft foundation to increase its thickness. Although the retrofitted building, as per Retrofitting Proposal I, was also found to be non-compliant with Eurocode requirements, it was included as a case study in this research to evaluate the extent of structural resilience enhancement achieved through the proposed retrofitting intervention.

4.7. Summary

In this chapter, linear elastic modeling, analysis, and design of four buildings, including a typical office building, a school building, a university building, and a hospital building, were carried out per the Eurocodes and their Sri Lankan national annexes. The final output of this chapter, which is the structural design of members, forms the basis for the next chapter, which focuses on non-linear inelastic modeling.

Additionally, an existing building suspected to be defective was subjected to a design review to confirm its inadequacy in resisting design loads. The proposed retrofitting to strengthen this defective building was also evaluated for its capability to enhance the building's load-carrying capacity. Since the retrofitting proposal was found to meet the client's needs for strengthening the building, the structural details of this defective building and the retrofitted building will also be used in the next chapter on non-linear inelastic modeling.

CHAPTER 5 : NON-LINEAR INELASTIC MODELING OF BUILDINGS

5.1. General

Linear elastic models can accurately predict the structural performance of structures within their elastic limits, where structural responses linearly vary with the applied forces. However, materials, cross sections, structural components, and structures exhibit significant non-linear and inelastic behavior in extreme loading events, and conventional linear elastic models cannot accurately predict structural performance during these extreme events.

Non-linear inelastic modeling can predict complex structural behavior under extreme loading conditions, including seismic events. This chapter investigates the principles and application of non-linear inelastic modeling, forming the basis for non-linear analysis of a typical building and three specific case study buildings: a school, a university, and a hospital. For this task, the present study harnesses the power of PERFORM-3D software - a comprehensive and robust software developed by Computers & Structures Inc. (CSI) for advanced non-linear modeling, analysis, and performance assessment of 3D structures. Its ability to simulate structures' inelastic behavior and provide insights into their performance under extreme loading conditions instills confidence in the accuracy and reliability of the results.

5.2. Non-linear inelastic modeling of buildings

Structures' responses mainly depend on complex interactions between materials, structural components' geometry, and the magnitude and duration of external loading. Under low to moderate loads, structures generally exhibit linear elastic behavior in which the deformations are directly proportional to the applied forces. In linear behavior, the materials return to their original shapes upon removing loads. In contrast, structures exhibit non-linear inelastic behavior under extreme loads, which cannot return to the structural element's original status.

The non-linear behavior of structures can be categorized into material non-linearity, geometric non-linearity, and inelastic behavior. Material non-linearity occurs when material strength exceeds the elastic limit. This causes structural elements to undergo plastic deformations, resulting in permanent deformations and potential damage. Geometric non-linearity occurs due to large deformations of structures that alter the structure's configuration, thus impacting load distribution and overall stability. Moreover, materials display inelastic behavior to dissipate excess energy using mechanisms like cracking, yielding, and hysteresis. Structural ductility in materials, structural components, and structures determines the capacity of a structure to endure such substantial plastic deformations without a sudden loss of strength, permitting it to absorb and dissipate energy.

Structural ductility can be determined at different levels, such as (i) at the material level by stress-strain plots of materials, (ii) at the cross-sectional level by moment-curvature curves and axial force–bending moment interaction curves, (iii) at the member level by moment-deformation curves, and (iv) at the structural level by load-displacement curves. This chapter first discusses material non-linearity, followed by cross-sectional and member-level non-linearity. It establishes the basis for structural-level non-linearity, which will be discussed in Chapters 6 and 7.

5.2.1. Structural ductility at the material level by stress-strain plot of materials

5.2.1.1. Stress-strain plots of concrete

The stress-strain curve of concrete presents a graphical representation of the behavior of concrete under loading by plotting the concrete compressive strength against the concrete strain. The idealized curve of the stress-strain plot of concrete is a parabolic shape up to a strain of 0.0020 and constant up to a strain of 0.0035, which is the limit state. The tensile strength of concrete is generally neglected. Figure 5.1 shows a stress-strain model for unconfined concrete with a cylindrical compressive strength of 25N/mm^2 based on the design parameters shown in Table 5.1 below. These design parameters are recommended according to European Standards.

Table 5.1: Design parameters for unconfined concrete

Parameters of Unconfined Concrete	Design Values
Directional symmetry type	Isotropic
Modulus of Elasticity (E)	31 GPa
Poisson ratio (U)	0.2
Coefficient of thermal expansion (A)	0.00001
Shear modulus (G)	12916667
Weight per unit volume	24.9926kN/m^3
Mass per unit volume	2.5485× 10^3 kg/m^3
Specified concrete compressive strength – f_c’	25 MPa / 25 N/mm^2
Expected concrete compressive strength	25 MPa / 25 N/mm^2
Hysteresis type	Concrete
Stress-strain curve definition option	Parametric (Mander)
Strain at unconfined compressive strength, f_c’	1.613 × 10^{-3}
Ultimate unconfined strain capacity	5.000 × 10^{-3}
Final compression slope (Multiplier on E)	-0.1

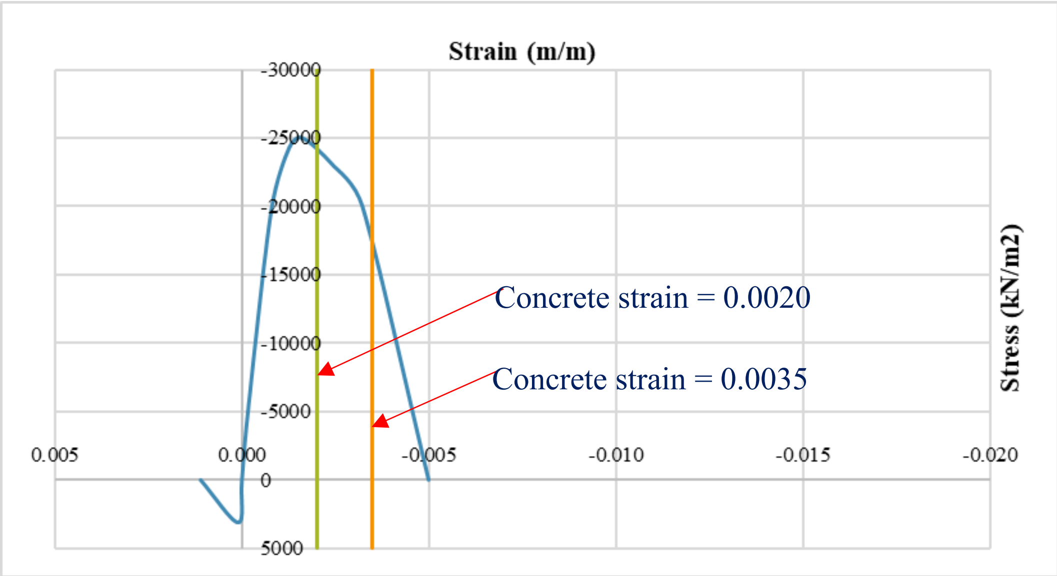

Figure 5.1: Stress-strain curve for unconfined concrete

Figure 5.1 shows that the concrete stress-strain curve has a parabolic shape up to a strain of approximately 0.0020. Contrary to constantly staying up to a strain of 0.0035, the concrete stress decreases beyond the point at 0.0020 as the strain increases, signifying that the concrete withstands less stress as the load rises. However, the confined concrete can withstand higher stresses than the unconfined concrete on the descending stress-strain curve.

Considering the confinement provided by the shear reinforcements, stress-strain models for the confined concrete in each element in the typical building and the three specific case study buildings were developed using the section designer option in SAP2000. Tables 5.2-5.5 below indicate the confinement in each main structural element of the typical and the three specific case study buildings.

Table 5.2: Confinement details of the main structural elements in the typical building

Structural Element	Confinement Reinforcement	C/C Spacing
Beams (X-direction)	R6	125mm
Beams (Y-direction)	R6	125mm
Columns	R8	150mm

Table 5.3: Confinement details of the main structural elements in the school building

Structural Element	Confinement Reinforcement	C/C Spacing
Beams (X-direction)	R6 (2)	200mm
Beams (Y-direction)	R6 (2)	225mm
Columns	R6 (2)	150mm

Table 5.4: Confinement details of the main structural elements in the university building

Structural Element	Confinement Reinforcement	C/C Spacing
Beams (X-direction)	R6 (2)	125mm
Beams (Y-direction)	R6 (2)	125mm
Columns	R8 (2)	150mm

Table 5.5: Confinement details of the main structural elements in the hospital building

Structural Element	Confinement Reinforcement	C/C Spacing
Beams (X-direction)	R8 (4)	125mm
Beams (Y-direction)	R8 (4)	125mm
Columns	R8 (2)	150mm

Figures 5.2-5.5 illustrate the stress-strain relationships of the confined concrete in beams spanning in the X- and Y-directions and the columns of each building, along with the stress-strain curve for unconfined concrete material.

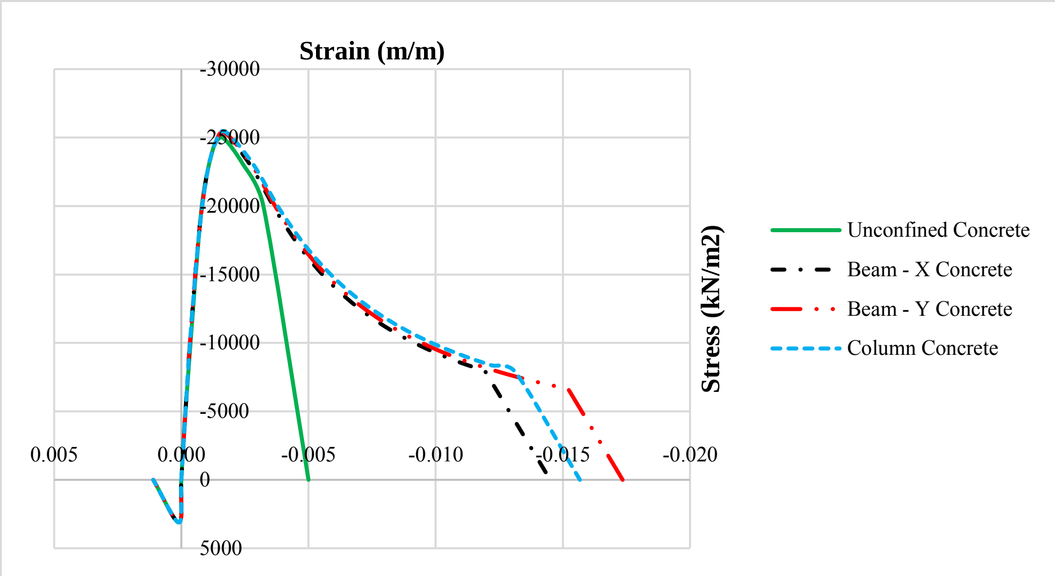

Figure 5.2: Stress-strain plots for concrete in the basic structural elements of the typical building

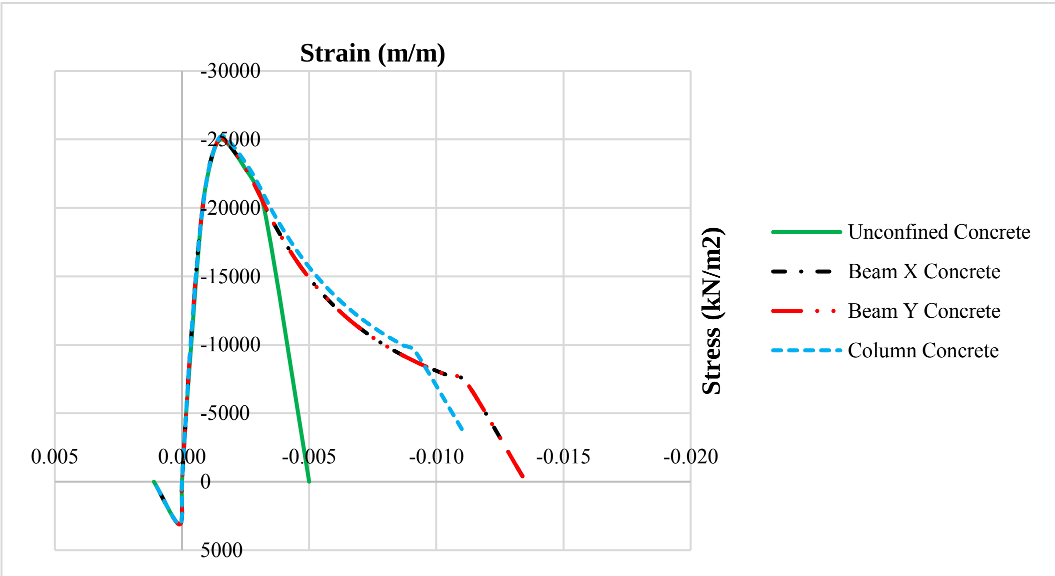

Figure 5.3: Stress-strain plots for concrete in the basic structural elements of the school building

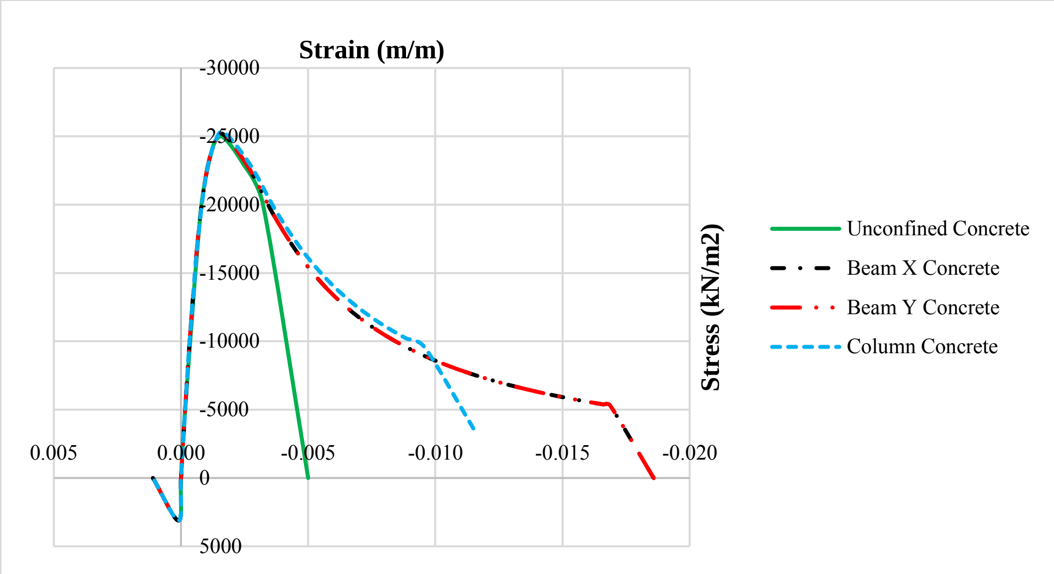

Figure 5.4: Stress-strain plots for concrete in the basic structural elements of the university building

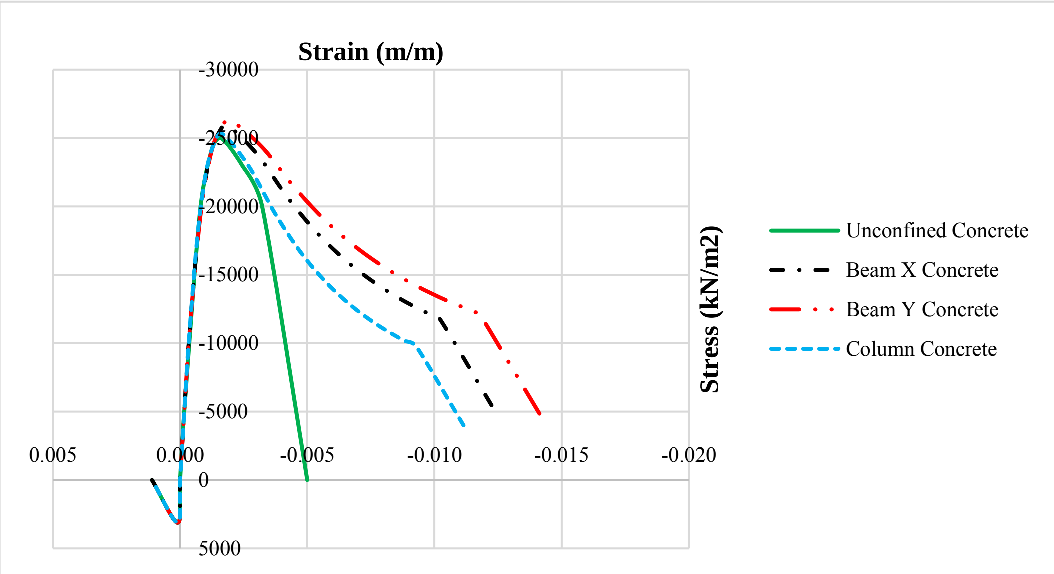

Figure 5.5: Stress-strain plots for concrete in the basic structural elements of the hospital building

Similarly, stress-strain plots for all different beams and columns in the Defective and Retrofitted mixed-use buildings were derived based on their confinement data.

5.2.1.2. Stress-strain plots of steel reinforcement bars

The stress-strain curve of steel represents steel's elastic and inelastic behavior under applied force. It is produced by plotting the steel stress against the strain in a uniaxial tensile test. The present study developed stress-strain plots of high-strength and mild steel reinforcements using the section designer option in SAP2000, utilizing the design parameters in Table 5.6 below.

Table 5.6: Design parameters for steel reinforcement bars

Parameters of Rebar	Design Values	
	High-Strength Steel Reinforcement Bars	**Mild Steel Reinforcement Bars**
Directional symmetry type	Uniaxial	Uniaxial
Modulus of Elasticity (E)	1.999×10^8kPa	1.999×10^8kPa
Poisson ratio (U12)	0	0
Coefficient of thermal expansion (A1)	1.170×10^{-5}	1.170×10^{-5}
Shear modulus (G12)	0	0
Weight per unit volume	76.97kN/m^3	76.97kN/m^3
Mass per unit volume	7.849×10^3kg/m^3	7.849×10^3kg/m^3
Minimum Yield Stress (Fy)	413685.50kPa	227272.73kPa
Minimum Tensile Stress (Fu)	620528.20kPa	340909.09kPa
Expected Yield Stress (Fye)	455054kPa	250000kPa
Expected Tensile Stress (Fue)	682581kPa	375000kPa
Hysteresis type	Kinematic	Kinematic
Stress-strain curve definition option	Parametric (Simple)	Parametric (Simple)
Strain at the onset of strain hardening	0.01	0.01
Ultimate strain capacity	0.09	0.09
Final slope (Multiplier on E)	-0.1	-0.1

The stress-strain curves of high-strength and mild steel mainly depend on their minimum yield and tensile stress. The properties of high-strength steel reinforcement bars provided in Table 5.6 are in line with European Standards. According to the conclusions drawn from a study undertaken by Bandara et al. (2017), the long-term characteristic yield strength (f_y) of Quenched and Self-Tempered (QST) RB 500 steel reinforcement bars used in Sri Lanka is 493 MPa (without segregation on the diameter), which is less than the expected strength of 500 MPa. The minimum value of the larger diameter bars' characteristic yield strength (f_{yk}) is less than 450 MPa. Therefore, the recommended parameters in the European Standards for the minimum and expected yield stresses of high-strength steel reinforcements show a reasonable alignment with the local high-strength steel reinforcements.

Without experimental data on the properties of mild steel reinforcement bars used in Sri Lanka, the anticipated yield stress of these bars was assumed to be 250 MPa. Based on this assumption, the minimum yield, tensile, and expected tensile stresses of the mild steel reinforcements were calculated.

Expected yield (F_{ye}) and expected tensile (F_{ue}) stresses are the products of code-prescribed factors and the expected strength of the materials. This study used conversion factors of 1.1 and 1.5, as prescribed by FEMA 356, to convert the predicted yield stress to the minimum yield stress and the minimum yield stress to the minimum tensile stress, respectively. This conversion is similar to European Standards' high-strength steel reinforcement bar property conversion.

Stress-strain curves for the high-strength and mild steel are presented in Figure 5.6 below.

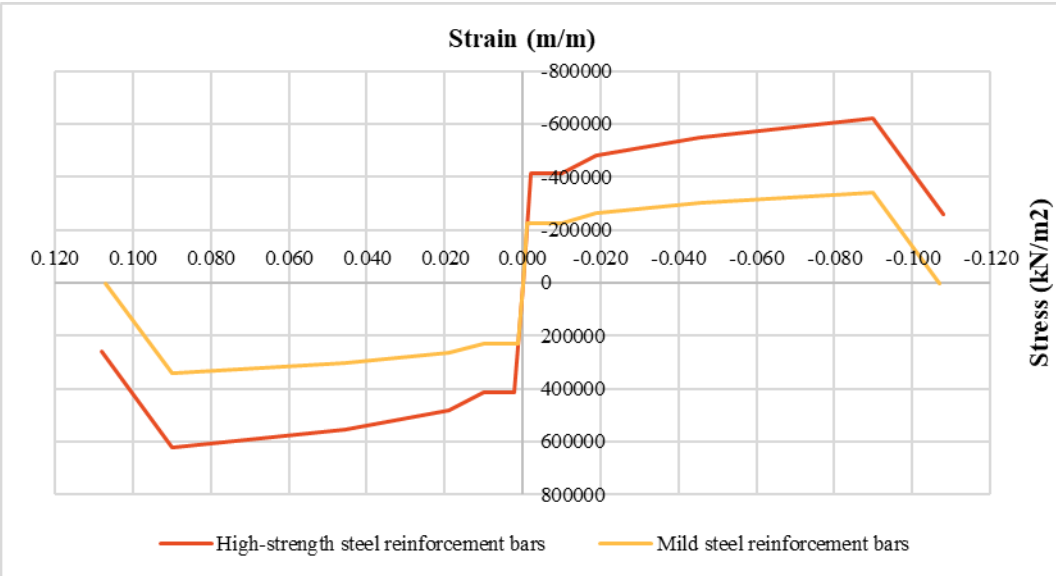

Figure 5.6: Stress-strain curve for the high-strength and mild steel reinforcement bars

5.2.2. Structural ductility at the cross-sectional level by force-deformation curves (moment-curvature curves and P-M-M interaction curves)

Chapter 4 discussed all material properties and structural design details, including the section sizes and the reinforcement details of the beams and columns for each building, as obtained from the structural design. The moment-curvature curves and P-M-M (Axial force – Major axis bending moment – Minor axis bending moment) interaction curves represent the cross-sectional non-linearity of structural elements as specified by the American Society of Civil Engineers (ASCE) in ASCE 41 – 13 (ASCE, 2014) and cross-sectional analyses in the SAP2000 section designer. These moment-curvature curves and the P-M-M interaction curves for beams and columns were developed based on the end cross sections, where plastic hinges are assumed to be formed when buildings are subject to extreme lateral loads.

Figure 5.7 shows the moment-curvature curves of beams and columns of the typical building.

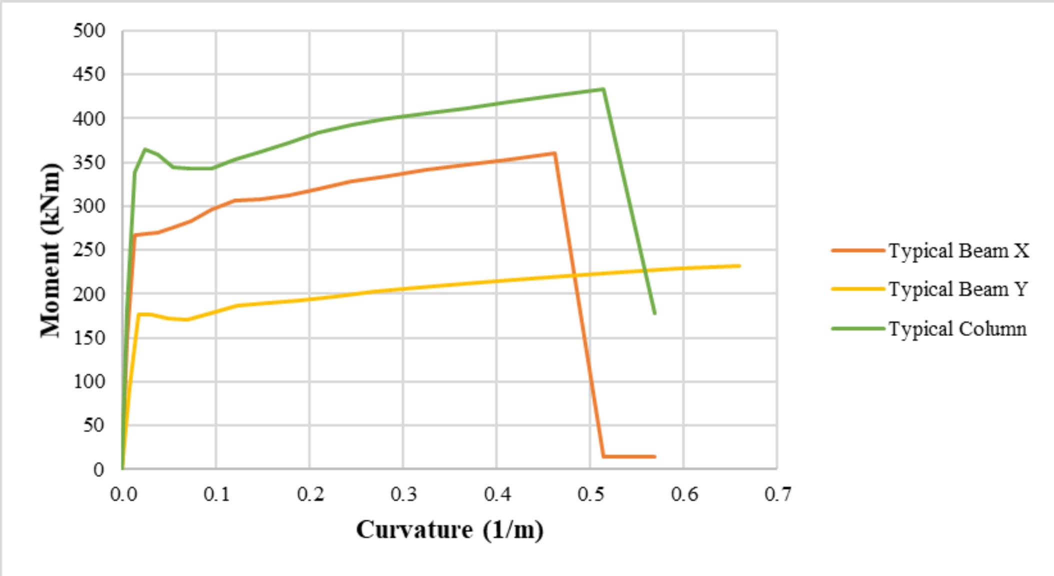

Figure 5.7: Moment-curvature curve for beams and columns of the typical building

P-M-M interaction curves for columns are three-dimensional plots with three axes: P (Axial Force), M2-2 (Major Axis Bending Moment), and M3-3 (Minor Axis Bending Moment). For a given cross-section, the section analysis in SAP2000 produces 24 curves in this 3D space, each spaced at 15-degree intervals.

Table 5.7 below provides the coordinates of Curve #24 generated for the columns of the typical building, and Figure 5.8 presents the P-M-M interaction curves.

Table 5.7: Coordinates of the 24th P-M-M interaction curve for the columns of the typical building

P(kN)	M2-2(kNm)	M3-3(kNm)
-3198.00	0.00	0.00
-3198.00	-27.13	76.41
-3025.00	-38.57	134.61
-2496.00	-43.28	191.06
-1859.00	-49.89	234.00
-1081.00	-59.69	265.20
-509.07	-68.21	302.83
234.12	-76.89	291.20
1118.00	-69.54	174.05
1993.29	-31.35	34.79
2193.69	0.00	0.00

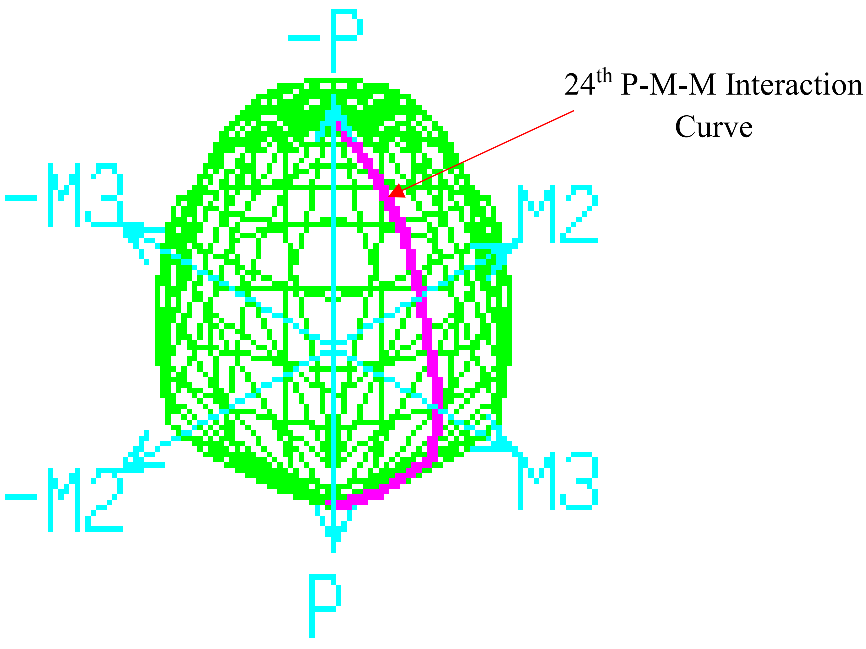

Figure 5.8: P-M-M interaction curve for columns of the typical building

Similarly, moment-curvature and P-M-M interaction curves were developed for each structural element of the school building, university building, hospital building, defective building, and retrofitted building.

5.2.3. Structural ductility at the member level by force-deformation (moment-rotation) curves

The structural ductility at the member level was determined using the cross-sectional level ductility estimated in the previous section. This is simply a conversion of moment-curvature curves to moment-rotation curves. In short, moment-curvature is a 'force-deformation' relationship at the section level, necessitating only sectional properties, such as flexural rigidity. Conversely, moment-rotation is a 'force-deformation' relationship at the member level, requiring the properties of the entire member.

PERFORM-3D software provides an F-D relationship as a guide to establish a member-level non-linearity through action-deformation curves. The PERFORM-3D Action-Deformation (F-D) relationship at the member level is denoted in Figure 5.9.

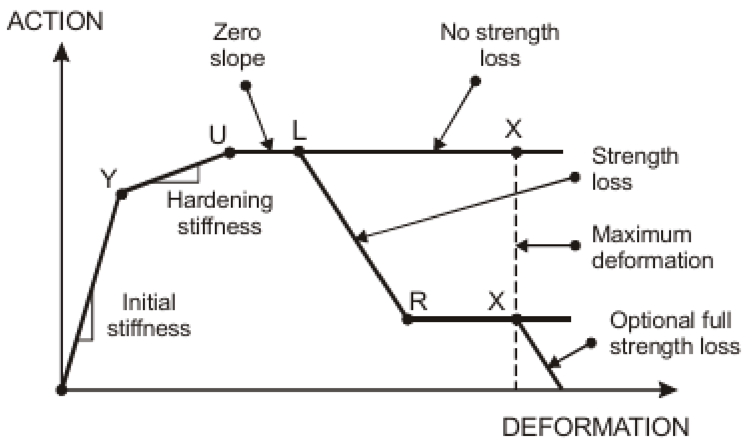

Figure 5.9: PERFORM-3D action deformation relationship

Most inelastic components in PERFORM-3D have the same form for the F-D relationship. This relationship for asymmetric components can vary for positive and negative deformations. As illustrated in Figure 5.9, this F-D relationship is trilinear with the optional strength loss. Explanations for the key points Y, U, L, R, and X in the above PERFORM-3D Action-Deformation relationship are provided in Table 5.8.

Table 5.8: Explanation of PERFORM-3D action-deformation relationship

Point	Description
Y	The first yield point - substantial nonlinear behavior starts
U	The ultimate strength point - maximum strength is reached
L	The ductile limit point - substantial strength loss starts
R	The residual strength point - minimum residual strength is reached
X	Large deformation - further analysis is unnecessary

Usually, the analyses are terminated if any structural component is deformed beyond Point X on the Action-Deformation plot. However, if necessary, the analysis can be continued beyond Point X. In the present study, the moment-curvature curves determined using the SAP2000 section designer option were transformed into moment-rotation curves, facilitating the non-linear analysis requirements in PERFORM-3D software. Rotation is the curvature integrated over the plastic hinge length. Hence, the values of curvatures were multiplied by the plastic hinge lengths of each structural component to obtain the rotations. Figure 5.10 shows the moment-rotation curves of beams and columns of the typical building.

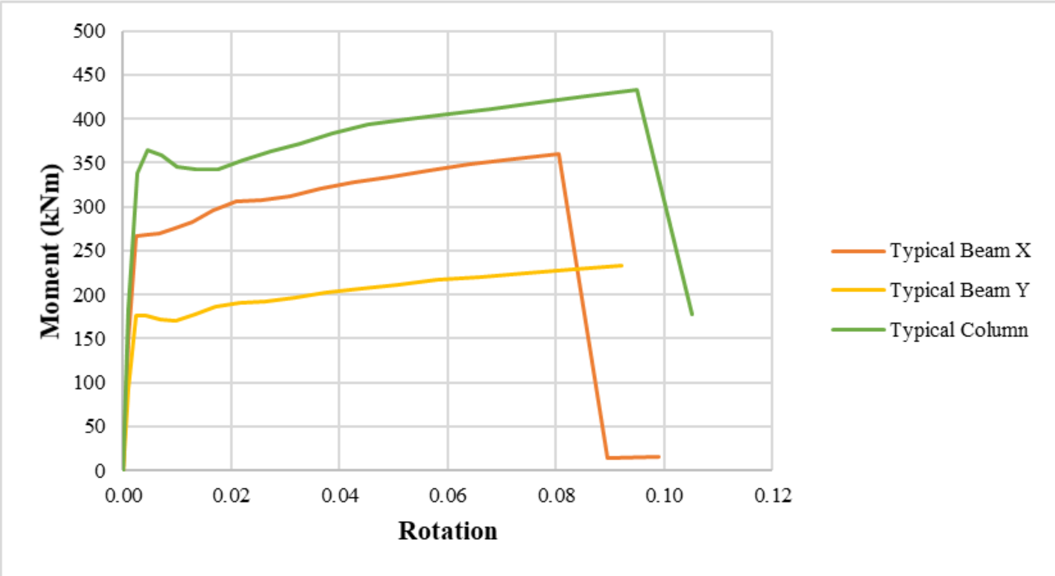

Figure 5.10: Moment-rotation curve for beams and columns of the typical building

5.2.4. Assigning hinge properties

When buildings experience extreme lateral loading, hinges are formed at the end sections of structural elements, specifically in the beams and columns. This is a common phenomenon in reinforced concrete-framed structures, where plastic hinges are created at beams' ends and columns' bases to lessen the impact of extreme lateral loads. Therefore, the present study used compound elements to assign hinge properties to the end sections of beams and columns.

Working from one end to another, a typical compound beam comprises an end zone, a FEMA beam/non-linear reinforced concrete beam, an inflection point, a FEMA beam/non-linear reinforced concrete beam, and an end zone, as presented in Figure 5.11. Further, a FEMA /non-linear reinforced concrete beam comprises a hinge and an elastic frame next to the hinge. Here, the hinge presents linear and non-linear properties, while the elastic frame denotes only the linear properties.

PERFORM-3D sets the end zone for a beam based on the size of the adjacent beams and columns. The length of the FEMA beam or non-linear reinforced concrete beam is 0.5 times the total beam length.

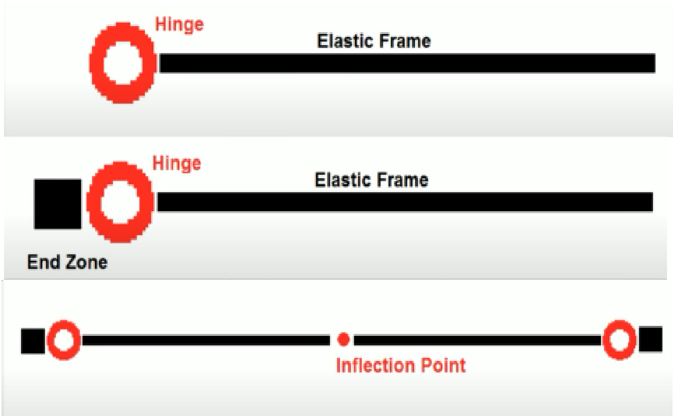

Figure 5.11: Structure of a typical compound beam

Working from the bottom up, a compound column on the ground floor level comprises a linear P/V/M hinge or release (to indicate a pinned support), FEMA column, inflection point, FEMA column, and column end zone. Since the inflection point is at the bottom of a pinned column, the heights of the FEMA columns are 0.02 and 0.98 times the total column height, respectively. For columns, PERFORM-3D sets the end zone based on the size of the adjacent beams.

Starting from the bottom, a compound column on the upper floor level consists of an end zone, a FEMA column, an inflection point, a FEMA column, and a column end zone. Because the inflection point is in the middle of the column, the heights of the FEMA columns are each 0.5 times the total column height.

5.3. Summary

PERFORM-3D software supports detailed modeling of materials with non-linear and inelastic properties. The software employs a component-based approach, modeling individual structural elements, like beams and columns, with non-linear characteristics. These capabilities allow accurate simulation of cracking, yielding, and other inelastic phenomena. This enables a detailed analysis of local behaviors and interactions by creating non-linear building models and assessing building performance under extreme loading conditions by integrating material and geometric non-linearities with advanced element formulations. The details in this chapter establish the basis for performing non-linear analyses of case study buildings, as discussed in Chapters 6 and 7.

CHAPTER 6 : ANALYSIS OF BUILDINGS FOR EXTREME WIND LOADING

6.1. General

To guarantee sufficient structural resilience, new and existing buildings must be tested for wind loads beyond the typical design level considered by building design codes and standards. The current codes and standards do not utilize the non-linear behavior of structural elements when designing for wind loading. Hence, the structural elements are designed to behave in the linear range at the design-level wind loading. However, during the building's life span, it may undergo more extreme wind events than stipulated in the building design codes and standards. Therefore, the structural elements may surpass their linear range and start behaving in the non-linear range. Therefore, non-linear analytical techniques must be utilized to analyze buildings against extreme wind-loading scenarios with a reduced probability of occurrence compared to those stated in building design codes.

The non-linear static pushover analysis (NSPA) can be utilized to estimate non-linear structural responses of buildings against static lateral loading. Furthermore, using these predicted responses is necessary to identify the methods to evaluate the building's performance. In the present study, NSPA was applied to six new, defective, and retrofitted versions of buildings. This study adopts the wind performance objective matrix introduced by Griffis et al. (2013) to evaluate the structural performance of the case-study buildings.

6.2. Non-linear static pushover analysis of the buildings

Since the non-linear static pushover analysis depends on the direction of the applied load, the analysis considered two main directions for each building: the typical office building, school building, university building, hospital building, defective mixed-use (offices and apartments) building, and its retrofitted version. Figure 6.1 shows the designated X- and Y-directions for each of these buildings.

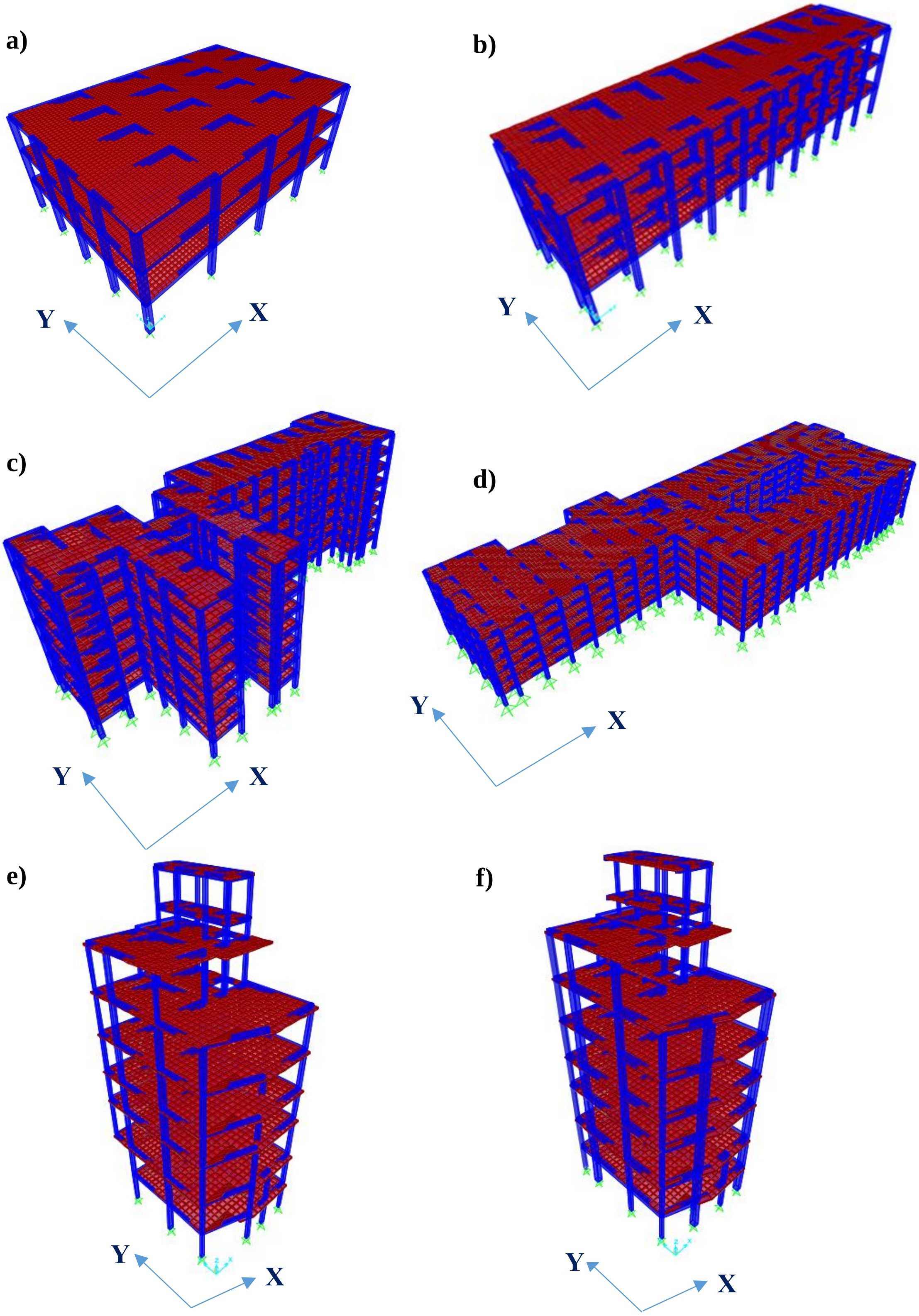

Figure 6.1: Principal directions of the buildings a) typical building, b) school building, c) university building, d) hospital building, e) defective building, f) retrofitted building

Each building floor was modeled as a rigid diaphragm where the entire floor moves in the diaphragm plane as a rigid body, providing an infinite in-plane stiffness. Before the pushover analysis, non-linear models of the Eurocode-based typical building, school building, university building, hospital building, and the non-code-compliant defective building, and its retrofitted building were assigned with gravity loads comprising the total dead load and 30% of the live load. In non-linear analyses, such as pushover analysis, only 30% of the live load is typically considered, as live loads are transient in nature and it is unlikely that their full magnitude will be present during an extreme event. Although the existing building was unoccupied at the time, 30% of the live load was also considered for the defective building, as the objective of this study is to evaluate its vulnerability, assuming it is put into use without the implementation of retrofitting strategies. The wind forces on each floor of each building were determined by multiplying the pressure distribution derived from the code with the contributory area, according to the calculation procedure outlined in Eurocode 1: Actions on structures - Part 1-4: General actions - Wind actions (EN 1991-1-4:2005). This contributory area calculation involved multiplying half the height of adjacent stories by the width of the building's windward and leeward sides.

According to EN 1991-1-4:2005, the wind loads on the first-floor, second-floor, and roof levels of the three-storied typical building are 56kN, 56kN, and 28kN, respectively, resulting in a base shear of 140kN, when the building is exposed to a wind incident with a 50-year return period in the X-direction. The wind forces on the first-floor, second-floor, and roof levels in the Y-direction are 92kN, 92kN, and 46kN for a wind event with a 50-year return period. These loads result in a base shear value of 230kN. The wind loads on the first-floor, second-floor, and roof levels of the three-storied school building are 22kN, 22kN, and 12kN, respectively, when the building is exposed to a wind incident with a 50-year return period in the X-direction. The wind forces on the first-floor, second-floor, and roof levels in the Y-direction are 124kN, 124kN, and 62kN for a wind event with a 50-year return period. The resulting base shear of this school building is 56kN and 310kN when subjected to wind forces in its X- and Y-directions, respectively. The lateral load pattern in the X-direction of the university building consisted of a 133kN wind force from the first-floor level to the seventh-floor level and 67kN at the roof level, causing a base shear value of 1000kN. In the Y-direction, the lateral load pattern comprised wind forces with magnitude 340kN, from the first-floor level to the seventh-floor level of the building and 170kN at the roof level, causing a base shear of 2553kN. As calculated from the Eurocode 1: Actions on structures - Part 1-4: General actions - Wind actions (EN 1991-1-4:2005), the lateral load pattern along the X-direction of the hospital building comprised of a wind force of 176kN, from the first-floor level to the fifth-floor level of the building and 88kN at the roof level, amounting to a base shear of 967kN. In the Y-direction, the lateral load pattern comprised a wind force of 462kN, from the first-floor level to the fifth-floor level of the building, and 231kN at the roof level, causing a base shear of 2540kN.

A case study building, identified as defective, failed to meet the required capacity for withstanding the expected gravity and wind loading. This building was not designed and constructed to cater to the wind loading recommended by Eurocode 1: Actions on structures - Part 1-4: General actions - Wind actions (EN 1991-1-4:2005) for a design return period of 50 years which is reasonable to consider for this type of a mixed-use building in the city. According to the calculation procedure outlined in Eurocode 1: Actions on structures - Part 1-4: General actions - Wind actions (EN 1991-1-4:2005), the wind loads on the seven-storied mixed-use building result in base shear of 378kN and 273kN, when the building is exposed to a wind incident with a 50-year return period in its principal directions, X and Y, respectively. The retrofitted version of this defective building was determined to have the required capacity for withstanding the anticipated gravity, and wind loading compared to the original defective building. Despite the design flaws in this existing building, this defective building, as well as its retrofitted version, were also considered as case studies for conducting non-linear static pushover analysis, following the load pattern recommended in Eurocode 1: Actions on structures - Part 1-4: General actions - Wind actions (EN 1991-1-4:2005).

Then, non-linear models of the buildings were assigned with these calculated static lateral wind loading at all story levels to perform non-linear static pushover analyses in their two principal directions, X and Y.

Since the typical building is symmetrical about its X- and Y-axis, the loads were applied at the central nodes of each floor. The wind loading in X- and Y-directions of the typical building followed the shape of the load pattern shown in Figures 6.2 and 6.3, respectively.

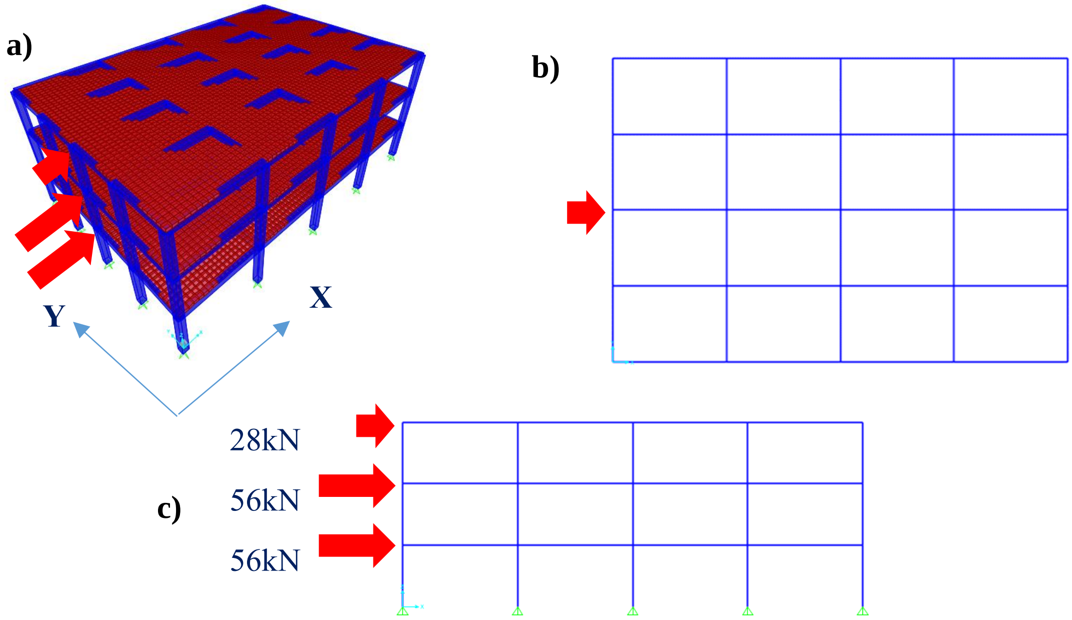

Figure 6.2: Wind load application in the X-direction a) 3D view, b) plan view, c) elevation view

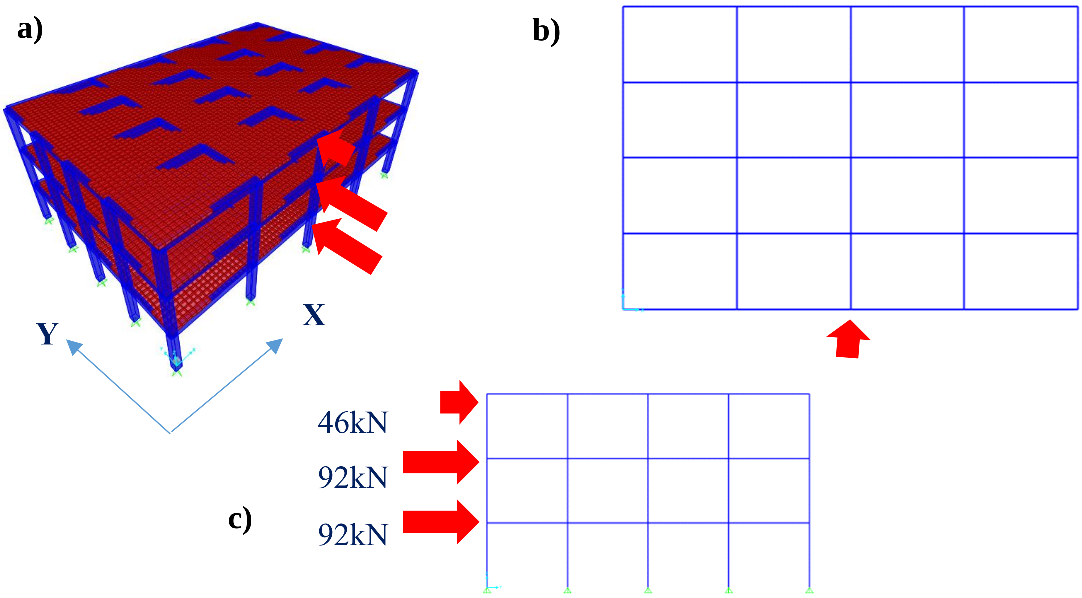

Figure 6.3: Wind load application in the y-direction a) 3d view, b) plan view, c) elevation view

In the Y-direction of the school building, the computed floor loads were assigned to the central nodes of each floor, considering its symmetry along the Y-axis. However, because the school building is not symmetrical along the X-axis, and the university, hospital, defective, and retrofitted buildings are asymmetrical along both the X- and Y-axes, wind loads were applied as nodal loads based on the contributory area for each node due to modeling restrictions in PERFORM-3D for defining an extra node along the centerline of each floor.

In the pushover analysis, non-linear models of these buildings were subjected to the combined action of these gravity loads and monotonically increasing static lateral wind loading vertically distributed along the building heights as recommended in Eurocode 1: Actions on structures - Part 1-4: General actions - Wind actions (EN 1991-1-4:2005). Starting from a zero wind loading, and increasing the static wind loading on the building by equal load increments while maintaining constant gravity loading, the non-linear static pushover analyses were conducted until the buildings encountered lateral instability. The P-Δ geometric nonlinear effect, which accounts for additional moments resulting from axial loads acting on a lateral displacement, was also considered for the nonlinear pushover analysis.

In the pushover analysis of the typical building, the center point of the top level was selected as the target node or displacement control point for both the X- and Y-directions. For the school building, the center point of the top level was used as the target node for the Y-direction analysis, while multiple control nodes were considered for the X-direction analysis due to the building's asymmetry along the X-axis. Similarly, multiple control nodes were used for the X- and Y-direction pushover analyses of the university, hospital, defective, and retrofitted buildings, because of their asymmetry along both the X- and Y-axes. Displacements at these target roof nodes were recorded at each load increment.

The pushover capacity curves were developed based on the relationship between the base shear induced by the monotonically increasing static lateral wind load and the roof drift of the target nodes.

Figures 6.4 and 6.5 show the pushover capacity curves for the typical building and the school building subjected to a monotonically increasing lateral wind load in the X- and Y-directions. Figures 6.6 – 6.9 illustrate the pushover capacity curves recorded at various control points on the roof of the university building, hospital building, defective building, and retrofitted building under the monotonically increasing lateral wind load in the X- and Y-directions. These curves, plotted for both principal directions (X and Y) for each building on the same graph, highlight how the changes in pushover capacity curves depend on the direction of the applied load. The notations "FO", "O", "LS", and "NC" represent the four damage limit states: Fully Operational, Operational, Life Safe, and Near Collapse, respectively. "X" and "Y" refer to the analyses conducted in the principal X- and Y-directions.

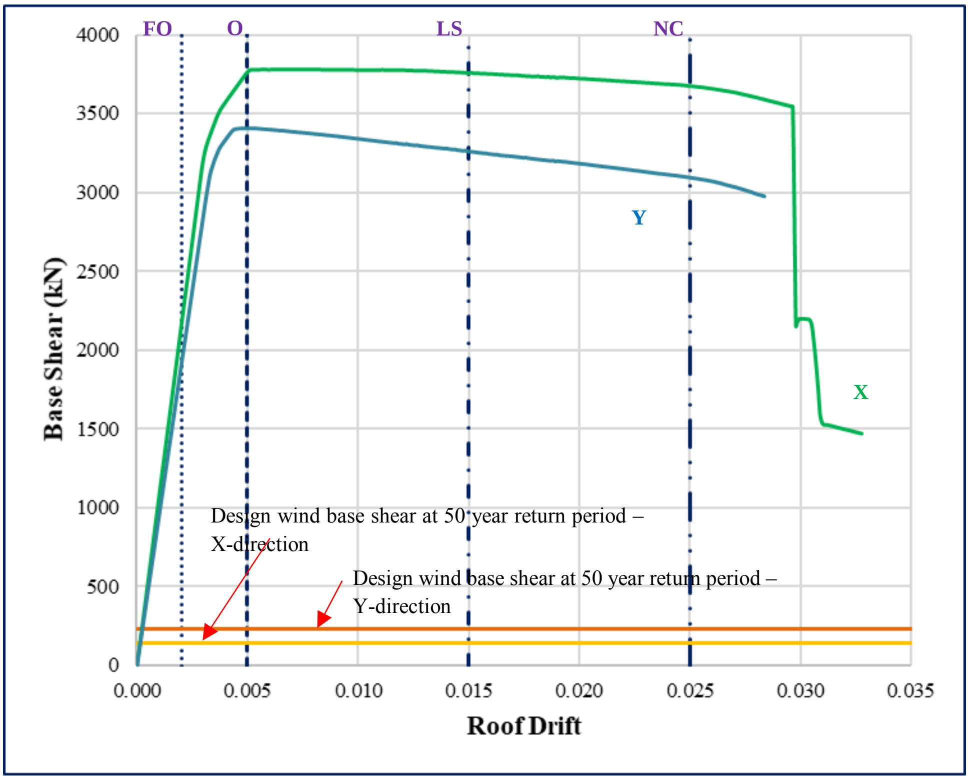

Figure 6.4: Pushover capacity curves in principal directions of the typical building

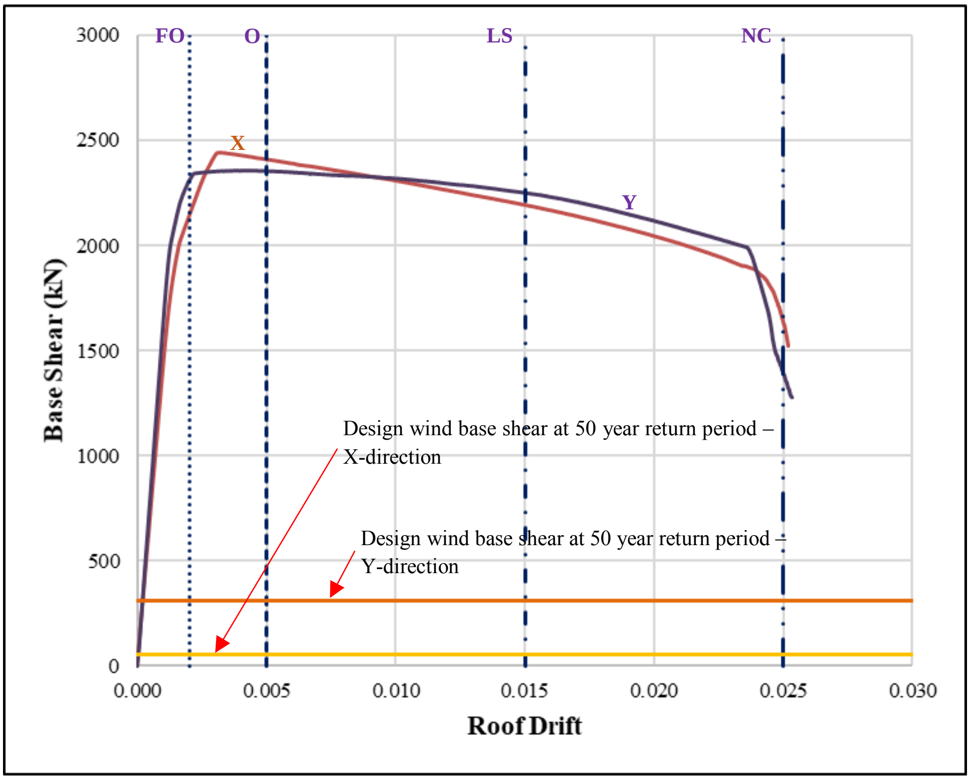

Figure 6.5: Pushover capacity curves in principal directions of the school building

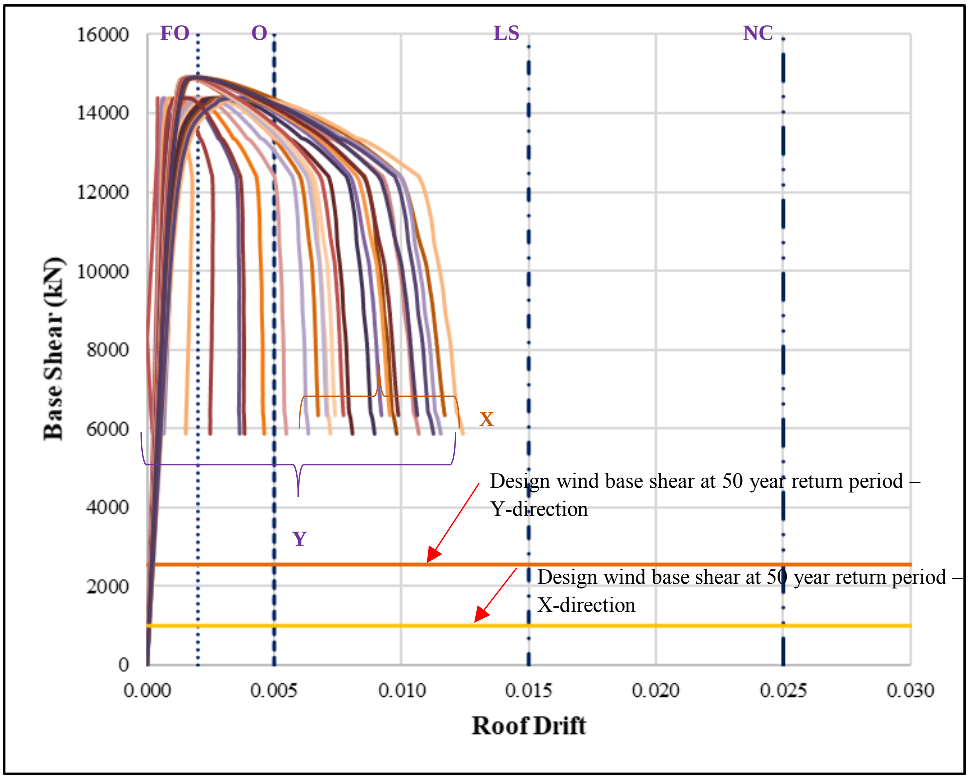

Figure 6.6: Pushover capacity curves in principal directions of the university building

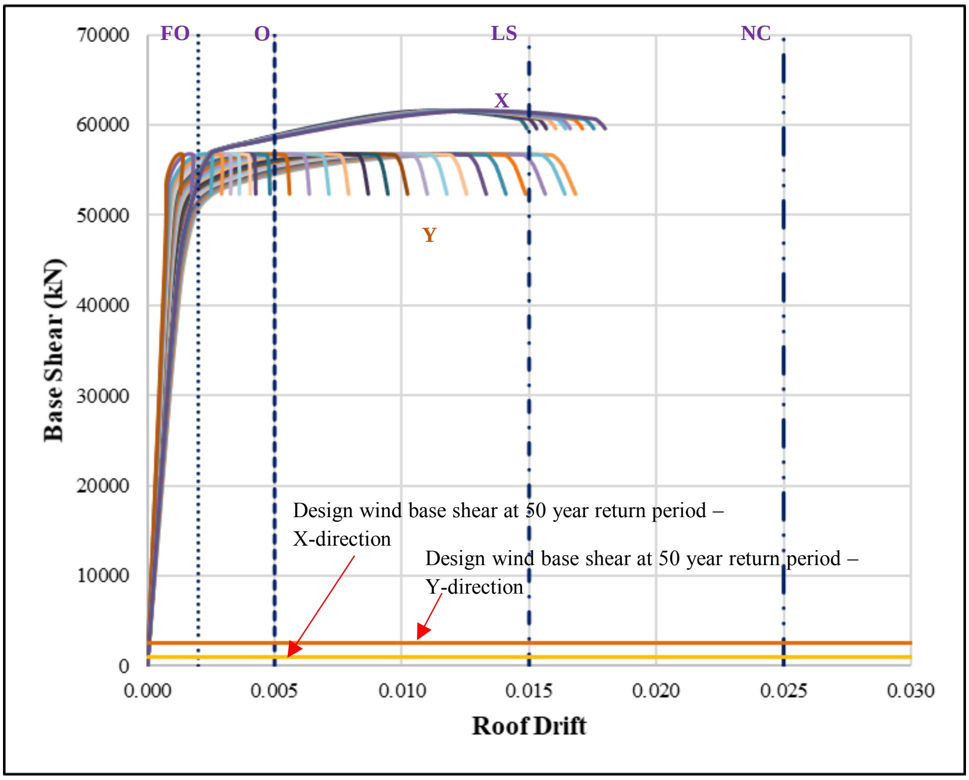

Figure 6.7: Pushover capacity curves in principal directions of the hospital building

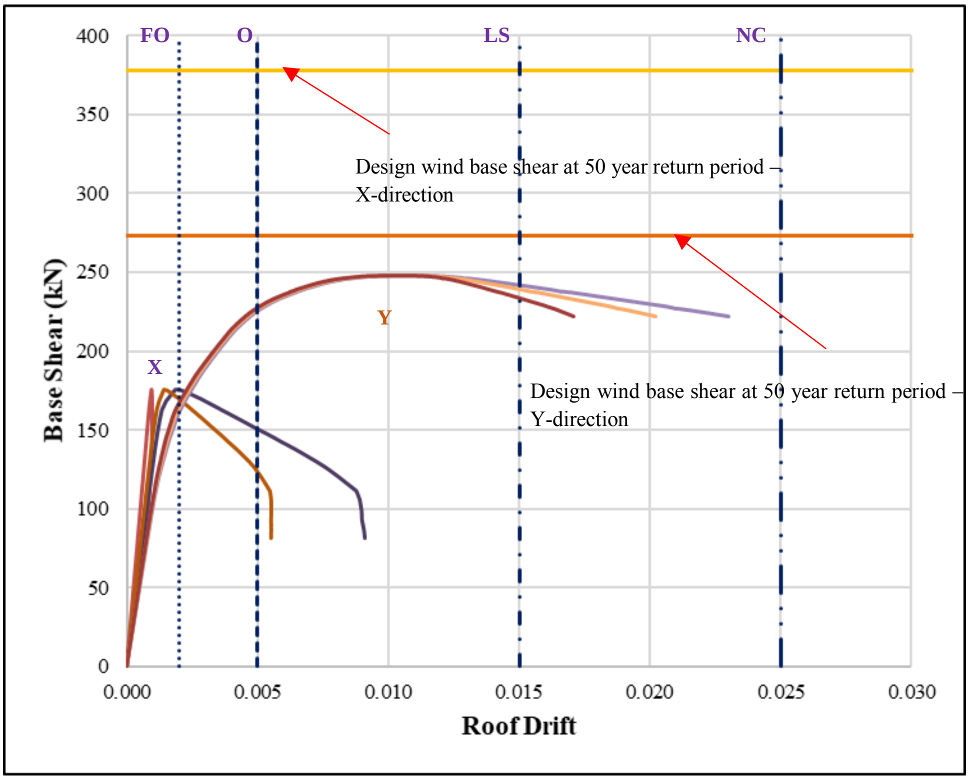

Figure 6.8: Pushover capacity curves in principal directions of the defective building

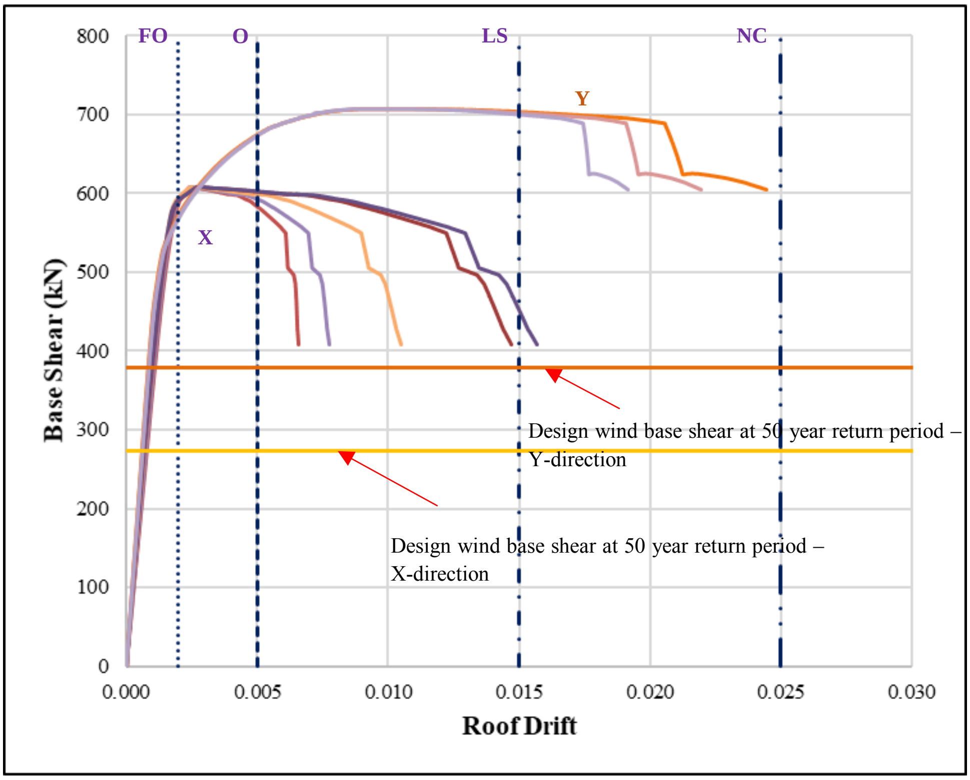

Figure 6.9: Pushover capacity curves in principal directions of the retrofitted building

According to Whittaker et al. (2003)'s work illustrated in Figure 2.11, a building reaches the immediate occupancy state when the base shear reaches the point where the pushover capacity curve shifts from the linear to the non-linear range. The collapse prevention state is reached just before the base shear begins to drop significantly on the pushover curve, with the life safety state occurring between the immediate occupancy and collapse prevention points.

The pushover capacity curves for the typical building and its performance levels align well with the study by Whittaker et al. (2003), wherein the qualitative performance levels from FEMA 273/274 were overlaid on a global force-displacement relationship for a representative building. The school building's pushover curves also show good alignment with the illustration in Figure 2.8. However, a noteworthy mismatch persists between these pushover capacity curves of the university and hospital buildings and the performance levels considered in the illustration presented by Whittaker et al. (2003). This alignment differs in that these buildings exceed the fully operational, operational, life-safe, and near-collapse damage limits before reaching the pre-defined roof drifts for these damage limit states. This suggests that the buildings deviate from these pre-defined damage limits as their structural configurations and geometries become more complex, and stresses the importance of considering each of the roof nodes as a target node to capture the worst-case scenario, especially in buildings where the center of mass does not overlap with the center of rigidity.

As also depicted in Figures 6.4 – 6.7, these typical, school, university, and hospital buildings account for higher non-linear capacities when experiencing extreme loads in the X-direction, compared to the Y-direction. This outcome derived from the pushover analysis is logical because the building's geometry provides higher stiffness when its shorter faces are subjected to lateral loads than when its larger faces are. However, as depicted in Figures 6.8 and 6.9, defective and retrofitted buildings yielded higher non-linear capacities along the Y-direction compared to the X-direction. These defective and retrofitted buildings do not have significantly different geometries when viewed from the X- and Y-directions, similar to typical, school, university, and hospital buildings. However, the differences in their structural arrangements in these two directions have influenced the variations observed in the X- and Y-direction analyses results.

Similar displacements of roof nodes were recorded in the X- and Y-directional pushover analysis of the typical building and the Y-directional pushover analysis of the school building at a given level of loading, hence resulting in the same pushover capacity curves across different target nodes. This result is reasonable since the center of mass of these buildings overlaps with their center of rigidity. The pushover capacity plots in Figures 6.6 and 6.7, corresponding to X-directional analyses, indicate that the displacements of the selected nodes at the roof level vary even when exposed to the same level of loading. However, the displacements of the target nodes follow a similar path in the linear range of the pushover capacity curves. Therefore, the pushover capacity plots recorded at different target nodes, initially exhibit a similar pattern along a substantial portion of the pushover curve, but then split into distinct paths. Therefore, towards the ends of the pushover capacity curves, the displacements of the nodes at the roof level of the building vary when exposed to the same level of loading. Hence, the behavior of the building beyond the linear region, and before reaching the lateral instability is mainly dependent on the target node being considered for the analysis. However, the pushover capacity curves for the Y-directional response of the university and hospital buildings demonstrate that the displacements of the nodes at the roof level of these buildings for a given level of loading vary in a wide range, even starting from their linear segments of the pushover capacity curves, compared to their X-directional response. Such dependencies of the loci of the pushover capacity curves on the target nodes are mainly attributed to the non-coinciding of the center of mass of the building with the center of the rigidity. Therefore, this underlines the importance of considering several target nodes to capture the worst-case scenario especially when the center of mass and center of rigidity of the buildings do not overlap. These discussed differences between the X- and Y-directional responses of the building are again attributed to the different structural arrangements in these two directions, making these buildings more vulnerable and unpredictable to lateral loading in the Y-direction.

The design wind base shear of the typical building as calculated per the Eurocode 1: Actions on structures - Part 1-4: General actions - Wind actions (EN 1991-1-4:2005) is 140kN for the X-direction and 230kN for the Y-direction. As depicted in Figure 6.4, the non-linear behavior of the building permitted an ultimate lateral resistance capacity of 3779kN for the X-direction and 3411kN for the Y-direction. Therefore, the wind over-strength, which is known as the ratio of the ultimate lateral resistance capacity to the design wind base shear, is 26.61 for the X-direction and 14.83 for the Y-direction.

With almost similar responses in the two principal directions, the nonlinear behavior of the school building marked ultimate lateral resistances equal to 2444kN and 2356kN when subjected to wind forces in the X- and Y-directions, respectively. Therefore, the wind over strength in two main directions, X and Y is 43.64 and 7.60 respectively.

The peak base shear responses, as well as the base shear values at lateral instability, when the university and hospital buildings are subjected to extreme loads in either X or Y-direction, are almost matching, even when recorded at different target nodes, although the roof displacements vary significantly for a given level of loading. With nearly matching peak base shear responses and the base shear at lateral instability in the two principal directions, the nonlinear behavior of the university building lead to ultimate lateral resistances of 14918kN and 14391kN when subjected to extreme wind forces in the X- and Y-directions, respectively. Accordingly, the wind overstrength in the two major directions, X and Y, is 14.91 and 5.64, respectively. The peak base shear responses and the base shear at lateral instability in the two principal directions of the hospital building do not match each other. The nonlinear response of the hospital building resulted in ultimate lateral resistances of 61595kN and 56818kN when subjected to extreme wind forces in the X- and Y-directions, respectively. Consequently, the wind over strength in the two main directions, X and Y, are 63.70 and 22.37, respectively.

The design efficiency, inherent design conservatism, and the influence of gravity framing in resisting the lateral loads on the low-rise buildings can attribute to this high over-strength.

As stated in the wind performance objective matrix, the buildings in the highest importance class, such as disaster-resilient buildings, should maintain the performance levels; continued occupancy, operational, and limited interruption during wind events with return periods of 100, 300, and 1700 years, respectively.

As presented in Figure 6.4, the typical building surpasses the fully operational, operational, life-safe, and near-collapse damage limit states at base shear values of 2133kN, 3749kN, 3757kN, and 3674kN, in the X-direction, and at 1890kN, 3411kN, 3265kN, and 3099kN, in the Y-direction, when subjected to extreme wind forces. As shown in Figure 6.5, for the school building, these limits are exceeded at 2138kN, 2414kN, 2195kN, and 1637kN in the X-direction, and 2301kN, 2353kN, 2250kN, and 1403kN in the Y-direction. All these base shear values are well beyond the design base shear values of these buildings, at the 1700-year return period, which is the maximum return period in the wind performance objective matrix suggested by Griffis et al. (2013).

As presented in Figures 6.6 and 6.7, the base shear values at which the university and hospital buildings surpassed each damage limit state are largely dependent on the target node being considered. Nonetheless, none of the pushover capacity curves derived for these buildings fail to achieve the wind performance criteria stated in the wind performance objective matrix proposed by Griffis et al. (2013) since the design base shear values at the return periods specified in this matrix intersect the pushover capacity curves in their linear segments.

As illustrated in Figure 6.8, the ultimate non-linear capacities of the defective building are lower than the design base shear of the building at a wind event of a 50-year return period. According to the wind performance objective matrix proposed by Griffis et al. (2013), this type of mixed-use building should not exceed the damage limit states, continued occupancy, operational, and limited interruption at wind events of 10, 50, and 300-year return periods. Therefore, this mixed-use building does not meet the recommended performance objectives.

However, as illustrated in Figure 6.9 above, the ultimate non-linear capacities of the retrofitted building are higher than the design base shear of the building at a wind event of a 50-year return period. Therefore, this mixed-use building does not exceed the recommended performance objectives in the matrix proposed by Griffis et al. (2013), wherein this type of building should not exceed continued occupancy, operational, and limited interruption at wind events of 10, 50, and 300-year return periods.

Figures 6.10 and 6.11 illustrate the ultimate non-linear capacity enhancement achieved in the X- and Y-directional responses of the defective building by employing the retrofitting proposal on the existing defective building. Each figure pertains to the specific principal direction considered in the pushover analysis.

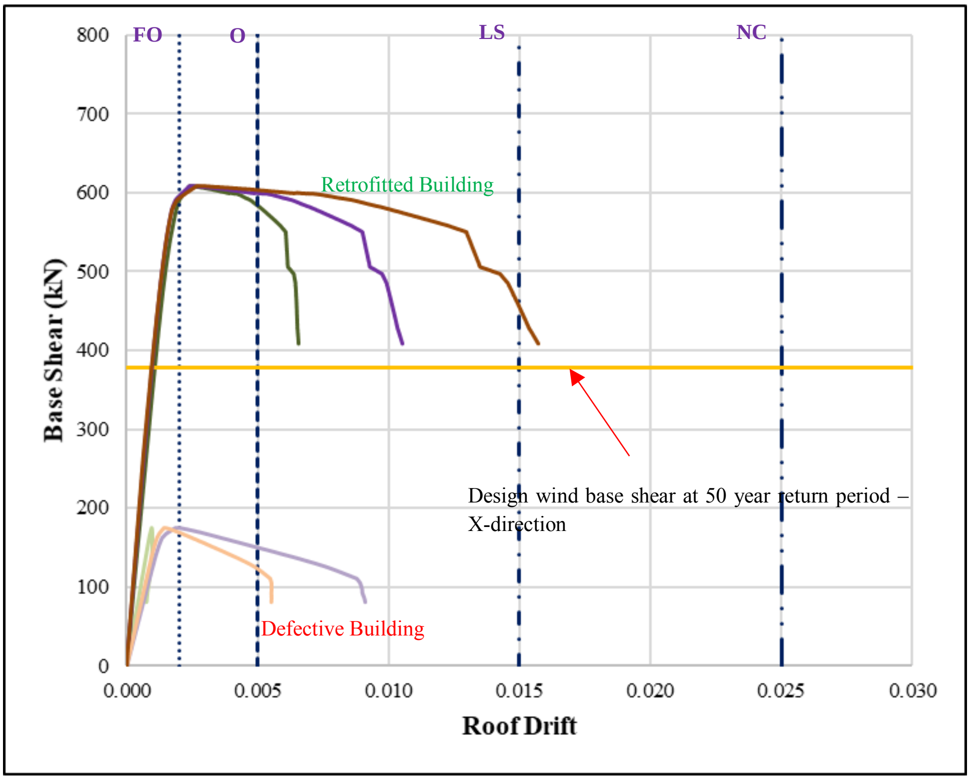

Figure 6.10: Comparison of pushover capacity curves of defective and retrofitted buildings – X-direction

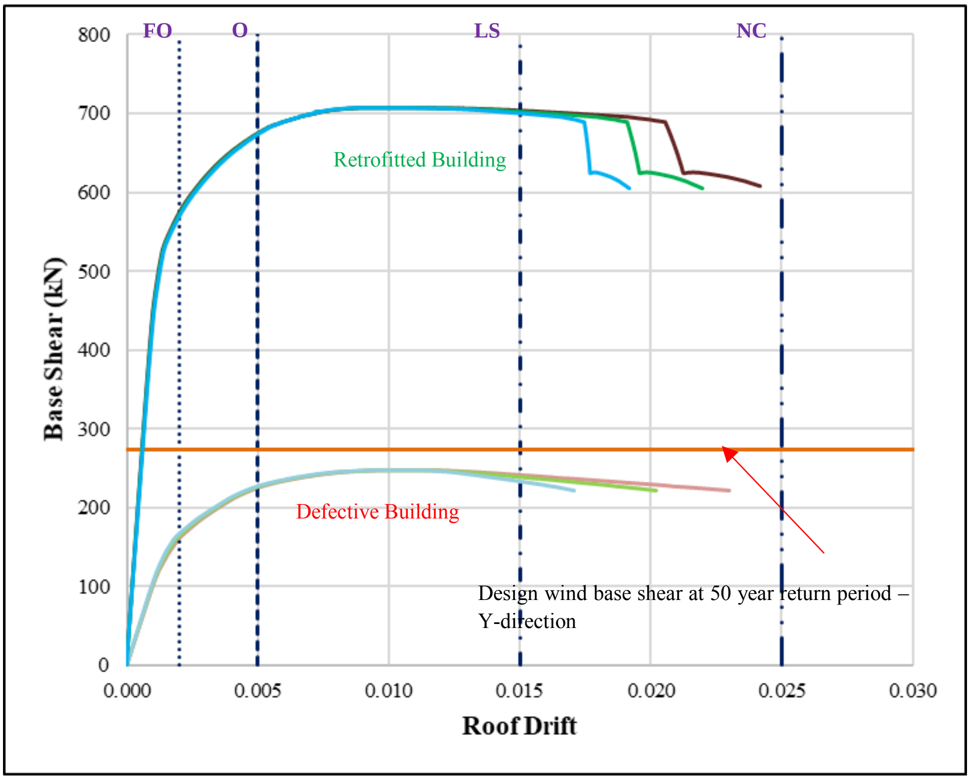

Figure 6.11: Comparison of pushover capacity curves of defective and retrofitted buildings – Y-direction

Accordingly, the proposed retrofitting proposal for the defective building has raised the ultimate non-linear capacity of the building in the X-direction from 176kN to 609kN. Similarly, in the Y-direction, the ultimate non-linear capacity has increased from 248kN to 707kN.

In this way, the non-linear static pushover analyses carried out in this study demonstrated the greater non-linear capacities of Eurocode-based buildings under extreme wind loading, and how these capacities are reduced if the buildings are not designed and constructed according to the relevant building codes and standards.

6.3. Summary

This chapter of the thesis presented the non-linear static pushover analysis results of four Eurocode-based buildings, a defective building, and its retrofitted building, using PERFORM-3D software, which has in-built features for conducting non-linear building analyses. This chapter also provided the structural evaluation of these buildings' pushover capacity curves with a wind performance objective matrix. The results presented in this chapter are vital in drawing conclusions, recommendations, and future work on the implications of adopting Eurocodes for designing disaster-resilient buildings in Sri Lanka.

CHAPTER 7 : ANALYSIS OF BUILDINGS FOR EXTREME EARTHQUAKE LOADING

7.1. General

It is imperative to test new and existing buildings against earthquake loadings beyond the design level earthquake loadings considered by building design codes and standards to ensure adequate structural resilience. Unlike the conventional procedure of designing buildings to withstand wind loads, earthquake-resistant designs rely on non-linear structural behavior. Therefore, the structural elements are originally intended to behave in their non-linear range at design-level earthquake loading. Since buildings may undergo extreme earthquake loading beyond that stipulated in the building design codes and standards during their life span, the structural elements might exceed their anticipated non-linear behavior at the design stage. Therefore, it is crucial to check whether these structural elements excessively utilize the non-linear capacity of the elements, hence requiring non-linear analytical techniques to test buildings against extreme earthquake-loading scenarios that have a reduced probability of occurrence compared with those stated in building design codes.

Non-linear-static-pushover analysis (NSPA) can be utilized to predict the structural response of buildings when subjected to static lateral loading. Moreover, non-linear dynamic analysis techniques, like non-linear dynamic time-history analysis coupled with incremental dynamic analysis, can accurately predict the non-linear response of the buildings against extreme earthquake loading. Due to the inherent dynamic characteristics in earthquake loading, non-linear dynamic analyses are widely accepted over non-linear static procedures when predicting the structural responses of buildings against seismic loading.

In the present study, non-linear dynamic time-history analysis and incremental dynamic analysis were adopted to estimate the structural response of five buildings, including three Eurocode-based new buildings, an existing building found to have defects, and its retrofitted version under the seismic excitation of extreme earthquake loading. Further to these analysis techniques, fragility assessment was utilized to interpret the responses predicted by time-history and incremental dynamic analysis. Finally, the estimated fragilities were compared with the Vision 2000 recommended seismic performance objectives in the context of structural resilience.

7.2. Ground motion selection

Since Sri Lanka is less vulnerable to earthquakes, it does not have a comprehensive database of historical ground motion time histories. Therefore, when conducting dynamic earthquake analysis on its structures, which requires earthquake time histories, it is necessary to consult other available databases.

The Pacific Earthquake Engineering Research (PEER) ground motion database is widely recognized and comprises an array of ground motion time histories that can be utilized in dynamic earthquake evaluations. It allows users to filter time histories of ground motion accelerations via an interactive web-based application, depending on the availability of ground motion time histories for a given set of criteria. The user can specify the design ground motions by the mean of target response spectrums and the expected features of the seismic ground motions. These ground motion characteristics include fault type, earthquake magnitude, source-to-site distance, and other general features. Upon the input ground motion characteristics, the database filters the requested number of ground motions that satisfy the stated selection criteria and provide good fits to the specified target response spectrum.

For this study, a suite of ground motions was filtered from the Pacific Earthquake Engineering Research (PEER) Centre database (PEER Ground Motion Database - PEER Centre, 2013) based on the selection criteria below.

7.2.1. Spectrum model

The ground motion time histories in the PEER database exhibit different response spectra. The spectrum model option in the PEER database can be utilized to obtain the ground motions that best fit the target response spectrum. The spectrum model can be a built-in target response spectrum, such as the PEER NGA-West2 spectrum, the ASCE Code spectrum, or a user-defined spectrum. In this study, ground motions were not matched with the country's response spectrum using the PEER database. Instead, raw ground motions were downloaded from the database, and the spectral matching was carried out independently.

7.2.2. Record characteristics

Ground motions can be selected based on the record characteristics such as Record Sequence Number (RSN), event name, and station name. The Record Sequence Number (RSN) is a unique identifier assigned to a ground motion event (RSN1,..RSNn). This option can filter a ground motion if its corresponding RSN number is known. The ground motion time histories of a particular event recorded at different stations can be filtered based on the event name. Conversely, filtering ground motions based on station name will provide a series of ground motions recorded at that station. In the current study, the filter criteria built on these record characteristics were not considered necessary since the PEER database does not contain earthquake records relevant to Sri Lanka.

7.2.3. Search parameters

Utilizing search parameters for filtering ground motions is a well-recognized approach, particularly when searching ground motions for a country not considered in the PEER database. These search parameters require information on the seismic source that governs the seismic hazard at the site, and they can be selected to represent the seismicity of the particular site in consideration.

7.2.3.1. Fault type

Ground motions can be filtered based on different faulting mechanisms accountable for triggering earthquakes. These faulting mechanisms include strike-slip, normal/oblique, reverse/oblique, strike-slip and normal, strike-slip and reverse, and normal and reverse.

Since Sri Lanka is situated in the Northwestern region of the Indo-Australian tectonic plate, far from the tectonic plate borders, Sri Lanka is less vulnerable to earthquakes triggered by interplate actions. However, Sri Lanka remains susceptible to intraplate earthquakes, which are triggered by enormous stress within the plate and initiated by ancient fault lines and rift zones. In 2020, Seneviratne et al. (2020) conducted a study based on historical records to estimate seismicity near Sri Lanka. Their study concluded that the activities within the Mannar rift zone are the major causes of seismic threats to Sri Lanka. The Mannar basin has faulted blocks of the continent and an approximately 10km thick sedimentary layer on the faulted sea floor. Continued thickening of the sedimentary layer can induce relative motion of the faulted rock blocks, generating some seismicity.

The type of faulting mechanism that could generate an earthquake within a tectonic plate is different from the faulting mechanisms that trigger an interplate earthquake. Since the specific fault mechanism that could trigger a future earthquake is presently unknown, the exact faulting mechanism was not considered during the ground motion filtering. Instead, all types of possible faults were considered.

7.2.3.2. Magnitude (min, max)

Earthquake magnitude indicates the size of the earthquake. Seneviratne et al. (2020) established a relationship between the return period and magnitude of earthquakes utilizing the procedure described by Gutenberg and Richter. Accordingly, they estimated magnitudes of 6.9 and 8.4 for the earthquakes with return periods of 475 and 2500 years, respectively. However, they emphasized that it is impossible to witness the occurrence of an earthquake with a magnitude more than 7.0 due to a seismic scenario expected in the Mannar rift zone. Therefore, an earthquake incident with a 2500-year return period is considered to have a maximum magnitude of 7.0 from a seismological perspective.

Therefore, in the current study, earthquakes with magnitudes ranging from 6.0 to 7.0 were considered to retrieve the required ground motions.

7.2.3.3. R_JB (km) min, max

R_JB, or the Joyner-Boore distance, designates the source-to-site distance as the closest horizontal distance from the site to the projection of the surface rupture. As highlighted in the study carried out by Seneviratne et al. (2020) and confirmed by the recent seismic records obtained from the Geological Survey and Mines Bureau (GSMB), an earthquake can occur at a depth of 10-15 km in the Western Ocean. However, presently, it is problematic to trace the exact location of an earthquake event that originated in this fault zone. Therefore, for the current study, R_JB distance is assumed to be within the range of 90-100km since the ocean-continental boundary is located about 90 km away from the Western coastline of Sri Lanka.

7.2.3.4. R_rup (km) min, max

R_rup indicates the closest distance from the site to the rupturing fault plane. In the present study, this distance is supposed to be 90-100km due to the inability to trace the exact location of an upcoming earthquake event based on the available data.

7.2.3.5. Vs30 (m/s) min, max

$V_{s,30}$, the average shear wave velocity defines the site class. The site of concern is assumed to have a stratigraphic profile with a shear wave velocity in the range of 360-780 m/s.

7.2.3.6. D5-95 (sec) min, max

D5-95 is the significant duration of the earthquake during which 5% to 95% of the energy or 90% of the total energy is concentrated. In this study, the significant duration is 15 – 60 seconds.

7.2.3.7. Pulse

Pulse-like ground motion records are expected at near-fault sites or sites located less than 10 km from the fault line. These kinds of ground motions have a single large pulse, and all the other values are less than that large pulse.

Since Sri Lanka is a far-fault site, no-pulse-like records were chosen from the database.

7.2.4. Additional characteristics

7.2.4.1. Max no. of records (<=100)

In addition to the specific characteristics, the user can request a maximum of 100 ground motion records.

Although these filtered ground motions have the same characteristics defined by the user, their inherent dynamic characteristics vary from one ground motion to another, resulting in different structural responses when utilized in a structural analysis. Therefore, it is imperative to consider multiple ground motion time histories to produce reasonably accurate results through probabilistic analyses. Thus, it is crucial to determine the number of ground motions to be considered for a given assessment.

Various building codes specify the suitable no. of ground motions to utilize in earthquake analyses in different ways. According to ASCE 7-10, earthquake analyses should consider seven ground motions, whereas ATC 40 suggests utilizing eleven. As recommended in UBC 1997, IBC 2000, FEMA 356, and EC 8, the number of ground motions should be selected in the range where the minimum and maximum are three and seven, respectively. However, some of the previous studies (Vamvatsikos & Cornell, 2004) Bhagat & Wijeyewickrema (2018)) have utilized a suite of 20 ground motions to yield more accuracy in the estimation of seismic demands, while some of the studies (Awchat et al., 2023) have restricted the ground motion suite to the number of ground motions stipulated in code provisions.

In the current study, a set of 20 far-fault ground motions satisfying the above criteria was filtered from the Pacific Earthquake Engineering Research (PEER) Center database to offer adequate accuracy in predicting seismic demands on structures. In summary, these selected ground motions represent relatively large magnitudes ranging from 6.0 to 7.0 and moderate distances of 90 – 100km, all logged on firm soil.

Out of the three components of a ground motion, namely H1 (horizontal component), H2 (horizontal component), and V (vertical component), as defined in the PEER database, only the H1 component was considered for the analysis.

7.3.Ground motion matching

Ground motion time histories downloaded from the PEER database relate to different response spectra. Therefore, it is essential to match these ground motions with the country’s response spectrum before using them in an analysis.

7.3.1. Target response spectrum of Sri Lanka

Still, Sri Lanka does not have a response spectrum to estimate the response of structures. However, recent research has been undertaken to develop a response spectrum for Sri Lanka.

In 2013, Kularathna et al. (2013) conducted a study to compare the various response spectra recommended in several seismic codes, namely Eurocode 8, Indian seismic code (IS 1893-1: 2002), and Australian code (AS 1170.4: 2007) normalized by the peak ground acceleration for nearly equivalent soil forms. Figures 7.1 – 7.3 illustrate Kularathna et al.'s comparative analysis for code response spectra based on three different soil types.

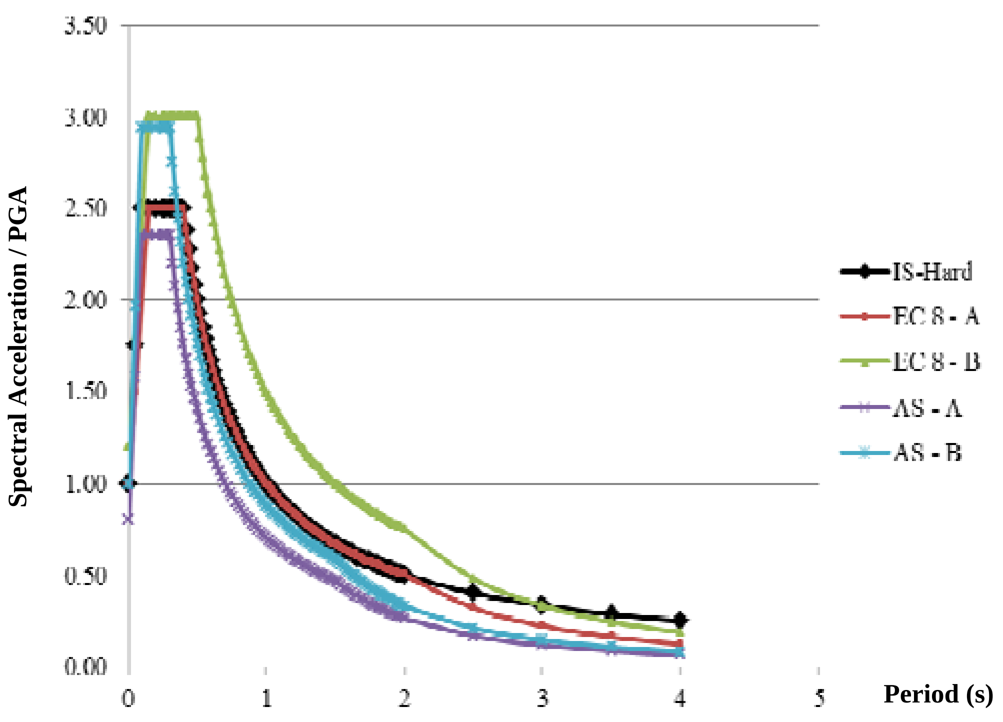

Figure 7.1: Comparison of code response spectra for hard soil

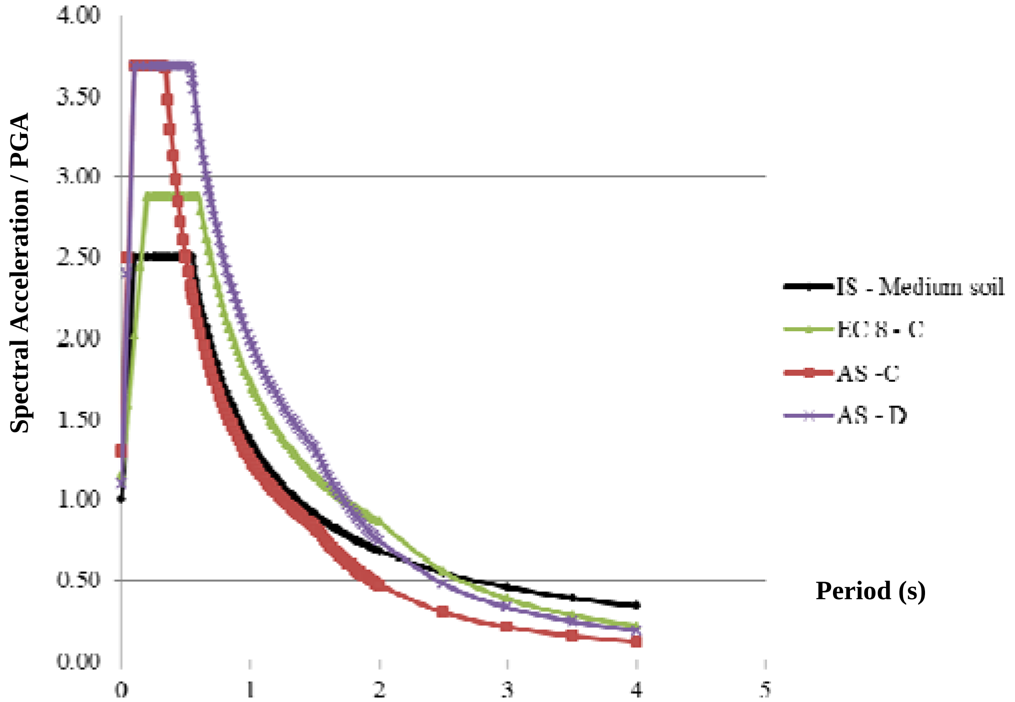

Figure 7.2: Comparison of code response spectra for medium soil

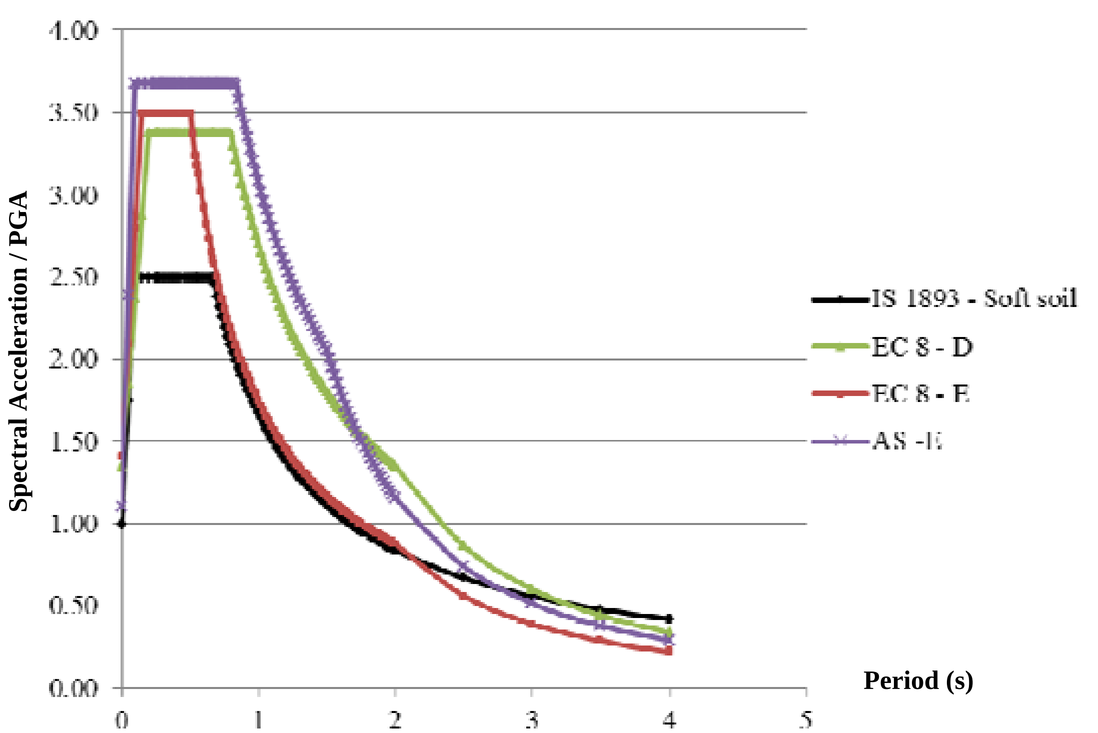

Figure 7.3: Comparison of code response spectra for soft soil

Their comparison showed that the response spectra vary from code to code, even when normalized response spectra are considered for approximately equivalent soil types.

Consequently, they highlighted that it is not reasonable to select a particular code spectrum as the most appropriate spectrum representing the local conditions of Sri Lanka without conducting a proper seismic hazard assessment.

Nonetheless, Kularathna et al. (2013) justified the adaptation of the response spectrum recommended in the Indian seismic code to Sri Lanka since the Indian seismic code provision is a well-recognized seismic code in the South Asia region, and Sri Lanka is situated close to India. Also, they assumed that both Sri Lanka and India possess approximately similar levels of seismicity and ground conditions. Kularathna et al. (2013) further confirmed their justification by comparing the response spectrum developed by Uduweriya et al. (2013) for a rock site in Colombo with the response spectrum recommended in the Indian seismic code. These two spectra demonstrate a reasonable alignment, as presented in Figure 7.4 below.

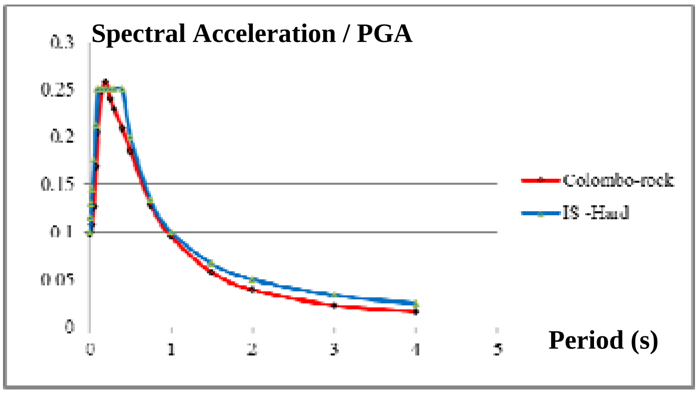

Figure 7.4: Comparison of response spectrum in Indian seismic code for hard rock with response spectrum for Colombo rock site. Adapted from (Uduweriya et al., 2013)

The response spectrum developed by Uduweriya et al. (2013) was considered for the present study.

7.3.2. Original Accelerograms and Matched Accelerograms

Each ground motion in the suite was matched with Sri Lanka's target response spectrum using SeismoMatch software. Figure 7.5 shows the original acceleration time history, the matched acceleration time history, and the scaling of ground motion no. 01 with the target response spectrum.

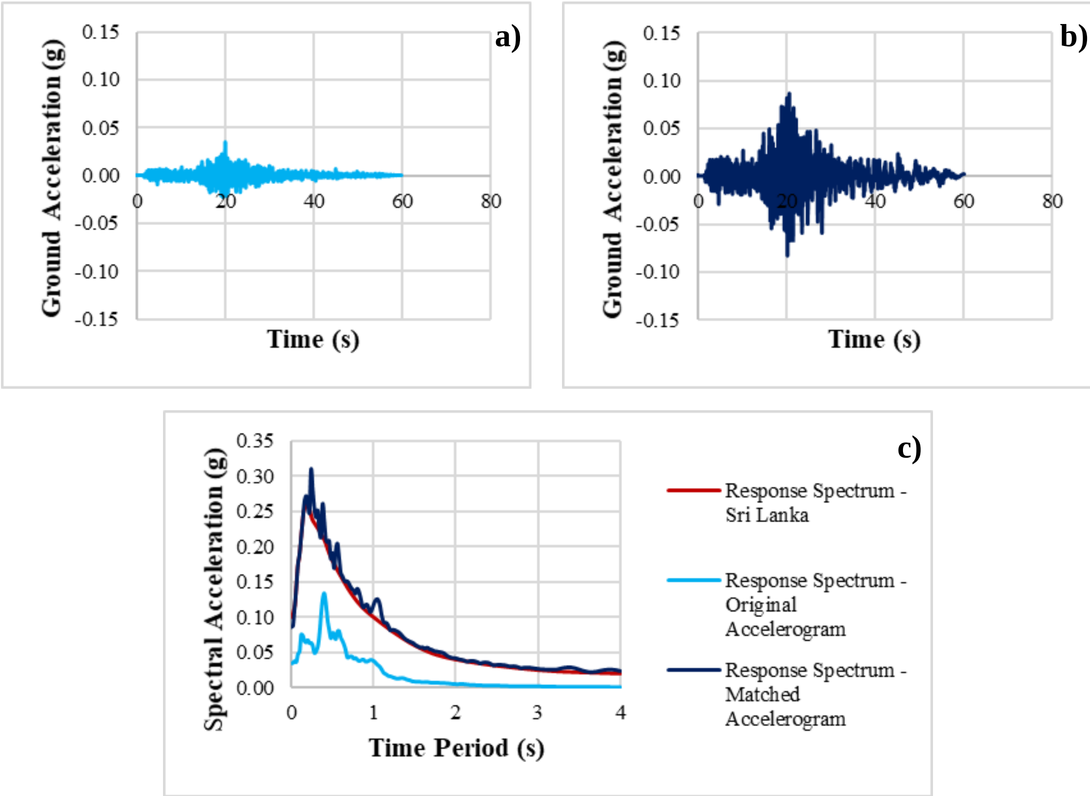

Figure 7.5: Ground motion 1 a) original accelerogram b) matched accelerogram c) response spectra

7.4.Non-linear dynamic time-history analysis, incremental dynamic analysis, and fragility assessment of buildings

Non-linear dynamic time-history analysis (NDTHA) combined with incremental dynamic analysis (IDA) provides more reliable structural performance predictions of buildings under seismic loading compared to non-linear static pushover analysis (NSPA). Non-linear dynamic time-history analysis is a well-recognized analysis technique used to investigate the structural responses under seismic excitations. It predicts more realistic responses since buildings are subjected to actual ground motions in the non-linear dynamic time-history analysis procedure. Incremental dynamic analysis is an extended version of the non-linear dynamic time-history analysis. In incremental dynamic analysis, a particular ground motion is scaled to different intensities to produce the response of structures at the desired intensities via a series of non-linear dynamic time-history analyses. Incremental dynamic analysis curves illustrate the relationship between the response of a structure measured in terms of an appropriate engineering demand parameter and the selected intensity measure.

In this context, the intensity measure is a property of the externally applied loads or the ground motion time histories. Such characteristics of ground motion time histories include peak ground acceleration, peak spectral acceleration, peak spectral velocity, peak spectral displacement, or any other suitable measure.

Various opinions persist regarding the most suitable intensity measure for incremental dynamic analysis. As mentioned by Nazri (2011), peak ground acceleration is frequently used intensity measure. This can be confirmed by the number of studies wherein the peak ground acceleration had been utilized as the intensity measure compared to the rarely used intensity measures such as peak spectral acceleration, peak spectral velocity, peak spectral displacement, etc (Nazri & Alexander, 2012).

However, it is worth emphasizing that peak ground acceleration refers to the acceleration sensed by the earth during an earthquake, and peak spectral acceleration pertains to the acceleration experienced by a structure. Therefore, peak ground acceleration and peak spectral acceleration, respectively, for a specific event and a structure, are not identical unless the structure holds an infinite stiffness. In the case of a real structure, the whole magnitude of peak ground acceleration does not transfer to a given structure; hence, peak ground acceleration cannot be considered as an intensity measure for a structure, though it is a solid representation of the ground motion.

Over time, there has been a growing interest in using meaningful intensity measures for incremental dynamic analysis. For instance, Bhagat & Wijeyewickrema (2018) considered 5% damped spectral acceleration at the fundamental period of the building (S_aT_1) as the intensity measure for incremental dynamic analysis. They also emphasized that 5% damped spectral acceleration at the fundamental period of the building (S_aT_1) is a more appropriate parameter to characterize the earthquake intensity while reducing the uncertainty in the seismic demand of the structure, which is high when peak ground acceleration is selected as the intensity measure.

The engineering demand parameter represents the building's structural response. Examples include roof drift and inter-storey drift. Bhagat and Wijeyewickrema (2018) considered the maximum inter-storey drift ratio, an engineering demand parameter, as they believed it closely relates to the superstructure's damaged state.

Since the features of ground motions vary from one to another, non-linear dynamic time-history analyses based on different ground motions result in dissimilar responses. However, their deviation is minimal when intensity measures such as peak spectral acceleration are chosen. Therefore, it is advisable to consider multiple ground motion time histories when making decisions on the response of structures. This results in several incremental dynamic analysis curves.

Seismic fragility assessment is a broadly accepted method for interpreting the outcomes of incremental dynamic analysis. Seismic fragility curves quantify the likelihood of a structure surpassing different performance levels at diverse intensities, as required for seismic performance evaluations.

Non-linear dynamic time-history analysis combined with incremental dynamic analysis was employed in the present study to observe the probable structural behavior of the buildings against various ground motions scaled at different intensities. Spectral acceleration at the fundamental period of the building Sa(T1) and the maximum interstorey drift was chosen as the intensity measure and the engineering demand parameter, respectively, for the incremental dynamic analysis. Fragility assessments were conducted following the incremental dynamic analysis, and its results were compared with the Vision 2000 recommended seismic performance objectives to evaluate the degree of structural resilience of the case study buildings.

Non-linear models of buildings were assigned with the total dead load, superimposed dead load, and 30% of the anticipated live load. Each building floor was modeled as a rigid diaphragm where all the floor nodes move in the diaphragm plane as a rigid body, providing infinite in-plane stiffness. The fundamental period of the three-storied typical building, three-storied school building, eight-storied university building, six-storied hospital building, seven-storied defective building, and its retrofitted building was found to be 0.72, 0.49, 0.84, 0.70, 2.43, and 1.28 seconds respectively. Therefore, the peak spectral acceleration at these fundamental periods of the buildings (S_aT_1) are 0.135g, 0.184g, 0.118g, 0.138g, 0.033g, and 0.076g, respectively, as indicated on the country's response spectrum in Figure 7.6.

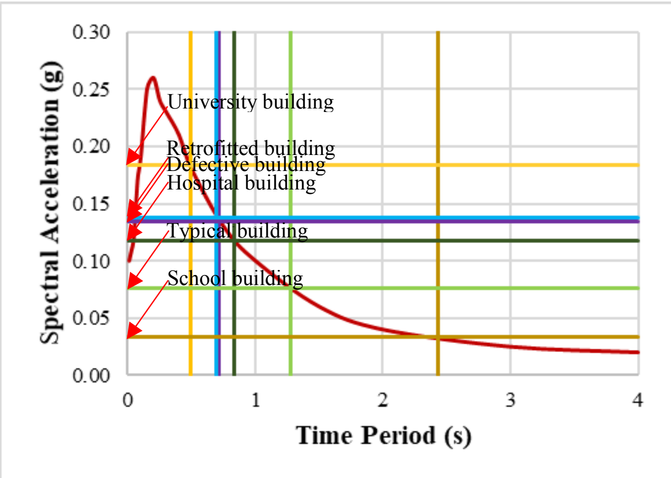

Figure 7.6: Peak spectral accelerations at the fundamental period of the buildings

Although each ground motion was matched with the country's response spectrum, the matched response spectra generated from the selected 20 ground motions did not precisely align with the country's response spectrum, resulting in different peak spectral accelerations at the fundamental period of vibration of the building. Therefore, the peak spectral acceleration at the fundamental period of the building (S_aT_1) was determined from each of the response spectra derived from each ground motion.

In the aftermath, each ground motion time-history with the above peak spectral accelerations at the fundamental period of the building was scaled to fit peak spectral accelerations from 0.1g up to 1.0g.

Next, the nonlinear models of the buildings were subjected to nonlinear dynamic time-history analyses in its X-direction. During this process, it was exposed to 20 ground motion time histories, each scaled to ten spectral accelerations from 0.1g to 1.0g, one at a time, and the interstorey drift values were recorded at each application.

For illustration, Figure 7.7 presents the interstorey drifts recorded at Location X3 of the typical building under the excitation of the first ground motion with 0.1g peak spectral acceleration.

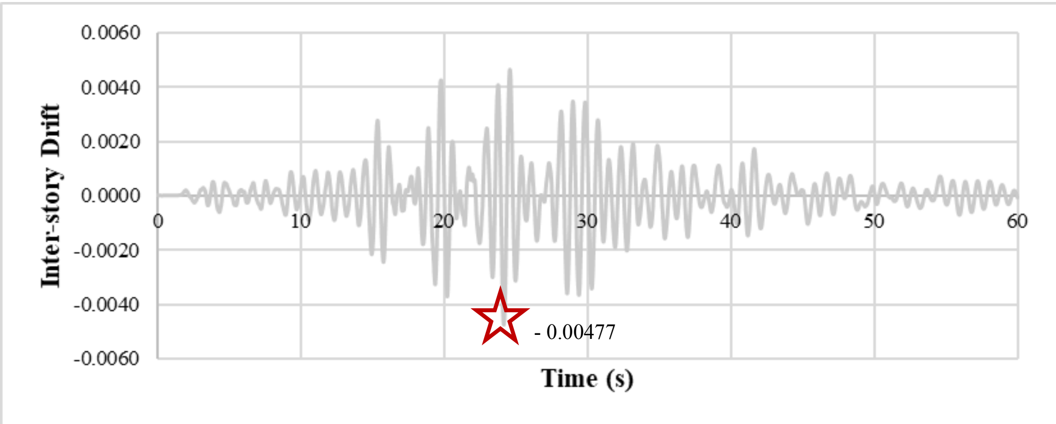

Figure 7.7: Interstorey drift (X3) of the typical building under the seismic excitation of ground motion 1 with 0.1g peak spectral acceleration

As illustrated in Figure 7.7, the maximum interstorey drift recorded at the provided circumstances is 0.00477 in the opposite X-direction amounting to a story displacement of 15 mm.

Figures 7.8-7.17 show the incremental dynamic analysis (IDA) curves drawn based on the analysis results for the X- and Y-directional responses; i.e., maximum interstorey drifts of the typical building, school building, university building, defective building, and retrofitted building when they are subjected to 20 ground motions, each scaled to peak spectral accelerations ranging from 0.1g to 1.0g, along their X- and Y-directions.

Each curve on the IDA plot represents the relationship between the peak spectral acceleration of a particular ground motion and the resulting maximum inter-storey drift of a particular building subjected to the seismic excitation of that specific ground motion.

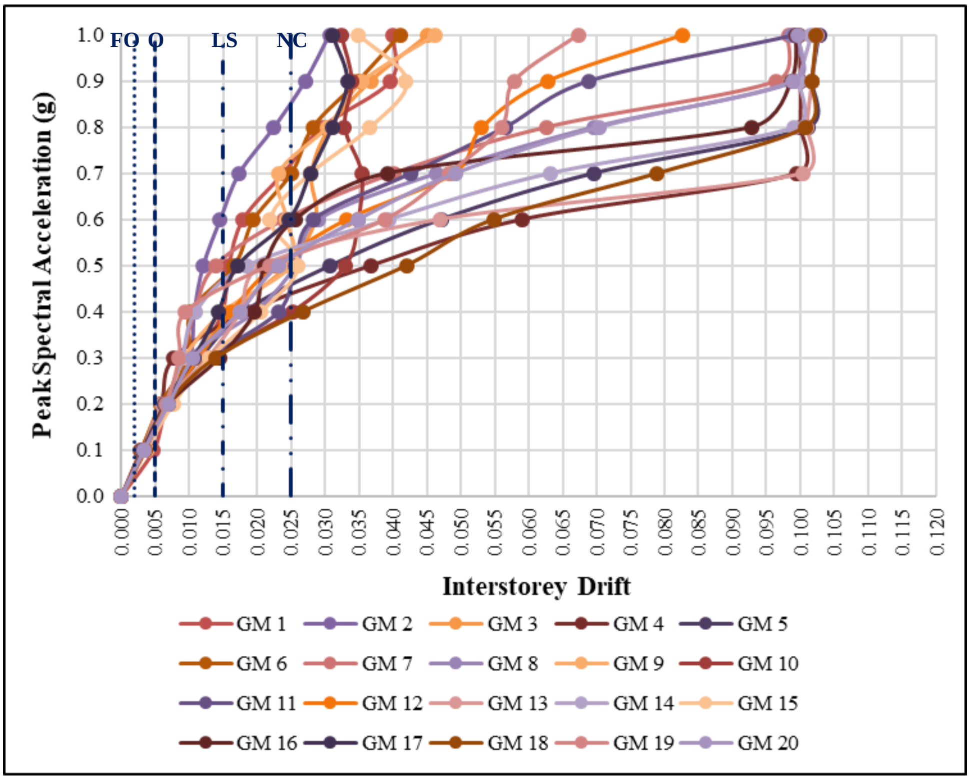

Figure 7.8: Incremental dynamic analysis curves for the maximum interstorey drift in the X-directional response of the typical building

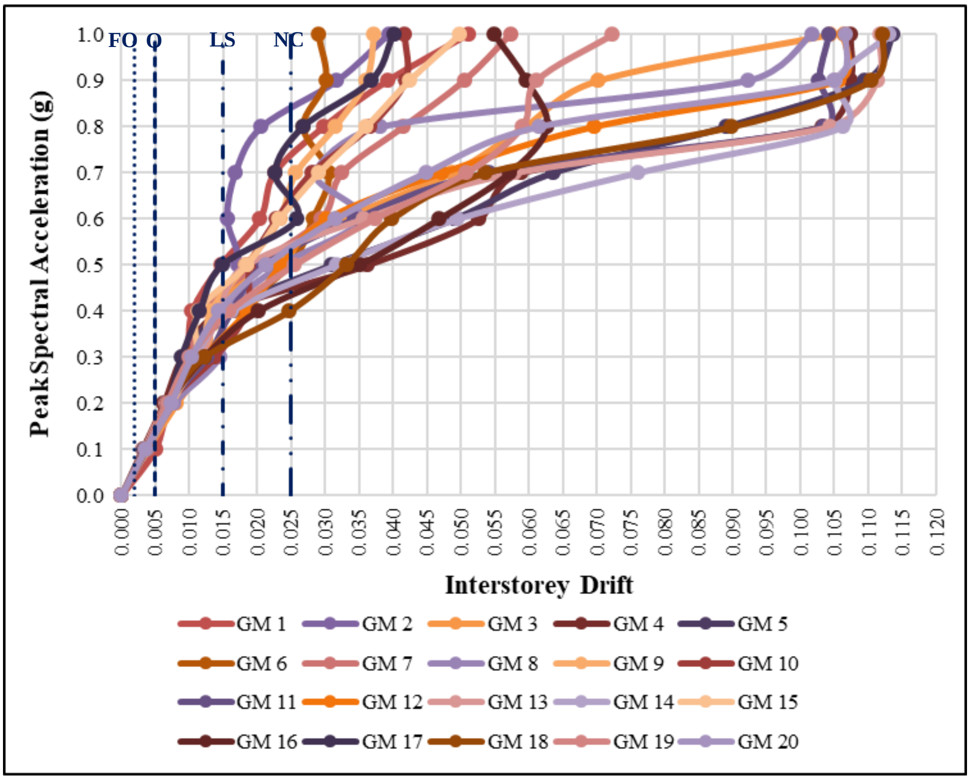

Figure 7.9: Incremental dynamic analysis curves for the maximum interstorey drift in the Y-directional response of the typical building

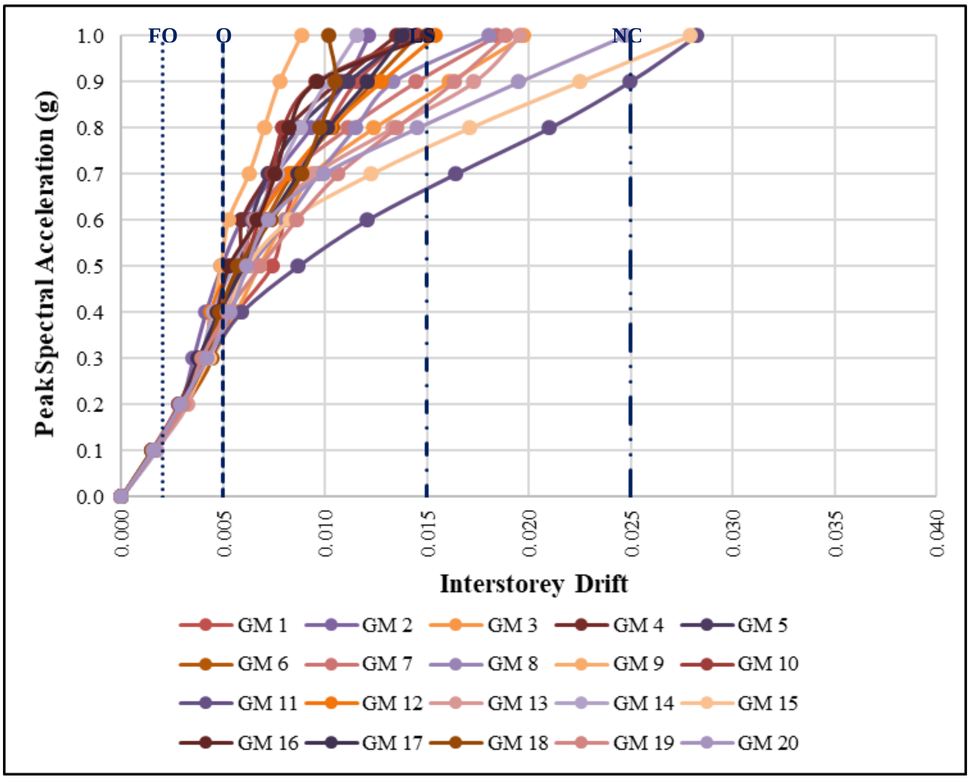

Figure 7.10: Incremental dynamic analysis curves for the maximum interstorey drift in the X-directional response of the school building

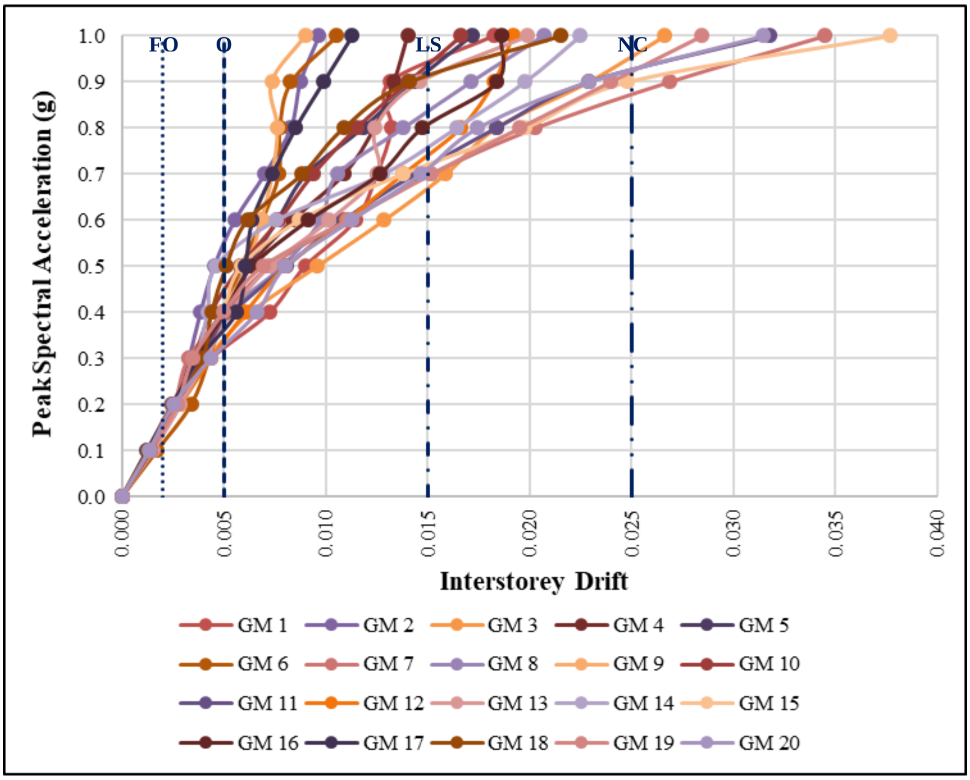

Figure 7.11: Incremental dynamic analysis curves for the maximum interstorey drift in the Y-directional response of the school building

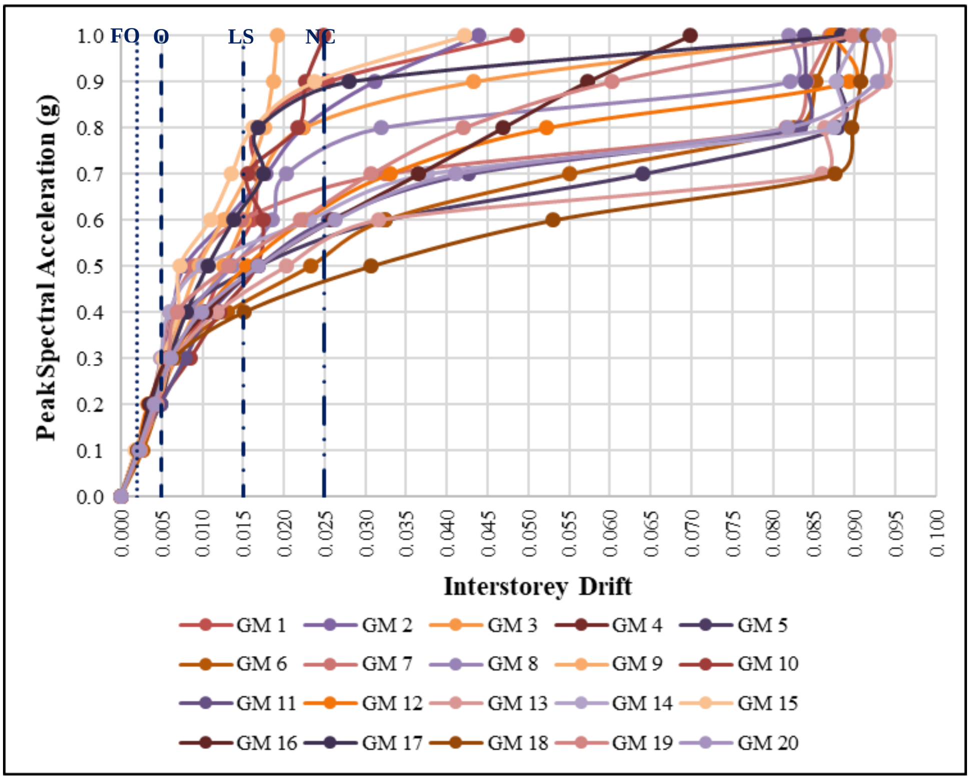

Figure 7.12: Incremental dynamic analysis curves for the maximum interstorey drift in the X-directional response of the university building

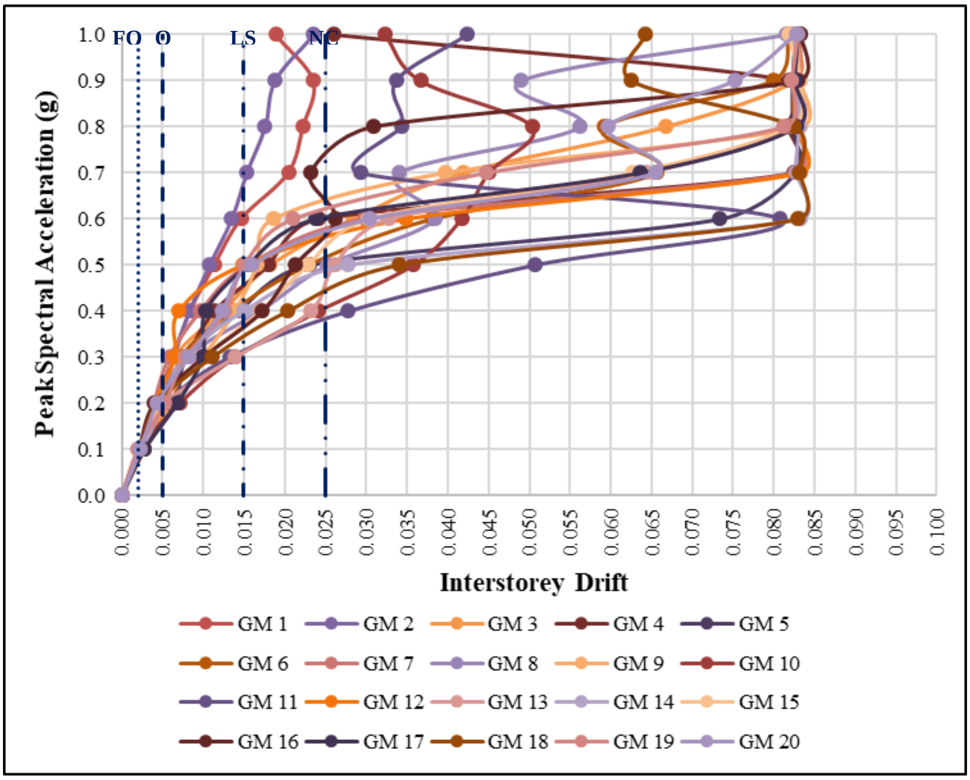

Figure 7.13: Incremental dynamic analysis curves for the maximum interstorey drift in the Y-directional response of the university building

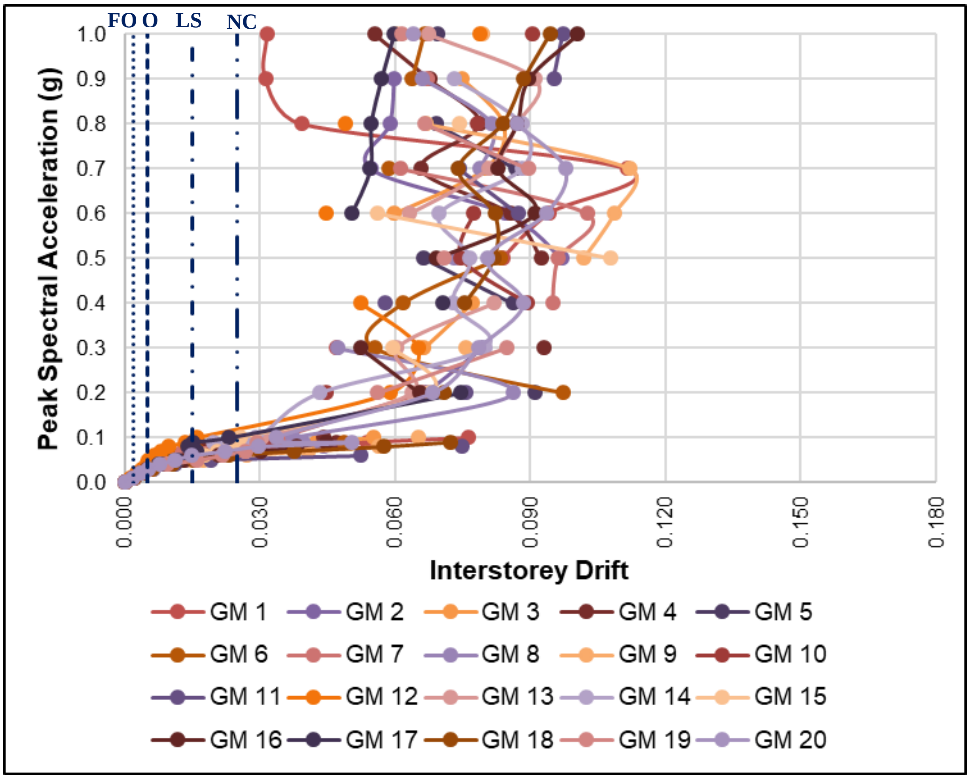

Figure 7.14: Incremental dynamic analysis curves for the maximum interstorey drift in the X-directional response of the defective building

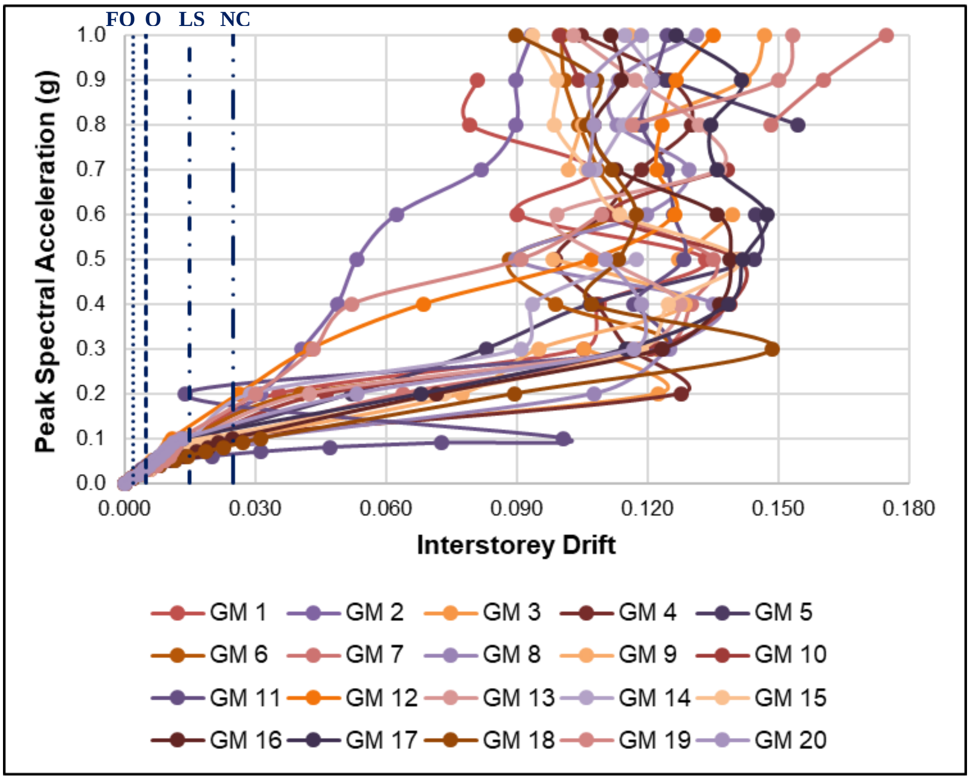

Figure 7.15: Incremental dynamic analysis curves for the maximum interstorey drift in the Y-directional response of the defective building

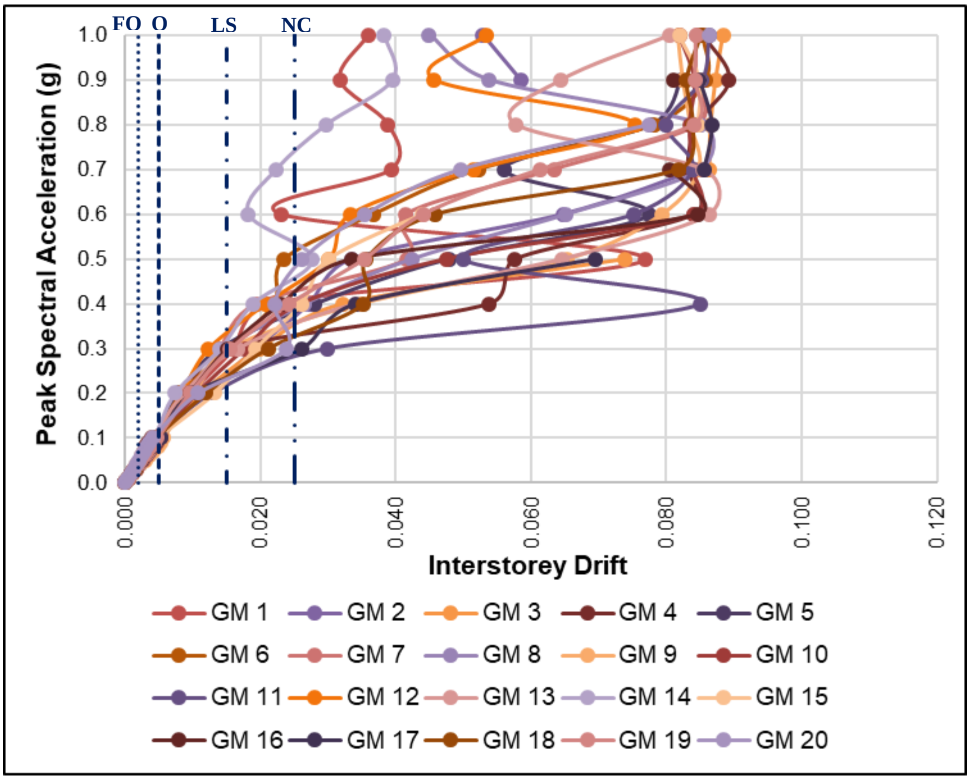

Figure 7.16: Incremental dynamic analysis curves for the maximum interstorey drift in the X-directional response of the retrofitted building

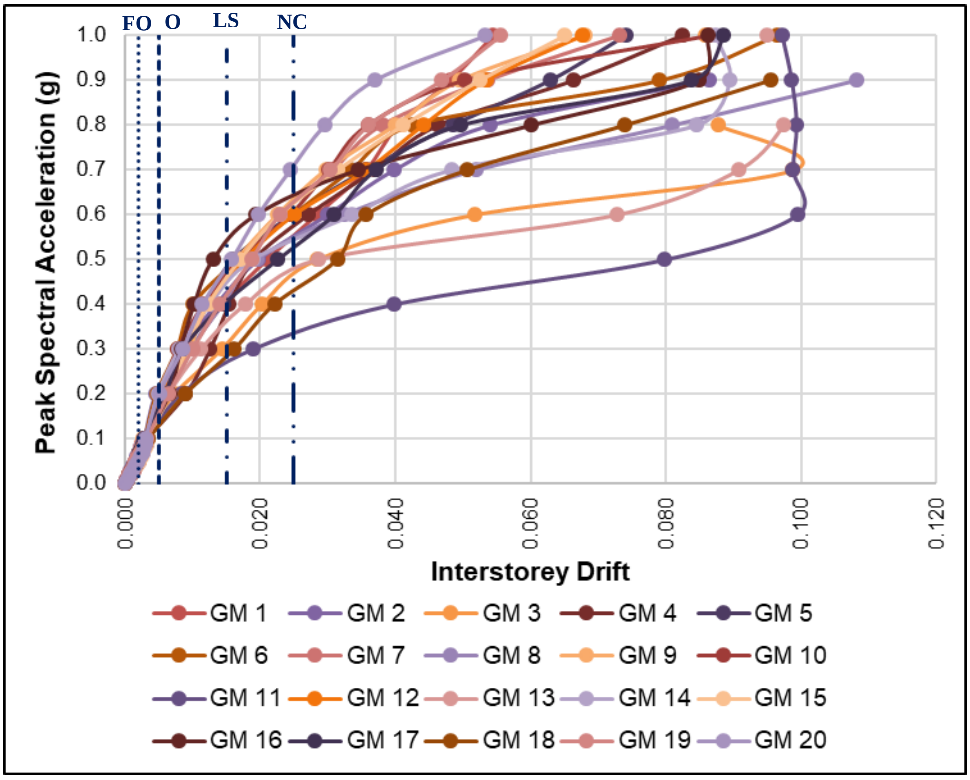

Figure 7.17: Incremental dynamic analysis curves for the maximum interstorey drift in the Y-directional response of the retrofitted building

As evident from the IDA curves presented in Figures 7.8 – 7.17, each building exhibits different performance levels at various intensity measures (IMs); i.e. peak spectral accelerations. The typical building, school building, university building, defective building, and retrofitted building, transits from elastic to yielding at the coordinates (peak spectral acceleration, interstorey drift): (0.2g, 0.007), (0.2g, 0.003), (0.2g, 0.004-0.005), (0.03g, 0.005), and (0.06g, 0.003-0.002), respectively. All Eurocode-based buildings remain elastic over a broader range of intensity measures (peak spectral acceleration) compared to that of the defective building, and the typical building demonstrates comparatively greater resilience to ground motions, as it stays elastic over a wider range of intensity measures.

Past the point of transition from elastic to yielding, these incremental dynamic analysis curves deviate significantly from each other. Therefore, interstorey drifts for a given peak spectral acceleration of the ground motion suite distribute over a broad range, as the peak spectral acceleration increases. Until the collapse point, these IDA curves exhibit various behaviors such as softening, hardening, etc.

A fragility assessment was conducted based on the abovementioned incremental dynamic analysis results. In the fragility calculation, four damage limit states; fully operational, operational, life-safe, and near collapse was assumed at interstorey drifts of 0.2% (0.002), 0.5% (0.005), 1.5% (0.015), and 2.5% (0.025), respectively.

Figures 7.18-7.27 show the fragility curves for the X- and Y-directional behavior of the typical, school, university, defective, and retrofitted buildings. Threshold limits at the four damage limit states are also marked on the IDA curve plots.

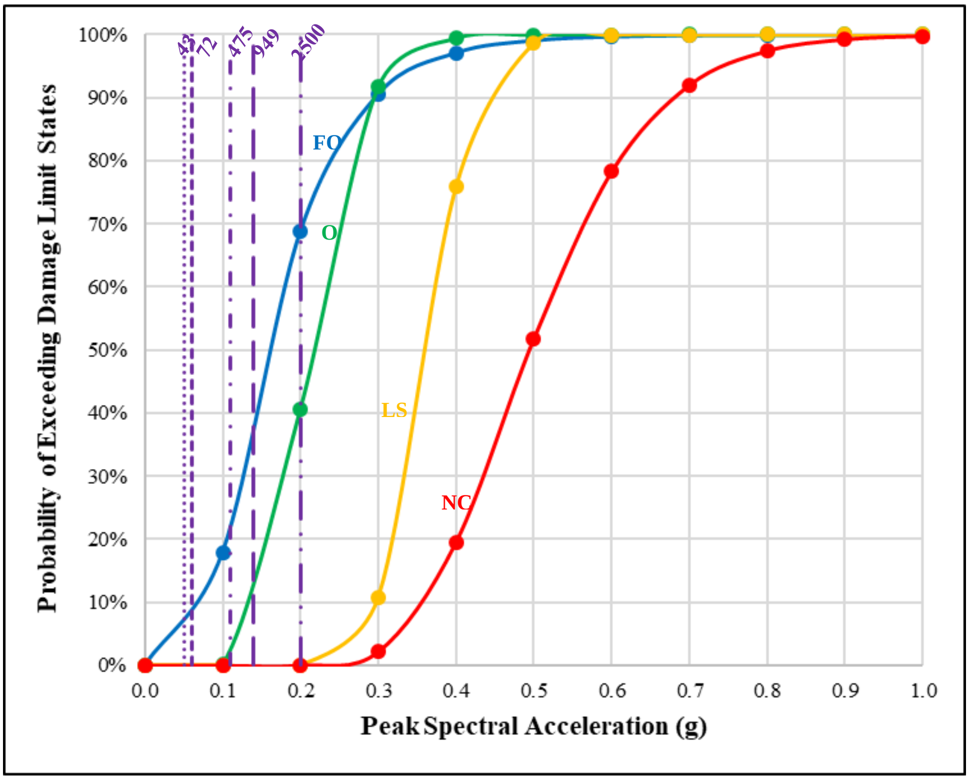

Figure 7.18: Fragility curves for the X-directional response of the typical building

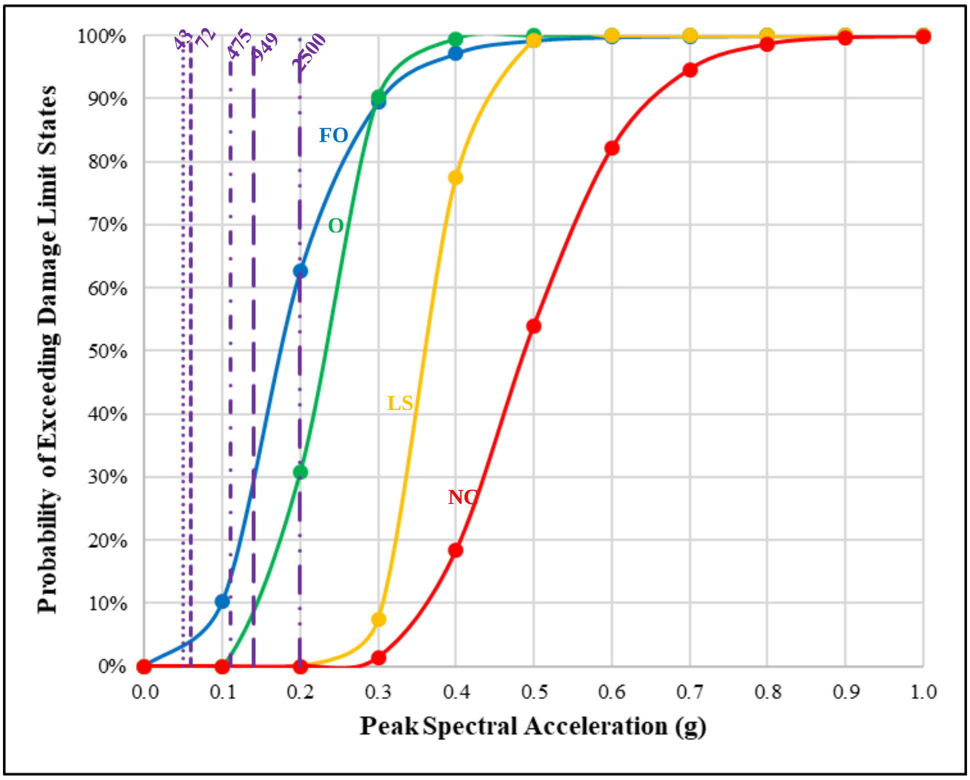

Figure 7.19: Fragility curves for the Y-directional response of the typical building

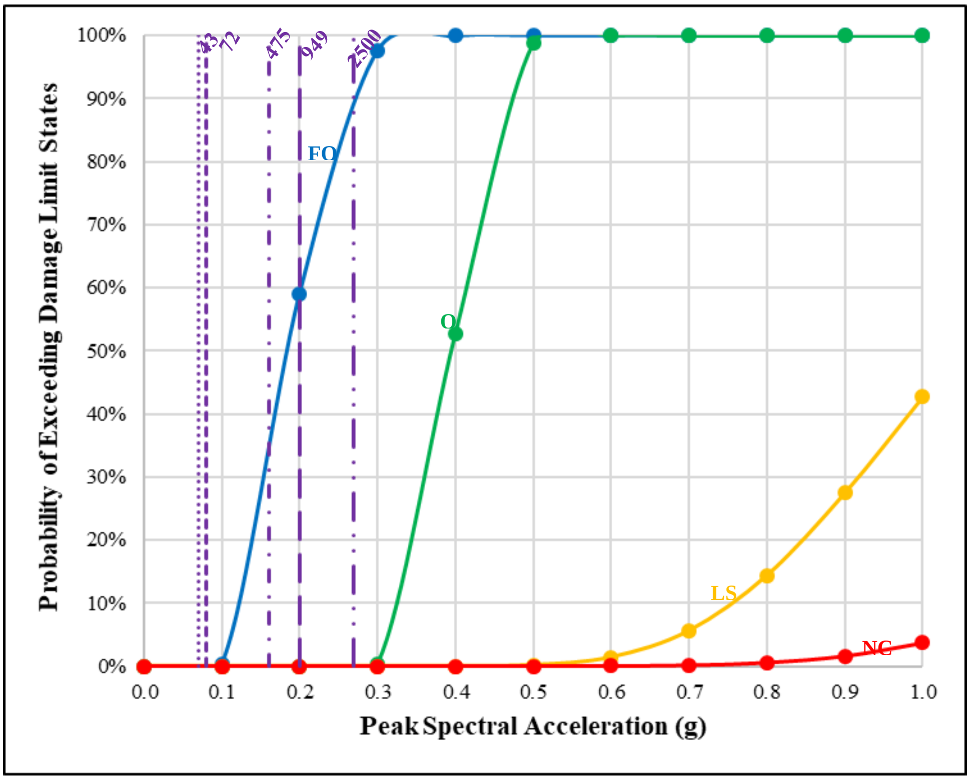

Figure 7.20: Fragility curves for the X-directional response of the school building

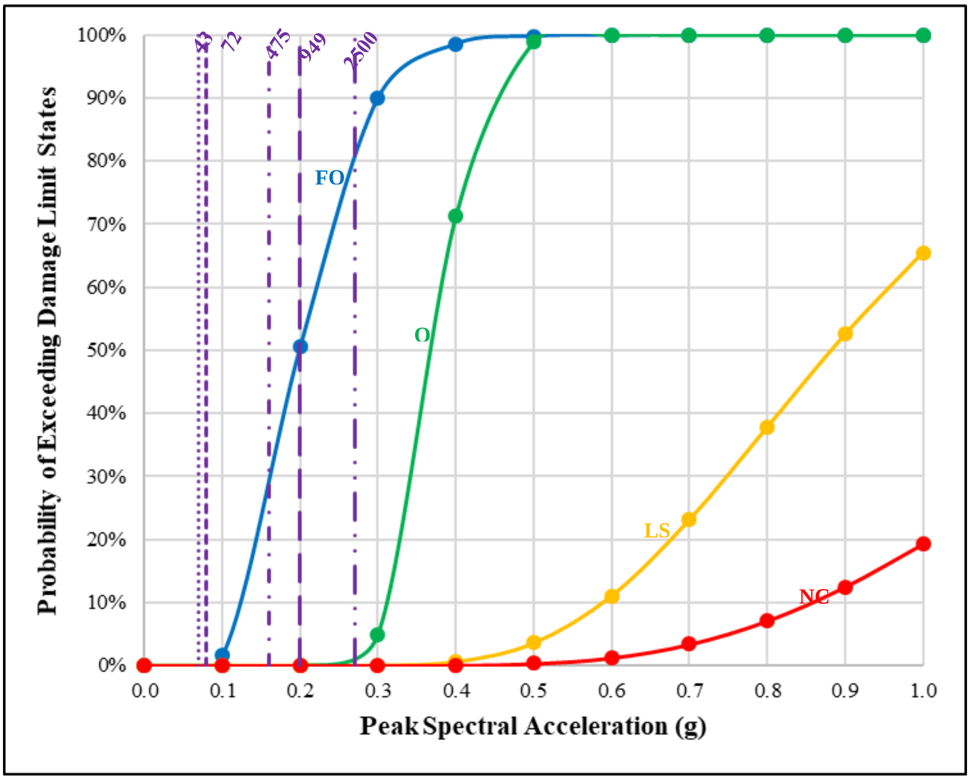

Figure 7.21: Fragility curves for the Y-directional response of the school building

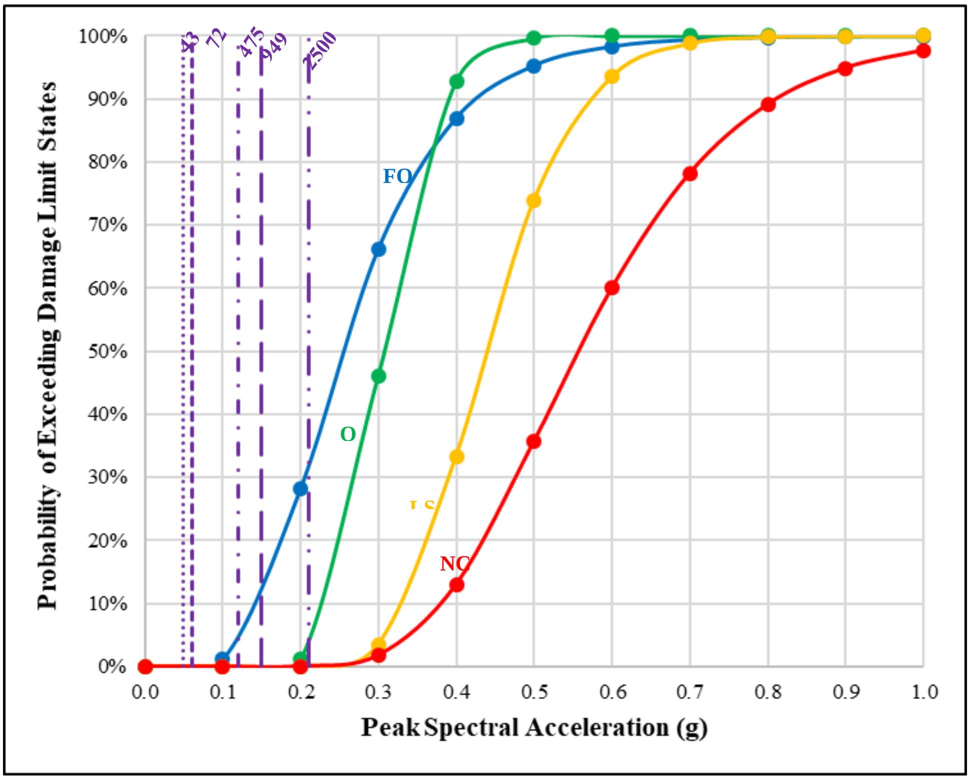

Figure 7.22: Fragility curves for the X-directional response of the university building

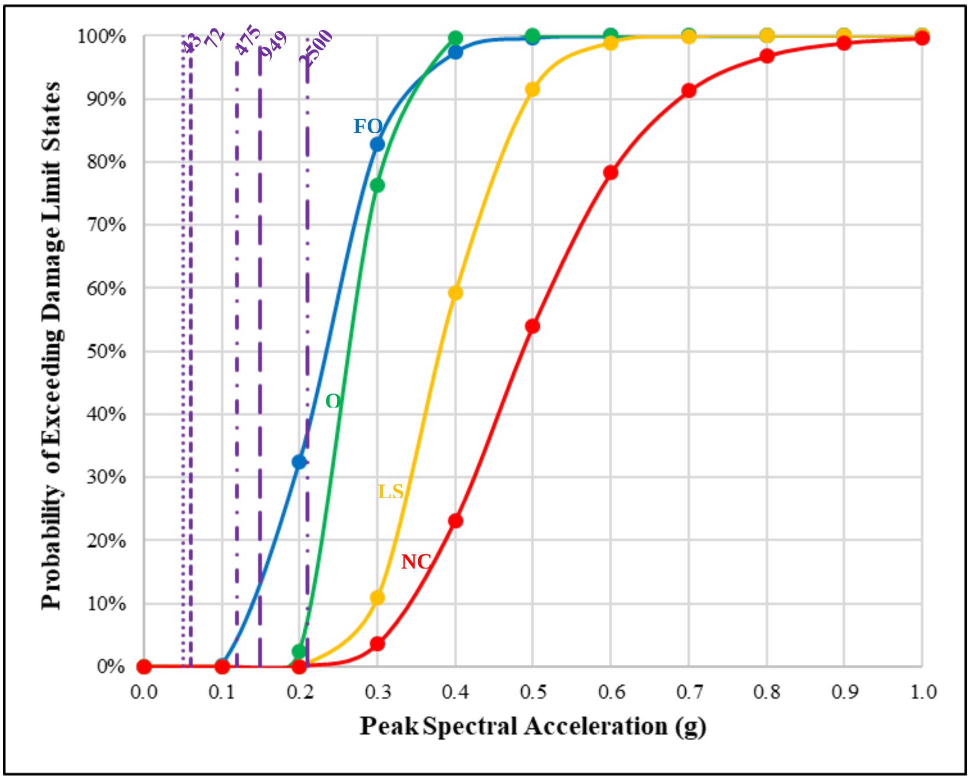

Figure 7.23: Fragility curves for the Y-directional response of the university building

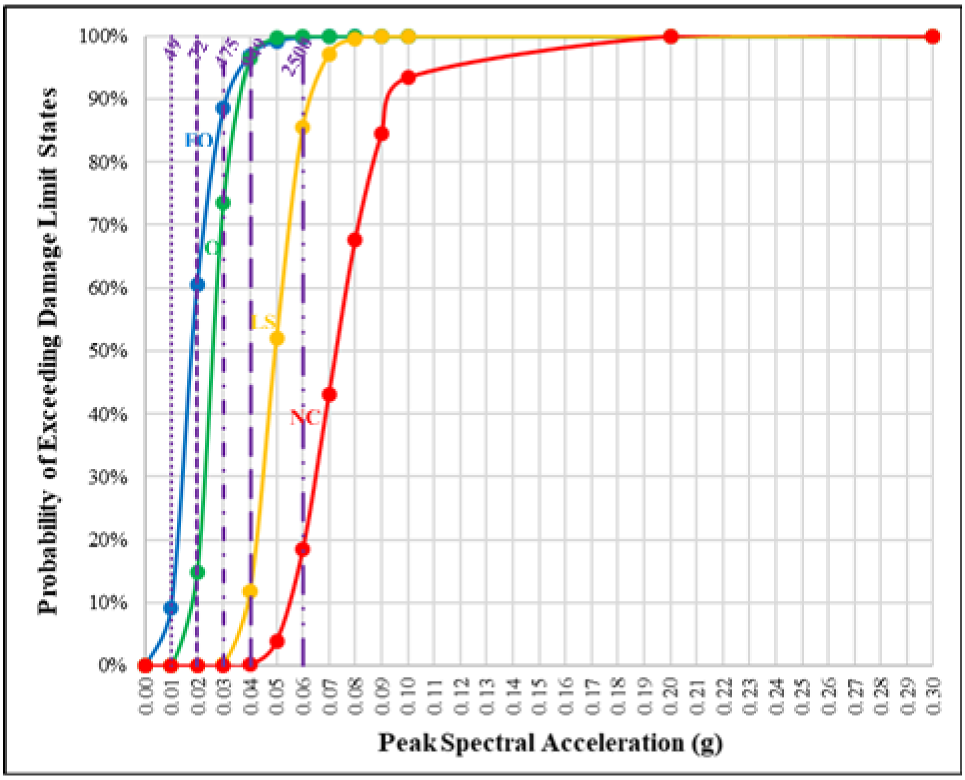

Figure 7.24: Fragility curves for the X-directional response of the defective building

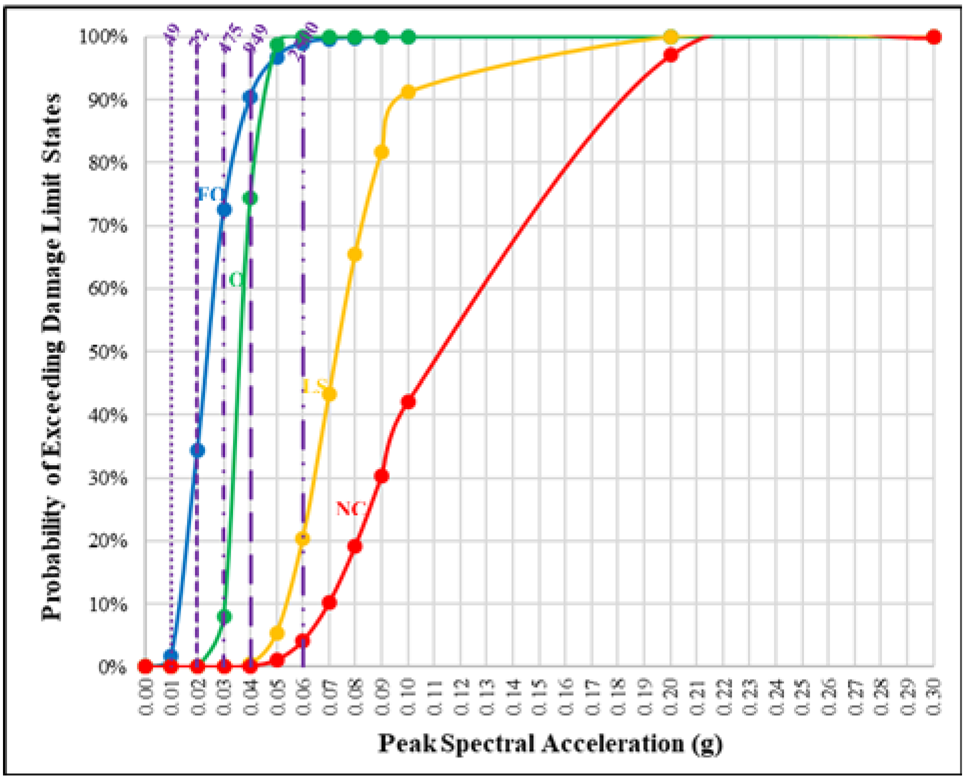

Figure 7.25: Fragility curves for the Y-directional response of the defective building

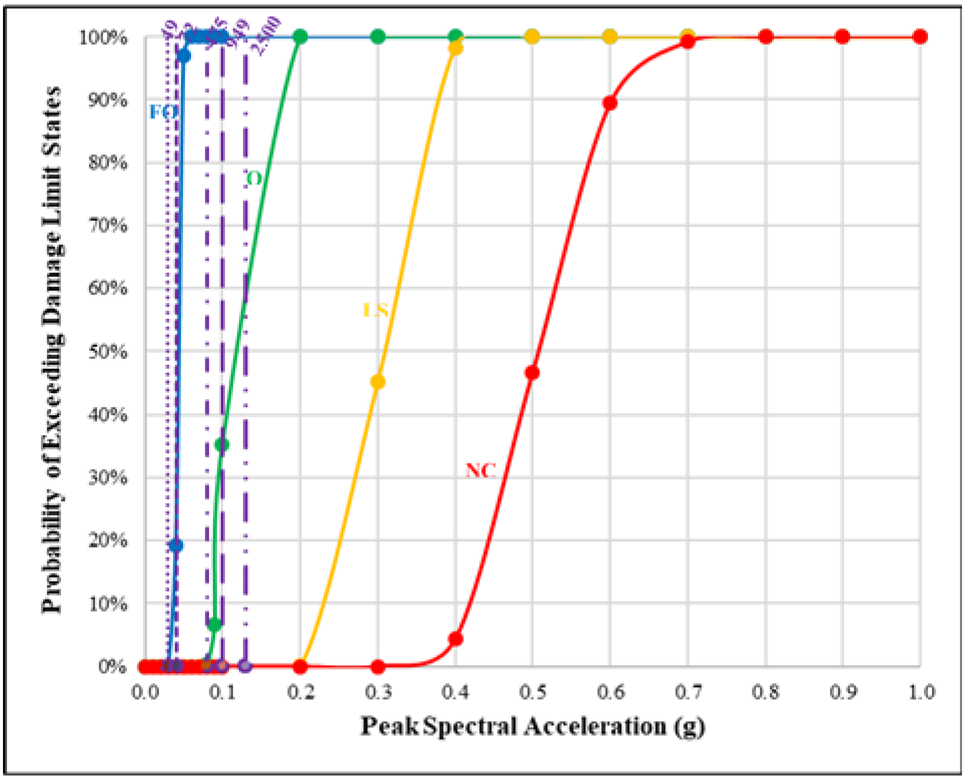

Figure 7.26: Fragility curves for the X-directional response of the retrofitted building

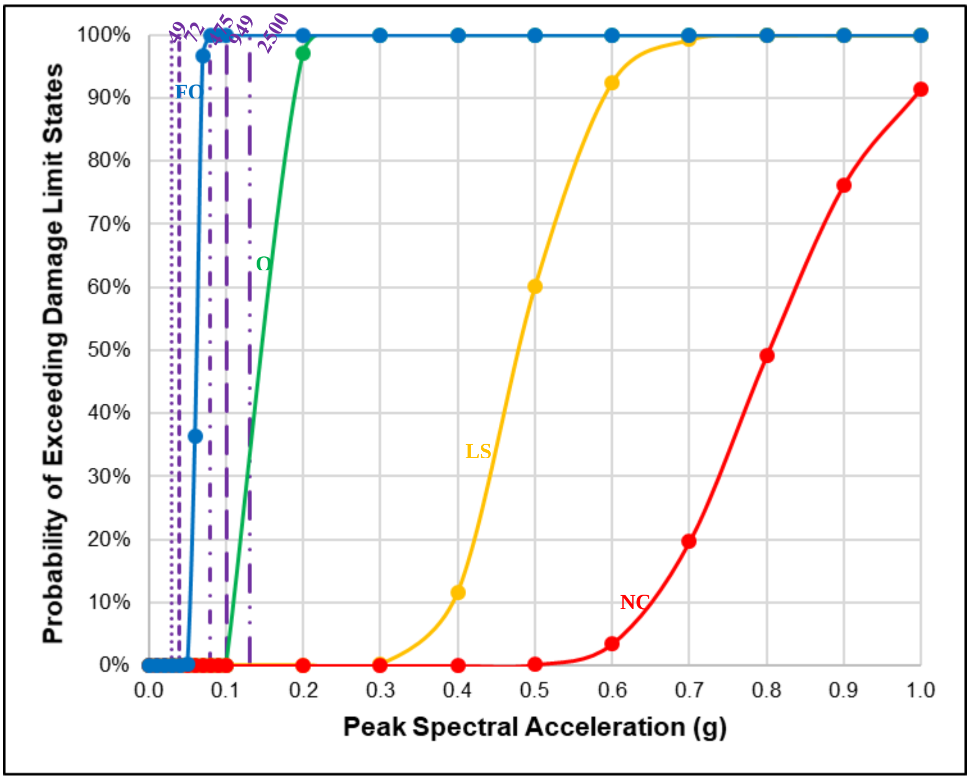

Figure 7.27: Fragility curves for the Y-directional response of the retrofitted building

As shown in Figures 7.18-7.23, the typical building exceeds the fully operational damage limit state under seismic excitations at all return periods in the Vision 2000 seismic performance objectives, while the school and university buildings exceed this limit state only at the 475- and 949-year return periods. The typical building also surpasses the operational damage limit at the 475- and 949-year return periods, whereas the school and university buildings do not exceed this limit at any return period. None of the buildings - typical, school, or university - exceed the life safety or near-collapse damage limit states at any return period.

According to Vision 2000 seismic performance objectives, buildings with safety-critical objectives, such as disaster-resilient buildings, should maintain thier performance levels; fully operational and operational during seismic events with return periods of 475 and 949 years, respectively. The typical building, school building, and university building exhibit an approximate probability of 10-20%, 30-40%, and 0-10%, respectively, of surpassing the fully operational damage limit state at a 475-year return period. Additionally, the typical building shows a 5-15% likelihood of exceeding the operational damage limit state at a 949-year return period. Therefore, the Eurocode-based design of the typical building, school building, and university building does not comply with the Vision 2000 recommended seismic performance objectives for safety-critical requirements.

According to Vision 2000's seismic performance objectives, buildings serving the basic objective should maintain the performance levels; fully operational, operational, life-safe, and near collapse during earthquake events with return periods of 43, 72, 475, and 949 years, respectively. As illustrated in Figure 7.24, this defective building fails to meet these four requirements for a building with a basic objective. As illustrated in Figure 7.25, this defective building fails to meet three requirements: fully operational, life-safe, and near collapse, set in the Vision 2000 recommended seismic performance objectives for a building with a primary objective. Hence, this defective building does not comply with the Vision 2000 recommended seismic performance objectives. This output from the fragility assessment is logical since the building is not even designed to cater to the expected gravity loads.

As illustrated in Figure 7.26 and Figure 7.27, this retrofitted building does not exceed the fully operational, operational, life-safe, and near-collapse damage limit states when exposed to seismic events with 43, 72, 475, and 949 return periods, respectively. Hence, this retrofitted building achieves the requirements set in the Vision 2000 recommended seismic performance objectives for a building serving primary objectives. Figures 7.28 and 7.29 illustrate the improvement in seismic performance from the defective building to the retrofitted building. The fragility curves shown with broken lines represent the defective building, while the solid lines depict its retrofitted version.

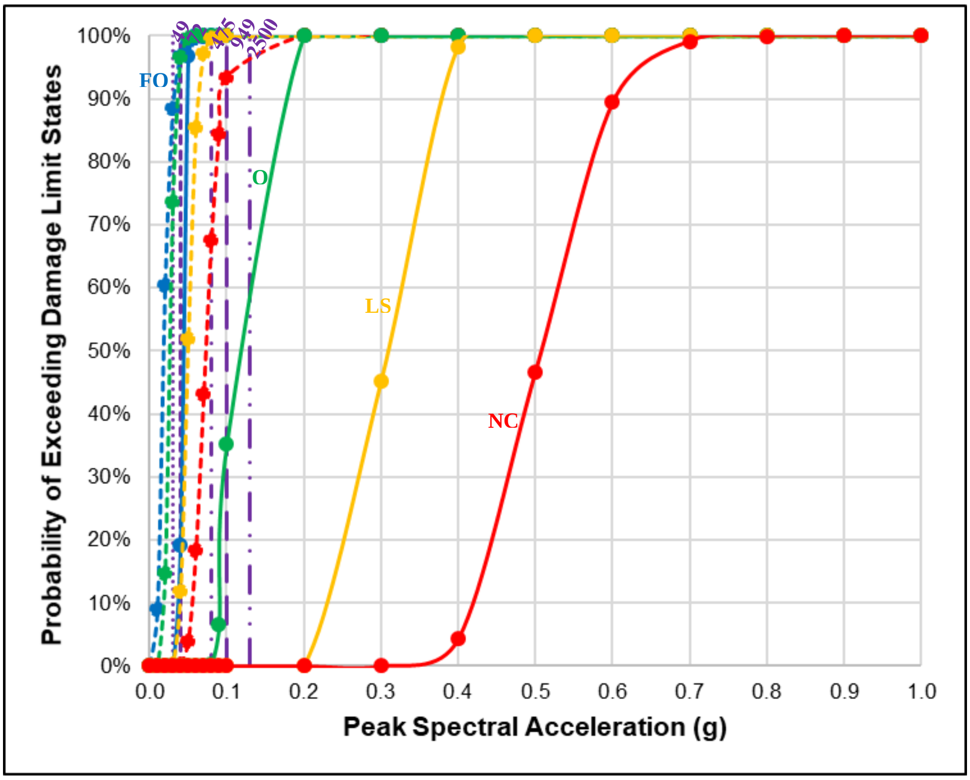

Figure 7.28: Comparison of fragility curves for X-directional response of defective and retrofitted buildings

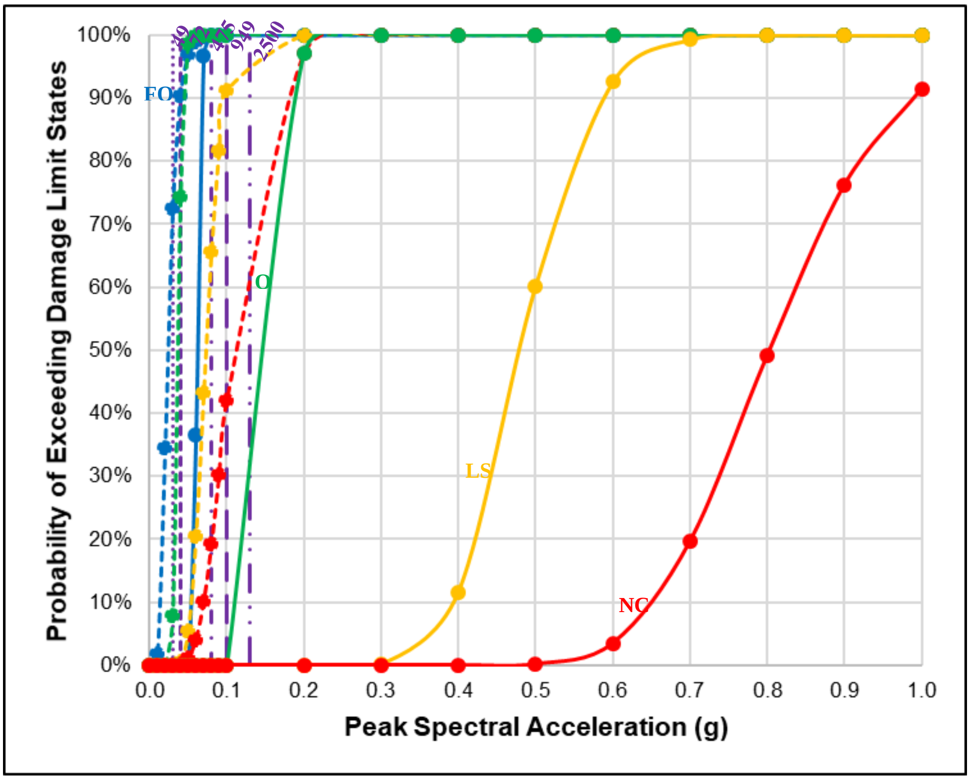

Figure 7.29: Comparison of fragility curves for Y-directional response of defective and retrofitted buildings

As depicted in Figure 7.28 and Figure 7.29, the retrofitted building exhibits enhancements across different damage limit states; fully operational, operational, life-safe, and near-collapse, for both X and Y-directional responses. This assessment of the seismic performance of defective and retrofitted buildings indicated that the retrofitting proposal had improved the defective building's capacity to withstand extreme seismic loadings up to the resilience requirements outlined in the Vision 2000 recommended seismic performance objectives under the basic objective.

Figures 7.30 – 7.33 compare each type of fragility curve—fully operational, operational, life-safe, and near collapse—across the buildings considered in this study.

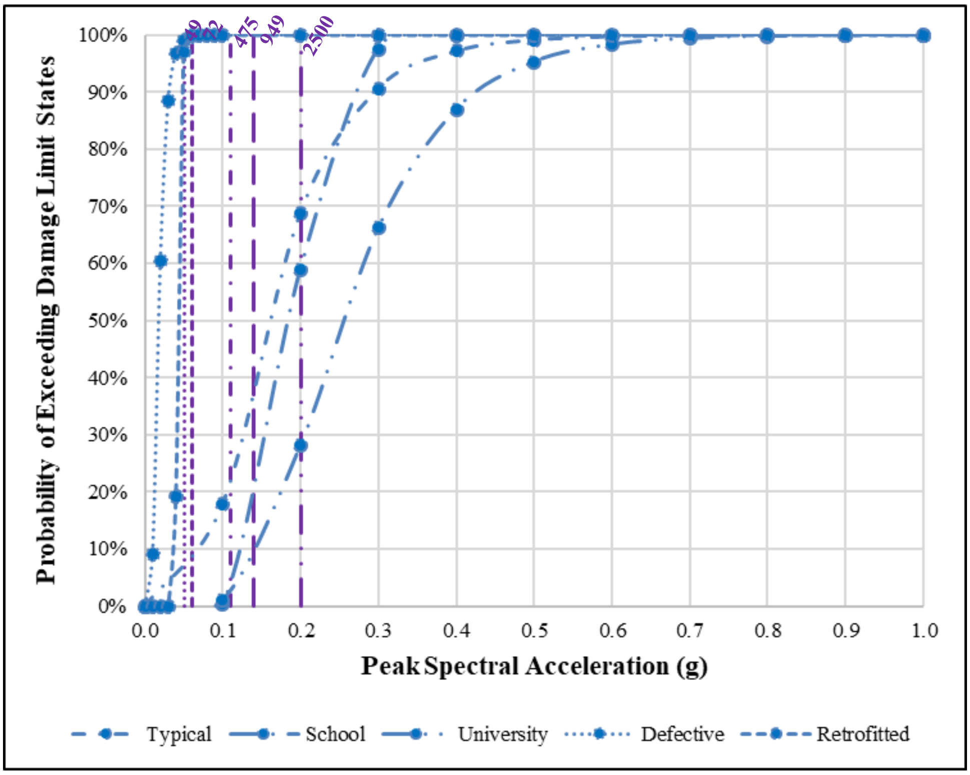

Figure 7.30: Comparison of "Fully Operational" fragility curves for X-directional response of the buildings

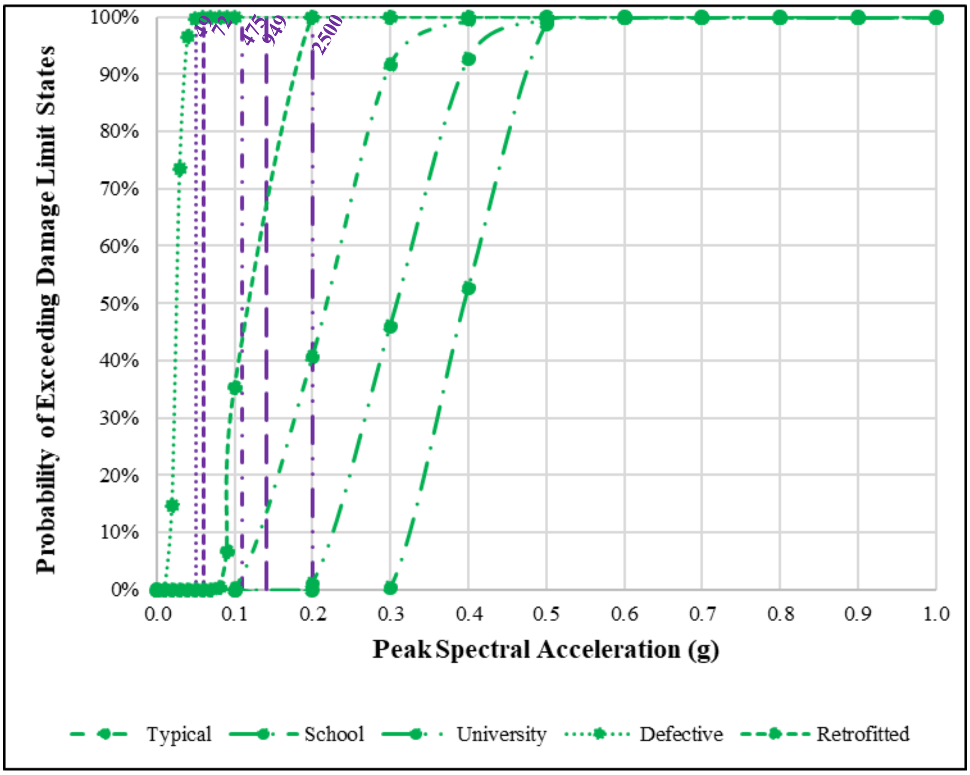

Figure 7.31: Comparison of "Life Safe" fragility curves for X-directional response of the buildings

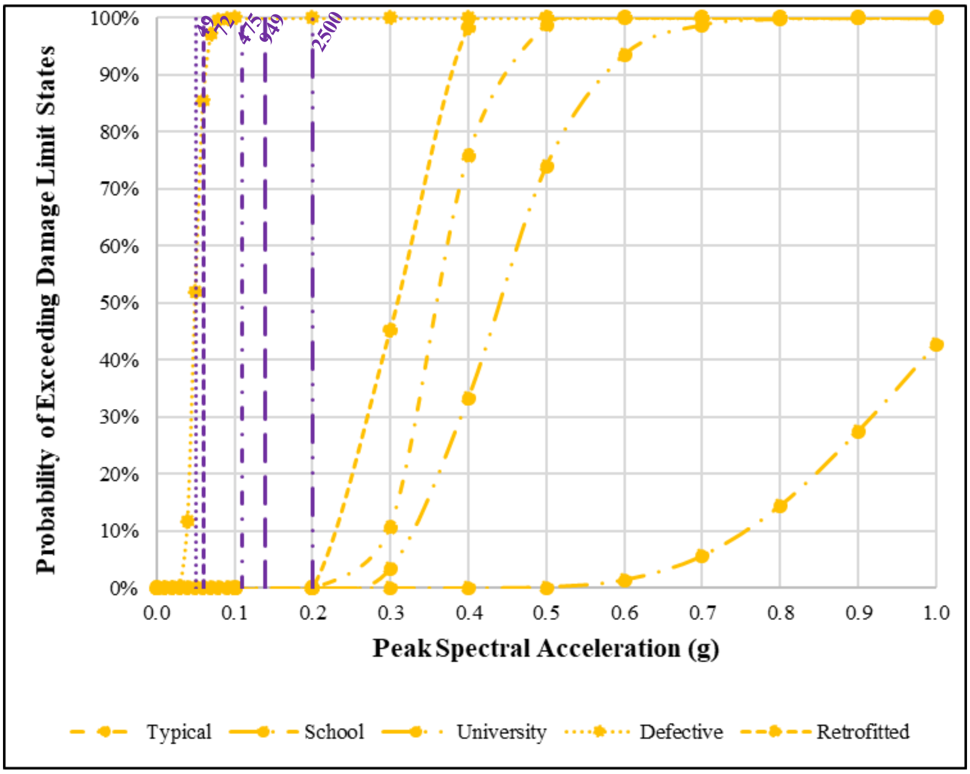

Figure 7.32: Comparison of "Operational" fragility curves for X-directional response of the buildings

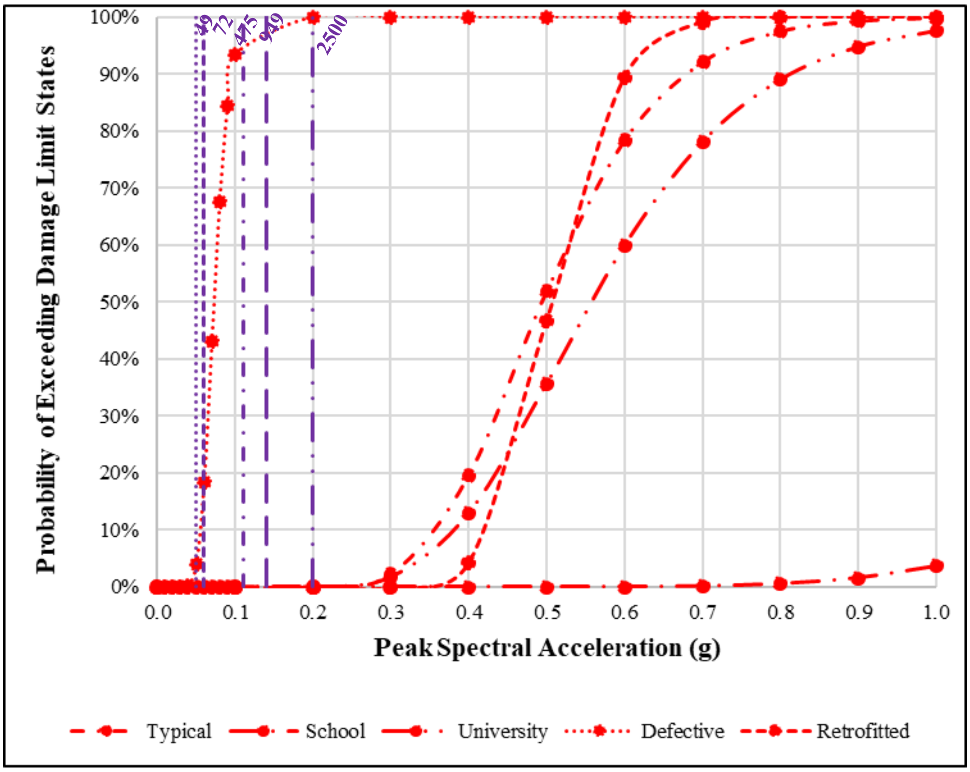

Figure 7.33: Comparison of "Near Collapse" fragility curves for X-directional response of the buildings

As depicted in Figures 7.30 – 7.33, the fragility curves for each damage limit state - fully operational, operational, life safe, and near collapse - vary significantly from building to building. For instance, at a peak spectral acceleration of 0.1g, for the fully operational damage limit state, the corresponding fragility values are 100% for both the defective and retrofitted buildings, 17.90% for the typical building, 1.13% for the university building, and 0.29% for the school building. For the operational damage limit state, the fragility values at 0.1g are 100% for the defective building, 35.27% for the retrofitted building, 0.13% for the typical building, and 0.00% for both the university and school buildings. For the life-safe damage limit state at 0.1g, the defective building has a fragility value of 99.99%, while all other buildings (retrofitted, typical, university, and school) have 0.00%. Similarly, for the near collapse limit state at 0.1g, the defective building shows 93.44%, while all other buildings show 0.00%. This illustrates how buildings perform differently under similar seismic demands, influenced by factors such as the capacities of individual structural elements, overall structural integrity, and stability.

The university building has the lowest probability of disrupting the fully operational damage limit state and can maintain fully operational functionality for the longest period. The school building can withstand more damage before reaching the operational damage limit state. The seismic intensity required for the school building to exceed the life-safe limit, which is critical for human safety, is the highest. Therefore, it has the lowest likelihood of surpassing this damage limit relative to the other buildings, making it the most resilient regarding life safety. Regarding collapse fragility, the defective building shows the steepest increase, followed by retrofitted building, typical building, and university building. The school building remains stable at higher seismic intensities and is expected to perform best during extreme events.

In most damage limit states, the curves become progressively flatter from the defective building, retrofitted building, typical building, and university building to the school building. Steeper slope gradients indicate that buildings are more sensitive to increases in seismic intensity, and the gradient reflects the vulnerability of each building. The flatter curves for most damage states in the school building suggest that it is more resilient, withstanding increasing seismic intensity without quickly reaching these damage limit states.

In overall, the defective building poses the highest risk of exceeding all damage limit states. The retrofitting of the defective building has significantly impacted the loci of the fragility curves marking a reduction in the likelihood of surpassing different damage states compared to the original defective building. The school building, which was pre-planned with disaster-resilient features, shows the lowest risk of exceeding these damage limit states, except for the fully operational damage limit state, where the university building has the lowest risk of exceeding this limit.

Further, Eurocode 8 for the Design of Structures for Earthquake Resistance intends to satisfy “No Collapse Requirement” at a seismic event with a 475-year return period and “Damage Limitation Requirement” at a seismic event with a 95-year return period provided that the building design followed the prescriptive standards and guidelines outlined in the code [Eurocode 8]. However, some of the Eurocode-based buildings considered in this study fail to meet the “damage limitation” requirement at a seismic event with a 95-year return period, confirming that the code alone does not ensure these performance levels.

7.5.Summary

This chapter of the thesis presented the results of the non-linear dynamic time-history analysis, incremental dynamic analysis, and fragility assessment of four Eurocode-based buildings, a defective building, and its retrofitted building, using PERFORM-3D software which has in-built features to conduct non-linear analysis of buildings. This chapter also provided the structural evaluation of these results with recommended seismic performance objectives. The results presented in this chapter are vital in drawing conclusions, recommendations, and future work on the implications of adopting Eurocodes for designing disaster resilient buildings in Sri Lanka.

CHAPTER 8 : COST IMPLICATIONS OF ADOPTING EUROCODES OVER BRITISH STANDARDS FOR A BUILDING SUBJECTED TO GRAVITY LOADING

8.1. General

The building analysis and design provisions differ between various standards, leading to variations in section sizes and reinforcements in building components. Similarly, the differences in the outlined procedures in Eurocodes and British Standards for the analysis and design of structures can result in different construction costs. This chapter discusses the cost implications of adopting Eurocodes and British Standards to design a typical reinforced concrete building under gravity loading.

8.2. Design data of the typical building

Table 8.1 provides the basic details of the typical building, including its location, dimensions, and key design parameters.

Table 8.1: Basic details of the typical building

Building Description	Typical Building
Location	Colombo
Structure type	Multi-story (low-rise) reinforced concrete frame
Roof type	Reinforced concrete slab
Number of stories	Three (ground floor + two upper floors)
Story height	3.2 m
Plan view shape	Rectangular
Plan dimensions	24.0 m × 16.0 m

Table 8.2 below presents the material densities/unit weights used for the typical building.

Table 8.2: Unit weights of materials for the typical building

Material	Unit Weight (kN/m^3)
Reinforced concrete	25.0 (For Eurocode-based analysis) 24.0 (For British Standard-based analysis)
Steel reinforcement	78.5
Block masonry	21.0

Tables 8.3 and 8.4 below present the superimposed dead loads and imposed loads of the building.

Table 8.3: Superimposed dead loads on the typical building

	Superimposed Dead Loads (kN/m^2)	
	Typical Floors	**Roof Floor**
Partitions	1.0	0.0
Finishes	1.8	2.3 (including waterproofing)
Ceiling and Services	0.5	0.5
Total	3.3	3.3

Table 8.4: Imposed loads on the typical building

	Imposed Loads (kN/m^2)	
	Typical Floors	**Roof Floor**
Live load	2.0	0.4

As shown in Tables 8.1 - 8.4, all design data have been kept consistent for the two design codes under consideration, except for the concrete unit weight, which is 25 kN/m^3 for the Eurocodes and 24 kN/m^3 for the British Standards.

8.3. Preliminary design of the typical building

Table 8.5 summarizes the preliminary design of the typical building according to the two codes: Eurocodes and British Standards.

Table 8.5: A summary of the preliminary design

Building Description	**Cross Section Sizes (mm × mm) & Slab Thicknesses (mm)**	
	Eurocode-based Typical Building	**British Standard-based Typical Building**
Columns	225 × 225	225 × 225
Beams in the X-direction	225 × 375	225 × 450
Beams in the Y-direction	225 × 275	225 × 350
Slabs	125	125

The preliminary design procedures in Eurocodes and British Standards resulted in different beam sizes, as shown in Table 8.5. The British Standards require larger beam sizes compared to the Eurocodes. To maintain consistency in the design data during the initial stage and to better understand how the detailed design procedures and equations of the two codes affect final member sizes and reinforcement requirements, initial member sizes were kept similar for both codes. Since the initial member sizes based on the British Standards' procedure also meet Eurocode requirements, and because Eurocode sizes do not satisfy British Standards' requirements, the member sizes specified by the British Standards were considered for the practicality of this particular building construction. Therefore, the initial design based on the British Standards was used in this study.

8.4. Structural analysis of the typical building

8.4.1. Load combinations

For gravity loading conditions, the load combinations 1.35Gk + 1.50Qk and 1.4Gk + 1.6Qk were used for the Eurocodes and British Standards analyses, respectively. Here, Gk represents permanent (dead) loads, and Qk represents variable (imposed) loads.

8.4.2. Structural analysis results

Given the building's symmetry, the structural analysis outcomes for the beams are presented in six sets: beams in Type 1-6 frames. The notation for the six frame types is as shown in Figure 8.1.

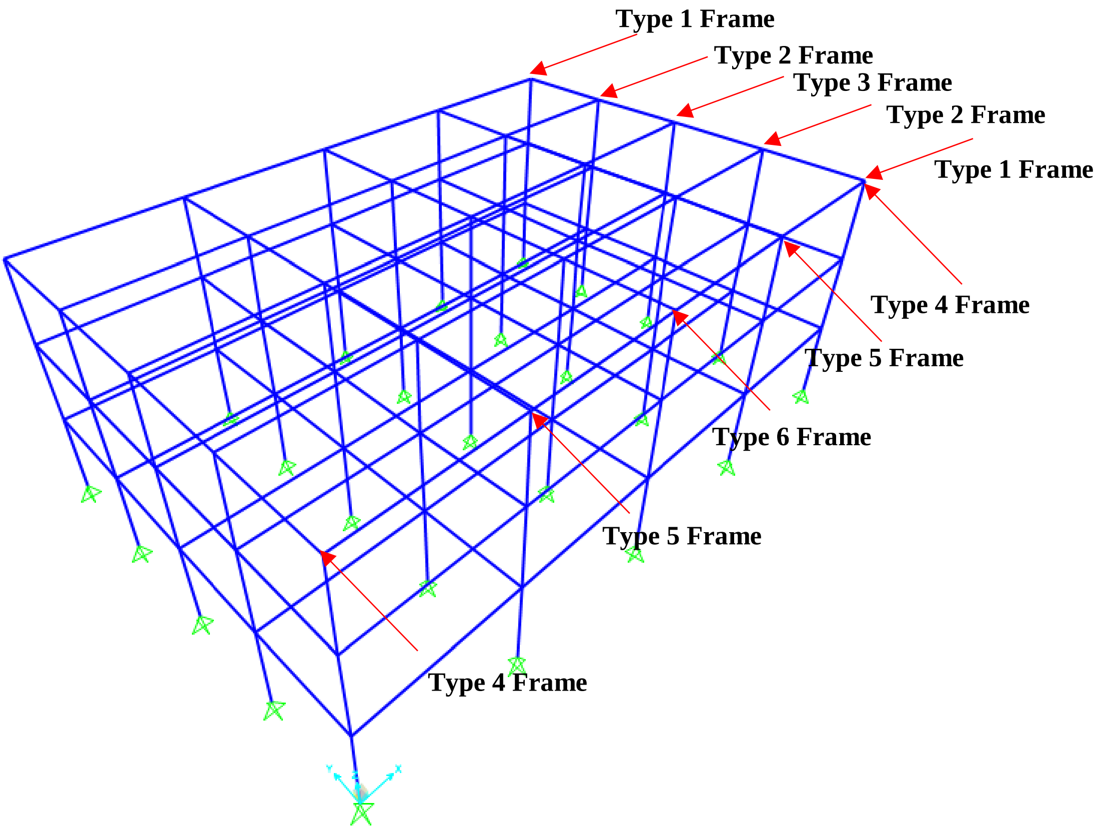

Figure 8.1: Frame identification

Appendix F of the thesis provides the bending moment diagrams for sagging and hogging bending moments and shear force diagrams of the beams in Type 1-6 frames of the typical building, as calculated using the Eurocodes and the British Standards analysis procedure.

Similarly, per the building's symmetry, the structural analysis outcomes for the columns are presented in nine sets: Type 1-9 at each floor of the building. The notation for the nine-column types is as shown in Figure 8.2.

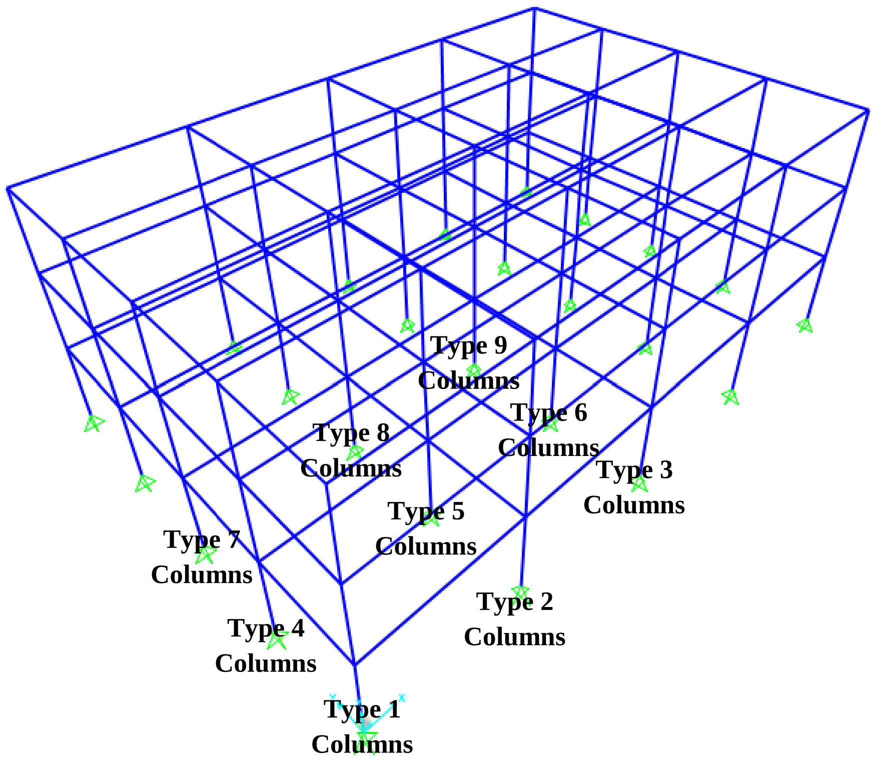

Figure 8.2: Column identification

Appendix F of the thesis provides the axial force diagrams and bending moment illustrations (M22 and M33) of Type 1-9 columns on the building's first, second, and roof floors, as calculated using the Eurocodes and the British Standards analysis procedure.

8.4.2.1. Comparison of axial force diagrams of columns

Figures 8.3 and 8.4 show the axial force diagrams for the columns of the typical building, highlighting the maximum, derived using the Eurocode and British Standard analysis procedures for the envelope of the specified load combinations.

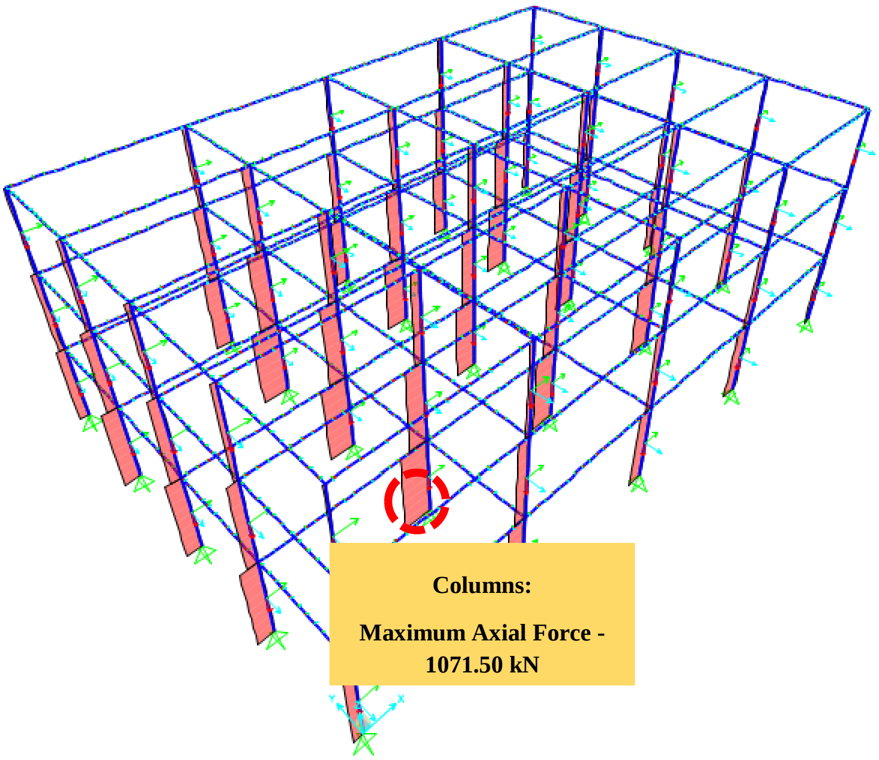

Figure 8.3: Axial force diagrams - Eurocode-based typical building

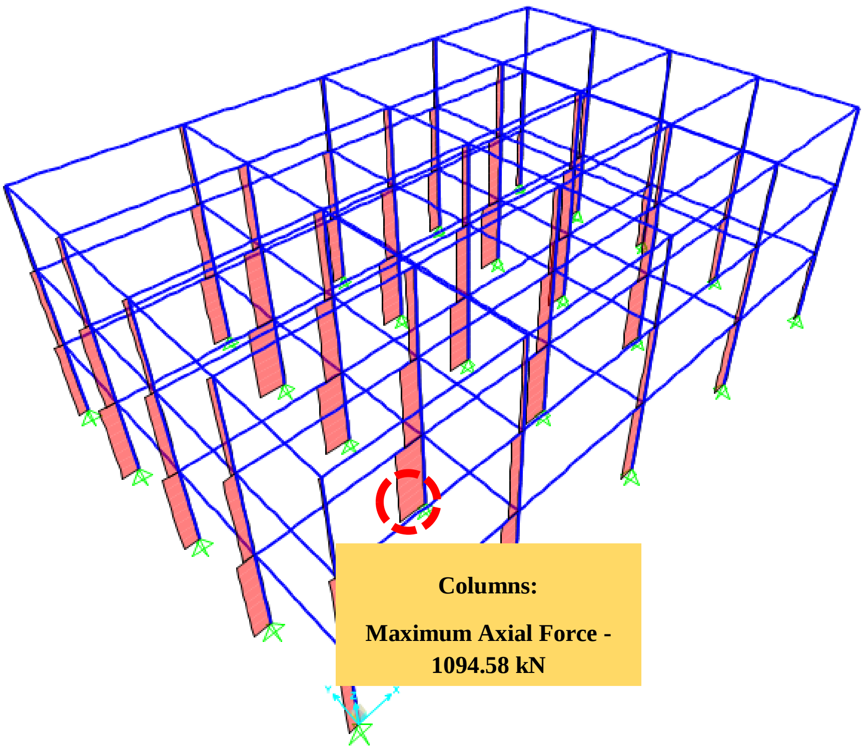

Figure 8.4: Axial force diagrams – British Standard-based typical building

As shown in Figures 8.3 and 8.4, the British Standard-based analysis predicted higher axial forces on columns compared to the Eurocode-based analysis.

8.4.2.2. Comparison of bending moment diagrams of columns and beams

Figures 8.5 and 8.6 present the bending moment diagrams (M22) for the columns of the typical building in the 2-2 direction, highlighting the maximum, derived using Eurocode and British Standard analysis procedures for the envelope of the specified load combinations.

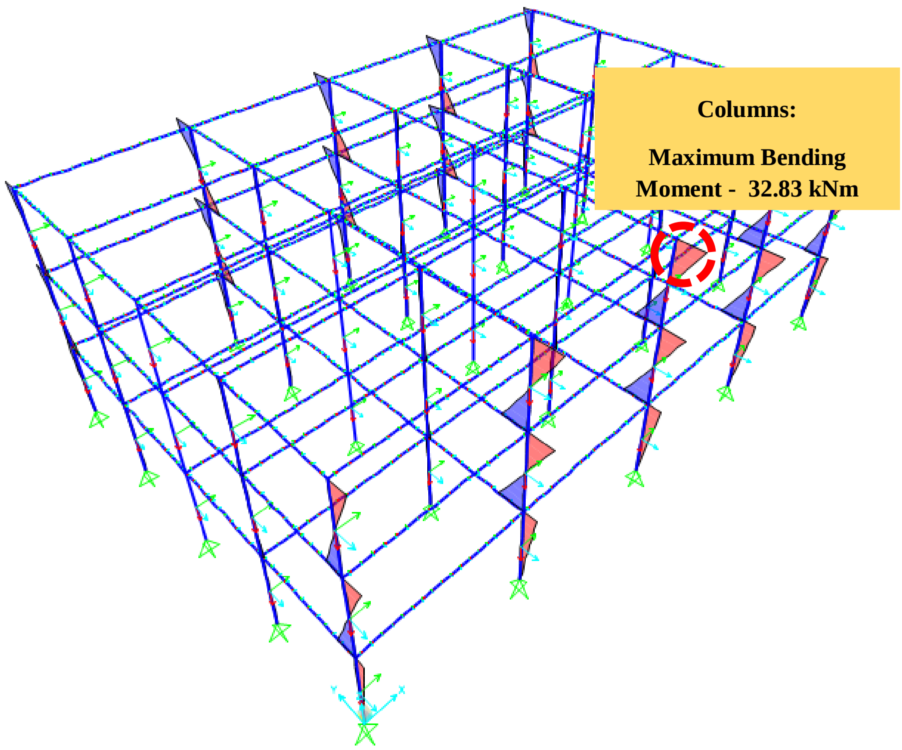

Figure 8.5: Bending moment diagrams (M22) - Eurocode-based typical building

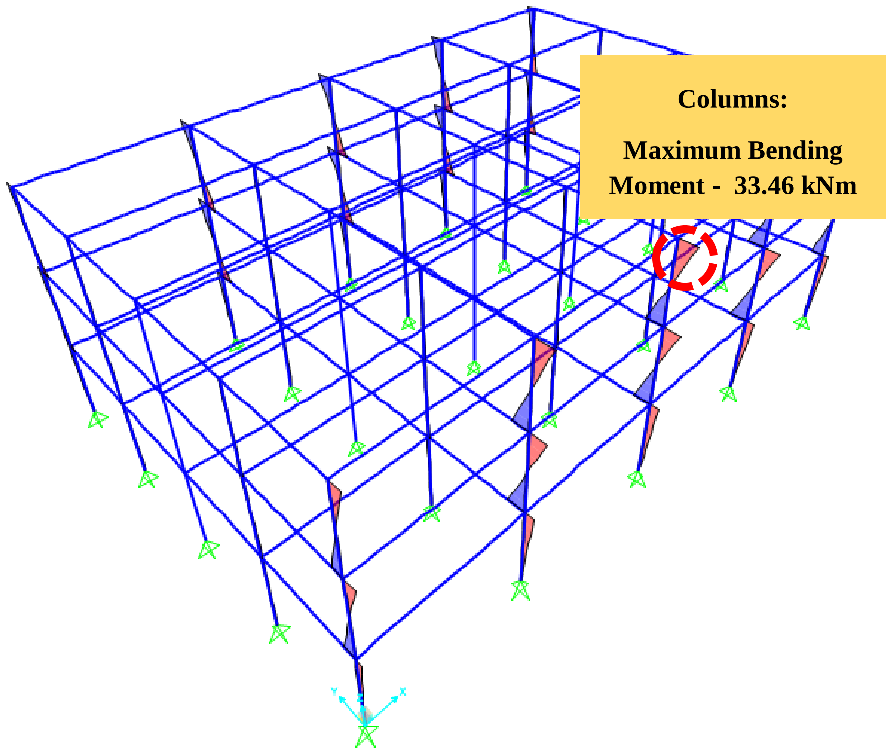

Figure 8.6: Bending moment diagrams (M22) - British Standard-based typical building

According to Figures 8.5 and 8.6, the British Standard-based analysis incurs higher bending moments (M22) on columns compared to the Eurocode-based analysis.

Figures 8.7 and 8.8 present the bending moment diagrams (M33) for the columns of the typical building in the 3-3 direction and the hogging and sagging bending moments of the beams along the two directions, highlighting the maximum, derived using Eurocode and British Standard analysis procedures for the envelope of the specified load combinations.

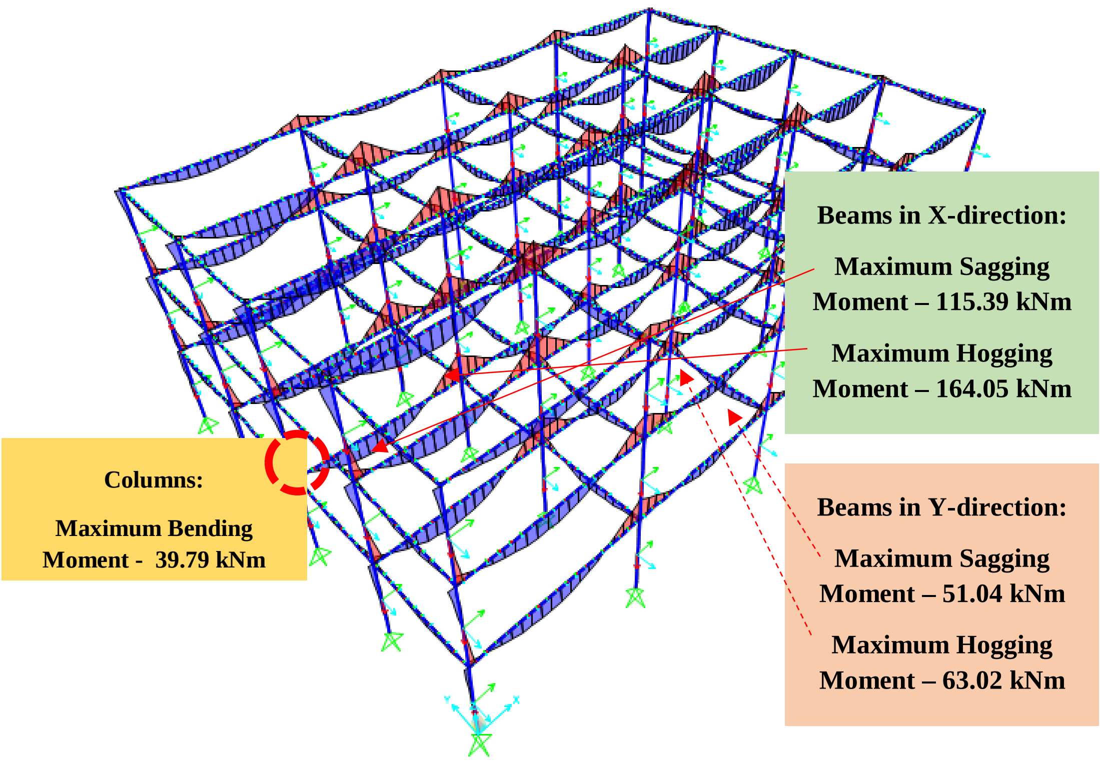

Figure 8.7: Bending moment diagrams (M33) - Eurocode-based typical building

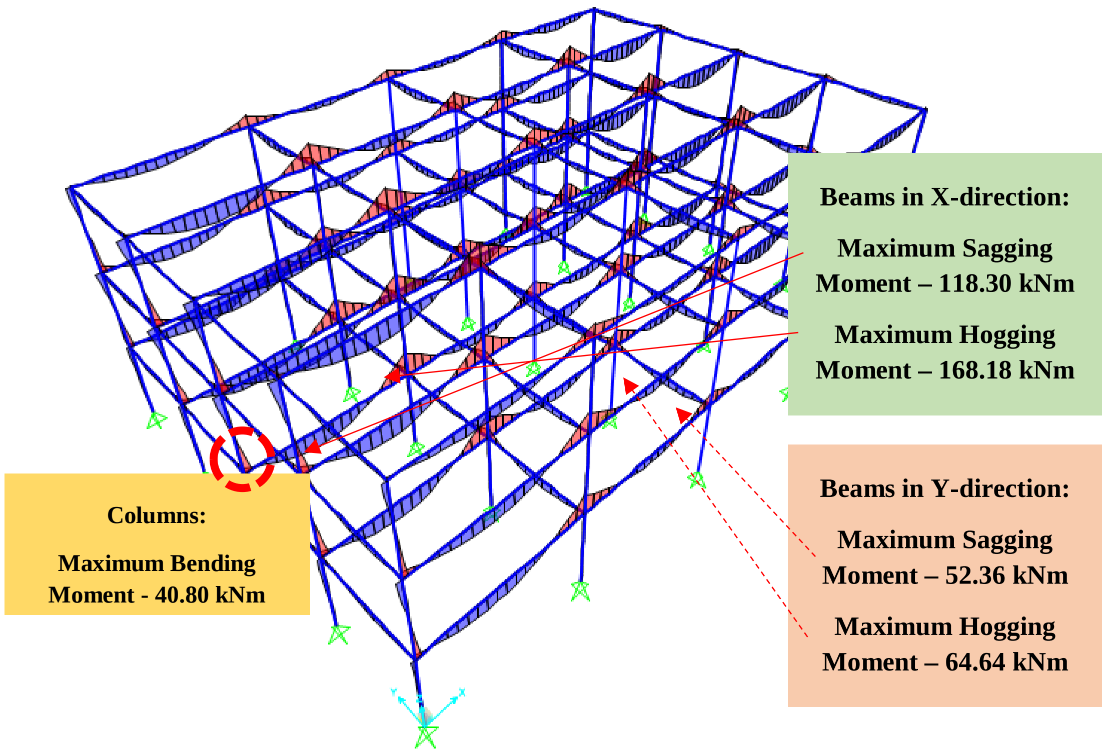

Figure 8.8: Bending moment diagrams (M33) - British Standard-based typical building

Figures 8.7 and 8.8 indicate that the British Standard-based analysis results in higher bending moments (M33) on columns compared to the Eurocode-based analysis.

Additionally, the British Standard-based analysis produces higher sagging and hogging bending moments (M33) on beams in both directions compared to the Eurocode-based analysis.

8.4.2.3. Comparison of shear force diagrams of beams

Figures 8.9 and 8.10 present the shear force diagrams for the beams along the two directions of the typical building, highlighting the maximum, derived using Eurocode and British Standard analysis procedures for the envelope of the specified load combinations.

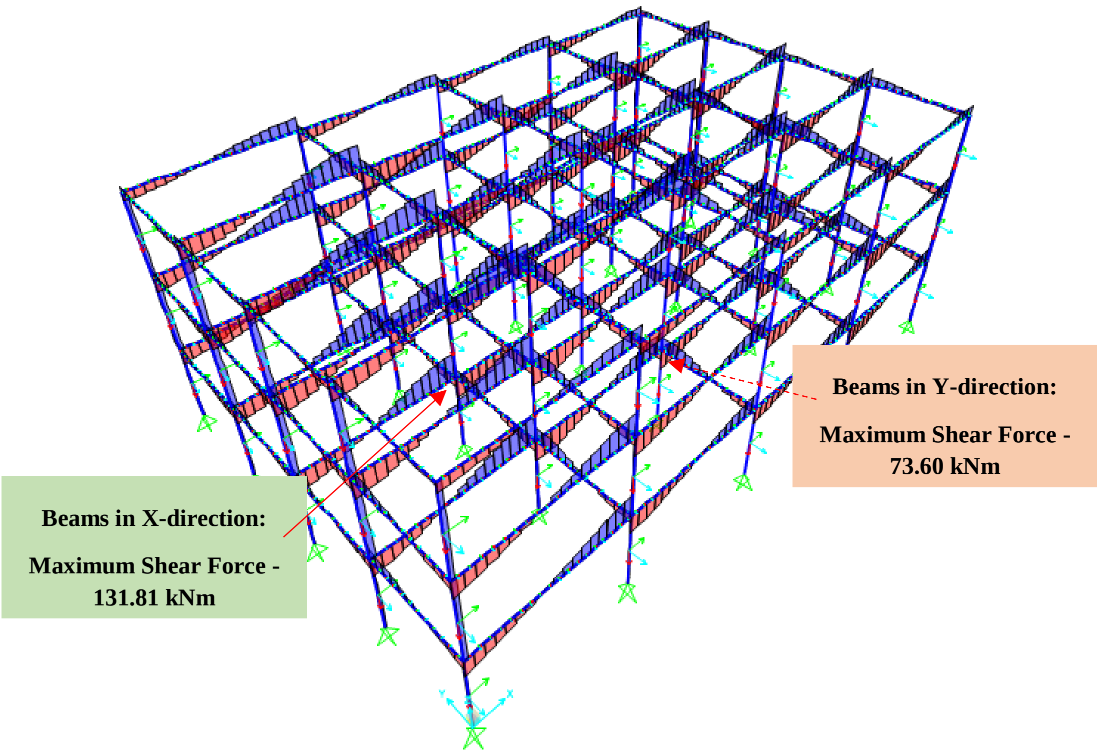

Figure 8.9: Shear force diagrams - Eurocode-based typical building

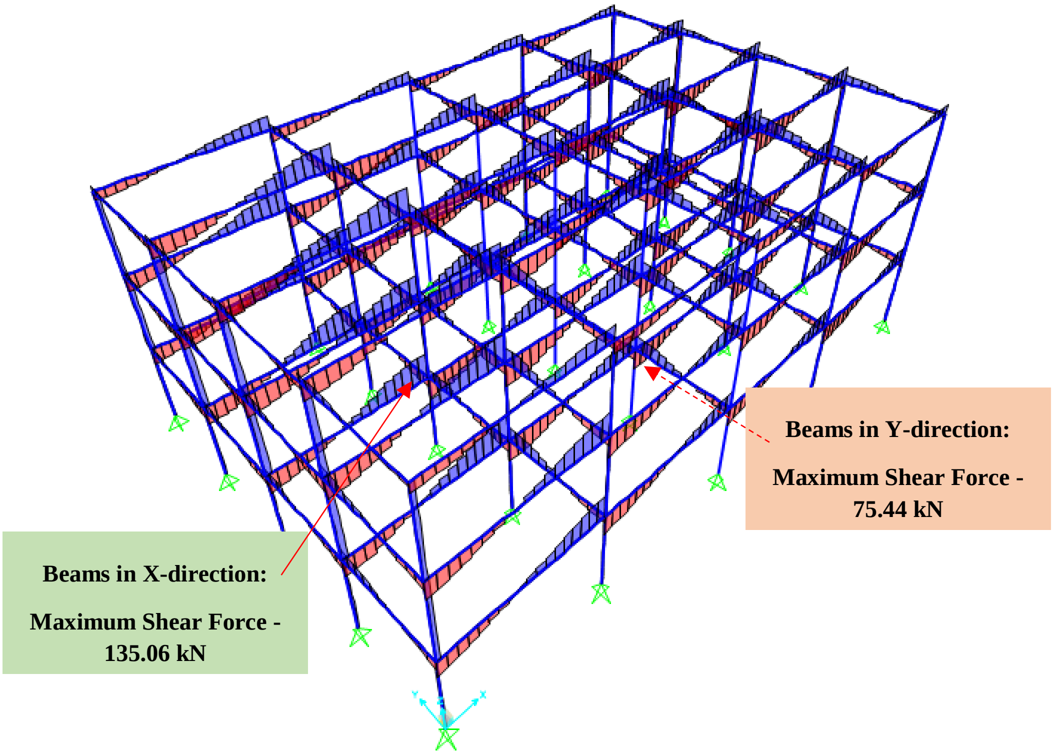

Figure 8.10: Shear force diagrams – British Standard-based typical building

Figures 8.9 and 8.10 indicate that the British Standard-based analysis results in higher shear forces on beams in both directions than the Eurocode-based analysis.

8.5. Structural design of the beams and columns

8.5.1. Structural design of the beams for flexure and shear

Tables 8.6 and 8.7 compare the Eurocode- and British Standard-based structural design results of the beam with the maximum hogging bending moment, sagging bending moment, and shear force in the X- and Y-directions of the typical building for flexure and shear. Appendix F of the thesis provides summary tables of the structural design carried out for each continuous beam.

Table 8.6: Design of beams in the X-direction of the typical building for flexure and shear

First/Second Floor/Type 3 Beam	Euro	BS	% Difference
Design for Maximum Hogging Moment			
Maximum Hogging Moment (kNm)	164.05	168.18	2.52%
Amount of Reinforcement Required (mm^2)	1260.00	1209.00	-4.05%
Number of Reinforcements	2T25+1T20	2T25+1T20	Similar
Amount of Reinforcement Provided (mm^2)	1295.25	1295.25	0.00%
Utilization	0.97	0.93	-4.05%
Design for Maximum Sagging Moment			
Maximum Sagging Moment (kNm)	115.39	118.30	2.52%
Amount of Reinforcement Required (mm^2)	761.00	714.00	-6.18%
Number of Reinforcements	2T20+1T16	2T20 + 1T12	Dissimilar
Amount of Reinforcement Provided (mm^2)	828.96	741.04	-10.61%
Utilization	0.92	0.96	4.96%
Design for Maximum Shear Force			
Maximum Shear Force (kN)	131.81	135.06	2.47%
Amount of Reinforcement Required (mm^2)	552.01	659.66	19.50%
Number of Reinforcements	R6 @ 100	R6 @ 75	Dissimilar
Amount of Reinforcement Provided (mm^2)	565.20	753.60	33.33%
Utilization	0.98	0.88	-10.37%

Table 8.7: Design of beams in the Y-direction of the typical building for flexure and shear

First/Second Floor/Type 6 Beam	Euro	BS	% Difference
Design for Maximum Hogging Moment			
Maximum Hogging Moment (kNm)	63.02	64.64	2.57%
Amount of Reinforcement Required (mm^2)	588.00	559.00	-4.93%
Number of Reinforcements	3T16	3T16	Similar
Amount of Reinforcement Provided (mm^2)	602.88	602.88	0.00%
Utilization	0.98	0.93	-4.93%
Design for Maximum Sagging Moment			
Maximum Sagging Moment (kNm)	51.04	52.36	2.59%
Amount of Reinforcement Required (mm^2)	588.00	419.00	-28.74%
Number of Reinforcements	3T16	2T16 + 1T12	Dissimilar
Amount of Reinforcement Provided (mm^2)	602.88	514.96	-14.58%
Utilization	0.98	0.81	-16.58%
Design for Maximum Shear Force			
Maximum Shear Force (kN)	73.60	75.44	2.50%
Amount of Reinforcement Required (mm^2)	382.20	421.05	10.16%
Number of Reinforcements	R6 @ 125	R6 @ 125	Similar
Amount of Reinforcement Provided (mm^2)	452.16	452.16	0.00%
Utilization	0.85	0.93	10.16%

As shown in Tables 8.6 and 8.7, the beam analysis based on British Standards results in higher hogging and sagging bending moments as well as shear forces compared to the analysis based on Eurocodes. However, when designing the beam for hogging bending moments according to Eurocodes, a greater amount of reinforcement area was required, although the reinforcement bar diameters were similar to those specified by the British Standards. For sagging bending moments, the Eurocodes also required more reinforcement area and larger bar diameters for one of the three suggested reinforcement bars compared to the British Standards. In contrast, the design for shear forces according to Eurocodes required a smaller reinforcement area than the British

Standards. While the bar diameter remained the same, the spacing was either greater or unchanged compared to the British Standards.

8.5.2. Structural design of the columns for axial loading and flexure

Tables 8.8, 8.9, and 8.10 compare the Eurocode- and British Standard-based structural design results of columns with the most critical combinations of axial forces and bending moments in the typical building for axial loading and flexure. Appendix F of the thesis includes summary tables of the structural design performed for each column on each floor of the building.

Table 8.8: Design of columns of the typical building with the maximum axial force

Ground Floor/Type 9 Column	Euro	BS	% Difference
Axial Force (kN)	918.98	938.5	2.12%
Bending Moment (M22) -Bottom	0.00	0.00	0.00%
Bending Moment (M22) -Top	0.00	0.00	0.00%
Bending Moment (M33) -Bottom	0.00	0.00	0.00%
Bending Moment (M33) -Top	0.00	0.00	0.00%
Cross Section Size (mm × mm)	225 × 225	225 × 225	Similar
Amount of Reinforcement Required (mm^2)	1100.54	1327.78	20.65%
Number of Reinforcements	4T20	4T25	Dissimilar
Amount of Reinforcement Provided (mm^2)	1256	1962.5	56.25%
Utilization	0.88	0.68	-22.79%
Shear Link Diameter (mm)	6	8	Similar
Shear Link Spacing (mm)	225	275	Similar

Table 8.9: Design of columns of the typical building with the critical combination of axial force and uniaxial bending moment

Second Floor/Type 7 Column	Euro	BS	% Difference
Axial Force (kN)	126.84	128.62	1.40%
Bending Moment (M22) -Bottom	0.00	0.00	0.00%
Bending Moment (M22) -Top	0.00	0.00	0.00%
Bending Moment (M33) -Bottom	38.24	39.09	2.22%
Bending Moment (M33) -Top	39.78	40.52	1.86%
Cross Section Size (mm × mm)	225 × 225	225 × 225	Similar
Amount of Reinforcement Required (mm^2)	1100.54	1265.63	15.00%
Number of Reinforcements	4T20	4T25	Dissimilar
Amount of Reinforcement Provided (mm^2)	1256	1962.5	56.25%
Utilization	0.88	0.64	-26.40%
Shear Link Diameter (mm)	6	8	Similar
Shear Link Spacing (mm)	225	275	Similar

Table 8.10: Design of columns of the typical building with the critical combination of axial force and biaxial bending moments

Second Floor/Type 1 Column	Euro	BS	% Difference
Axial Force (kN)	63.50	64.27	1.21%
Bending Moment (M22) -Bottom	19.69	20.16	2.39%
Bending Moment (M22) -Top	19.49	19.87	1.95%
Bending Moment (M33) -Bottom	26.75	27.39	2.39%
Bending Moment (M33) -Top	24.89	25.37	1.93%
Cross Section Size (mm × mm)	225 × 225	225 × 225	Similar
Amount of Reinforcement Required (mm^2)	1444.46	1670.63	15.66%
Number of Reinforcements	4T25	4T25	Similar
Amount of Reinforcement Provided (mm^2)	1962.5	1962.5	0.00%
Utilization	0.74	0.85	15.66%
Shear Link Diameter (mm)	8	8	Similar
Shear Link Spacing (mm)	225	275	Dissimilar

As shown in Tables 8.8, 8.9, and 8.10, the column analysis based on British Standards results in slightly higher axial forces and bending moments (M22 and M33) than the analysis based on Eurocodes. In all three critical cases presented, the Eurocode-based design required less reinforcement area, leading to smaller or similar bar diameters compared to the British Standards-based design. However, when providing shear links according to Eurocodes, the reinforcement bar diameter remained the same, but the spacing was reduced compared to the British Standards.

8.6. Summary

This chapter of the thesis compared the design outcomes of a gravity-loaded typical case study building using Eurocodes and British Standards, focusing on the key structural design aspects such as material properties, material safety factors, load combinations, and design equations.

Critical structural elements, including beams and columns, were analyzed to examine differences in the design procedures in the two codes.

The column analysis showed that British Standards resulted in slightly larger member forces, with percentage differences of 1.21%-2.35% for axial forces, 0.00%-3.08% for M22 bending moments, and 0.00%-3.01% for M33 bending moments. These differences led to a 0%-100% variation in the required reinforcements, causing larger bar diameters in some columns. However, not all columns were affected, as the impact depended on the capacity range associated with specific column dimensions and the chosen bar diameters.

Similarly, the beam analysis indicated that British Standards produced slightly larger member forces, with percentage differences of 1.35%-2.85% for hogging bending moments, 1.42%-2.79% for sagging bending moments, and 1.32%-2.85% for shear forces. Despite this, the Eurocode-based design required slightly more reinforcement (3.98%-6.96% for hogging bending moments and 5.87%-28.74% for sagging bending moments), resulting in larger bar diameters for some beams. On the other hand, British Standards necessitated more shear reinforcement (4.61%-140.59%), leading to closer shear link spacing in some beams. Again, these differences did not affect all beams, as the outcome depended on the capacity range associated with specific beam dimensions and the selected bar diameters. As understood from this study, these variations were driven by the more conservative design equations in Eurocodes for the beam design, which compensated for the differences in member forces.

Overall, the analysis of this typical building under gravity loading showed that Eurocodes generally required slightly less material (reinforcements) than British Standards. This difference is primarily due to the more conservative partial safety factors in British Standards' load combinations rather than the higher concrete material density specified in Eurocodes. However, for this building, the difference in reinforcement requirement did not significantly impact the bar diameters used.

However, the impact of this difference in reinforcement requirement can largely vary based on the kind of building, its parameters, usage, and the types of loads considered (such as wind and seismic loads, in addition to gravity loads). This variation can lead to significant differences in member sizes and reinforcement arrangements, which can significantly affect the cost performance of buildings.

CHAPTER 9 : CONCLUSION, RECOMMENDATIONS, AND FUTURE WORK

9.1.General conclusion

Given the increasing frequency and severity of natural disasters as well as man-made hazards in the built environment, Sri Lanka has prioritized the preparation and establishment of a National Building Code. The Sri Lankan National Building Code needs to establish robust design standards that guarantee the safety and resilience of structures. In addition, a priority is to examine the suitability of the latest Eurocodes and Sri Lankan national annexes to serve as the structural design standard for the forthcoming National Building Code of Sri Lanka in place of the well-known British Standards, which ceased updating as of 2010.

This thesis examined this timely national need for the implications of adopting Eurocodes for designing disaster-resilient buildings in Sri Lanka. Since Eurocodes provide comprehensive guidelines for both wind and seismic loading scenarios, this study underlined the flexibility of the Eurocodes supplied through the national annexes to address country-specific design parameters. Also, it emphasized the suitability of adopting Eurocodes over traditional design codes and standards, as they incorporate a performance-based approach to a certain extent.

The present study focused on reinforced concrete, low-rise buildings designed following the Eurocodes and Sri Lankan national annexes/national guidelines. It assessed the structural resilience of these buildings against wind and seismic loading. This study proposed a novel framework combining linear elastic analysis, design, non-linear inelastic modeling, non-linear static/dynamic analysis, fragility assessment, and structural performance evaluation. The effectiveness of this framework was demonstrated by evaluating a three-story reinforced concrete typical building designed according to the Eurocodes and Sri Lankan national annexes/national guidelines. The proposed framework confirmed its capability to examine the structural resilience of reinforced concrete buildings. This framework was subsequently utilized to evaluate the structural resilience of three case study buildings: a school, a university, and a hospital. The same framework was later applied to a mixed-use medium-rise building in Sri Lanka. Since this building was identified as defective in terms of gravity and lateral load-bearing capacities, the retrofitting proposal to strengthen its gravity load-bearing and lateral load-bearing capacity was assessed using the proposed framework. This study also examined the cost implications of adopting the Eurocodes and Sri Lankan national annexes over British Standards by comparing the Eurocode- and British Standard-based structural designs of a typical building subjected to gravity loading.

The significant findings of this study can be listed as follows:

1. The first framework (Figure 9.1) proposed in this study can assess the structural resilience of new buildings against extreme wind and seismic loading.
2. The second framework (Figure 9.2) proposed in this study (a slightly modified version of the first framework) can assess the vulnerability of existing buildings, including code-compliant and non-code-compliant buildings, against design-level gravity, wind, and seismic loading and extreme wind and seismic loading.
3. The proposed second framework can also evaluate the efficiency of building retrofitting proposals in enhancing defective buildings' gravity, wind, and seismic load-bearing capacity. This study, therefore, showcases the potential of the proposed tool in estimating the danger involved with poorly designed and constructed buildings and appraising the effectiveness of retrofitting proposals.
4. The buildings designed according to the Eurocodes and Sri Lankan national annexes present a remarkably high structural resilience against extreme wind loading compared to the wind performance objective matrix developed by Griffis et al. (2013).
5. The inherent wind over strength observed in the case study buildings can be attributed to several aspects, such as design conservatism in the wind design approach, less impact from the wind loading on low-rise buildings' structural frame, the contribution of the gravity load bearing system in resisting lateral wind loading, and the design being governed by the seismic loading.
6. The buildings designed per the Eurocodes and Sri Lankan national annexes present a reasonably good level of structural resilience against extreme seismic loading compared to the Vision 2000 recommended seismic performance objectives. However, some specific case study buildings failed to meet stringent performance levels, such as fully operational and acceptable performance at the specified return periods recommended by the Vision 2000 seismic performance objectives.
7. Eurocode-based designs are not always structurally resilient; sometimes, they compromise meeting the standard performance objectives for measuring structural resilience.
8. Per the structural design results of the typical building under gravity loading, the Eurocodes generally required slightly less material (reinforcements) than British Standards primarily due to the more conservative partial safety factors in British Standards's load combinations rather than the higher concrete material density specified in Eurocodes.
9. The impact of the design procedures in Eurocodes and British Standards on the section sizes and reinforcement requirements largely varies based on the kind of building, its parameters, usage, and the types of loads considered (such as wind and seismic loads, in addition to gravity loads). This variation can lead to significant differences in member sizes and reinforcement arrangements, which can significantly affect the cost performance of buildings.

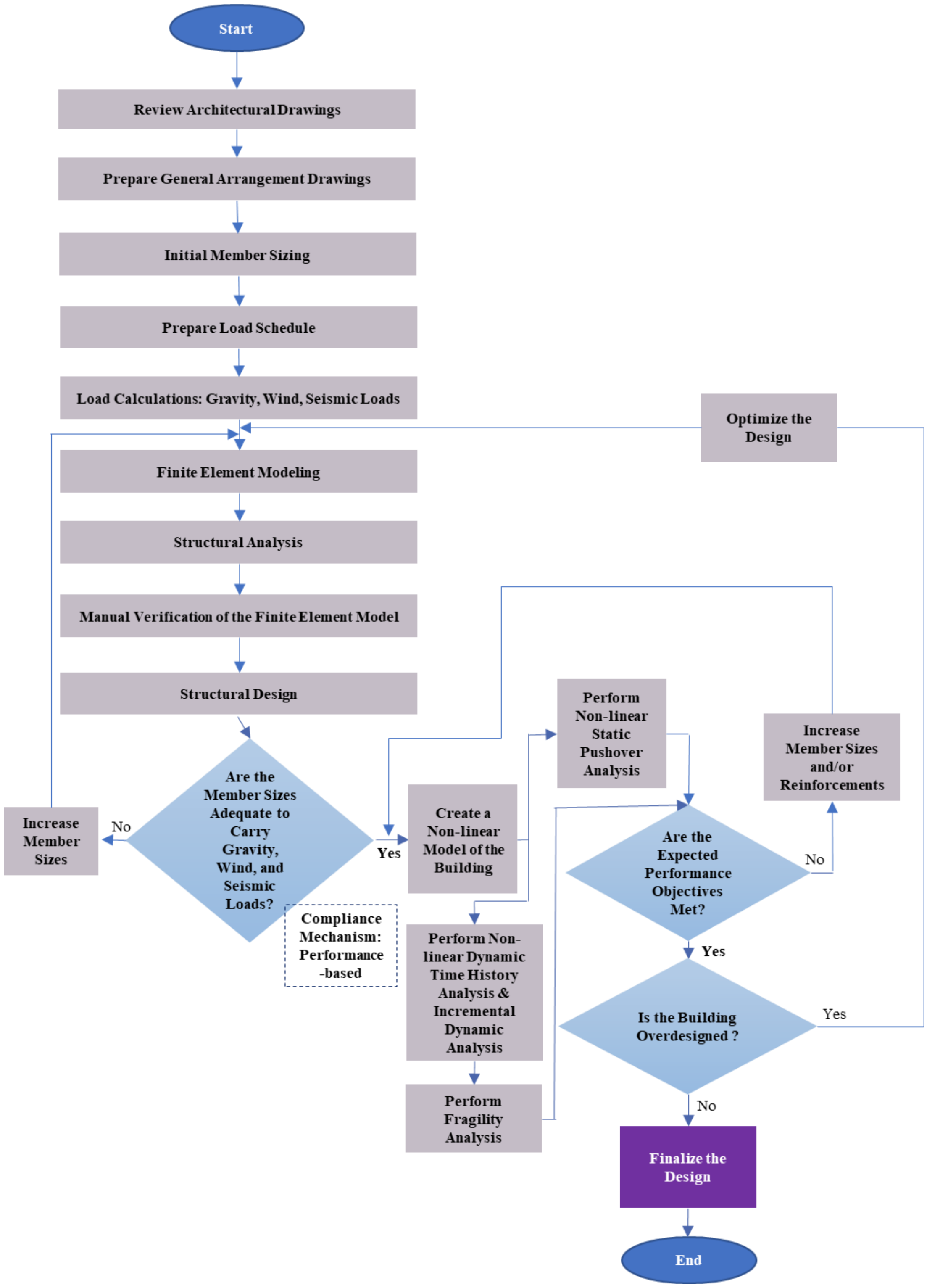

Figure 9.1: Framework to evaluate the degree of structural resilience of new building designs

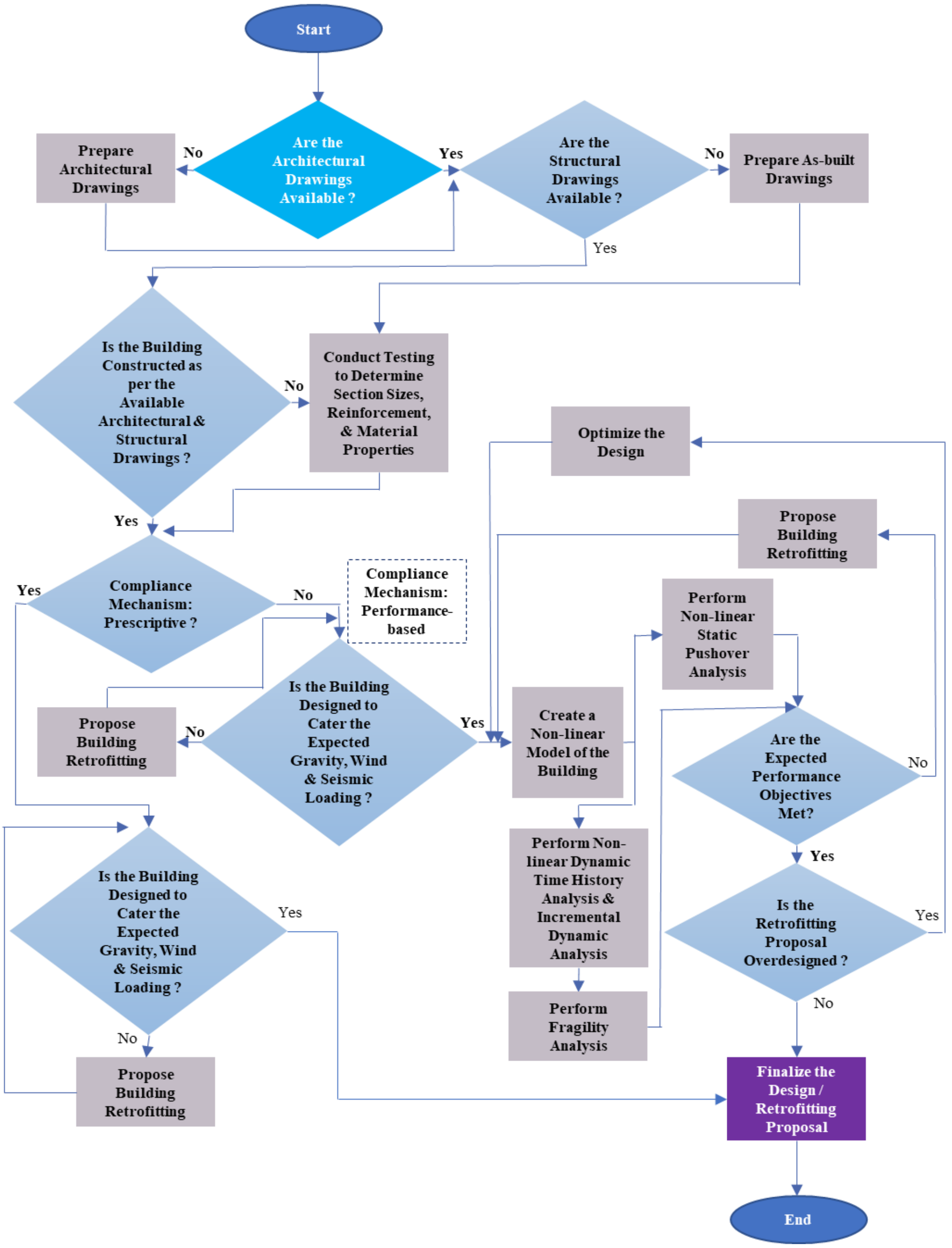

Figure 9.2: Framework to evaluate the degree of vulnerability in existing buildings

In conclusion, implementing Eurocodes and national annexes in the Sri Lankan context is a promising step to address disaster resilience in the built environment amidst the growing risks from natural and artificial hazards. Since this study is one of the first to assess the disaster resilience features of the latest Eurocodes in the Sri Lankan context, further research must be conducted to fill the existing gaps and unexplored research areas. By addressing the knowledge gaps and tailoring the standards to local needs, Sri Lanka can significantly improve the safety and resilience of its built environment, ultimately protecting lives and property against natural disasters.

9.2.Recommendations

The following recommendations can be presented based on the findings of the analysis of buildings against extreme wind loading:

1. Pushover analysis should be conducted for the principal directions of the building, unless for square-shaped buildings with symmetric structural arrangements, which are capable of generating the same response in both directions.
2. It is advisable to consider multiple control nodes when conducting non-linear static pushover analysis, wherein the center of mass of the buildings does not overlap with the center of rigidity.

The following recommendations can be presented based on the findings of the analysis of buildings against extreme seismic loading:

1. Since building responses are susceptible to ground motions extracted from the PEER database, it is recommended to determine these features as accurately as possible. In the absence of country-specific data for precise decision-making, it is advisable to select the worst-case scenario. For instance, the D5-95 scenario, which is the significant duration of the earthquake during which 5% to 95% of the energy or 90% of the total power is concentrated, is a governing factor that decides the ground motions to be used in the analysis. Since Sri Lanka does not experience earthquakes frequently, it does not have a database of its historical earthquake records. Since it is difficult to decide such parameters precisely, analyzing ground motion sets with different ranges of D5-95 is recommended to recognize the worst-case scenario.
2. Since code-based building designs do not always satisfy the structural resilience requirements, it is recommended to follow the proposed framework to assess the buildings' structural resilience. This allows appropriate revisions to the original design while maintaining the client's structural resilience requirements. Additionally, it is advisable to develop a country-specific resilience rating system rather than adopting those from other countries with different seismicity levels.

3. Sri Lanka's forthcoming unified multidisciplinary national building code can adopt Eurocodes and Sri Lankan national annexes as its structural design standard, provided revisions will be made to the original designs if a particular Eurocode-based design does not meet the expected resilience requirements.

9.3.Future work

This study recognized the importance of adapting the Eurocodes to fit into the Sri Lankan context. It also stressed the necessity of amending the proposed framework as new knowledge becomes available. Most importantly, future research should focus on expanding the scope of the present study to encompass a broader range of relevant research areas, including the existing building stock in Sri Lanka.

The following can be presented as potential areas for further research.

1. Although this study's findings indicate the adequacy of the Eurocodes to design the selected case-study buildings with disaster resilience qualities, this should be confirmed by analyzing the structures not considered in this study and using other performance objectives, such as the life-cycle cost.
2. This study had a limited scope, concentrating solely on the performance assessment of low to medium-rise reinforced concrete buildings. Future research should expand this scope to include high-rise reinforced concrete buildings and buildings built with steel, composite materials, etc. Moreover, the study could incorporate various engineering structures, like telecommunication towers, bridges, etc.
3. The current study focused on wind and seismic hazards, two natural disasters likely to occur in Sri Lanka. The framework and the methodology built accordingly can also consider other risks, such as floods, tsunamis, blasts, impacts, etc.
4. The framework presented in this study was primarily utilized to evaluate the capacity of a retrofitting proposal to enhance the lateral-load-bearing capacity of a defective building. This retrofitting proposal included column and beam jacketing as the retrofitting method. The same framework can be extended to assess the performance of other retrofitting methods, like fiber-reinforced polymer wrapping.
5. The framework proposed in this study can also be utilized to identify the most effective building plans, structural arrangements, and lateral load-resisting systems to resist extreme loading.
6. This study focused on assessing the performance of the superstructure of low to medium-rise buildings in Sri Lanka against extreme wind and seismic events. It provided general guidelines on designing and constructing substructures to withstand extreme loading. However, it does not provide insights into how building substructures, ground profiles, and their interactions perform during extreme lateral loading, particularly during seismic events. Therefore, this research

should be expanded to assess the superstructure-substructure-soil interaction during a seismic event.

7. Further, the present study can be expanded to provide the implications of adopting performance-based design over code-based design by analyzing optimized designs of the same structures with predetermined performance levels.

The following are potential areas for further research within the wind engineering discipline.

1. Although wind loading on structures is often treated as equivalent to static loading, it is inherently dynamic in nature. Therefore, if wind time histories are available, the proposed framework can be extended to incorporate fragility analysis, specifically for high-rise buildings.
2. The framework proposed in this study focused solely on the structural resilience of reinforced concrete column-beam frames. The framework can also be developed to evaluate the strength of the roof structure and its connections, as these are the most vulnerable components of low-rise buildings exposed to extreme winds.

The following are potential areas for further research within the seismic engineering discipline.

1. Since Sri Lanka is in a low seismicity zone compared to earthquake-prone regions in the world, it has paid less attention to developing its earthquake loading standard despite the historical earthquake events and continuous reports of minor tremors across the country. Identifying the importance of the impact of earthquakes on structures, Sri Lanka has initiated the development of the Sri Lankan national annex for Eurocode 8. Since seismic engineering is a relatively new engineering discipline in Sri Lanka, developing the Sri Lankan national annex for Eurocode 8 will require extensive research to determine earthquake parameters. This research must also be carried out continuously since the Sri Lankan national annex must be updated periodically after its first implementation.
2. Since the Sri Lankan national annex for Eurocode 8 was not available at the time of this study, national guidelines for seismic analysis and design of (engineered) buildings in Sri Lanka, published by Kularathna et al. (2013), and the response spectrum developed for a rock site in Colombo by Uduweriya et al. (2013) were utilized in the present study. However, discrepancies exist between their studies' parameters, response spectrum, and the upcoming Sri Lankan national annex to Eurocode 8, such as the design peak ground acceleration for a given return period. Moreover, the concept of a return period for defining the seismicity of the country might not be feasible since Sri Lanka does not have sufficient earthquake records to determine the design peak ground acceleration on a probabilistic basis. Hence,

a deterministic approach might better suit the Sri Lankan context. Therefore, the present study might require amendments once the Sri Lankan national annex to Eurocode 8 is established.

3. Since Sri Lanka does not have a database of past seismic activity, ground motions were extracted from the PEER database and matched with the response spectrum proposed by Uduweriya et al. (2013) for Sri Lanka. Filtering ground motions from the PEER ground motion database necessitated a detailed list of features of probable seismic events in Sri Lanka. These ground motion features include fault type, magnitude, R_JB/Joyner-Boore distance (the source-to-site distance as the closest horizontal distance from the site to the projection of the surface rupture), R_rup (the nearest distance from the site to the rupturing fault plane), $V_{s,30}$ (the average shear wave velocity), and D5-95 (the significant duration of the earthquake during which 5% to 95% of the energy or 90% of the total power is concentrated). Accurate data on the fault types of seismic sources that triggered earthquakes and those that might trigger earthquakes are unavailable in Sri Lanka. As a result, several assumptions were made when selecting ground motion time histories from the PEER database. Therefore, the country requires a detailed continental and oceanic geological assessment to identify fault mechanisms.
4. This study utilized Vision 2000 recommended seismic performance objectives to assess the structural resilience of the case study buildings against extreme seismic loading. However, Sri Lanka should produce its performance objectives based on historical seismic data and damage without adopting the performance objectives designed for high seismic vulnerability zones. Less stringent performance objectives tailored to low seismic hazards can optimize the safety and economy of the construction industry.

REFERENCES

Almufti, I., & Willford, M. (2013). *REDi^{TM} Rating System: Resilience-based Earthquake Design Initiative for the Next Generation of Buildings*. https://doi.org/10.13140/RG.2.2.20267.75043

Anwar, N., & Ahmed, W. (2021). *Performance Based Structural Design: Why Do We Need It?*

Awchat, G., Patil, A., More, A., & Dhanjode, G. (2023). Incremental Dynamic Analysis and Seismic Fragility Analysis of Reinforced Concrete Frame. *Civil and Environmental Engineering*, *19*(1), 444–451. https://doi.org/10.2478/cee-2023-0039

Bandara, C., Jayasinghe, J. A. S. C., & Dissanayake, R. (2017, November 24). *Characteristic Strength of Reinforcing Steel Bars Used in Sri Lanka—A Proposal to Sri Lankan National Annex of Eurocode 2*.

Brett, C., & Lu, Y. (2013). Assessment of robustness of structures: Current state of research. *Frontiers of Structural and Civil Engineering*, *7*(4), 356–368. https://doi.org/10.1007/s11709-013-0220-z

Bruneau, M., Chang, S., Eguchi, R., Lee, G., O'Rourke, T., Reinhorn, A., Shinozuka, M., Tierney, K., Wallace, W., & Winterfeldt, D. (2003). A Framework to Quantitatively Assess and Enhance the Seismic Resilience of Communities. *Earthquake Spectra - EARTHQ SPECTRA*, *19*. https://doi.org/10.1193/1.1623497

Cels, J., Rossetto, T., Dias, P., Thamboo, J., Wijesundara, K., Baiguera, M., & Del Zoppo, M. (2023). Engineering surveys of Sri Lankan schools exposed to tsunami. *Frontiers in Earth Science*, *11*, 1075290. https://doi.org/10.3389/feart.2023.1075290

Cyclone Events 1900 – 2000, Available Source, www. meteo.gov.lk, 2009

Disaster | UNDRR. (2007, August 30). http://www.undrr.org/terminology/disaster

Disaster Resilience: A National Imperative (with Committee on Increasing National Resilience to Hazards and Disasters, Committee on Science, Engineering, and Public Policy, Policy and Global Affairs, & National Academies). (2012). National Academies Press. https://doi.org/10.17226/13457

Ellingwood, B., Rosowsky, D., Li, Y., & Kim, J. (2004). Fragility Assessment of Light-Frame Wood Construction Subjected to Wind and Earthquake Hazards. *Journal of Structural Engineering-Asce - J STRUCT ENG-ASCE*, *130*. https://doi.org/10.1061/(ASCE)0733-9445(2004)130:12(1921)

EN1990. (2005). Eurocode - Basis of structural design . European Committee for Standardization: Brussels, Belgium.

EN 1991-1-1. (2002). Eurocode 1: Actions on structures - Part 1-1: General actions - Densities, self-weight, imposed loads for buildings. European Committee for Standardization: Brussels, Belgium.

EN 1991-1-4. (2010). Eurocode 1: Actions on structures - Part 1-4: General actions - Wind actions. European Committee for Standardization: Brussels, Belgium.

EN 1992-1-1. (2004). Eurocode 2: Design of concrete structures - Part 1-1: General rules and rules for buildings. European Committee for Standardization: Brussels, Belgium.

EN 1998-1. (2013). Eurocode 8: Design of structures for earthquake resistance - Part 1: General rules, seismic actions and rules for buildings. European Committee for Standardization: Brussels, Belgium.

Gazetas, G., Apostolou, M., & Anastasopoulos, J. (2004). *Seismic Bearing Capacity Failure and Overturning of 'Terveler' Building in Adapazari, 1999*. https://www.semanticscholar.org/paper/Seismic-Bearing-Capacity-Failure-and-Overturning-of-Gazetas-Apostolou/5635873b46ae0995255d1276d349bd56621929ee

Ghobarah, A. (2001). Performance-based design in earthquake engineering: State of development. *Engineering Structures*, *23*(8), 878–884. https://doi.org/10.1016/S0141-0296(01)00036-0

Goulet, C. A., Haselton, C. B., Mitrani-Reiser, J., Beck, J. L., Deierlein, G. G., Porter, K. A., & Stewart, J. P. (2007). Evaluation of the seismic performance of a code-conforming reinforced-concrete frame building—From seismic hazard to collapse safety and economic losses. *Earthquake Engineering & Structural Dynamics*, *36*(13), 1973–1997. https://doi.org/10.1002/eqe.694

Griffis, L., Patel, V., Muthukumar, S., & Baldava, S. (2013). *A Framework for Performance-Based Wind Engineering*. 1205–1216. https://doi.org/10.1061/9780784412626.105

Hyderkhan, P., & Murnal, D. P. B. (2018). *COMPARISON OF INCREMENTAL DYNAMIC ANALYSIS CURVE WITH PUSHOVER CURVE*. *05*(10).

Joyner, M. D., & Sasani, M. (2018). Multihazard Risk-Based Resilience Analysis of East and West Coast Buildings Designed to Current Codes. *Journal of Structural Engineering*, *144*(9), 04018156. https://doi.org/10.1061/(ASCE)ST.1943-541X.0002132

Khan, M. A. (2013). Chapter Ten—Seismic Design for Buildings. In M. A. Khan (Ed.), *Earthquake-Resistant Structures* (pp. 283–315). Butterworth-Heinemann. https://doi.org/10.1016/B978-1-85617-501-2.00010-9

Kularathna, S., Lewangamage, C., & Jayasinghe, M. T. R. (2013a). *(PDF) DEVELOPMENT OF NATIONAL GUIDELINES FOR SEISMIC ANALYSIS AND DESIGN OF (ENGINEERED) BUILDINGS DEVELOPMENT OF NATIONAL GUIDELINES FOR SEISMIC ANALYSIS AND DESIGN OF (ENGINEERED) BUILDINGS IN SRI LANKA*. https://www.researchgate.net/publication/304281326_DEVELOPMENT_OF_NATIONAL_GUIDELINES_FOR_SEISMIC_ANALYSIS_AND_DESIGN_OF_ENGINEERED_BUILDINGS_DEVELOPMENT_OF_NATIONAL_GUIDELINES_FOR_SEISMIC_ANALYSIS_AND_DESIGN_OF_ENGINEERED_BUILDINGS_IN_SRI_LANKA

Kularathna, S., Lewangamage, C., & Jayasinghe, M. T. R. (2013b, January 1). *DEVELOPMENT OF NATIONAL GUIDELINES FOR SEISMIC ANALYSIS AND DESIGN OF (ENGINEERED) BUILDINGS DEVELOPMENT OF NATIONAL GUIDELINES FOR SEISMIC ANALYSIS AND DESIGN OF (ENGINEERED) BUILDINGS IN SRI LANKA*.

Mohammadi, A., Azizinamini, A., Griffis, L., & Irwin, P. (2019). Performance Assessment of an Existing 47-Story High-Rise Building under Extreme Wind Loads. *Journal of Structural Engineering*, *145*(1), 04018232. https://doi.org/10.1061/(ASCE)ST.1943-541X.0002239

Nazri, F. M. (2011). *Predicting the Collapse Potential of Structures in Earthquakes*. University of Bristol.

Nazri, F. M., & Alexander, N. A. (2012). *Predicting the Collapse Potential of Structures*.

Nissanka, S., Amaratunga, P., & Haigh, R. (2020, October 17). *DISASTER RESILIENT BUILDING CODES IN SRI LANKA*.

Patil, S., & Kori, J. (2021). Performance Evaluation of RC Building Subjected to Repeated Earthquake Load. *Reliability Engineering and Resilience*, *3*(2). https://doi.org/10.22115/rer.2022.346922.1047

Paulotto, C., Ciampoli, M., & Augusti, G. (2004). Some proposals for a first step towards a Performance Based Wind Engineering. *Int. J.*

(PDF) REDi™ Rating System: Resilience-based Earthquake Design Initiative for the Next Generation of Buildings. (n.d.). Retrieved January 20, 2024, from https://www.researchgate.net/publication/326331951_REDi_Rating_System_Resilience-

based_Earthquake_Design_Initiative_for_the_Next_Generation_of_Buildings

Pearson, C., & Delatte, N. (2005). Ronan Point Apartment Tower Collapse and its Effect on Building Codes. *Journal of Performance of Constructed Facilities*, *19*(2), 172–177. https://doi.org/10.1061/(ASCE)0887-3828(2005)19:2(172)

Pecker, A., & Pender, M. (2000). Earthquake resistant design of foundations: New construction. *GeoEng Conference, Melbourne*, *1*.

Pierre, A. J., & Hidayat, I. (2020). Seismic performance of reinforced concrete structures with pushover analysis. *IOP Conference Series: Earth and Environmental Science*, *426*(1), 012045. https://doi.org/10.1088/1755-1315/426/1/012045

Porter, K. (2003). *An Overview of PEER's Performance-Based Earthquake Engineering Methodology*. https://www.semanticscholar.org/paper/An-Overview-of-PEER%27s-Performance-Based-Earthquake-Porter/3b3f4192a485c6ae6ab584b8f1b9ff40820f1913

Puri, V. K., & Prakash, S. (2013). *Shallow Foundations for Seismic Loads: Design Considerations*.

PURI, V., & Prakash, S. (2007). *ON FOUNDATIONS UNDER SEISMIC LOADS*.

Rosowsky, D., & Ellingwood, B. (2002). Performance-Based Engineering of Wood Frame Housing: Fragility Analysis Methodology. *Journal of Structural Engineering-Asce - J STRUCT ENG-ASCE*, *128*. https://doi.org/10.1061/(ASCE)0733-9445(2002)128:1(32)

Seneviratne, H. N., Perera, L. R. K., Wijesundara, K. K., Dananjaya, R. M. S., & De S. Jayawardena, U. (2020). Seismicity around Sri Lanka from Historical Records and its Engineering Implications. *Engineer: Journal of the Institution of Engineers, Sri Lanka*, *53*(2), 47. https://doi.org/10.4038/engineer.v53i2.7412

Seneviratne, N., Wijesundara, K., Perera, L. R. K., & Dissanayake, R. (2020). A Macro Seismic Hazard Zonation for Sri Lanka. *Engineer*, *53*, 37–44. https://doi.org/10.4038/engineer.v53i3.7418

Spence, S., & Arunachalam, S. (2022). Performance-Based Wind Engineering: Background and State of the Art. *Frontiers in Built Environment*, *8*. https://doi.org/10.3389/fbuil.2022.830207

Stochino, F., Bedon, C., Sagaseta, J., & Honfi, D. (2019). Robustness and Resilience of Structures under Extreme Loads. *Advances in Civil Engineering*, *2019*, e4291703. https://doi.org/10.1155/2019/4291703

Taghinezhad, R., Taghinezhad, A., Mahdavifar, V., & Soltangharaei, V. (2018). Evaluation of Story Drift under Pushover Analysis in Reinforced Concrete Moment Frames. *International Journal of Research and Engineering*, *5*, 296–302.

Tavares, D. C. R., & Krausmann, E. (2021, October 29). *Impacts of Natural Hazards and Climate Change on EU Security and Defence*. JRC Publications Repository. https://doi.org/10.2760/244397

Uduweriya, S. B., Wijesundara, K., & Dissanayake, P. (2013). *SEISMIC RISK IN COLOMBO – PROBABILISTIC APPROACH*. https://www.semanticscholar.org/paper/SEISMIC-RISK-IN-COLOMBO-%E2%80%93-PROBABILISTIC-APPROACH-Uduweriya-Wijesundara/7a77f3010520586fcbdb6704e06701dcd671d0d4

Vamvatsikos, D., & Cornell, C. (2004). Applied Incremental Dynamic Analysis. *Earthquake Spectra - EARTHQ SPECTRA*, *20*. https://doi.org/10.1193/1.1737737

Whittaker, A., Hamburger, R., Comartin, C., Bachman, R., & Rojahn, C. (2003, October 1). *Performance based engineering of buildings and infrastructure for extreme loadings*.

World Bank Group. (2016). *Fiscal Disaster Risk Assessment and Risk Financing Options*. World Bank, Washington, DC. https://doi.org/10.1596/24689

Zięba, Z., Krokowska, M., Wyjadłowski, M., Kozubal, J. V., Kania, T., & Mońka, J. (2023). Assessing the Scale Effect on Bearing Capacity of Undrained Subsoil: Implications for Seismic Resilience of Shallow Foundations. *Materials*, *16*(16), Article 16. https://doi.org/10.3390/ma16165631

APPENDIX A –- GENERAL ARRANGEMENT DRAWINGS OF BUILDINGS

A.1. Typical building

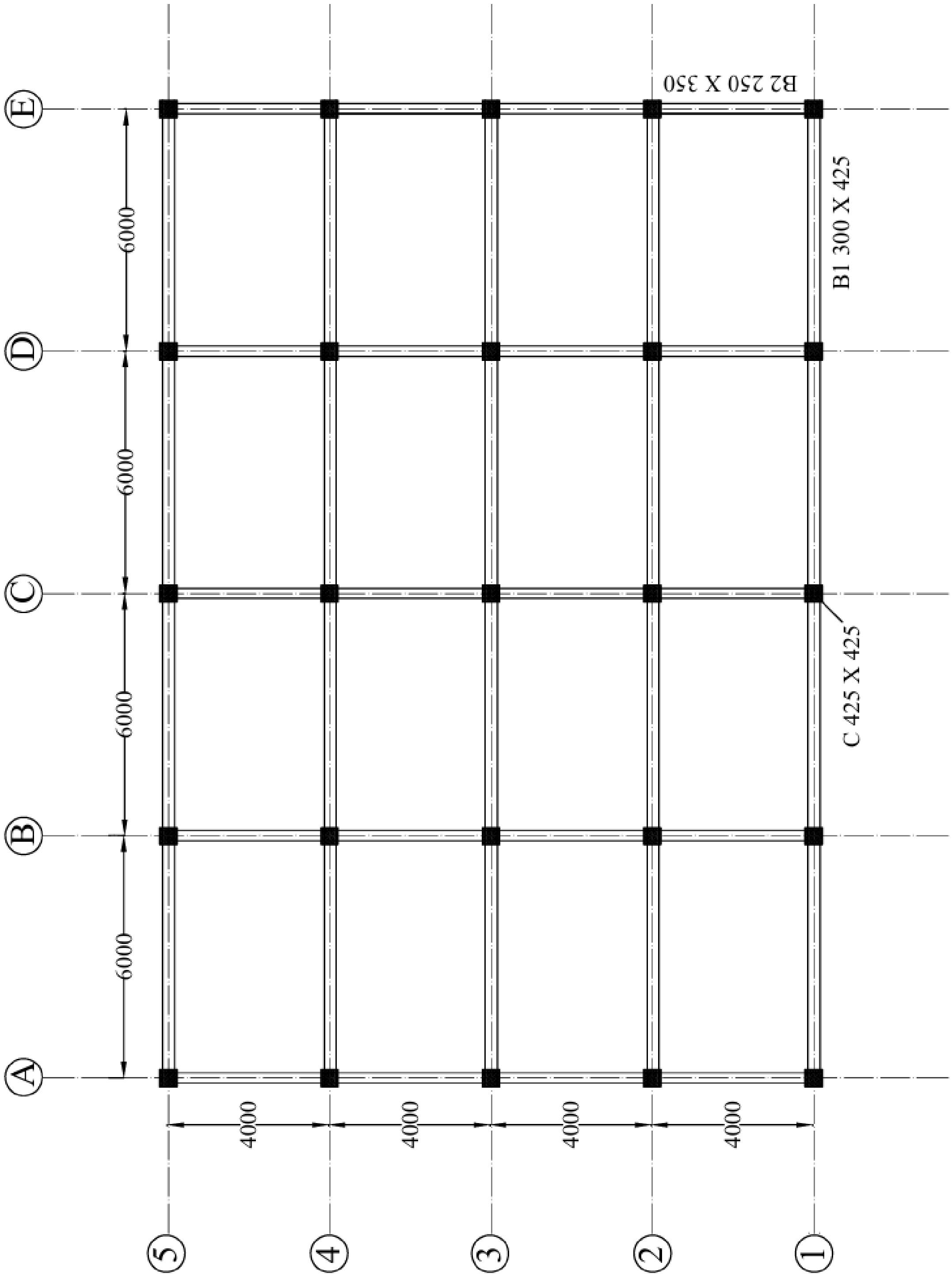

Figure A.1: General arrangement of the typical building

A.2. School building

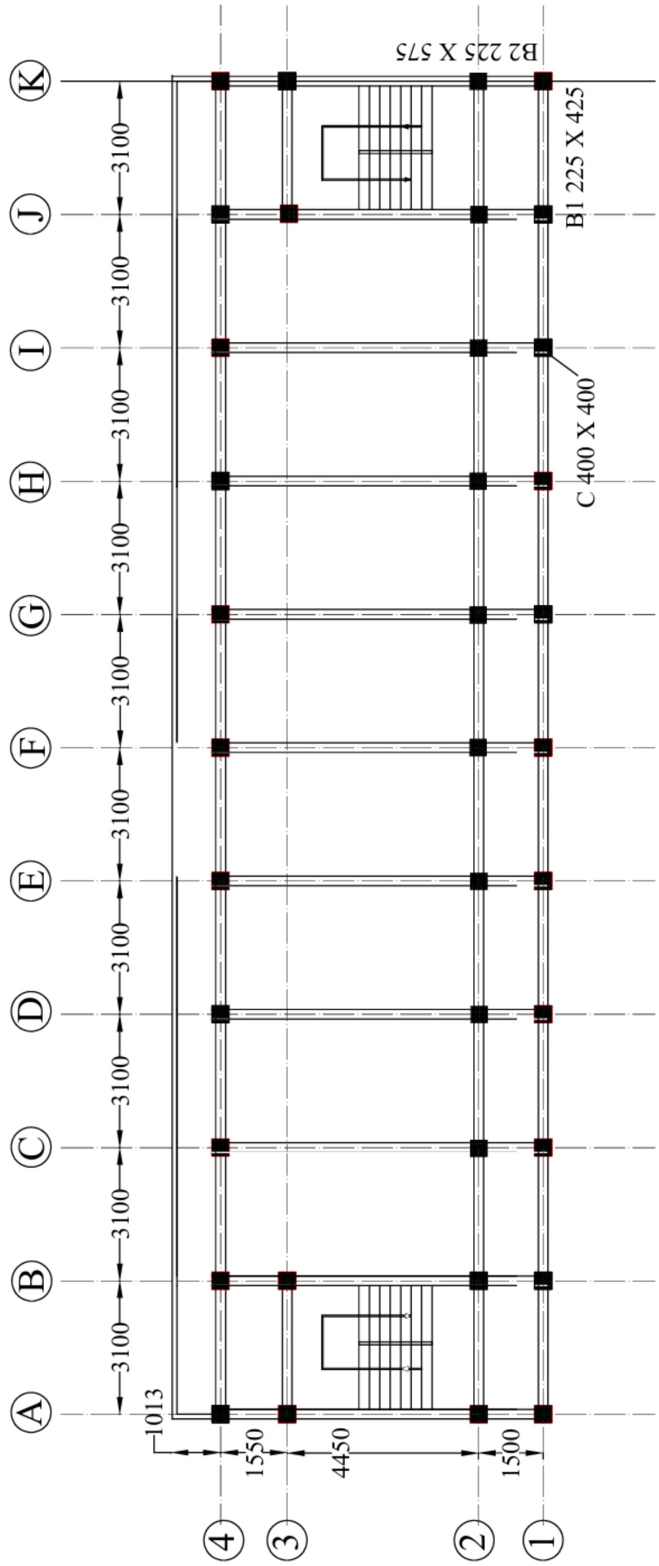

Figure A.2: General arrangement of the school building

A.3. University building

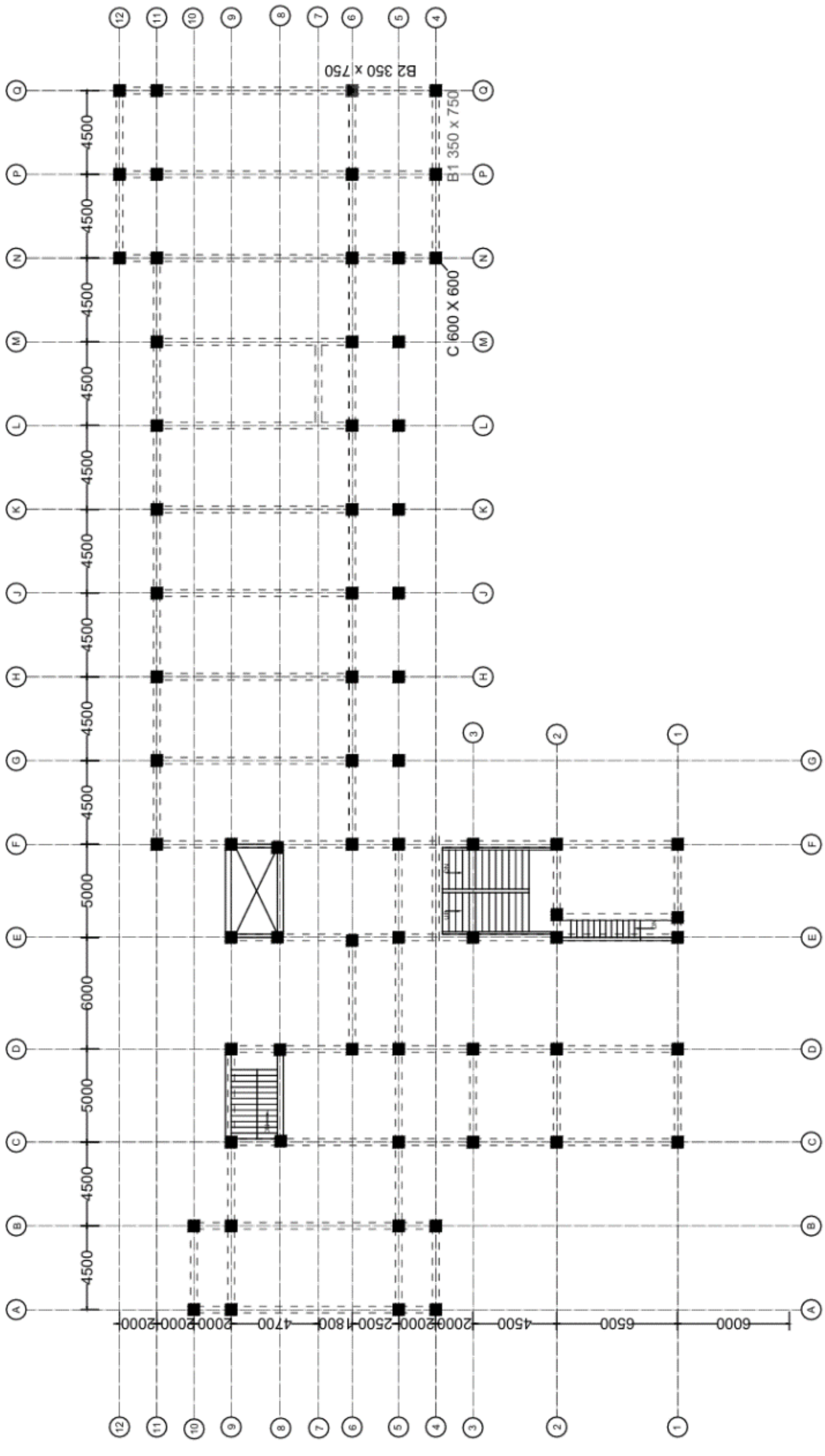

Figure A.3: General arrangement of the university building

A.4. Hospital building

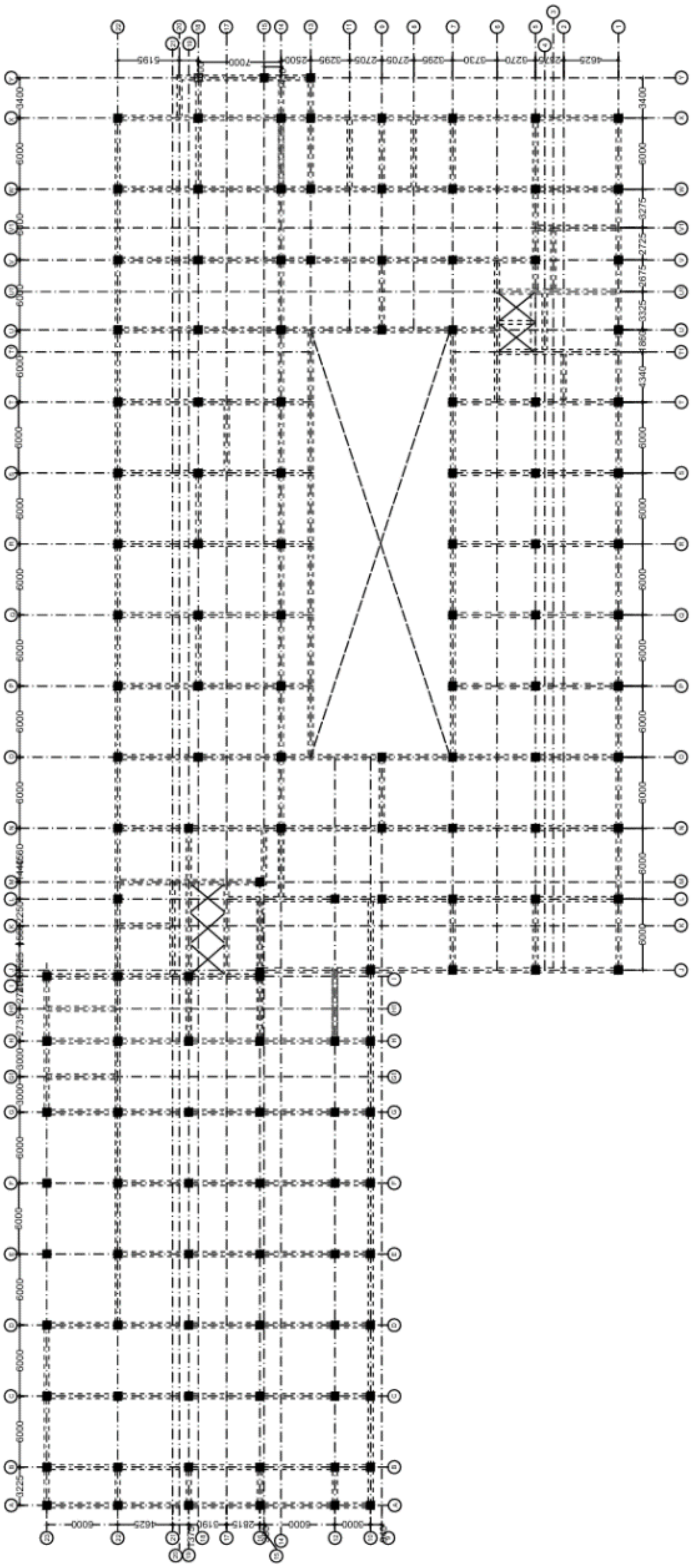

Figure A.4: General arrangement of the hospital building

A.5. Defective building

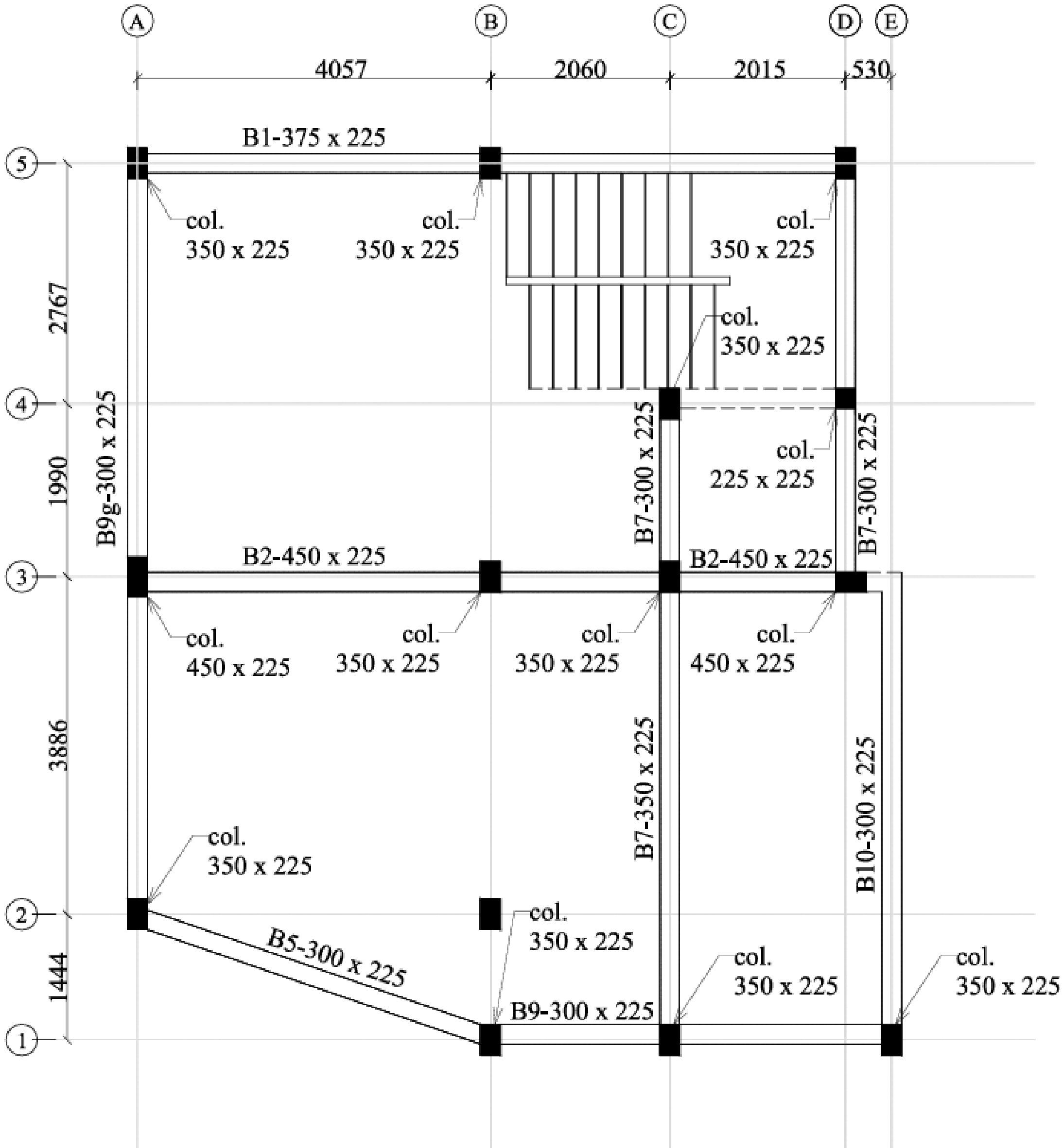

Figure A.5: General arrangement of the defective building

A.6. Retrofitted building

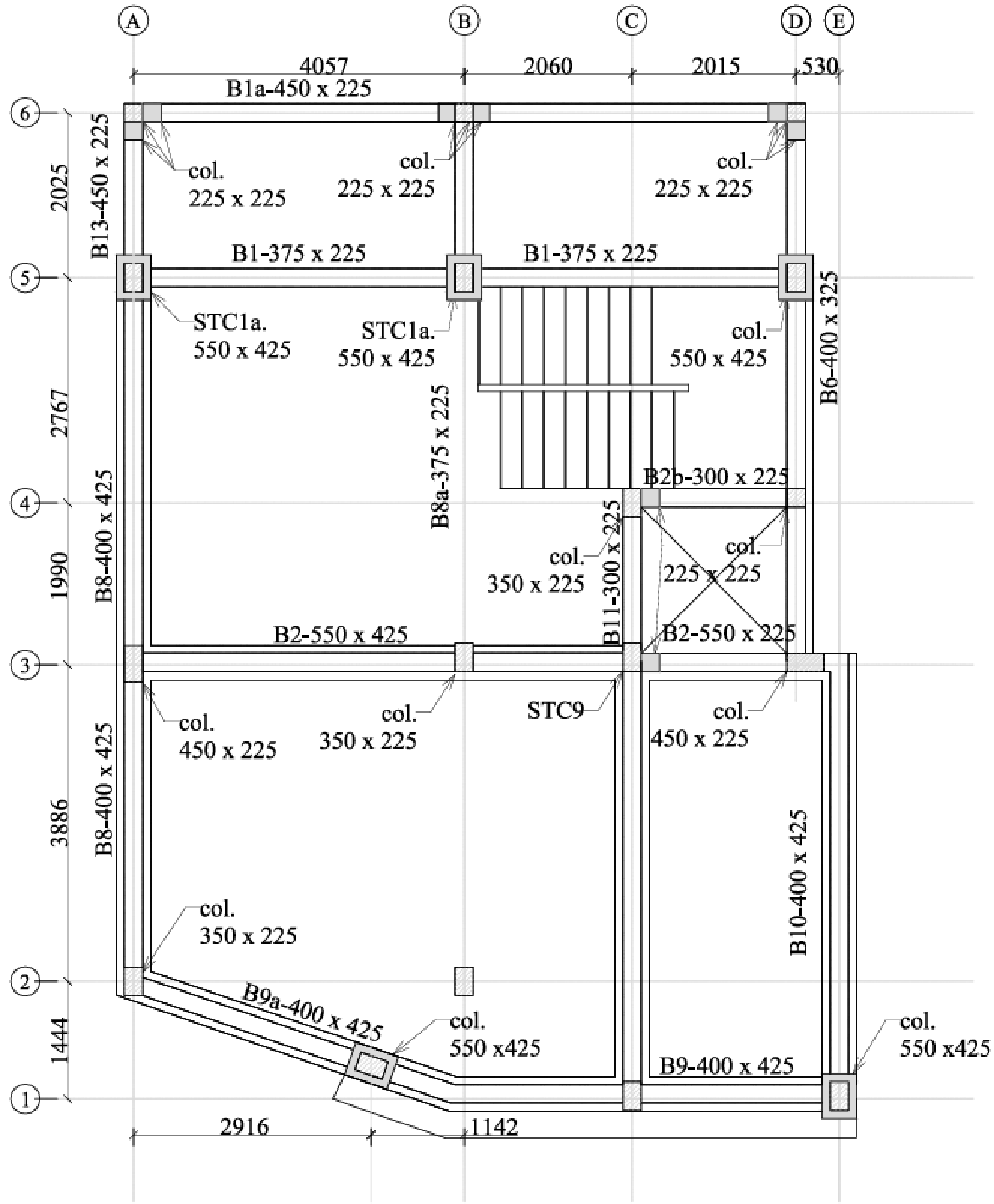

Figure A.6: General arrangement of the retrofitted building

APPENDIX B – SUMMARY OF WIND LOADS ON BUILDINGS

Table B.1: Wind loads on the typical building

Floor	Design Wind Load X-direction	Design Wind Load Y-direction
First floor	56.74kN	91.54kN
Second floor	56.74kN	91.54kN
Roof floor	28.37kN	45.77kN
Design Base shear	**141.85kN**	**228.85kN**

Table B.2: Wind loads on the school building

Floor	Design Wind Load X-direction	Design Wind Load Y-direction
First floor	22.18kN	124.01kN
Second floor	22.18kN	124.01kN
Roof floor	11.68kN	62.01kN
Design Base shear	**56.04kN**	**310.03kN**

Table B.3: Wind loads on the university building

Floor	Design Wind Load X-direction	Design Wind Load Y-direction
First floor	133.29kN	340.44kN
Second floor	133.29kN	340.44kN
Third floor	133.29kN	340.44kN
Fourth floor	133.29kN	340.44kN
Fifth floor	133.29kN	340.44kN
Sixth floor	133.29kN	340.44kN
Seventh floor	133.29kN	340.44kN
Roof floor	66.65kN	170.22kN
Design Base shear	**999.68kN**	**2553.30kN**

Table B.4: Wind loads on the hospital building

Floor	Design Wind Load X-direction	Design Wind Load Y-direction
First floor	176.10kN	461.73kN
Second floor	176.10kN	461.73kN
Third floor	176.10kN	461.73kN
Fourth floor	176.10kN	461.73kN
Fifth floor	176.10kN	461.73kN
Roof floor	88.05kN	230.87kN
Design Base shear	**968.55kN**	**2539.52kN**

APPENDIX C – SUMMARY OF SEISMIC LOADS ON BUILDINGS

Table C.1: Seismic loads on the typical building

Floor	Design Seismic Load
First floor	251.69kN
Second floor	503.38kN
Roof floor	595.51kN
Base Shear	1350.58kN

Table C.2: Seismic loads on the school building

Floor	Design Seismic Load
First floor	212.23kN
Second floor	424.46kN
Roof floor	386.27kN
Base shear	1030.56kN

Table C.3: Seismic loads on the university building

Floor	Design Seismic Load
First floor	165.52kN
Second floor	331.04kN
Third floor	496.57kN
Fourth floor	662.09kN
Fifth floor	827.61kN
Sixth floor	993.13kN
Seventh floor	1158.65kN
Roof floor	935.67kN
Base shear	5570.28kN

Table C.4: Seismic loads on the hospital building

Floor	Design Seismic Load
First floor	948.65kN
Second floor	1897.30kN
Third floor	2845.95kN
Fourth floor	3794.60kN
Fifth floor	4743.25kN
Roof floor	4552.75kN
Base shear	18782.49kN

APPENDIX D – SUMMARY OF STRUCTURAL ANALYSIS OF BUILDINGS

Table D.1: Summary of the structural analysis of the typical building

Element	Member Force	Value
Beams – X-direction	Bending Moment (Hogging)	240kNm
	Bending Moment (Sagging)	100kNm
	Shear Force	138kN
Beams – Y-direction	Bending Moment (Hogging)	163kNm
	Bending Moment (Sagging)	116kNm
	Shear Force	108kN
Columns	Axial Force	1164kN
	Bending Moment (M22)	193kNm
	Bending Moment (M33)	195kNm

Table D.2: Summary of the structural analysis of the school building

Element	Member Force	Value
Beams – X-direction	Bending Moment (Hogging)	82kNm
	Bending Moment (Sagging)	57kNm
	Shear Force	82kN
Beams – Y-direction	Bending Moment (Hogging)	136kNm
	Bending Moment (Sagging)	96kNm
	Shear Force	136kN
Columns	Axial Force	740kN
	Bending Moment (M22)	114kNm
	Bending Moment (M33)	93kNm

Table D.3: Summary of the structural analysis of the university building

Element	Member Force	Value
Beams – X-direction	Bending Moment (Hogging)	426kNm
	Bending Moment (Sagging)	369kNm
	Shear Force	500kN
Beams – Y-direction	Bending Moment (Hogging)	643kNm
	Bending Moment (Sagging)	424kNm
	Shear Force	415kN
Columns	Axial Force	4180kN
	Bending Moment (M22)	436kNm
	Bending Moment (M33)	370kNm

Table D.4: Summary of the structural analysis of the hospital building

Element	Member Force	Value
Beams – X-direction	Bending Moment (Hogging)	436kNm
	Bending Moment (Sagging)	428kNm
	Shear Force	607kN
Beams – Y-direction	Bending Moment (Hogging)	461kNm
	Bending Moment (Sagging)	399kNm
	Shear Force	670kN
Columns	Axial Force	5458kN
	Bending Moment (M22)	457kNm
	Bending Moment (M33)	426kNm

APPENDIX E – SUMMARY OF STRUCTURAL DESIGN OF BUILDINGS

Table E.1: Summary of the structural design of the typical building

Element	Section Size (mm × mm)	Reinforcements	Shear Reinforcements
Beams – X-direction	300×425	3T25 and 2T20 @ top 3T25 and 2T20 @ bottom	2×R6 @ 125c/c
Beams – Y-direction	250×350	3T20 and 3T20 @ top 3T20 and 3T20 @ bottom	2×R6 @ 125c/c
Columns	425×425	4T25/side	R8 @ 150c/c

Table E.2: Summary of the structural design of the school building

Element	Section Size (mm × mm)	Reinforcements	Shear Reinforcements
Beams – X-direction	225×425	2T20 @ top 2T20 @ bottom	2×R6 @ 200c/c
Beams – Y-direction	225×575	2T20 @ top 2T20 @ bottom	2×R6 @ 225c/c
Columns	400×400	3T20/side	R6 @ 150c/c

Table E.3: Summary of the structural design of the university building

Element	Section Size (mm × mm)	Reinforcements	Shear Reinforcements
Beams – X-direction	350×750	4T20 and 2T20 @ top 4T20 and 2T20 @ bottom	2×R8 @ 125c/c
Beams – Y-direction	350×750	4T25 and 2T25 @ top 4T25 and 2T25 @ bottom	2×R8 @ 125c/c
Columns	600×600	4T25/side	R8 @ 150c/c

Table E.4: Summary of the structural design of the hospital building

Element	Section Size (mm × mm)	Reinforcements	Shear Reinforcements
Beams – X-direction	400×650	4T20 and 4T20 @ top 4T20 and 4T20 @ bottom	4×R8 @ 150c/c
Beams – Y-direction	400×650	4T20 and 4T20 @ top 4T20 and 4T20 @ bottom	4×R8 @ 125c/c
Columns	625×625	5T25/side	R8 @ 150c/c

APPENDIX F – SUMMARY OF THE RESULTS FOR COMPARISON OF STRUCTURAL ANALYSIS AND DESIGN OF A GRAVITY-LOADED TYPICAL BUILDING BASED ON EUROCODES AND BRITISH STANDARDS

F.1. Structural analysis and design of beams for flexure

F.1.1. Structural analysis and design of beams in type 1 frame for flexure

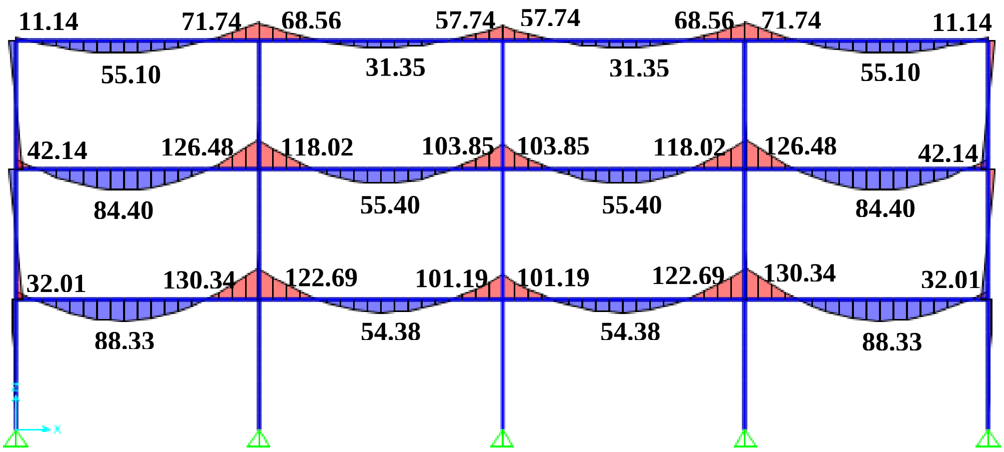

Figure F.1: Bending moment diagrams – Eurocode-based typical building (X-direction – type 1 frame)

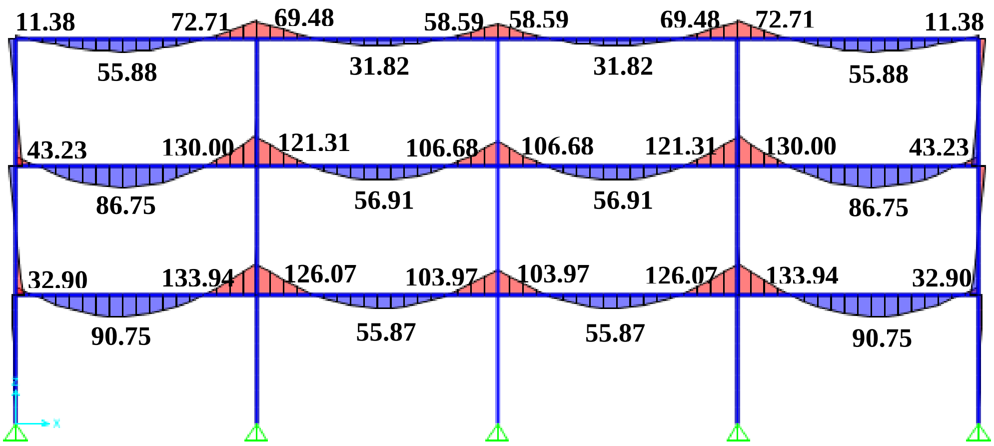

Figure F.2: Bending moment diagrams – British Standard-based typical building (X-direction – type 1 frame)

Table F.1: Design of beams for flexure (X-direction - type 1 frame - first/second floor)

Parameters - Design for Hogging Moment	Euro	BS	% Difference
Maximum Hogging Moment (kNm)	130.34	133.94	2.76%
Amount of Reinforcement Required (mm^2)	942.00	899.00	-4.56%
Number of Reinforcements	3T20	3T20	Similar
Amount of Reinforcement Provided (mm^2)	942.00	942.00	0.00%
Utilization	1.00	0.95	-4.56%
Parameters - Design for Sagging Moment	**Euro**	**BS**	**% Difference**
Maximum Sagging Moment (kNm)	88.33	90.75	2.74%
Amount of Reinforcement Required (mm^2)	579.00	545.00	-5.87%
Number of Reinforcements	3T16	3T16	Similar
Amount of Reinforcement Provided (mm^2)	602.88	602.88	0.00%
Utilization	0.96	0.90	-5.87%

Table F.2: Design of beams for flexure (X-direction - type 1 frame - roof floor)

Parameters - Design for Hogging Moment	Euro	BS	% Difference
Maximum Hogging Moment (kNm)	71.74	72.71	1.35%
Amount of Reinforcement Required (mm^2)	479.00	447.00	-6.68%
Number of Reinforcements	2T16+1T12	2T16+1T12	Similar
Amount of Reinforcement Provided (mm^2)	514.96	514.96	0.00%
Utilization	0.93	0.87	-6.68%
Parameters - Design for Sagging Moment	**Euro**	**BS**	**% Difference**
Maximum Sagging Moment (kNm)	55.10	55.88	1.42%
Amount of Reinforcement Required (mm^2)	361.00	334.00	-7.48%
Number of Reinforcements	2T16	3T12	Dissimilar
Amount of Reinforcement Provided (mm^2)	401.92	339.12	-15.63%
Utilization	0.90	0.98	9.65%

F.1.2. Structural analysis and design of beams in type 2 frame for flexure

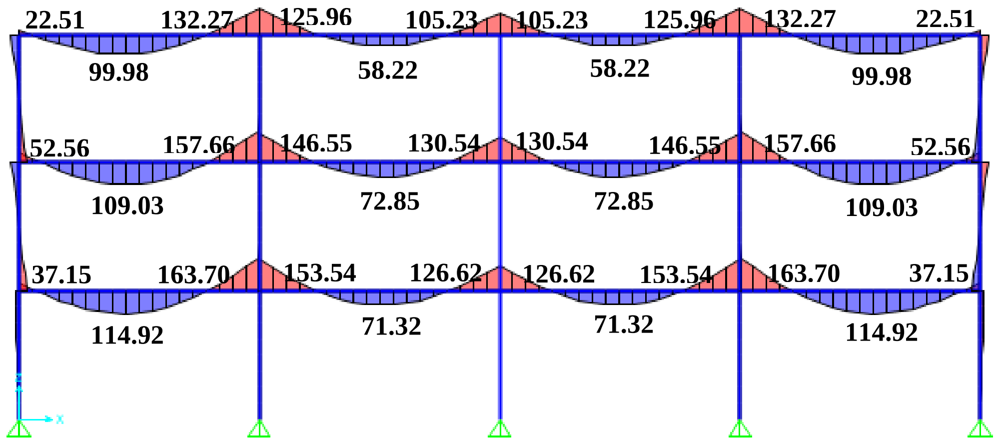

Figure F.3: Bending moment diagrams – Eurocode-based typical building (X-direction – type 2 frame)

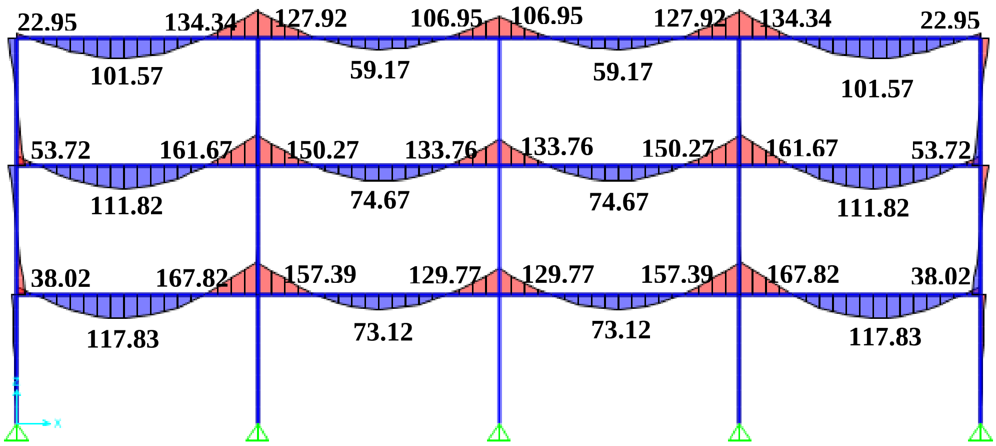

Figure F.4: Bending moment diagrams – British Standard-based typical building (X-direction – type 2 frame)

Table F.3: Design of beams for flexure (X-direction - type 2 frame - first/second floor)

Parameters - Design for Hogging Moment	Euro	BS	% Difference
Maximum Hogging Moment (kNm)	163.70	167.82	2.52%
Amount of Reinforcement Required (mm^2)	1256.00	1206.00	-3.98%
Number of Reinforcements	2T25+1T20	2T25+1T20	Similar
Amount of Reinforcement Provided (mm^2)	1295.25	1295.25	0.00%
Utilization	0.97	0.93	-3.98%
Parameters - Design for Sagging Moment	**Euro**	**BS**	**% Difference**
Maximum Sagging Moment (kNm)	114.92	117.83	2.53%
Amount of Reinforcement Required (mm^2)	758.00	711.00	-6.20%
Number of Reinforcements	2T20+1T16	2T20 + 1T12	Dissimilar
Amount of Reinforcement Provided (mm^2)	828.96	741.04	-10.61%
Utilization	0.91	0.96	4.93%

Table F.4: Design of beams for flexure (X-direction - type 2 frame - roof floor)

Parameters - Design for Hogging Moment	Euro	BS	% Difference
Maximum Hogging Moment (kNm)	132.27	134.34	1.56%
Amount of Reinforcement Required (mm^2)	967.00	903.00	-6.62%
Number of Reinforcements	2T25	3T20	Dissimilar
Amount of Reinforcement Provided (mm^2)	981.25	942.00	-4.00%
Utilization	0.99	0.96	-2.73%
Parameters - Design for Sagging Moment	**Euro**	**BS**	**% Difference**
Maximum Sagging Moment (kNm)	99.98	101.57	1.59%
Amount of Reinforcement Required (mm^2)	659.00	613.00	-6.98%
Number of Reinforcements	2T20+1T12	2T20	Dissimilar
Amount of Reinforcement Provided (mm^2)	741.04	628.00	-15.25%
Utilization	0.89	0.98	9.76%

F.1.3. Structural analysis and design of beams in Type 3 frame for flexure

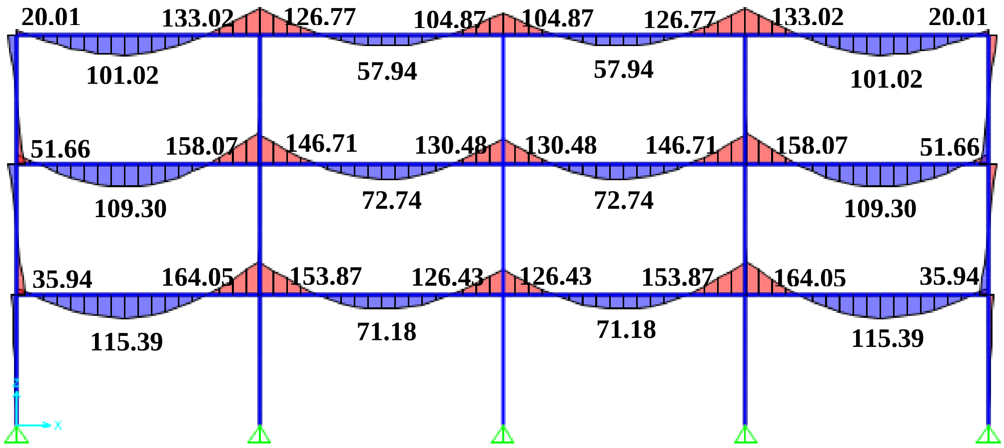

Figure F.5: Bending moment diagrams – Eurocode-based typical building (X-direction – type 3 frame)

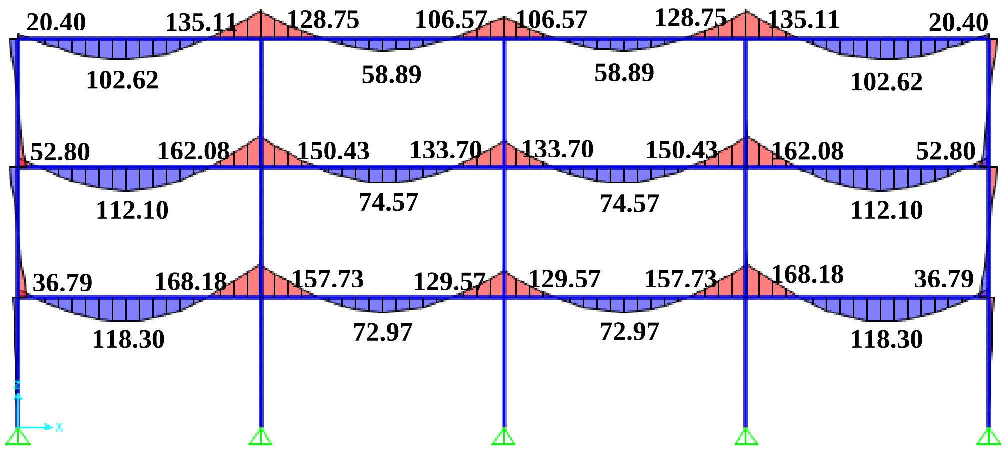

Figure F.6: Bending moment diagrams – British Standard-based typical building (X-direction – type 3 frame)

Table F.5: Design of beams for flexure (X-direction - type 3 frame - first/second floor)

Parameters - Design for Hogging Moment	**Euro**	**BS**	**% Difference**
Maximum Hogging Moment (kNm)	164.05	168.18	2.52%
Amount of Reinforcement Required (mm^2)	1260.00	1209.00	-4.05%
Number of Reinforcements	2T25+1T20	2T25+1T20	Similar
Amount of Reinforcement Provided (mm^2)	1295.25	1295.25	0.00%
Utilization	0.97	0.93	-4.05%
Parameters - Design for Sagging Moment	**Euro**	**BS**	**% Difference**
Maximum Sagging Moment (kNm)	115.39	118.30	2.52%
Amount of Reinforcement Required (mm^2)	761.00	714.00	-6.18%
Number of Reinforcements	2T20+1T16	2T20 + 1T12	Dissimilar
Amount of Reinforcement Provided (mm^2)	828.96	741.04	-10.61%
Utilization	0.92	0.96	4.96%

Table F.6: Design of beams for flexure (X-direction - type 3 frame - roof floor)

Parameters - Design for Hogging Moment	**Euro**	**BS**	**% Difference**
Maximum Hogging Moment (kNm)	133.02	135.11	1.57%
Amount of Reinforcement Required (mm^2)	973.00	909.00	-6.58%
Number of Reinforcements	2T25	3T20	Dissimilar
Amount of Reinforcement Provided (mm^2)	981.25	942.00	-4.00%
Utilization	0.99	0.96	-2.68%
Parameters - Design for Sagging Moment	**Euro**	**BS**	**% Difference**
Maximum Sagging Moment (kNm)	101.02	102.62	1.58%
Amount of Reinforcement Required (mm^2)	666.00	620.00	-6.91%
Number of Reinforcements	2T20+1T12	2T20	Dissimilar
Amount of Reinforcement Provided (mm^2)	741.04	628.00	-15.25%
Utilization	0.90	0.99	9.85%

F.1.4. Structural analysis and design of beams in type 4 frame for flexure

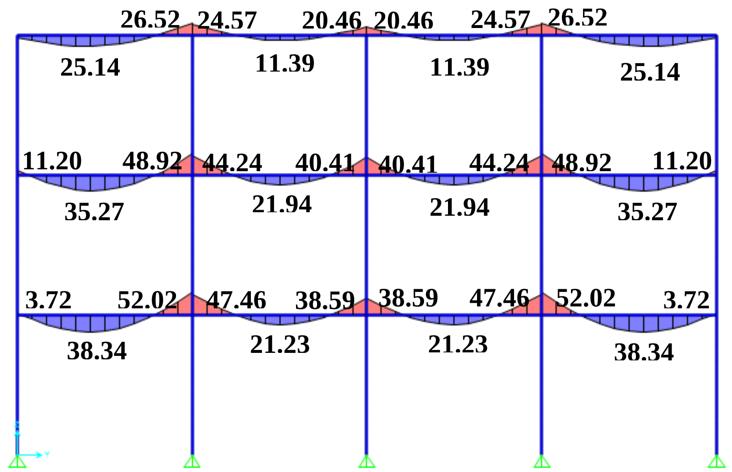

Figure F.7: Bending moment diagrams – Eurocode-based typical building (Y-direction – Type 4 frame)

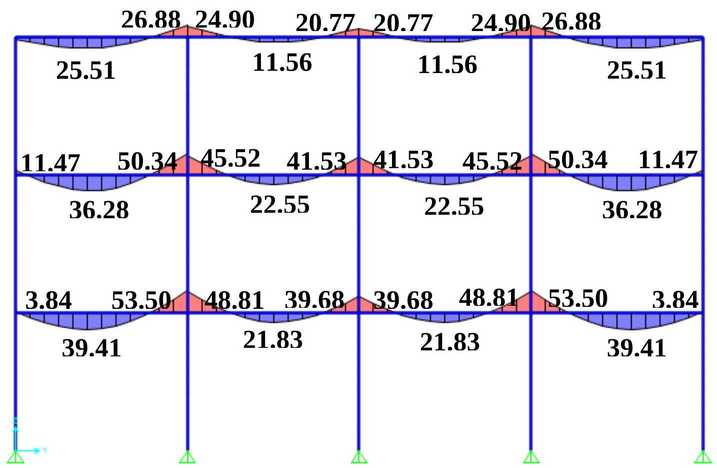

Figure F.8: Bending moment diagrams – British Standard-based typical building (Y-direction – type 4 frame)

Table F.7: Design of beams for flexure (Y-direction - type 4 frame - first/second floor)

Parameters - Design for Hogging Moment	Euro	BS	% Difference
Maximum Hogging Moment (kNm)	52.02	53.50	2.85%
Amount of Reinforcement Required (mm^2)	474.00	450.00	-5.06%
Number of Reinforcements	2T16+1T12	2T16 + 1T12	Similar
Amount of Reinforcement Provided (mm^2)	514.96	514.96	0.00%
Utilization	0.92	0.87	-5.06%
Parameters - Design for Sagging Moment	**Euro**	**BS**	**% Difference**
Maximum Sagging Moment (kNm)	38.34	39.41	2.79%
Amount of Reinforcement Required (mm^2)	333.00	313.00	-6.01%
Number of Reinforcements	3T12	3T12	Similar
Amount of Reinforcement Provided (mm^2)	339.12	339.12	0.00%
Utilization	0.98	0.92	-6.01%

Table F.8: Design of beams for flexure (Y-direction - type 4 frame - roof floor)

Parameters - Design for Hogging Moment	Euro	BS	% Difference
Maximum Hogging Moment (kNm)	26.52	26.88	1.36%
Amount of Reinforcement Required (mm^2)	230.00	214.00	-6.96%
Number of Reinforcements	3T12	2T12	Dissimilar
Amount of Reinforcement Provided (mm^2)	339.12	226.08	-33.33%
Utilization	0.68	0.95	39.57%
Parameters - Design for Sagging Moment	**Euro**	**BS**	**% Difference**
Maximum Sagging Moment (kNm)	25.14	25.51	1.47%
Amount of Reinforcement Required (mm^2)	218.00	203.00	-6.88%
Number of Reinforcements	2T12	2T12	Similar
Amount of Reinforcement Provided (mm^2)	226.08	226.08	0.00%
Utilization	0.96	0.90	-6.88%

F.1.5. Structural analysis and design of beams in type 5 frame for flexure

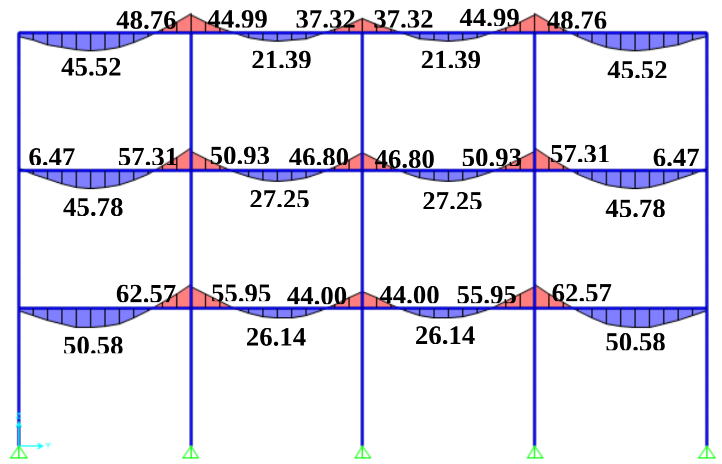

Figure F.9: Bending moment diagrams – Eurocode-based typical building (Y-direction – type 5 frame)

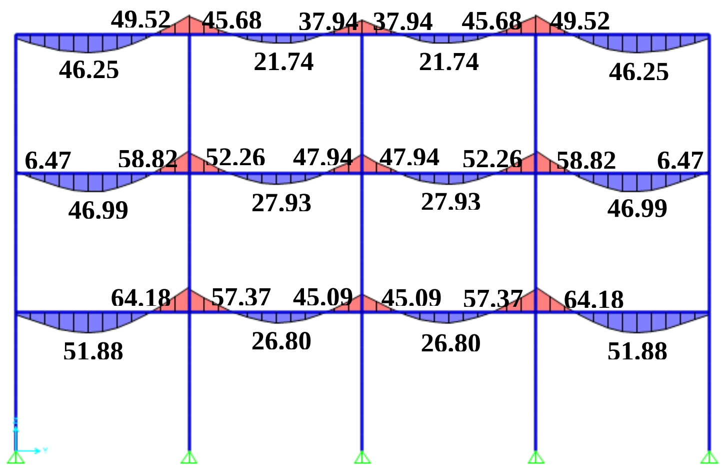

Figure F.10: Bending moment diagrams – British Standard-based typical building (Y-direction – type 5 frame)

Table F.9: Design of beams for flexure (Y-direction - type 5 frame - first/second floor)

Parameters - Design for Hogging Moment	Euro	BS	% Difference
Maximum Hogging Moment (kNm)	62.57	64.18	2.57%
Amount of Reinforcement Required (mm^2)	583.00	554.00	-4.97%
Number of Reinforcements	3T16	3T16	Similar
Amount of Reinforcement Provided (mm^2)	602.88	602.88	0.00%
Utilization	0.97	0.92	-4.97%
Parameters - Design for Sagging Moment	**Euro**	**BS**	**% Difference**
Maximum Sagging Moment (kNm)	50.58	51.88	2.57%
Amount of Reinforcement Required (mm^2)	442.00	415.00	-6.11%
Number of Reinforcements	2T16+1T12	2T16 + 1T12	Similar
Amount of Reinforcement Provided (mm^2)	514.96	514.96	0.00%
Utilization	0.86	0.81	-6.11%

Table F.10: Design of beams for flexure (Y-direction - type 5 frame - roof floor)

Parameters - Design for Hogging Moment	Euro	BS	% Difference
Maximum Hogging Moment (kNm)	48.76	49.52	1.56%
Amount of Reinforcement Required (mm^2)	441.00	413.00	-6.35%
Number of Reinforcements	2T16+1T12	2T16 + 1T12	Similar
Amount of Reinforcement Provided (mm^2)	514.96	514.96	0.00%
Utilization	0.86	0.80	-6.35%
Parameters - Design for Sagging Moment	**Euro**	**BS**	**% Difference**
Maximum Sagging Moment (kNm)	45.52	46.25	1.60%
Amount of Reinforcement Required (mm^2)	398.00	370.00	-7.04%
Number of Reinforcements	2T16	2T16	Similar
Amount of Reinforcement Provided (mm^2)	401.92	401.92	0.00%
Utilization	0.99	0.92	-7.04%

F.1.6: Structural analysis and design of beams in type 6 frame for flexture

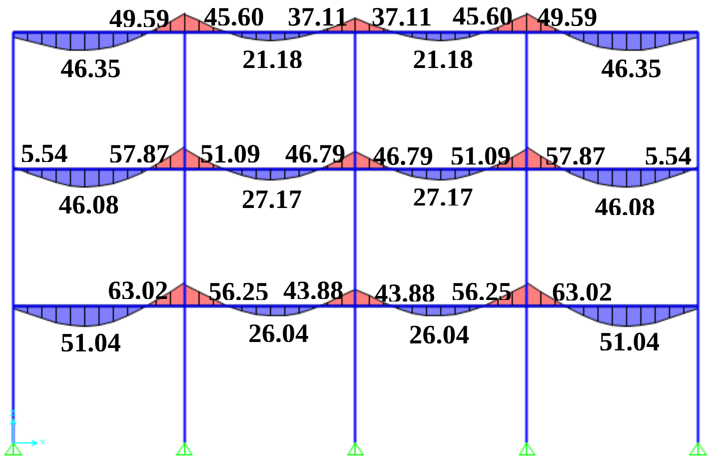

Figure F.11: Bending moment diagrams – Eurocode-based typical building (Y-direction – type 6 frame)

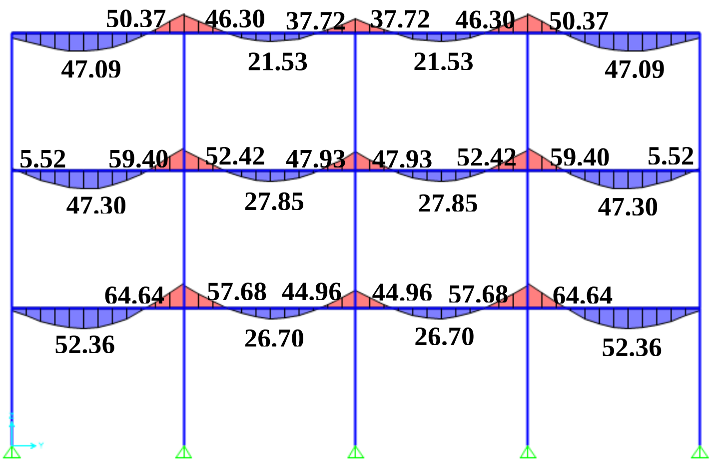

Figure F.12: Bending moment diagrams – British Standard-based typical building (Y-direction – type 6 frame)

Table F.11: Design of beams for flexure (Y-direction- type 6 frame- first/second floor)

Parameters - Design for Hogging Moment	Euro	BS	% Difference
Maximum Hogging Moment (kNm)	63.02	64.64	2.57%
Amount of Reinforcement Required (mm^2)	588.00	559.00	-4.93%
Number of Reinforcements	3T16	3T16	Similar
Amount of Reinforcement Provided (mm^2)	602.88	602.88	0.00%
Utilization	0.98	0.93	-4.93%
Parameters - Design for Sagging Moment	**Euro**	**BS**	**% Difference**
Maximum Sagging Moment (kNm)	51.04	52.36	2.59%
Amount of Reinforcement Required (mm^2)	588.00	419.00	-28.74%
Number of Reinforcements	3T16	2T16 + 1T12	Dissimilar
Amount of Reinforcement Provided (mm^2)	602.88	514.96	-14.58%
Utilization	0.98	0.81	-16.58%

Table F.12: Design of beams for flexure (Y-direction - type 6 frame - roof floor)

Parameters - Design for Hogging Moment	Euro	BS	% Difference
Maximum Hogging Moment (kNm)	49.59	50.37	1.57%
Amount of Reinforcement Required (mm^2)	450.00	421.00	-6.44%
Number of Reinforcements	2T16+1T12	2T16 + 1T12	Similar
Amount of Reinforcement Provided (mm^2)	514.96	514.96	0.00%
Utilization	0.87	0.82	-6.44%
Parameters - Design for Sagging Moment	**Euro**	**BS**	**% Difference**
Maximum Sagging Moment (kNm)	46.35	47.09	1.60%
Amount of Reinforcement Required (mm^2)	405.00	377.00	-6.91%
Number of Reinforcements	2T16+1T12	2T16	Dissimilar
Amount of Reinforcement Provided (mm^2)	514.96	401.92	-21.95%
Utilization	0.79	0.94	19.27%

F.2. Design of beams for shear

F.2.1. Structural analysis and design of beams in type 1 frame for shear

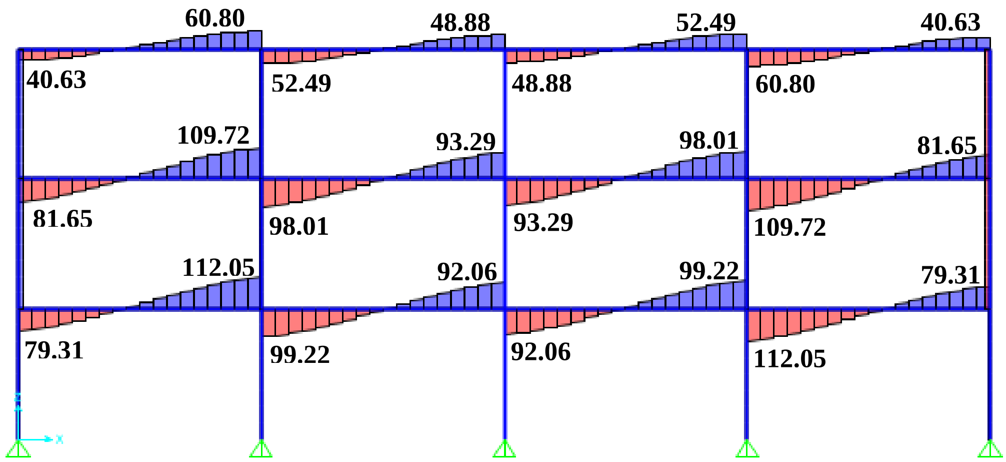

Figure F.13: Shear force diagrams – Eurocode-based typical building (X-direction – type 1 frame)

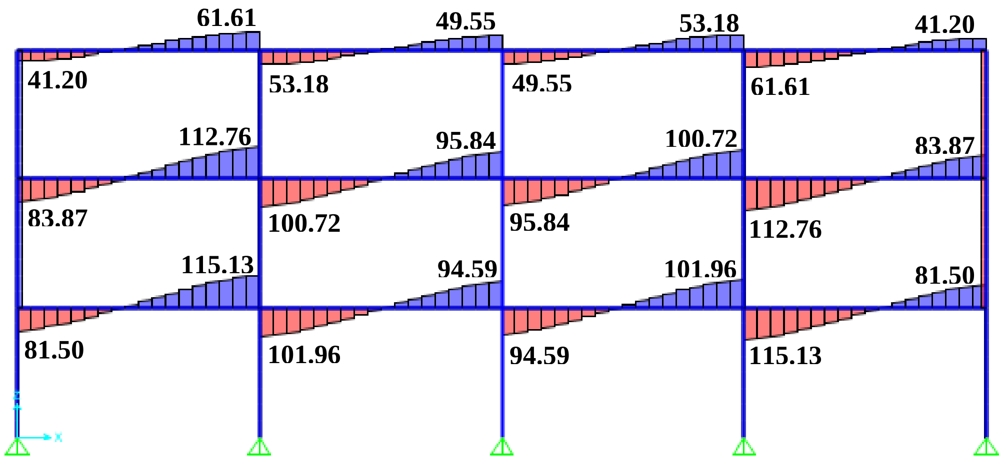

Figure F.14: Shear force diagrams – British Standard-based typical building (X-direction – type 1 frame)

Table F.13: Design of beams for shear (X-direction - type 1 frame - first/second floor)

Parameters – Design for Shear	Euro	BS	% Difference
Maximum Shear Force (kN)	112.05	115.13	2.75%
Amount of Reinforcement Required (mm^2)	465.84	520.91	11.82%
Number of Reinforcements	R6 @ 100	R6 @ 100	Similar
Amount of Reinforcement Provided (mm^2)	565.20	565.20	0.00%
Utilization	0.82	0.92	11.82%

Table F.14: Design of beams for shear (X-direction - type 1 frame - roof floor)

Parameters – Design for Shear	Euro	BS	% Difference
Maximum Shear Force (kN)	60.80	61.61	1.33%
Amount of Reinforcement Required (mm^2)	251.30	421.05	67.55%
Number of Reinforcements	R6 @ 200	R6 @ 125	Dissimilar
Amount of Reinforcement Provided (mm^2)	282.60	452.16	60.00%
Utilization	0.89	0.93	4.72%

F.2.2. Structural analysis and design of beams in the type-2 frame for shear

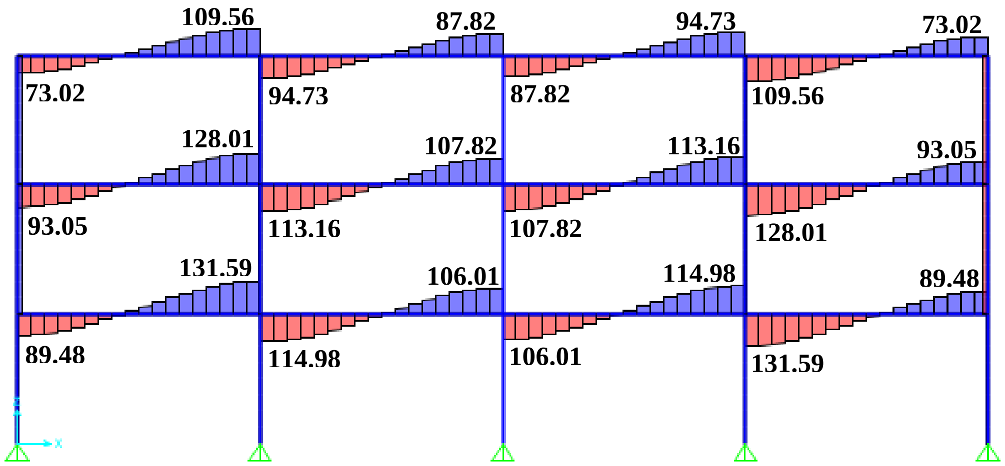

Figure F.15: Shear force diagrams – Eurocode-based typical building (X-direction – type 2 frame)

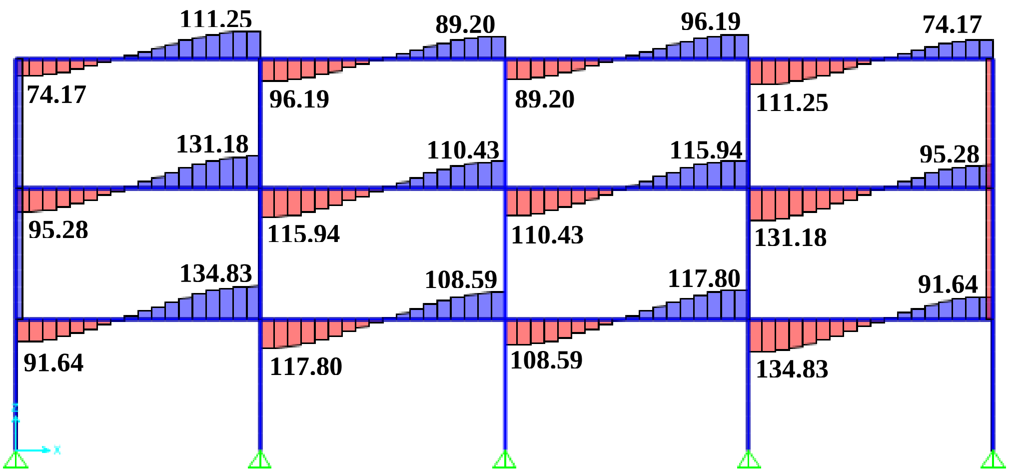

Figure F.16: Shear force diagrams – British Standard-based typical building (X-direction – type 2 frame)

Table F.15: Design of beams for shear (X-direction - type 2 frame - first/second floor)

Parameters – Design for Shear	Euro	BS	% Difference
Maximum Shear Force (kN)	131.59	134.83	2.46%
Amount of Reinforcement Required (mm^2)	551.09	657.21	19.26%
Number of Reinforcements	R6 @ 100	R6 @ 75	Dissimilar
Amount of Reinforcement Provided (mm^2)	565.20	753.60	33.33%
Utilization	0.98	0.87	-10.56%

Table F.16: Design of beams for shear (X-direction - type 2 frame - roof floor)

Parameters – Design for Shear	Euro	BS	% Difference
Maximum Shear Force (kN)	109.56	111.25	1.54%
Amount of Reinforcement Required (mm^2)	458.83	479.97	4.61%
Number of Reinforcements	R6 @ 100	R6 @ 100	Similar
Amount of Reinforcement Provided (mm^2)	565.20	565.20	0.00%
Utilization	0.81	0.85	4.61%

F.2.3. Structural analysis and design of beams in type 3 frame for shear

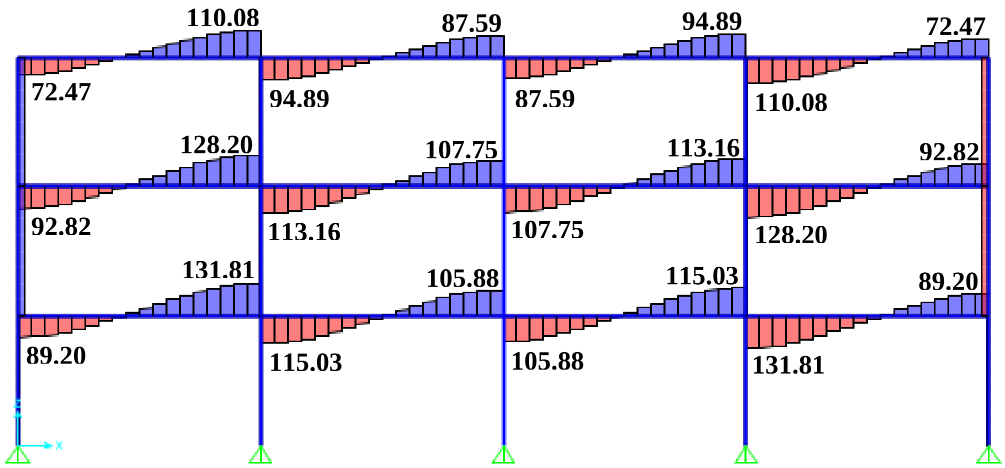

Figure F.17: Shear force diagrams – Eurocode-based typical building (X-direction – type 3 frame)

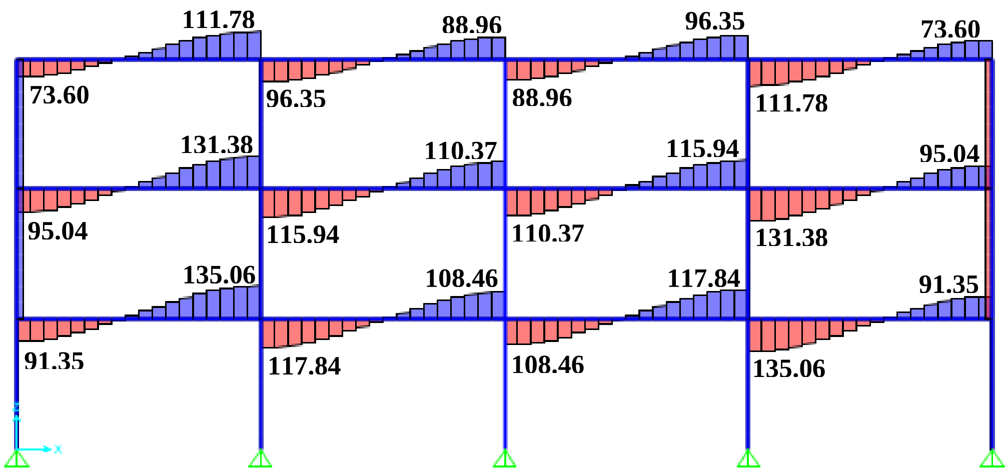

Figure F.18: Shear force diagrams – British Standard-based typical building (X-direction – type 3 frame)

Table F.17: Design of beams for shear (X-direction - type 3 frame - first/second floor)

Parameters – Design for Shear	Euro	BS	% Difference
Maximum Shear Force (kN)	131.81	135.06	2.47%
Amount of Reinforcement Required (mm^2)	552.01	659.66	19.50%
Number of Reinforcements	R6 @ 100	R6 @ 75	Dissimilar
Amount of Reinforcement Provided (mm^2)	565.20	753.60	33.33%
Utilization	0.98	0.88	-10.37%

Table F.18: Design of beams for shear (X-direction - type 3 frame - roof floor)

Parameters – Design for Shear	Euro	BS	% Difference
Maximum Shear Force (kN)	110.08	111.78	1.54%
Amount of Reinforcement Required (mm^2)	461.01	485.56	5.33%
Number of Reinforcements	R6 @ 100	R6 @ 100	Similar
Amount of Reinforcement Provided (mm^2)	565.20	565.20	0.00%
Utilization	0.82	0.86	5.33%

F.2.4. Structural analysis and design of beams in type 4 frame for shear

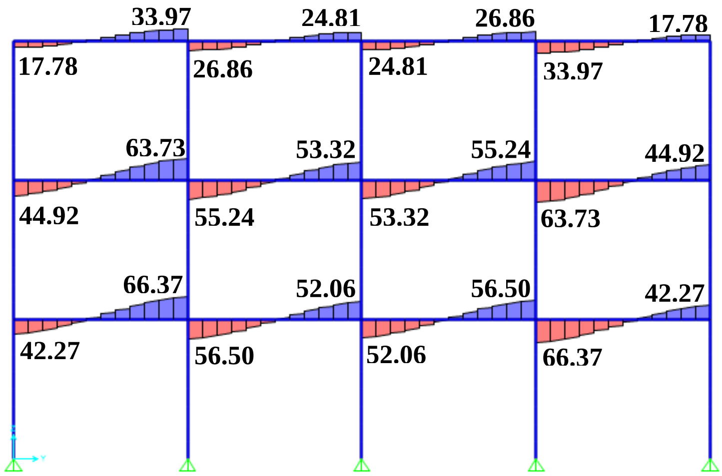

Figure F.19: Shear force diagrams – Eurocode-based typical building (Y-direction – type 4 frame)

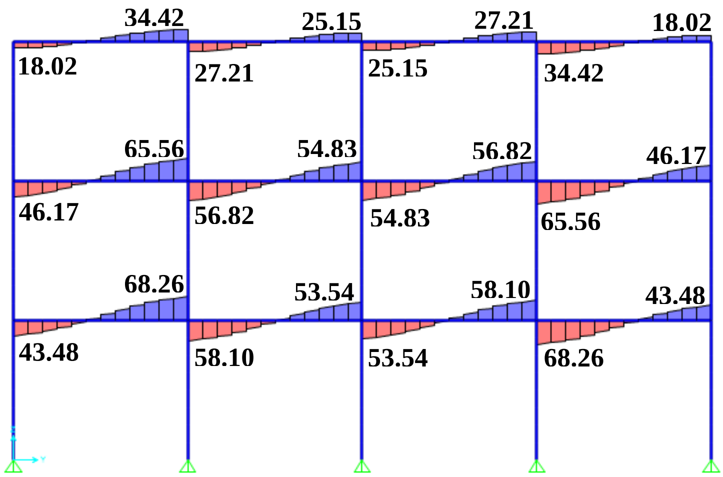

Figure F.20: Shear force diagrams – British Standard-based typical building (Y-direction – type 4 frame)

Table F.19: Design of beams for shear (Y-direction - type 4 frame - first/second floor)

Parameters – Design for Shear	Euro	BS	% Difference
Maximum Shear Force (kN)	66.37	68.26	2.85%
Amount of Reinforcement Required (mm^2)	344.66	421.05	22.16%
Number of Reinforcements	R6 @ 150	R6 @ 125	Dissimilar
Amount of Reinforcement Provided (mm^2)	376.80	452.16	20.00%
Utilization	0.91	0.93	1.80%

Table F.20: Design of beams for shear (Y-direction - type 4 frame - roof floor)

Parameters – Design for Shear	Euro	BS	% Difference
Maximum Shear Force (kN)	33.97	34.42	1.32%
Amount of Reinforcement Required (mm^2)	175.01	421.05	140.59%
Number of Reinforcements	R6 @ 225	R6 @ 125	Dissimilar
Amount of Reinforcement Provided (mm^2)	251.20	452.16	80.00%
Utilization	0.70	0.93	33.66%

F.2.5. Structural analysis and design of beams in type 5 frame for shear

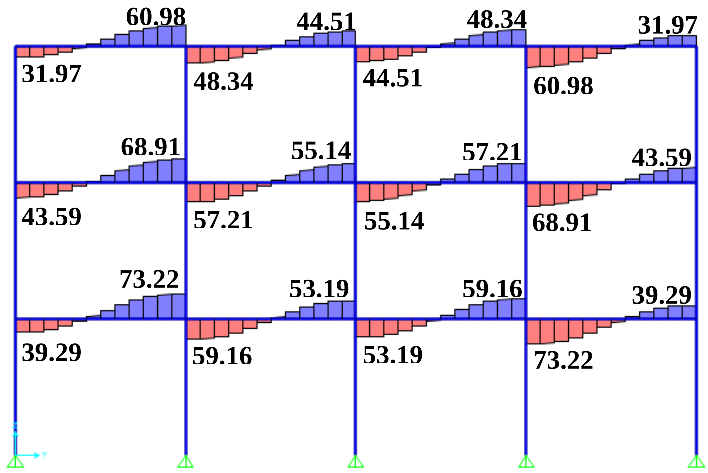

Figure F.21: Shear force diagrams – Eurocode-based typical building (Y-direction – type 5 frame)

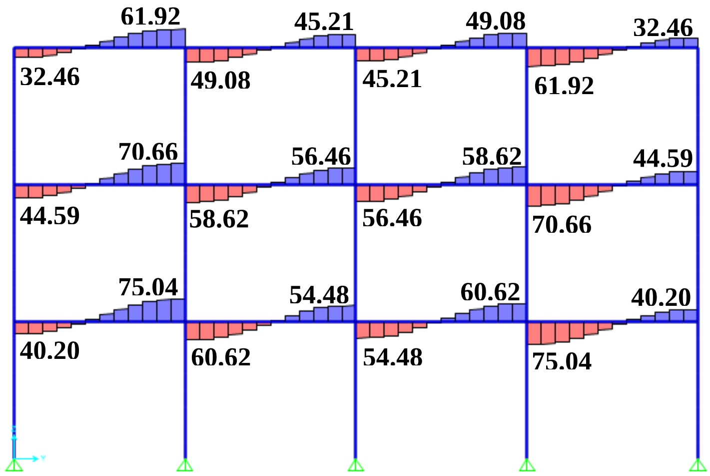

Figure F.22: Shear force diagrams – British Standard-based typical building (Y-direction – type 5 frame)

Table F.21: Design of beams for shear (Y-direction - type 5 frame - first/second floor)

Parameters – Design for Shear	Euro	BS	% Difference
Maximum Shear Force (kN)	73.22	75.04	2.49%
Amount of Reinforcement Required (mm^2)	380.23	421.05	10.74%
Number of Reinforcements	R6 @ 125	R6 @ 125	Similar
Amount of Reinforcement Provided (mm^2)	452.16	452.16	0.00%
Utilization	0.84	0.93	10.74%

Table F.22: Design of beams for shear (Y-direction - type 5 frame - roof floor)

Parameters – Design for Shear	Euro	BS	% Difference
Maximum Shear Force (kN)	60.98	61.92	1.54%
Amount of Reinforcement Required (mm^2)	316.67	421.05	32.96%
Number of Reinforcements	R6 @ 175	R6 @ 125	Dissimilar
Amount of Reinforcement Provided (mm^2)	322.97	452.16	40.00%
Utilization	0.98	0.93	-5.03%

F.2.6. Structural analysis and design of beams in type 6 frame for shear

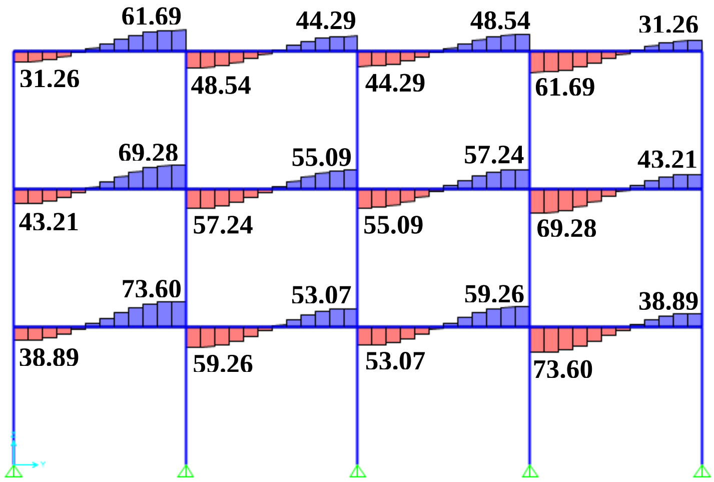

Figure F.23: Shear force diagrams – Eurocode-based typical building (Y-direction – type 6 frame)

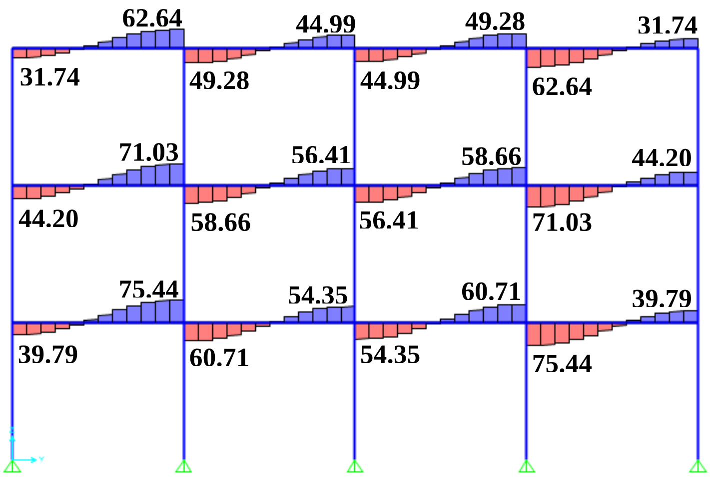

Figure F.24: Shear force diagrams – British Standard-based typical building (Y-direction – type 6 frame)

Table F.23: Design of beams for shear (Y-direction - type 6 frame - first/second floor)

Parameters – Design for Shear	Euro	BS	% Difference
Maximum Shear Force (kN)	73.60	75.44	2.50%
Amount of Reinforcement Required (mm^2)	382.20	421.05	10.16%
Number of Reinforcements	R6 @ 125	R6 @ 125	Similar
Amount of Reinforcement Provided (mm^2)	452.16	452.16	0.00%
Utilization	0.85	0.93	10.16%

Table F.24: Design of beams for shear (Y-direction - type 6 frame - roof floor)

Parameters – Design for Shear	Euro	BS	% Difference
Maximum Shear Force (kN)	61.69	62.64	1.54%
Amount of Reinforcement Required (mm^2)	320.35	421.05	31.43%
Number of Reinforcements	R6 @ 175	R6 @ 125	Dissimilar
Amount of Reinforcement Provided (mm^2)	322.97	452.16	40.00%
Utilization	0.99	0.93	-6.12%

F.3. Structural analysis and design of columns for axial force and bending moments

			Notation Axial Force M22-Top, M22-Bottom
528.81 0,0	1010.50 0, 0	918.98 0, 0	M33-Top, M33-Bottom
0, 20.87 572.18 0, 1.77	0, 3.64 1071.50 0, 2.41	0, 0 984.54 0, 2.51	
0, 20.68 321.67 0, 11.52	0, 3.56 661.04 0, 16.51	0, 0 595.71 0, 16.74	

Figure F.25: Column member forces – ground floor - Eurocode-based typical building

			Notation Axial Force M22-Top, M22-Bottom
330.90 0, 0	653.51 0, 0	597.32 0, 0	M33-Top, M33-Bottom
39.79, 38.25 355.23 3.05, 2.59	6.49, 5.76 688.78 4.04, 3.30	0, 0 635.89 4.22, 3.47	
39.48, 37.99 195.07 21.84, 20.85	6.34, 5.63 405.90 31.21, 29.72	0, 0 368.13 31.59, 30.01	

Figure F.26: Column member forces – first floor - Eurocode -based typical building

			Notation Axial Force M22-Top, M22-Bottom
126.84 0, 0	298.09 0, 0	267.86 0, 0	M33-Top, M33-Bottom
38.24, 39.78 138.61 2.21, 2.29	5.56, 6.10 317.72 3.06, 3.54	0, 0 289.96 3.29, 3.86	
37.84, 39.16 63.50 19.69, 19.49	5.37, 5.82 150.00 30.24, 32.26	0, 0 133.76 30.62, 32.83	

Figure F.27: Column member forces – roof floor - Eurocode-based typical building

			Notation Axial Force M22-Top, M22-Bottom
540.84 0,0	1032.09 0, 0	938.50 0, 0	M33-Top, M33-Bottom
0, 21.40 585.29 0, 1.82	0, 3.73 1094.58 0, 2.47	0, 0 1005.64 0, 2.57	
0, 21.20 329.24 0, 11.84	0, 3.65 676.38 0, 16.94	0, 0 609.48 0, 17.17	

Figure F.28: Column member forces – ground floor - British Standard-based typical building

			Notation Axial Force M22-Top, M22-Bottom
128.62 **0, 0**	**302.60** **0, 0**	**271.95** **0, 0**	M33-Top, M33-Bottom
39.09, 40.52 **140.52** **2.26, 2.33**	**5.69, 6.21** **322.49** **3.14, 3.61**	**0, 0** **294.36** **3.38, 3.93**	
38.68, 39.90 **64.27** **20.16, 19.87**	**5.49, 5.92** **151.96** **30.93, 32.88**	**0, 0** **135.55** **31.32, 33.46**	

Figure F.29: Column member forces – ground floor - British Standard-based typical building

			Notation Axial Force M22-Top, M22-Bottom
337.86 **0, 0**	**666.55** **0, 0**	**609.19** **0, 0**	M33-Top, M33-Bottom
40.80, 39.22 **362.74** **3.14, 2.67**	**6.66, 5.92** **702.59** **4.16, 3.41**	**0, 0** **648.61** **4.35, 3.58**	
40.48, 38.97 **199.29** **22.44, 21.44**	**6.51, 5.78** **414.56** **32.03, 30.51**	**0, 0** **375.97** **32.41, 30.80**	

Figure F.30: Column member forces – roof floor - British Standard-based typical building

F.3.1. Design of type 1 columns

Table F.25: Design of column type 1 (ground floor)

GF/Type 1 Column	Euro	BS	% Difference
Axial Force (kN)	321.67	329.24	2.35%
Bending Moment (M22) -Bottom	0.00	0.00	0.00%
Bending Moment (M22) -Top	11.52	11.84	2.78%
Bending Moment (M33) -Bottom	0.00	0.00	0.00%
Bending Moment (M33) -Top	15.92	16.36	2.76%
Cross Section Size	225 × 225	225 × 225	Similar
Amount of Reinforcement Required (mm^2)	220.11	253.13	15.00%
Number of Reinforcements	4T12	4T12	Similar
Amount of Reinforcement Provided (mm^2)	452.16	452.16	0.00%
Utilization	0.49	0.56	15.00%
Shear Link Diameter (mm)	6	6	Similar
Shear Link Spacing (mm)	125	125	Similar

Table F.26: Design of column type 1 (first floor)

1F/Type 1 Column	Euro	BS	% Difference
Axial Force (kN)	195.07	199.29	2.16%
Bending Moment (M22) -Bottom	21.84	22.44	2.75%
Bending Moment (M22) -Top	20.85	21.44	2.83%
Bending Moment (M33) -Bottom	30.54	31.38	2.75%
Bending Moment (M33) -Top	29.55	30.36	2.74%
Cross Section Size (mm × mm)	225 × 225	225 × 225	Similar
Amount of Reinforcement Required (mm^2)	1293.14	1620	25.28%
Number of Reinforcements	4T25	4T25	Similar
Amount of Reinforcement Provided (mm^2)	1962.5	1962.5	0.00%
Utilization	0.66	0.83	25.28%
Shear Link Diameter (mm)	8	8	Similar
Shear Link Spacing (mm)	225	300	Dissimilar

Table F.27: Design of column type 1 (second floor)

2F/Type 1 Column	Euro	BS	% Difference
Axial Force (kN)	63.50	64.27	1.21%
Bending Moment (M22) -Bottom	19.69	20.16	2.39%
Bending Moment (M22) -Top	19.49	19.87	1.95%
Bending Moment (M33) -Bottom	26.75	27.39	2.39%
Bending Moment (M33) -Top	24.89	25.37	1.93%
Cross Section Size (mm × mm)	225 × 225	225 × 225	Similar
Amount of Reinforcement Required (mm^2)	1444.46	1670.63	15.66%
Number of Reinforcements	4T25	4T25	Similar
Amount of Reinforcement Provided (mm^2)	1962.5	1962.5	0.00%
Utilization	0.74	0.85	15.66%
Shear Link Diameter (mm)	8	8	Similar
Shear Link Spacing (mm)	225	300	Dissimilar

F.3.2. Design of type 2 columns

Table F.28: Design of column type 2 (ground floor)

GF/Type 2 Column	Euro	BS	% Difference
Axial Force (kN)	661.04	676.38	2.32%
Bending Moment (M22) -Bottom	0.00	0.00	0.00%
Bending Moment (M22) -Top	16.51	16.94	2.60%
Bending Moment (M33) -Bottom	0.00	0.00	0.00%
Bending Moment (M33) -Top	2.83	2.9	2.47%
Cross Section Size (mm × mm)	225 × 225	225 × 225	Similar
Amount of Reinforcement Required (mm^2)	412.7	556.88	34.94%
Number of Reinforcements	4T12	4T16	Dissimilar
Amount of Reinforcement Provided (mm^2)	452.16	803.84	77.78%
Utilization	0.91	0.69	-24.10%
Shear Link Diameter (mm)	6	6	Similar
Shear Link Spacing (mm)	125	125	Similar

Table F.29: Design of column type 2 (first floor)

1F/Type 2 Column	Euro	BS	% Difference
Axial Force (kN)	405.9	414.56	2.13%
Bending Moment (M22) -Bottom	31.21	32.03	2.63%
Bending Moment (M22) -Top	29.72	30.51	2.66%
Bending Moment (M33) -Bottom	5.13	5.27	2.73%
Bending Moment (M33) -Top	4.65	4.79	3.01%
Cross Section Size (mm × mm)	225 × 225	225 × 225	Similar
Amount of Reinforcement Required (mm^2)	687.84	759.38	10.40%
Number of Reinforcements	4T16	4T16	Similar
Amount of Reinforcement Provided (mm^2)	803.84	803.84	0.00%
Utilization	0.86	0.94	10.40%
Shear Link Diameter (mm)	6	6	Similar
Shear Link Spacing (mm)	175	175	Similar

Table F.30: Design of column type 2 (second floor)

2F/Type 2 Column	Euro	BS	% Difference
Axial Force (kN)	150.00	151.96	1.31%
Bending Moment (M22) -Bottom	30.24	30.93	2.28%
Bending Moment (M22) -Top	32.26	32.88	1.92%
Bending Moment (M33) -Bottom	3.97	4.07	2.52%
Bending Moment (M33) -Top	3.75	3.82	1.87%
Cross Section Size (mm × mm)	225 × 225	225 × 225	Similar
Amount of Reinforcement Required (mm^2)	894.19	1012.5	13.23%
Number of Reinforcements	4T20	4T20	Similar
Amount of Reinforcement Provided (mm^2)	1256	1256	0.00%
Utilization	0.71	0.81	13.23%
Shear Link Diameter (mm)	6	6	Similar
Shear Link Spacing (mm)	225	225	Similar

F.3.3. Design of type 3 columns

Table F.31: Design of column type 3 (ground floor)

GF/Type 3 Column	Euro	BS	% Difference
Axial Force (kN)	595.71	609.48	2.31%
Bending Moment (M22) -Bottom	0.00	0.00	0.00%
Bending Moment (M22) -Top	16.74	17.17	2.57%
Bending Moment (M33) -Bottom	0.00	0.00	0.00%
Bending Moment (M33) -Top	0.00	0.00	0.00%
Cross Section Size (mm × mm)	225 × 225	225 × 225	Similar
Amount of Reinforcement Required (mm^2)	275.14	354.38	28.80%
Number of Reinforcements	4T12	4T12	Similar
Amount of Reinforcement Provided (mm^2)	452.16	452.16	0.00%
Utilization	0.61	0.78	28.80%
Shear Link Diameter (mm)	6	6	Similar
Shear Link Spacing (mm)	125	125	Similar

Table F.32: Design of column type 3 (first floor)

1F/Type 3 Column	Euro	BS	% Difference
Axial Force (kN)	368.13	375.97	2.13%
Bending Moment (M22) -Bottom	31.59	32.41	2.60%
Bending Moment (M22) -Top	30.01	30.8	2.63%
Bending Moment (M33) -Bottom	0	0	0.00%
Bending Moment (M33) -Top	0	0	0.00%
Cross Section Size (mm × mm)	225 × 225	225 × 225	Similar
Amount of Reinforcement Required (mm^2)	550.27	607.5	Similar
Number of Reinforcements	4T16	4T16	Similar
Amount of Reinforcement Provided (mm^2)	803.84	803.84	0.00%
Utilization	0.68	0.76	10.40%
Shear Link Diameter (mm)	6	6	Similar
Shear Link Spacing (mm)	175	175	Similar

Table F.33: Design of column type 3 (second floor)

2F/Type 3 Column	Euro	BS	% Difference
Axial Force (kN)	133.76	135.55	1.34%
Bending Moment (M22) -Bottom	30.62	31.32	2.29%
Bending Moment (M22) -Top	32.83	33.46	1.92%
Bending Moment (M33) -Bottom	0	0	0.00%
Bending Moment (M33) -Top	0	0	0.00%
Cross Section Size (mm × mm)	225 × 225	225 × 225	Similar
Amount of Reinforcement Required (mm^2)	687.84	961.88	39.84%
Number of Reinforcements	4T16	4T20	Dissimilar
Amount of Reinforcement Provided (mm^2)	803.84	1256.00	56.25%
Utilization	0.86	0.77	-10.50%
Shear Link Diameter (mm)	6	6	Similar
Shear Link Spacing (mm)	175	225	Dissimilar

F.3.4. Design of type 4 columns

Table F.34: Design of column type 4 (ground floor)

GF/Type 4 Column	Euro	BS	% Difference
Axial Force (kN)	572.18	585.29	2.29%
Bending Moment (M22) -Bottom	0.00	0.00	0.00%
Bending Moment (M22) -Top	1.77	1.82	2.82%
Bending Moment (M33) -Bottom	0.00	0.00	0.00%
Bending Moment (M33) -Top	20.68	21.2	2.51%
Cross Section Size (mm × mm)	225 × 225	225 × 225	Similar
Amount of Reinforcement Required (mm^2)	412.7	506.25	22.67%
Number of Reinforcements	4T12	4T16	Dissimilar
Amount of Reinforcement Provided (mm^2)	452.16	803.84	77.78%
Utilization	0.91	0.63	-31.00%
Shear Link Diameter (mm)	6	6	Similar
Shear Link Spacing (mm)	125	125	Similar

Table F.35: Design of column type 4 (first floor)

1F/Type 4 Column	Euro	BS	% Difference
Axial Force (kN)	355.23	362.74	2.11%
Bending Moment (M22) -Bottom	3.05	3.14	2.95%
Bending Moment (M22) -Top	2.59	2.67	3.09%
Bending Moment (M33) -Bottom	39.48	40.48	2.53%
Bending Moment (M33) -Top	37.99	38.97	2.58%
Cross Section Size (mm × mm)	225 × 225	225 × 225	Similar
Amount of Reinforcement Required (mm^2)	962.98	1265.63	31.43%
Number of Reinforcements	4T20	4T25	Dissimilar
Amount of Reinforcement Provided (mm^2)	1256	1962.5	56.25%
Utilization	0.77	0.64	-15.89%
Shear Link Diameter (mm)	6	6	Similar
Shear Link Spacing (mm)	225	225	Similar

Table F.36: Design of column type 4 (second floor)

2F/Type 4 Column	Euro	BS	% Difference
Axial Force (kN)	138.61	140.52	1.38%
Bending Moment (M22) -Bottom	2.21	2.26	2.26%
Bending Moment (M22) -Top	2.29	2.33	1.75%
Bending Moment (M33) -Bottom	37.84	38.68	2.22%
Bending Moment (M33) -Top	39.16	39.9	1.89%
Cross Section Size (mm × mm)	225 × 225	225 × 225	Similar
Amount of Reinforcement Required (mm^2)	990.00	1316.25	32.95%
Number of Reinforcements	4T20	4T25	Dissimilar
Amount of Reinforcement Provided (mm^2)	1256	1962.5	56.25%
Utilization	0.79	0.67	-14.91%
Shear Link Diameter (mm)	6	6	Similar
Shear Link Spacing (mm)	225	225	Similar

F.3.5. Design of type 5 columns

Table F.37: Design of column type 5 (ground floor)

GF/Type 5 Column	Euro	BS	% Difference
Axial Force (kN)	1071.5	1094.58	2.15%
Bending Moment (M22) -Bottom	0.00	0.00	0.00%
Bending Moment (M22) -Top	2.41	2.47	2.49%
Bending Moment (M33) -Bottom	0.00	0.00	0.00%
Bending Moment (M33) -Top	3.56	3.65	2.53%
Cross Section Size (mm × mm)	225 × 225	225 × 225	Similar
Amount of Reinforcement Required (mm^2)	1100.54	1164.38	5.80%
Number of Reinforcements	4T20	4T20	Similar
Amount of Reinforcement Provided (mm^2)	1256	1256	0.00%
Utilization	0.88	0.93	5.80%
Shear Link Diameter (mm)	6	6	Similar
Shear Link Spacing (mm)	225	225	Similar

Table F.38: Design of column type 5 (first floor)

1F/Type 5 Column	Euro	BS	% Difference
Axial Force (kN)	688.78	702.59	2.00%
Bending Moment (M22) -Bottom	4.04	4.16	2.97%
Bending Moment (M22) -Top	3.30	3.41	3.33%
Bending Moment (M33) -Bottom	6.34	6.51	2.68%
Bending Moment (M33) -Top	5.63	5.78	2.66%
Cross Section Size (mm × mm)	225 × 225	225 × 225	Similar
Amount of Reinforcement Required (mm^2)	206.35	303.75	47.20%
Number of Reinforcements	4T12	4T12	Similar
Amount of Reinforcement Provided (mm^2)	452.16	452.16	0.00%
Utilization	0.46	0.67	47.20%
Shear Link Diameter (mm)	6	6	Similar
Shear Link Spacing (mm)	125	125	Similar

Table F.39: Design of column type 5 (second floor)

2F/Type 5 Column	Euro	BS	% Difference
Axial Force (kN)	317.72	322.49	1.50%
Bending Moment (M22) -Bottom	3.06	3.14	2.61%
Bending Moment (M22) -Top	3.54	3.61	1.98%
Bending Moment (M33) -Bottom	5.37	5.49	2.23%
Bending Moment (M33) -Top	5.82	5.92	1.72%
Cross Section Size (mm × mm)	225 × 225	225 × 225	Similar
Amount of Reinforcement Required (mm^2)	202.50	202.50	0.00%
Number of Reinforcements	4T12	4T12	Similar
Amount of Reinforcement Provided (mm^2)	452.16	452.16	0.00%
Utilization	0.45	0.45	0.00%
Shear Link Diameter (mm)	6	6	Similar
Shear Link Spacing (mm)	125	125	Similar

F.3.6. Design of type 6 columns

Table F.40: Design of column type 6 (ground floor)

GF/Type 6 Column	Euro	BS	% Difference
Axial Force (kN)	984.54	1005.64	2.14%
Bending Moment (M22) -Bottom	0.00	0.00	0.00%
Bending Moment (M22) -Top	2.51	2.57	2.39%
Bending Moment (M33) -Bottom	0.00	0.00	0.00%
Bending Moment (M33) -Top	0.00	0.00	0.00%
Cross Section Size (mm × mm)	225 × 225	225 × 225	Similar
Amount of Reinforcement Required (mm^2)	770.38	860.63	11.71%
Number of Reinforcements	4T16	4T20	Dissimilar
Amount of Reinforcement Provided (mm^2)	803.84	1256	56.25%
Utilization	0.96	0.69	-28.50%
Shear Link Diameter (mm)	6	6	Similar
Shear Link Spacing (mm)	175	225	Dissimilar

Table F.41: Design of column type 6 (first floor)

1F/Type 6 Column	Euro	BS	% Difference
Axial Force (kN)	635.89	648.61	2.00%
Bending Moment (M22) -Bottom	4.22	4.35	3.08%
Bending Moment (M22) -Top	3.47	3.58	3.17%
Bending Moment (M33) -Bottom	0.00	0.00	0.00%
Bending Moment (M33) -Top	0.00	0.00	0.00%
Cross Section Size (mm × mm)	225 × 225	225 × 225	Similar
Amount of Reinforcement Required (mm^2)	202.5	202.5	0.00%
Number of Reinforcements	4T12	4T12	Similar
Amount of Reinforcement Provided (mm^2)	452.16	452.16	0.00%
Utilization	0.45	0.45	0.00%
Shear Link Diameter (mm)	6	6	Similar
Shear Link Spacing (mm)	125	125	Similar

Table F.42: Design of column type 6 (second floor)

2F/Type 6 Column	Euro	BS	% Difference
Axial Force (kN)	289.96	294.36	1.52%
Bending Moment (M22) -Bottom	3.29	3.38	2.74%
Bending Moment (M22) -Top	3.86	3.93	1.81%
Bending Moment (M33) -Bottom	0.00	0.00	0.00%
Bending Moment (M33) -Top	0.00	0.00	0.00%
Cross Section Size (mm × mm)	225 × 225	225 × 225	Similar
Amount of Reinforcement Required (mm^2)	202.50	202.50	0.00%
Number of Reinforcements	4T12	4T12	Similar
Amount of Reinforcement Provided (mm^2)	452.16	452.16	0.00%
Utilization	0.45	0.45	0.00%
Shear Link Diameter (mm)	6	6	Similar
Shear Link Spacing (mm)	125	125	Similar

F.3.7. Design of type 7 columns

Table F.43: Design of column type 7 (ground floor)

GF/Type 7 Column	Euro	BS	% Difference
Axial Force (kN)	528.81	540.84	2.27%
Bending Moment (M22) -Bottom	0.00	0.00	0.00%
Bending Moment (M22) -Top	0.00	0.00	0.00%
Bending Moment (M33) -Bottom	0.00	0.00	0.00%
Bending Moment (M33) -Top	20.87	21.4	2.54%
Cross Section Size (mm × mm)	225 × 225	225 × 225	Similar
Amount of Reinforcement Required (mm^2)	202.5	405	100.00%
Number of Reinforcements	4T12	4T12	Similar
Amount of Reinforcement Provided (mm^2)	452.16	452.16	0.00%
Utilization	0.45	0.90	100.00%
Shear Link Diameter (mm)	6	6	Similar
Shear Link Spacing (mm)	125	125	Similar

Table F.44: Design of column type 7 (first floor)

1F/Type 7 Column	Euro	BS	% Difference
Axial Force (kN)	330.9	337.86	2.10%
Bending Moment (M22) -Bottom	0.00	0.00	0.00%
Bending Moment (M22) -Top	0.00	0.00	0.00%
Bending Moment (M33) -Bottom	39.79	40.8	2.54%
Bending Moment (M33) -Top	38.25	39.22	2.54%
Cross Section Size (mm × mm)	225 × 225	225 × 225	Similar
Amount of Reinforcement Required (mm^2)	825.41	1139.06	38.00%
Number of Reinforcements	4T20	4T20	Similar
Amount of Reinforcement Provided (mm^2)	1256	1256	0.00%
Utilization	0.66	0.91	38.00%
Shear Link Diameter (mm)	6	6	Similar
Shear Link Spacing (mm)	225	225	Similar

Table F.45: Design of column type 7 (second floor)

2F/Type 7 Column	Euro	BS	% Difference
Axial Force (kN)	126.84	128.62	1.40%
Bending Moment (M22) -Bottom	0.00	0.00	0.00%
Bending Moment (M22) -Top	0.00	0.00	0.00%
Bending Moment (M33) -Bottom	38.24	39.09	2.22%
Bending Moment (M33) -Top	39.78	40.52	1.86%
Cross Section Size (mm × mm)	225 × 225	225 × 225	Similar
Amount of Reinforcement Required (mm^2)	1100.54	1265.63	15.00%
Number of Reinforcements	4T20	4T25	Dissimilar
Amount of Reinforcement Provided (mm^2)	1256	1962.5	56.25%
Utilization	0.88	0.64	-26.40%
Shear Link Diameter (mm)	6	6	Similar
Shear Link Spacing (mm)	225	225	Similar

F.3.8. Design of type 8 columns

Table F.46: Design of column type 8 (ground floor)

GF/Type 8 Column	Euro	BS	% Difference
Axial Force (kN)	1010.5	1032.09	2.14%
Bending Moment (M22) -Bottom	0.00	0.00	0.00%
Bending Moment (M22) -Top	0.00	0.00	0.00%
Bending Moment (M33) -Bottom	0.00	0.00	0.00%
Bending Moment (M33) -Top	3.64	3.73	2.47%
Cross Section Size (mm × mm)	225 × 225	225 × 225	Similar
Amount of Reinforcement Required (mm^2)	880.43	1012.5	15.00%
Number of Reinforcements	4T20	4T20	Similar
Amount of Reinforcement Provided (mm^2)	1256	1256	0.00%
Utilization	0.70	0.81	15.00%
Shear Link Diameter (mm)	6	6	Similar
Shear Link Spacing (mm)	225	225	Similar

Table F.47: Design of column type 8 (first floor)

1F/Type 8 Column	Euro	BS	% Difference
Axial Force (kN)	653.51	666.55	2.00%
Bending Moment (M22) -Bottom	0.00	0.00	0.00%
Bending Moment (M22) -Top	0.00	0.00	0.00%
Bending Moment (M33) -Bottom	6.49	6.66	2.62%
Bending Moment (M33) -Top	5.76	5.92	2.78%
Cross Section Size (mm × mm)	225 × 225	225 × 225	Similar
Amount of Reinforcement Required (mm^2)	202.5	202.5	0.00%
Number of Reinforcements	4T12	4T12	Similar
Amount of Reinforcement Provided (mm^2)	452.16	452.16	0.00%
Utilization	0.45	0.45	0.00%
Shear Link Diameter (mm)	6	6	Similar
Shear Link Spacing (mm)	125	125	Similar

Table F.48: Design of column type 8 (second floor)

2F/Type 8 Column	Euro	BS	% Difference
Axial Force (kN)	298.09	302.6	1.51%
Bending Moment (M22) -Bottom	0	0	0.00%
Bending Moment (M22) -Top	0	0	0.00%
Bending Moment (M33) -Bottom	5.56	5.69	2.34%
Bending Moment (M33) -Top	6.10	6.21	1.80%
Cross Section Size (mm × mm)	225 × 225	225 × 225	Similar
Amount of Reinforcement Required (mm^2)	202.50	202.50	0.00%
Number of Reinforcements	4T12	4T12	Similar
Amount of Reinforcement Provided (mm^2)	452.16	452.16	0.00%
Utilization	0.45	0.45	0.00%
Shear Link Diameter (mm)	6	6	Similar
Shear Link Spacing (mm)	125	125	Similar

F.3.9. Design of type 9 columns

Table F.49: Design of column type 9 (ground floor)

GF/Type 9 Column	Euro	BS	% Difference
Axial Force (kN)	918.98	938.5	2.12%
Bending Moment (M22) -Bottom	0.00	0.00	0.00%
Bending Moment (M22) -Top	0.00	0.00	0.00%
Bending Moment (M33) -Bottom	0.00	0.00	0.00%
Bending Moment (M33) -Top	0.00	0.00	0.00%
Cross Section Size (mm × mm)	225 × 225	225 × 225	Similar
Amount of Reinforcement Required (mm^2)	1100.54	1327.78	20.65%
Number of Reinforcements	4T20	4T25	Dissimilar
Amount of Reinforcement Provided (mm^2)	1256	1962.5	56.25%
Utilization	0.88	0.68	-22.79%
Shear Link Diameter (mm)	6	6	Similar
Shear Link Spacing (mm)	225	225	Similar

Table F.50: Design of column type 9 (first floor)

1F/Type 9 Column	Euro	BS	% Difference
Axial Force (kN)	597.32	609.19	1.99%
Bending Moment (M22) -Bottom	0.00	0.00	0.00%
Bending Moment (M22) -Top	0.00	0.00	0.00%
Bending Moment (M33) -Bottom	0.00	0.00	0.00%
Bending Moment (M33) -Top	0.00	0.00	0.00%
Cross Section Size (mm × mm)	225 × 225	225 × 225	Similar
Amount of Reinforcement Required (mm^2)	202.50	255.82	26.33%
Number of Reinforcements	4T12	4T12	Similar
Amount of Reinforcement Provided (mm^2)	452.16	452.16	0.00%
Utilization	0.45	0.57	26.33%
Shear Link Diameter (mm)	6	6	Similar
Shear Link Spacing (mm)	125	125	Similar

Table F.51: Design of column type 9 (second floor)

2F/Type 9 Column	Euro	BS	% Difference
Axial Force (kN)	267.86	271.95	1.53%
Bending Moment (M22) -Bottom	0.00	0.00	0.00%
Bending Moment (M22) -Top	0.00	0.00	0.00%
Bending Moment (M33) -Bottom	0.00	0.00	0.00%
Bending Moment (M33) -Top	0.00	0.00	0.00%
Cross Section Size (mm × mm)	225 × 225	225 × 225	Similar
Amount of Reinforcement Required (mm^2)	202.50	Negative	
Number of Reinforcements	4T12	4T12	Similar
Amount of Reinforcement Provided (mm^2)	452.16	452.16	0.00%
Utilization	0.45	0.00	-100.00%
Shear Link Diameter (mm)	6	6	Similar
Shear Link Spacing (mm)	125	125	Similar